

Technical Description

This section of the User Guide provides additional details and references on the theory and methods implemented in PIPESIM.

- [Flow Models](#)
- [Completion \(IPR\) Models](#)
- [Equipment](#)
- [Heat Transfer Models](#)
- [Fluids Models](#)

Flow regimes

Flow regimes classification for vertical two phase flow

The general problem of predicting the pressure drop for the simultaneous flow of gas and liquid is complex.

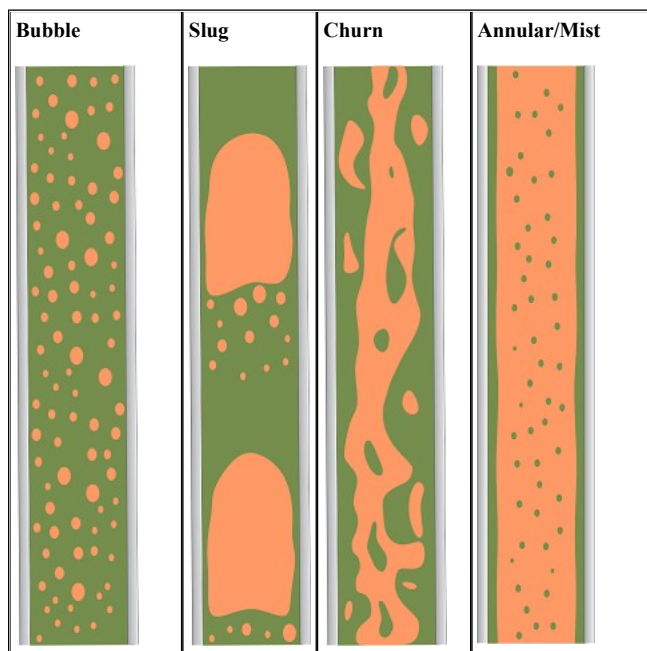
The problem consists of being able to predict the variation of pressure with distance along the length of the flow path for known conditions of flow. Multiphase vertical flow can be categorized into four different flow patterns or flow regimes, consisting of bubble flow, slug flow, slug-mist transition (churn) flow and mist flow.

A typical example of bubble flow is the liberation of solution gas from an undersaturated oil at and above the point in the flow path where its bubble point pressure is reached.

In slug flow, both the gas and liquid phases significantly contribute to the pressure gradient. the gas phase exists as large bubbles almost filling the pipe and separated by slugs of liquid. In transition flow, the liquid slugs between the gas bubbles essentially disappear, and at some point the liquid phases becomes discontinuous and the phase becomes continuous.

The pressure losses in transition (churn) flow are partly a result of the liquid phase, but are more the result of the gas phase. Mist flow is characterized by a continuous gas phase with liquid occurring as entrained droplets in the gas stream and as a liquid film wetting the pipe walls. A typical example of mist flow is the flow of gas and condensate in a gas condensate well.

PIPESIM Vertical Flow Patterns

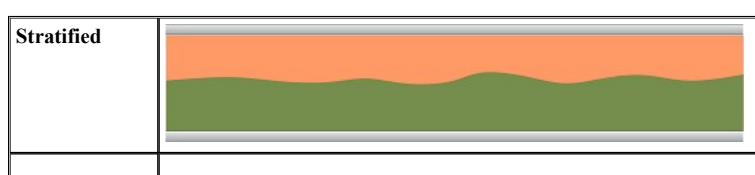


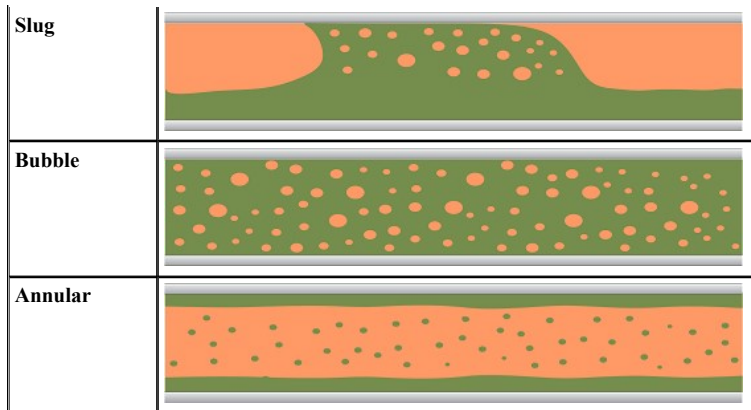
Flow regimes classification for horizontal two phase flow

Prediction of liquid holdup is less critical for pressure loss calculations in horizontal flow than for inclined or vertical flow, although several correlations will require a holdup value for calculating the density terms used in the friction and acceleration pressure drop components. The acceleration pressure drop is usually minor and is often ignored in design calculations; however, PIPESIM includes them.

As in the vertical flow, the two-phase horizontal flow can be divided into the following flow regimes: Stratified Flow (smooth, wavy), Intermittent Flow (plug and slug) and Distributed Flow (bubble and mist).

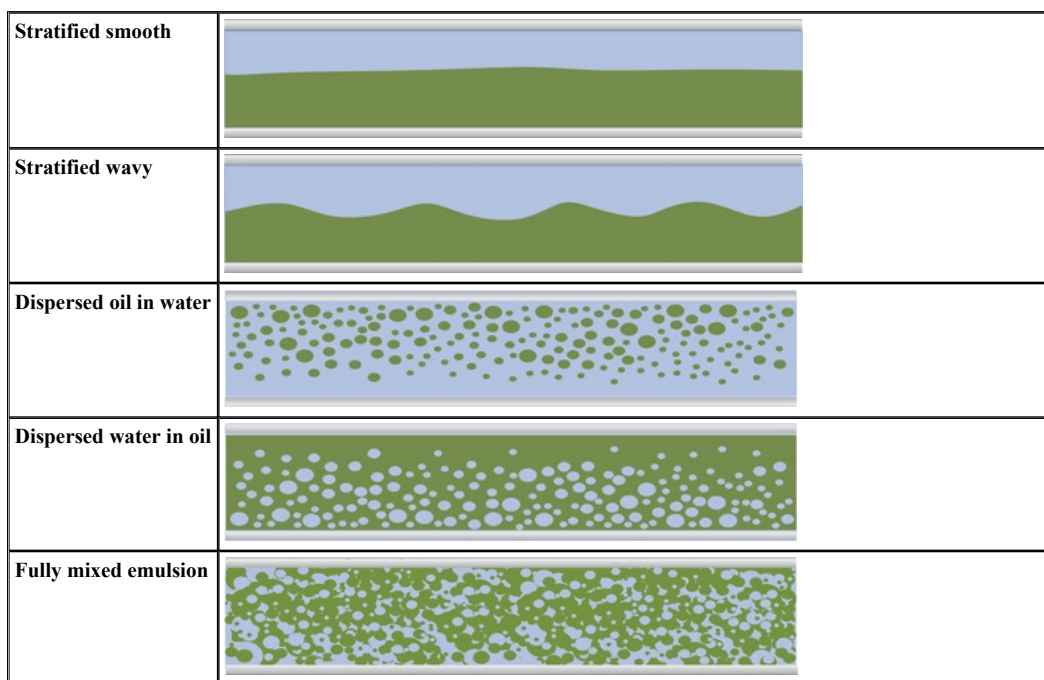
PIPESIM Horizontal Flow Patterns





PIPESIM oil-water flow regimes

Three-phase flow models (OLGAS, TUFFP Unified, LedaPM) will additionally report oil-water flow patterns. Oil-water flow patterns are largely dependent on fractions of each phase and velocity. Each flow model has its own method of calculating the effective viscosity of the oil-water mixture.



Flow regime number and flow pattern

The following flow regimes (patterns) are available for plotting:

- gas-liquid
- oil-water

The list of flow regimes listed below reflect the description provided by the original source though the naming may be slightly different. Generally, these flow regimes will correspond to the broader classifications provided above.

Gas-liquid

The following table shows the current gas-liquid regimes:

Flow Regime	Flow Map	Number
'Undefined'	'?'	-1
'Smooth'	'Sm'	00
'Stratified'	'St'	01
'Annular'	'A'	02
'Slug'	'Sl'	03
'Bubble'	'B'	04
'Segregated'	'Sg'	05
'Transition'	'T'	06
'Intermittent'	'I'	07

'Distributed'	'D'	08
'Strat. Smooth'	'Ss'	09
'Strat. Wavy'	'Sw'	10
'Strat. Dispersed'	'Sd'	11
'Annular Disp.'	'Ad'	12
'Intermit./Slug'	'Ts'	13
'Churn'	'C'	14
'Dispersed Bubble'	'Db'	15
'Single Phase'	'Sp'	16
'Mist'	'M'	17
'Liquid'	'L'	18
'Gas'	'G'	19
'Dense Phase'	'De'	20
'Annular Mist'	'Am'	21
'Two Phase'	'2'	22
'Wave'	'W'	23
'Dispersed'	'Dp'	24
'Plug'	'P'	25
'Tr. Bubble/Slug'	'Tb'	26
'Tr. Froth/Slug'	'Tf'	27
'Heading'	'H'	28
'Oil'	'O'	29
'Oil/Water'	'Ow'	30
'Water/Oil'	'Wo'	31
'Water'	'Wa'	32
'Froth'	'F'	33
'Strat. 3-phase'	'S3'	34
'Bubbly'	'B'	35

Oil-water

The following table shows the current oil-water regimes:

Flow Regime	Flow Map	Number
'Undefined'	'?'	-1
'Stratified'	'St'	00
'Strat. liq. film in slug flow'	'Sf'	01
'Oil/Water'	'Ow'	02
'Water/Oil'	'Wo'	03
'Water'	'Wa'	04
'Oil'	'O'	05
'Emulsion'	'Em'	06

Horizontal multiphase flow correlations

The following horizontal multiphase flow correlations are available:

Baker Jardine (BJA) correlation

[Baker Jardine](#) (now Schlumberger) has developed a correlation for two phase flow in gas-condensate pipelines. This model represents no major advance in theory, but rather a consolidation of various existing mechanistic models, combined with a modest amount of theoretical development and field data testing. The model uses the Taitel Dukler flow regime map and a modified set of the Taitel Dukler momentum balance to predict liquid holdup. The pressure loss calculation procedure is similar in approach to that proposed by Oliemans, but accounts for the increased interfacial shear resulting from the liquid surface roughness. The BJA correlation is used for pressure loss and holdup with flow regime determined by the Taitel Dukler correlation. The BJA correlation has been developed specifically for applications involving low liquid/gas ratios, for example gas/condensate pipelines with a no-slip liquid volume fraction of lower than 0.1.

Beggs and Brill original

ORIGINAL: The original [Beggs and Brill](#) correlation is used for pressure loss and liquid holdup. Flow regime is determined by either the Beggs and

Brill or Taitel Dukler correlation. The Beggs and Brill correlation was developed following a study of two-phase flow in horizontal and inclined pipes. The correlation is based upon a flow regime map which is first determined as if the flow was horizontal. A horizontal holdup is then calculated by correlations, and this holdup is corrected for the angle of inclination. The test system included two 90 ft long acrylic pipes, winched to a variable elevation in the middle, so as to model incline flow both upwards and downwards at angles of up to 90°.

Beggs and Brill revised

REVISED: As above except that the revised version of the Beggs and Brill correlation is used, with rough pipe friction factors, holdup limits and corrective constants as proposed by [Palmer](#) and [Payne](#). The following enhancements to the original method are used; (1) an extra flow regime of froth flow is considered which assumes a no-slip holdup, (2) the friction factor is changed from the standard smooth pipe model, to utilize a single phase friction factor based on the average fluid velocity.

Dukler, (AGA) and Flanigan

The AGA and Flanigan correlation was developed for horizontal and inclined two phase flow of gas-condensate gathering systems. The Taitel Dukler flow regime map is used which considers five flow regimes, stratified smooth, stratified wavy, intermittent, annular dispersed liquid, and dispersed bubble. The [Dukler](#) equation is used to calculate the frictional pressure loss and holdup, and the [Flanigan](#) equation is used to calculate the elevational pressure differential.

Dukler, (AGA) and Flanigan (Eaton Holdup)

As above but with liquid holdup calculated according to the [Eaton](#) correlation. The Eaton liquid holdup correlation is based on a study performed on 2 in. and 4 in. steel pipe using water and natural gas as test fluids. Test pressures ranged from 305 to 865 psia and liquid holdup measurements ranged from .006 - 0.732.

Eaton-Oliemans

The Eaton, Oliemans combination of methods uses the correlation developed by Eaton et al (1967) to predict liquid holdup and the Oliemans Pressure Drop Calculations correlation (1976) to predict frictional pressure losses. This set of correlations has been found to be reliable for gas-condensate systems in which the liquid loading varies from very small amounts to levels high above that which is normally found in gas gathering systems. Additionally, while the Eaton method tends to over-predict liquid holdup, the results for crude oil systems are generally reasonable. Note that since the Eaton et al correlation does not incorporate elevation change in its computation of liquid holdup, hydrostatic pressure losses can be significantly underestimated in cases of low flow rates over hilly terrain. For downhill flow, pressure recovery is based on the gas density, unlike the Baker Jardine version of the Oliemans model which uses mixture density for downhill pressure recovery.

The Oliemans correlation was developed following the study of large diameter condensate pipelines. The flow regime is predicted using the Taitel Dukler flow regime map, and a simple model, which obeyed the correct single phase flow limits was introduced to predict the pressure drop. The model was based on a limited amount of data from a 30-in, 100-km pipeline operating at pressures of 100 barg or higher.

Hughmark-Dukler

The [Hughmark \(1962\)](#) / [Dukler et al \(1964\)](#) method is the procedure that was recommended by the AGA /API (1970). This approach uses the Dukler model for pressure loss calculations and the Hughmark model for liquid holdup calculations.

The use of the Hughmark (1962) liquid volume fraction correlation for pipelines is somewhat anomalous since it was originally based solely on data for flow in vertical pipes. Hughmark did however, compare its predictions with some limited data from horizontal pipes and found the agreement to be reasonable. Since then, a number of studies (Dukler et al, 1964; Mandhane et al, 1975; Gregory, 1975; Gregory and Fogarasi, 1985) have confirmed it to be one of the better correlations for pipeline applications. For downhill flow, pressure recovery is based on the gas density.

It can generally be expected to give reasonable pressure drop and liquid holdup results for gas-crude oil pipelines. This procedure is not recommended however for gas-condensate systems, where the Hughmark correlation generally predicts excessive liquid holdups; errors of up to 600% have been observed.

LEDA

The Leda Point Model (PM) (<http://www.kongsberg.com/ledaflow>) is a mechanistic model applicable for all inclination angles, pipe diameters and fluid properties. The 2-phase model considers gas-liquid flow whereas the 3-phase model considers gas-oil-water flow.

The 3-phase Leda PM considers 9 fields in the mass (continuity) equations (oil, gas, water, oil in gas and water, gas in oil and water, water in oil and gas). Separate momentum equations are solved for oil, gas and water.

The 2-phase Leda PM considers 4 fields in the mass (continuity) equations (liquid, gas, liquid in gas and gas in liquid). Separate momentum equations are solved for gas and liquid phases. The flow regimes predicted by LedaPM are stratified smooth flow, stratified wavy flow, slug flow, annular and bubbly flow. The Leda 2-phase model uses the liquid viscosity associated with the fluid model defined in PIPESIM. The Leda 3-phase model assumes that the liquid viscosity is equal to that of the continuous phase; liquid viscosity options defined with the PIPESIM fluid model are ignored. The continuous phase is determined by the [Brauner-Ullman](#) inversion criteria.

The Leda Point Model is the steady-state version of the transient model developed by SINTEF in collaboration with Total and ConocoPhillips and commercialized by Kongsberg. The model has been calibrated against data collected at the SINTEF Multiphase Flow Laboratory near Trondheim Norway. Over 10,000 experimental data points have been collected for single-phase, two-phase (oil-water, water-gas) and three-phase (oil-water-gas) flow. Pipe diameters ranging from 4-12" were used at pressures up to 90 barg. The models have been validated with field data supplied by ConocoPhillips and Total.

Minami and Brill

The Minami and Brill correlation calculates liquid holdup though does not predict flow regime or pressure gradient. The experimental holdup data was obtained by passing spheres through a 1,333 ft long 3 steel horizontal pipe and measuring the liquid volumes removed. Holdup measurements ranged from .001 to .44. Fluids used in the experiment included air, kerosene and water with the liquid viscosities ranging from .6 cp to 2 cp.

Two correlations were proposed. The first (BRIMIN1) is valid for all ranges of liquid holdup; the second (BRIMIN2) is strictly for wet gas pipelines (holdup < .35).

The [Minami and Brill](#) holdup correlations can be used with any correlation except Mukherjee and Brill, No Slip, TUFFP, LEDA, and OLGA. To activate the Minami and Brill correlation, enter the appropriate engine keyword under Setup » Engine Options (for example, hcorr holdup = brimin1)

Mukherjee and Brill

The [Mukherjee and Brill](#) correlation is used for Pressure loss, Holdup and Flow Map. Note: selection of alternative flow maps and/or holdups will cause unpredictable results. The Mukherjee and Brill correlation was developed following a study of pressure drop behavior in two-phase inclined flow. The test facility consisted of a U-Shaped pipe that was inclinable +/-90°. Each leg of the U section was 56 ft with 22 ft entrance lengths and a 32 ft test sections on both sides. Fluids were air, kerosene and lube oil with liquid viscosities ranging from .9 to 75 cp. Approximately 1000 pressure drop measurements and 1500 liquid holdup measurements were obtained from a broad range of oil and gas flows.

For bubble and slug flow, a no-slip friction factor calculated from the Moody diagram was found adequate for friction head loss calculations. In downhill stratified flow, the friction pressure gradient is calculated based on a momentum balance equation for either phase assuming a smooth gas-liquid interface. For annular-mist flow, a friction factor correlation was presented that is a function of holdup ratio and no-slip Moody friction factor. Results agreed well with the experimental data and correlations were further verified with Prudhoe Bay and North Sea data.

NOSLIP correlation

The NOSLIP correlation assumes homogeneous flow with no slip between the phases. Fluid properties are taken as the average of the gas and liquid phases and friction factors are calculated using the single phase MOODY correlation.

OLGAS 2-phase / OLGAS 2000 3-phase

The OLGAS mechanistic models are applicable for all inclination angles, pipe diameters and fluid properties. The 2-phase [Bendiksen](#) model considers gas-liquid flow, whereas the 3-phase model considers gas-oil-water flow.

This model employs separate continuity equations for gas, liquid bulk and liquid droplets, which are coupled through interphase mass transfer. Two momentum equations are solved: one applied to the combined balance for the gas and liquid droplets, if present, and a separate momentum equation for the liquid film. OLGAS considers four flow regimes: stratified, annular, slug and dispersed bubble flow; and uses a unique minimum slip criteria to predict flow regime transitions.

The OLGA 2-Phase model uses the liquid viscosity model defined within the PIPESIM fluid property definition. The 3-Phase model uses the Pal and Rhodes emulsion correlation to calculate liquid viscosity based on the oil and water viscosities defined with the PIPESIM fluid model definition; liquid viscosity options defined with the PIPESIM fluid model are ignored.

OLGAS is based in large part on data from the SINTEF multiphase flow laboratory near Trondheim, Norway. The test facilities were designed to operate at conditions that approximated field conditions. The test loop is 800 m long and 8 inches in diameter. Operating pressures between 20 and 90 barg were studied. Gas superficial velocities of up to 13 m/s, and liquid superficial velocities of up to 4 m/s were obtained. In order to simulate the range of viscosities and surface tensions experienced in field applications, different hydrocarbon liquids were used (naphtha, diesel, and lube oil). Nitrogen was used as the gas. Pipeline inclination angles between 1° were studied in addition to flow up or down a hill section ahead of a 50m high vertical riser. Over 10,000 experiments were run on this test loop during an eight year period. The facility was run in both steady state and transient modes.

Oliemans

The [Oliemans](#) correlation was developed following the study of large diameter condensate pipelines. The flow regime is predicted using the Taitel Dukler flow regime map, and a simple model, which obeyed the correct single phase flow limits was introduced to predict the pressure drop. The model was based on a limited amount of data from a 30-in, 100-km pipeline operating at pressures of 100 barg or higher.

TUFFP unified mechanistic model (2-phase and 3-phase)

The TUFFP Unified Mechanistic Model is the collective result of many research projects performed by the Tulsa University Fluid Flow Projects (TUFFP) research consortium. The model determines flow pattern transitions, pressure gradient, liquid holdup and slug characteristics. A 2-phase version is available for gas-liquid flow [[Zhang et.al. development](#) and [validation](#)] and a 3-phase version is available for gas-oil-water pipe flow [[Zhang and Sarica](#)]. The model is valid for all inclination angles, pipe diameters and fluid properties.

The principle concept underlying the model is the premise that slug flow shares transition boundaries with all the other flow patterns. The flow pattern transition from slug flow to stratified and/or annular flow is predicted by solving the momentum equations for slug flow. The entire film zone is treated as the control volume and the momentum exchange between the slug body and the film zone is introduced into the combined momentum equation. This approach differs from traditional methods of using separate models for each transition. The advantage of a single hydrodynamic model is that the flow pattern transitions, slug characteristics, liquid holdup and pressure gradient are implicitly related.

The 3-phase model contains separate momentum balances for the gas, oil and water phases. The model determines whether the oil and water phases are separated or fully mixed. If the phases are separated, individual phase viscosities are used. If the phases are fully mixed, the liquid viscosity can be determined either by the method within the TUFFP model (emul default option) or overridden (emul override option) by the liquid viscosity method defined with the PIPESIM fluid model, which is useful when rheology data are available. In the latter case, for black oil fluid models, selecting the Brinkman emulsion viscosity method with the Brauner-Ullman watercut cutoff method will replicate the method used within the TUFFP model. For the 2-phase (gas-liquid) model, the liquid viscosity from PIPESIM is always used, so the emulsion options defined in the PIPESIM fluid definition always apply.

The closure relationships included in the model are based on focused experimental research programs at University of Tulsa and elsewhere. As new and improved closure relationships become available, the TUFFP Unified Model is updated and validated.

Note: The TUFFP Unified 2-Phase Model v 2007.1 is no longer supported in PIPESIM. Upon import, TUFFPU2P is used instead.

Xiao

The Xiao comprehensive mechanistic model was developed as part of the TUFFP research program. It was developed for gas-liquid two-phase flow in

horizontal and near horizontal pipelines. The model first predicts the existing flow pattern, and then calculates flow characteristics, primarily liquid holdup and pressure drop, for the stratified, intermittent, annular, or dispersed bubble flow patterns. The model was tested against a pipeline data bank. The data bank included large diameter field data culled from the AGA multiphase pipeline data bank, and laboratory data published in literature. Data included both black oil and compositional fluid systems. A new correlation was proposed which predicts the internal friction factor under stratified flow. The former has the advantage of making the film friction sensitive to both the gas and liquid velocities making the model as a whole more interconnected and a better holdup predictor. The Xiao et al. model is valid for all fluid types and pipe inclinations between -15° C and +15° C relative to horizontal.

Xiao (film modified)

The Xiao mechanistic model was developed as part of the TUFFP research consortia at the University of [Tulsa](#). The standard implementation was modified in the stratified flow pattern to produce a second method called Xiao film modified. Unlike the Baker-Jardine implementation (which is based on the TUFFP version of the code, yet also contains a film modification), the Neotec version was coded independently and therefore the numerical methods and film modification approach are slightly different.

The modification consists of using the [Ouyang and Aziz](#) two-phase correlation for film wall friction instead of the more traditional single phase correlation. The former has the advantage of making the film friction sensitive to both the gas and liquid velocities making the model as a whole more interconnected and a better holdup predictor. The Xiao et al. model is valid for all fluid types and pipe inclinations between -15degC and +15degC relative to horizontal.

Vertical multiphase flow correlations

Setup » Flow Correlations

See also: [Flow regimes](#), [Suggested flow correlation](#)

The flow correlations available are affected by the Moody friction Factor calculation method option. By default, PIPESIM uses the [Sonnad](#) explicit Moody friction factor calculation method.

The following vertical multiphase flow correlations are available:

Ansari

The Ansari mechanistic model was developed as part of the Tulsa University Fluid Flow Projects (TUFFP) research program. A comprehensive model was formulated to predict flow patterns and the flow characteristics of the predicted flow patterns for upward two-phase flow. The comprehensive mechanistic model is composed of a model for flow pattern prediction and a set of independent models for predicting holdup and pressure drop in bubble, slug, and annular flows. The model was evaluated by using the TUFFP well databank that is composed of 1775 well cases, with 371 of them from Prudhoe Bay data.

Aziz, Govier, and Fogarasi

The Aziz, Govier, and Fogarasi model was developed especially for wellbore pressure drop calculations for upward flow in production wells. The flow regime (for example, annular-mist, slug, etc.) is determined using the correlation of Govier and Aziz (1972). The flow pattern is predicted first, and then a corresponding correlation is used to calculate liquid holdup and frictional pressure loss. The Duns and Ros method is used for holdup and pressure calculations in the annular mist flow regime as recommended in the published work.

The correlation of Aziz, Govier, and Forgasi is used for pressure loss, holdup, and flow regime. The Govier, Aziz, and Fogarasi correlation was developed following a study of pressure drop in wells producing gas and condensate. Actual field pressure drop versus flowrate data from 102 wells with gas-liquid ratios ranging from 3,900 to 1,170,000 scf/bbl were analyzed in detail. The phase conditions in the well bore were determined by standard flash calculations. Pressure-gradient data for flow under single-phase conditions were compared with conventional predictions, and found generally to confirm them. For the test in which two-phase conditions were predicted throughout the well bore, the field data were compared with several wholly empirical prediction methods, with a previously proposed method, and with a new prediction method partly based on the mechanics of flow. The new prediction method incorporates an empirical estimate of the distribution of the liquid phase between that flowing as a film on the wall and that entrained in the gas core. It employs separate momentum equations for the gas-liquid mixture in the core and for the total contents of the pipe.

Note: This method tends to overpredict the minimum stable flow rate (minimum rate to lift liquids) and thus can overpredict pressure losses, especially for gas-water wells. Consider the Gregory method instead.

Beggs and Brill original

ORIGINAL: The Original [Beggs and Brill](#) correlation is used for pressure loss and holdup. Flow regime is determined by either the Beggs and Brill or Taitel Dukler correlation. The Beggs and Brill correlation was developed following a study of two-phase flow in horizontal and inclined pipes. The correlation is based upon a flow regime map which is first determined as if the flow was horizontal. A horizontal holdup is then calculated by correlations, and this holdup is corrected for the angle of inclination. The test system included two 90 ft long acrylic pipes, winched to a variable elevation in the middle, so as to model incline flow both upwards and downwards at angles of up to 90°.

Beggs and Brill revised

REVISED: As above except that the revised version of the Beggs and Brill correlation is used, with rough pipe friction factors, holdup limiters and corrective constants as proposed by [Palmer](#) and [Payne](#). The following enhancements to the original method are used; (1) an extra flow regime of froth flow is considered which assumes a no-slip holdup, (2) the friction factor is changed from the standard smooth pipe model, to utilize a single phase friction factor based on the average fluid velocity.

Duns and Ros

The Duns and Ros correlation is used for pressure loss and holdup with flow regime determination by either the [Duns and Ros](#) or the [Taitel Dukler](#) correlations. The Duns and Ros correlation was developed for vertical flow of gas and liquid mixtures in wells. Equations were developed for each of three flow regions, (I) bubble, plug and part of froth flow regimes, (II) remainder of froth flow and slug flow regimes, (III) mist flow regime. These regions have low, intermediate and high gas throughputs respectively. Each flow region has a different holdup correlation. The equations were based on

extensive experimental work using oil and air mixtures.

Gomez

The Gomez mechanistic flow model was developed at The University of [Tulsa](#), and the code written by Neotec based on the published work.

The Gomez et al. model is valid for all fluid types and inclinations between 0 and 90 degrees. (Recommended for 30-90 degrees).

Note: The Gomez model generally causes very slow runtimes.

Gomez enhanced

The standard Gomez et al. implementation was modified by Neotec to produce the Gomez et al. enhanced method.

The modification consists of using the [Oliemans](#) liquid entrainment correlation for vertical annular mist flow instead of the standard Wallis correlation. Even though the Oliemans correlation was developed using low pressure, mainly water-air, small diameter data, it does a good job of smoothing the response surface around the slug to annular mist transition region where the Gomez et al. correlation shows unusual behavior. This improves the statistical performance of this method in simulations of gas-lift wells as shown by [Adames](#). The result is an improved method that works well for all types of wells.

Note: The Gomez model generally causes very slow runtimes.

Govier and Aziz

The correlation of [Aziz, Govier, and Forgasi](#) is used for pressure loss, holdup, and flow regime. The Govier, Aziz, and Fogarasi correlation was developed following a study of pressure drop in wells producing gas and condensate. Actual field pressure drop versus flowrate data from 102 wells with gas-liquid ratios ranging from 3,900 to 1,170,000 scf/bbl were analyzed in detail. The phase conditions in the well bore were determined by standard flash calculations. Pressure-gradient data for flow under single-phase conditions were compared with conventional predictions, and found generally to confirm them. For the test in which two-phase conditions were predicted throughout the well bore, the field data were compared with several wholly empirical prediction methods, with a previously proposed method, and with a new prediction method partly based on the mechanics of flow. The new prediction method incorporates an empirical estimate of the distribution of the liquid phase between that flowing as a film on the wall and that entrained in the gas core. It employs separate momentum equations for the gas-liquid mixture in the core and for the total contents of the pipe.

Gray

The Gray Vertical Flow correlation is used for pressure loss and holdup. This correlation was developed by H E Gray of Shell Oil Company for vertical flow in gas and condensate systems which are predominantly gas phase. Flow is treated as single phase, and dropped out water or condensate is assumed to adhere to the pipe wall. It is considered applicable for vertical flow cases where the velocity is below 50 ft/s, the tube size is below 3.5 in, the condensate ratio is below 50 bbl/mmscf, and the water ratio is below 5 bbl/mmscf.

Gray modified

As above, but with the following modifications: (1) Actual Reynolds number used (Gray Original assumed Reynolds number to always be 1 million), and (2) Pseudo-roughness is constrained to be less than the pipe radius.

Gregory

The Gregory et al model (1989) is a modification of the Aziz, Govier, and Fogarasi (1972) method (described in [Aziz, Govier, and Fogarasi](#)). The Gregory et al model uses the Govier and Aziz flow pattern map (1972) except for the transition from annular-mist flow to froth flow. The transition between annular-mist (stable flow) and froth flow (unstable flow) is computed using the technique proposed by Turner et al (1969). Turner et al postulated that the minimum gas velocity required to lift liquids would correspond to the terminal velocity of the largest stable liquid droplet that would form. The Gregory model uses the procedure recommended by Coleman which does not include the 20% increase in velocity added by Turner. If the gas velocity (superficial gas velocity divided by the gas volume fraction in the input stream) is larger than the velocity expressed in the equation below, the flow pattern will be annular-mist, otherwise froth flow will be assumed.

$$V = 1.2979 \left[\frac{\sigma(\rho_L - \rho_G)}{C_D \rho_G^2} \right]^{1/4}$$

where

σ gas-liquid surface tension (dynes/cm)

C_D droplet drag coefficient

ρ_L liquid density (lbm/ft³)

ρ_G gas density (lbm/ft³)

V velocity at the boundary between froth and annular-mist (ft/s)

C_L liquid input volume fraction

The rest of the calculations are the same as for the Aziz, Govier, and Fogarasi method (described in Aziz, Govier, and Fogarasi), with the exception that the parameter V_{Gfm} (required for froth flow calculations) is computed as shown in the following equation: $V_{Gfm} = V(1 - C_L)$

A default value of 0.44 (which corresponds to a spherical droplet shape) is provided for the droplet drag coefficient. Additionally, the Gray modified

method for pressure drop is used instead of the Duns and Ros method in the annular-mist regime.

Hagedorn and Brown

The correlation of [Hagedorn and Brown](#) is used for pressure loss and holdup. While the Hagedorn and Brown correlation does not predict flow pattern, the flow pattern as predicted by Orkiszewski is reported. The Duns and Ros flow pattern prediction can also be reported. Neither of these flow pattern prediction methods affects any of the calculations. The Hagedorn and Brown correlation was developed following an experimental study of pressure gradients occurring during continuous two-phase flow in small diameter vertical conduits. A 1,500 ft experimental well was used to study flow through 1 in., 1.25 in., and 1.5 in. nominal size tubing. Air was the gas phase and four different liquids were used: water and crude oils with viscosities of about 10, 30 and 110 cp. Liquid holdup was not directly measured, rather a pseudo liquid-holdup value was determined that matched measured pressure gradients.

Further work by Brill and Hagedorn have led to two modifications: (1) If the Griffith and Wallis criteria predicted the occurrence of bubble flow, the Griffith bubble-flow method should be used to predict pressure gradient, and (2) If the predicted liquid holdup is less than the no-slip liquid holdup, then the no-slip liquid holdup is used.

All of the correlations involve only dimensionless groups, which is a condition usually sought for in similarity analysis but not always achieved.

Mukherjee and Brill

The [Mukherjee and Brill](#) correlation is used for Pressure loss, Holdup and flow map. Note: selection of alternative flow maps and/or holdups will cause unpredictable results. The Mukherjee and Brill correlation was developed following a study of pressure drop behavior in two-phase inclined flow. For bubble and slug flow, a no-slip friction factor calculated from the Moody diagram was found adequate for friction head loss calculations. In downhill stratified flow, the friction pressure gradient is calculated based on a momentum balance equation for either phase assuming a smooth gas-liquid interface. For annular-mist flow, a friction factor correlation was presented that is a function of holdup ratio and no-slip Moody friction factor. Results agreed well with the experimental data and correlations were further verified with Prudhoe Bay and North Sea data.

NOSLIP correlation

The NOSLIP correlation assumes homogeneous flow with no slip between the phases. Fluid properties are taken as the average of the gas and liquid phases and friction factors are calculated using the single phase MOODY correlation. Note: selection of alternative flow maps and/or holdups will cause unpredictable results.

OLGAS 2-phase/OLGAS 3-phase

The OLGAS mechanistic models are applicable for all inclination angles, pipe diameters and fluid properties. The 2-phase [Bendiksen](#) model considers gas-liquid flow, whereas the 3-phase model considers gas-oil-water flow.

This model employs separate continuity equations for gas, liquid bulk and liquid droplets, which are coupled through interphase mass transfer. Two momentum equations are solved: one applied to the combined balance for the gas and liquid droplets, if present, and a separate momentum equation for the liquid film. OLGAS considers four flow regimes: stratified, annular, slug and dispersed bubble flow; and uses a unique minimum slip criteria to predict flow regime transitions.

The OLGA 2-Phase model uses the liquid viscosity model defined within the PIPESIM fluid property definition. The 3-Phase model uses the Pal and Rhodes emulsion correlation to calculate liquid viscosity based on the oil and water viscosities defined with the PIPESIM fluid model definition; liquid viscosity options defined with the PIPESIM fluid model are ignored.

OLGAS is based in large part on data from the SINTEF multiphase flow laboratory near Trondheim, Norway. The test facilities were designed to operate at conditions that approximated field conditions. The test loop is 800 m long and 8 inches in diameter. Operating pressures between 20 and 90 barg were studied. Gas superficial velocities of up to 13 m/s, and liquid superficial velocities of up to 4 m/s were obtained. In order to simulate the range of viscosities and surface tensions experienced in field applications, different hydrocarbon liquids were used (naphtha, diesel, and lube oil). Nitrogen was used as the gas. Pipeline inclination angles between 1° were studied in addition to flow up or down a hill section ahead of a 50m high vertical riser. Over 10,000 experiments were run on this test loop during an eight year period. The facility was run in both steady state and transient modes.

LEDA 2-phase/3-phase

The ([Leda Point Model \(PM\)](#)) is a mechanistic model applicable for all inclination angles, pipe diameters and fluid properties. The 2-phase model considers gas-liquid flow whereas the 3-phase model considers gas-oil-water flow.

The 3-phase Leda PM considers 9 fields in the mass (continuity) equations (oil, gas, water, oil in gas and water, gas in oil and water, water in oil and gas). Separate momentum equations are solved for oil, gas and water.

The 2-phase Leda PM considers 4 fields in the mass (continuity) equations (liquid, gas, liquid in gas and gas in liquid). Separate momentum equations are solved for gas and liquid phases. The flow regimes predicted by LedaPM are stratified smooth flow, stratified wavy flow, slug flow, annular and bubbly flow. The Leda 2-phase model uses the liquid viscosity associated with the fluid model defined in PIPESIM. The Leda 3-phase model assumes that the liquid viscosity is equal to that of the continuous phase; liquid viscosity options defined with the PIPESIM fluid model are ignored. The continuous phase is determined by the [Brauner-Ullman](#) inversion criteria.

The Leda Point Model is the steady-state version of the transient model developed by SINTEF in collaboration with Total and ConocoPhillips and commercialized by Kongsberg. The model has been calibrated against data collected at the SINTEF Multiphase Flow Laboratory near Trondheim Norway. Over 10,000 experimental data points have been collected for single-phase, two-phase (oil-water, water-gas) and three-phase (oil-water-gas) flow. Pipe diameters ranging from 4-12" were used at pressures up to 90 barg. The models have been validated with field data supplied by ConocoPhillips and Total.

Orkiszewski

The [Orkiszewski](#) correlation is used for pressure loss, holdup, and flow regime. The Orkiszewski correlation was developed for the prediction of two phase pressure drops in vertical pipe. Four flow regimes were considered, bubble, slug, annular-slug transition, and annular mist. The method can accurately predict, to within 10%, the two phase pressure drops in naturally flowing and gas lifted production wells over a wide range of well conditions. The precision of the method was verified when its predicted values were compared against 148 measured pressure drops. Unlike most other methods,

liquid holdup is derived from observed physical phenomena, and is adjusted for angle of deviation.

TUFFP unified mechanistic model (2-phase and 3-phase)

The TUFFP Unified Mechanistic Model is the collective result of many research projects performed by the Tulsa University Fluid Flow Projects (TUFFP) research consortium. The model determines flow pattern transitions, pressure gradient, liquid holdup and slug characteristics. A 2-phase version is available for gas-liquid flow [[Zhang et.al. development](#) and [validation](#)] and a 3-phase version is available for gas-oil-water pipe flow [[Zhang and Sarica](#)]. The model is valid for all inclination angles, pipe diameters and fluid properties.

The principle concept underlying the model is the premise that slug flow shares transition boundaries with all the other flow patterns. The flow pattern transition from slug flow to stratified and/or annular flow is predicted by solving the momentum equations for slug flow. The entire film zone is treated as the control volume and the momentum exchange between the slug body and the film zone is introduced into the combined momentum equation. This approach differs from traditional methods of using separate models for each transition. The advantage of a single hydrodynamic model is that the flow pattern transitions, slug characteristics, liquid holdup and pressure gradient are implicitly related.

The 3-phase model contains separate momentum balances for the gas, oil and water phases. The model determines whether the oil and water phases are separated or fully mixed. If the phases are separated, individual phase viscosities are used. If the phases are fully mixed, the liquid viscosity can be determined either by the method within the TUFFP model (emul default option) or overridden (emul override option) by the liquid viscosity method defined with the PIPESIM fluid model, which is useful when rheology data are available. In the latter case, for black oil fluid models, selecting the Brinkman emulsion viscosity method with the Brauner-Ullman watercut cutoff method will replicate the method used within the TUFFP model. For the 2-phase (gas-liquid) model, the liquid viscosity from PIPESIM is always used, so the emulsion options defined in the PIPESIM fluid definition always apply.

The closure relationships included in the model are based on focused experimental research programs at University of Tulsa and elsewhere. As new and improved closure relationships become available, the TUFFP Unified Model is updated and validated.

Note: The TUFFP Unified 2-Phase Model v 2007.1 (available in PIPESIM 2012 and previous) is no longer supported in PIPESIM. Upon import, TUFFP version 2011.1 is used instead.

Suggested correlations

Use the Flow correlations tab to set flow correlation options at the global level or at local levels. If you set flow correlation options at the local level, the source, correlation, friction factor, and holdup factor appear as individual columns for both vertical and horizontal components.

If no production data are available, Schlumberger have found the following to give satisfactory results based on previous studies using field data:

Single phase system

[Moody](#)

Vertical oil well

[OLGA-S](#), [Hagedorn and Brown](#), Gregory, TUFFP, Ansari, Leda

Highly deviated oil well

[OLGA-S](#), [Hagedorn and Brown](#), [Duns and Ros](#), TUFFP, Leda

Gas/condensate well

[OLGA-S](#), [Hagedorn and Brown](#), Gregory, TUFFP, Xiao, Leda

Oil pipelines

[OLGA-S](#), [Oliemans](#), TUFFP, Xiao, Leda

Gas/condensate pipelines

[OLGA-S](#), [Baker Jardine](#), TUFFP, Oliemans, Xiao, Leda

Correlation	Vertical and Predominantly Vertical Oil Wells	Highly Deviated Oil Wells	Vertical Gas/Condensate Wells	Oil Pipelines	Gas/Condensate Pipelines
Duns and Ros	yes	yes	yes	no	no
Orkiszewski	yes	no	yes	no	no
Hagedorn and Brown	yes	yes	yes	no	no
Beggs and Brill Revised	yes	yes	yes	yes	yes
Beggs and Brill Original	yes	yes	yes	yes	yes
Mukherjee and Brill	yes	yes	yes	yes	yes
Govier, Aziz and Forgasi	yes	yes	no	no	no
NoSlip	yes	yes	yes	yes	yes
OLGAS	yes	yes	yes	yes	yes
Ansari	yes	no	yes	no	no
BJA for Condensates	no	no	yes	no	yes
AGA and Flanigan	no	no	no	no	yes
Oliemans	no	no	no	yes	yes
Gray	no	no	yes	no	no
Gray Modified	no	no	yes	no	no
Xiao	no	no	no	yes	yes
LEDA	yes	yes	yes	yes	yes

TUFFP	yes	yes	yes	yes	yes
Gregory	yes	no	yes	no	no

Friction and holdup factors

These two factors can be used to adjust the friction and holdup prediction of a particular flow correlation. By default these factors are 1.

A linear relationship is used for the friction pressure drop. Setting the friction factor to 0.5, for example, will mean that the friction element of pressure drop computed by the correlation will be halved.

A non-linear relationship is used to calculate the liquid holdup H_L from the value predicted by the correlation H_{Lc} :

$$H_L = f_H \cdot H_{Lc} + (1 - f_H) \cdot H_{Lc}^2 \quad [\text{Eq. 1772.1}]$$

This ensures that the liquid holdup is sensible $0 \leq H_L \leq 1$ when $0 \leq f_H \leq 2$.

These factors are often used as calibration factors when a good match to field data cannot be obtained by any other method. Changing these factors will affect the results and should be undertaken with care.

Single phase flow correlations

See also: [SPHASE Single Phase Flow Options](#)

The steady-state pressure gradient in single phase sections is given by the equation:

$$\frac{dp}{dL} = \left(\frac{dp}{dL} \right)_{elev.} + \left(\frac{dp}{dL} \right)_{fric.} + \left(\frac{dp}{dL} \right)_{acc.} \quad [\text{Eq. 1772.1}]$$

where elevation, friction and acceleration components of the pressure drop are:

$$\left(\frac{dp}{dL} \right)_{elev.} = - \rho g \sin \theta \quad [\text{Eq. 1772.2}]$$

$$\left(\frac{dp}{dL} \right)_{fric.} = - \frac{f \rho v^2}{2D} \quad [\text{Eq. 1772.3}]$$

$$\left(\frac{dp}{dL} \right)_{acc.} = - \rho v \frac{dv}{dL} \quad [\text{Eq. 1772.4}]$$

where

f	is the friction factor	dimensionless
ρ	is the fluid density	lb/ ft ³
v	is the fluid velocity	ft/ s
g	is the gravitational acceleration	ft/ s ²
θ	is the angle of the pipe to the horizontal	degrees
D	is the pipe diameter	ft
L	is the length of the pipe	ft

There are a number of different ways of calculating the friction factor, which usually depends on the Reynolds number:

$$Re = \frac{\rho v D}{\mu} \quad [\text{Eq. 1772.5}]$$

where:

μ	is the fluid viscosity	lb/ ft · s
-------	------------------------	------------

Moody (default for liquid or gas)

See [Sonnad and Goudar paper](#) and [Moody paper](#) for more technical details.

For laminar flow (Re < 2000)	$f_{Lam} = \frac{64}{Re}$
------------------------------	---------------------------

For turbulent flow ($\text{Re} > 4000$)	$\frac{1}{f_{Turb}^{1/2}} = a \left[\ln \left(\frac{c}{q} + \delta \right) \right]$
For transition flow ($2000 \leq \text{Re} \leq 4000$)	$f = \frac{(\text{Re} - \text{Re}_{\min})(f_{Turb} - f_{Lam})}{(\text{Re}_{\max} - \text{Re}_{\min})} + f_{Lam}$

where:

f_{Turb}	is the Moody friction factor
Re	is the Reynolds Number
a	is $\frac{2}{\ln(10)}$
ϵ	is the pipe roughness
D	is the pipe diameter
b	is $\frac{\epsilon/D}{3.7}$
c	is $\left(\frac{\ln(10)}{5.02} \right) \text{Re}$
s	is $bc + \ln(c)$
q	is $s^{\lceil s/(s+1) \rceil}$
z	is $\ln \left(\frac{q}{g} \right)$
g	is $bc + \ln \left(\frac{c}{q} \right)$
δ	is $\left(\frac{g}{g+1} \right) z$

The friction factor is interpolated in the transition region ($2000 < \text{Re} < 4000$). The limits for the transition zone and the interpolation method can be reset by the user.

The various friction factor calculation methods available are:

Friction Factor Calculation method	Approximation used	Equation
EXPLICIT or SONNAD	Sonnad 2007 linear approximation (default)	$\frac{1}{f_{Turb}^{1/2}} = a \left[\ln \left(\frac{c}{q} + \delta \right) \right]$
APPROXIMATE or MOODY	Moody 1947 approximation	$f_{Turb} = 0.0055 \left[1 + \left(20000 \frac{\epsilon}{D} + \frac{10^6}{\text{Re}} \right)^{1/3} \right]$
IMPLICIT or ITERATIVE	Colebrook-White equation (Moody chart)	$\frac{1}{f_{Turb}^{1/2}} = 1.74 - 2 \log_{10} \left(\frac{2\epsilon}{D} + \frac{18.7}{\text{Re} f_{Turb}^{1/2}} \right)$

AGA (for gas)

The AGA friction factor is the same as the Moody friction factor at high and low Reynolds numbers, but differs in between:

For laminar flow ($\text{Re} < 1000$)	$f = \frac{64}{\text{Re}}$
For transition flow ($1000 < \text{Re} < 4 \frac{C_2}{C_1} \left(\frac{3.7D}{\epsilon} \right)^{1/C_1} \log_{10} \left(\frac{3.7D}{\epsilon} \right)$)	$\frac{1}{f^{1/2}} = 2C_1 \log_{10} \left(\frac{\text{Re}}{2} \frac{C_1}{C_2} f^{1/2} \right)$
For turbulent flow ($\text{Re} > 4 \frac{C_2}{C_1} \left(\frac{3.7D}{\epsilon} \right)^{1/C_1} \log_{10} \left(\frac{3.7D}{\epsilon} \right)$)	$\frac{1}{f^{1/2}} = 2 \log_{10} \left(\frac{3.7D}{\epsilon} \right) = 1.74 - 2 \log_{10} \left(\frac{2\epsilon}{D} \right)$

where:

$C_1 = 0.98$	is the drag factor
$C_2 = 10^{0.15}$	is a constant

Cullender and Smith (for gas)

The total pressure drop can be calculated from

$$\frac{dp}{dL} = \frac{P_{down} - P_{up}}{L}$$

where:

$$P_{up}^2 = \frac{P_{down}^2 - a^2}{b}$$

where:

$$a^2 = \frac{25 f q_{vG}^2 \bar{T}^2 Z_G^2 (b - 1)}{0.0375(12D)^5}$$

$$b = \exp\left(\frac{0.0375 \gamma_G L}{\bar{T} Z_G}\right)$$

f	is the Moody friction factor	dimensionless
L	is the pipe length	ft
P_{down}	is the downstream pressure	psi
P_{up}	is the upstream pressure	psi
q_{vG}	is the stock tank gas volume flow rate	scf / day
\bar{T}	is the average temperature	° R
Z_G	is the gas compressibility factor	dimensionless
γ_G	is the gas specific gravity	dimensionless

Other friction pressure drops for gas

The friction pressure drop can be calculated from

$$\left(\frac{dp}{dL}\right)_{fric.} = \frac{P_{down} - P_{up}}{L}$$

where:

$$P_{up}^2 - P_{down}^2 = \frac{\bar{T} Z_G L}{5280} \left(\frac{P_s}{T_s} \right)^2 \left(\frac{1}{a_1} \cdot \frac{q_{vG}}{\eta} \cdot \frac{\gamma_G^{a_4}}{(12D)^{a_5}} \right)^{1/a_3}$$

where:

L	is the pipe length	ft
P_{down}	is the downstream pressure	psi
P_{up}	is the upstream pressure	psi
P_s	is the stock tank pressure	psi
q_{vG}	is the stock tank gas volume flow rate	scf / day
\bar{T}	is the average temperature	° R
T_s	is the stock tank temperature	° R
Z_G	is the gas compressibility factor	dimensionless
γ_G	is the gas specific gravity	dimensionless
η	is a flow efficiency factor	dimensionless

and the constants are given by

	a_1	a_3	a_4	a_5
Panhandle A	435.87	0.5394	0.4604	2.618
Panhandle B	737.00	0.5100	0.4900	2.530
Weymouth	433.50	0.5000	0.5000	2.667

Hazen-Williams (for liquid water)

The friction pressure drop can be calculated from:

$$\left(\frac{dp}{dL} \right)_{fric.} = \frac{0.015 \rho_m}{144(12D)^{4.87}} \cdot \left(\frac{q_{vL}}{c} \right)^{1.85} \quad [Eq. 1772.6]$$

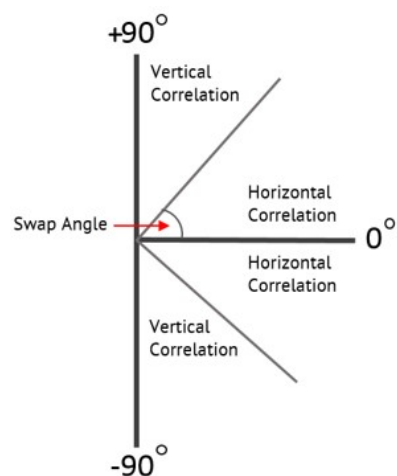
where:

c	is the pipe condition factor	
q_{vL}	is the liquid volume flow rate	bbl / day
ρ_m	is the mixture density	lb / ft ³

Swap angle

The multiphase flow correlations used to predict the pressure loss and holdup are split into two categories: vertical and horizontal. Each category lists the correlations that are appropriate for that type of flow.

By default the selected vertical correlation is used in the situation where the tubing/pipe is at an angle greater than 45 degrees from the 0 degree axis. For angles that are less than or equal to 45 degrees, the selected horizontal correlation is used. This angle can be changed.



Related links:

[Run data matching](#)

deWaard (1995) corrosion model

The [de Waard model](#) predicts the corrosion rate of carbon steel in the presence of water and CO₂. The model was developed primarily for use in predicting corrosion rates in pipelines where CO₂ is present in a vapor phase. The model has not been validated at high pressures where CO₂ is entirely in the liquid phase. Corrosion rate is calculated as a function of:

- Temperature
- Pressure
- Mol% CO₂
- Wt% Glycol (Multiflash and ScaleChem only)
- Liquid velocity
- Pipe Diameter
- pH

The model accounts for the flow-independent kinetics of the corrosion reaction as well as the flow-dependent mass transfer of dissolved CO₂ using a resistance model. Additionally, effects of protective scale at high temperatures are considered in addition to glycol inhibition.

Note: The equations that follow are based on the [de Waard 1995 model](#). This model is a revision to the [de Waard 1991 model](#). Some of the equations below appear only in the original paper].

General Equation

$$V_{cor} = \frac{CcFsFg}{\left[\frac{1}{V_r} + \frac{1}{V_m} \right]} \quad [Eq. 1772.1]$$

CO₂ Partial Pressure/Fugacity

$$p_{CO_2} = \frac{(mole \% CO_2 * P_{total})}{100} \quad [Eq. 1772.2]$$

$$\log(f_{CO_2}) = \log(pCO_2) + (.0031 - \frac{1.4}{t+273})P$$

Reaction Rate term (Vr)

$$\log(Vr) = 4.93 - \frac{1119}{T} + 0.58\log(fCO_2) - .34(pH_{act} - pH_{CO_2}) \quad [\text{Eq. 1772.3}]$$

pH

By default, the correlation assumes that the actual pH of the water is affected strictly by the presence of CO₂. However, the user may specify the actual pH of a water sample that accounts for the additional presence of electrolytes and dissolved FeCO₃ liberated from the pipe wall. Since pH is dependent on pressure and temperature, care must be taken when specifying this value. If a ScaleChem generated PVT file is used, the actual pH is taken from the ScaleChem fluid description.

$$pH_{CO_2} = 3.82 + .00384t - 0.5\log(fCO_2) \quad [\text{Eq. 1772.4}]$$

pH_{act} = assumed to equal *pH_{CO2}* unless user specified or ScaleChem PVT file is used

Mass Transfer rate term (Vm)

$$Vm = 2.45 \frac{U_L^{0.8}}{d^{0.2}} fCO_2 \quad [\text{Eq. 1772.5}]$$

Effect of Temperature (protective scale)

$$Ts = \frac{2400}{6.7 + 0.44\log(fCO_2)} \quad [\text{Eq. 1772.6}]$$

(if T > Ts)

$$\log(Fs) = 2400 \left[\frac{1}{T} - \frac{1}{Ts} \right] \quad [\text{Eq. 1772.7}]$$

Else,

$$Fs = 1 \quad [\text{Eq. 1772.8}]$$

Glycol Reduction Effect

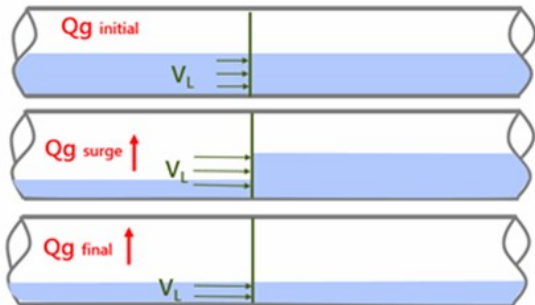
$$\log F_g = 1.6[\log(W\%) - 2] \quad [\text{Eq. 1772.9}]$$

Where W% is the weight percent of water in a water-glycol mixture (100% water results in a factor of 1.0). The Glycol component is only available when using Multiflash (MEG or DEG) or with ScaleChem (MEG).

Variable	Units	Description	Default	Acceptable Input Range	Variable Source
Vcor	(mm/yr)	corrosion rate			calc
T	°K	temperature			pipesim
t	°C	temperature			pipesim
pCO ²	atm	partial pressure of CO ₂			calc
fCO ²	atm	fugacity of CO ₂			calc
mol%CO ₂	—	mol % CO ₂ (comp, BO, ScaleChem PVT file)			pipesim
P _{total}	atm	pressure			pipesim
pH _{act}	—	actual pH of the system	pH _{CO2}	1.0–10.0	user spec
pH _{CO₂}	—	pH of dissolved CO ₂ in pure water			calc
U _L	m/s	liquid velocity			pipesim
d	m/s	pipe diameter			pipesim
W%	fraction	Weight percent water in a water-glycol mixture	100		pipesim
T _s	°K	Vcor inversion temperature			calc
F _s	—	scaling factor			calc
C _c	—	multiplier to correct for inhibitor efficiency or match to field data	1	0.1–10.0	user spec

Cunliffe's method for ramp up surge

When the flow rate into a pipeline increases, the overall liquid holdup typically decreases because the gas can more efficiently sweep out the liquid phase. When a rate increase (ramp-up) occurs, the liquid volume in the pipeline is accelerated resulting in a surge. A ramp-up operation is illustrated in the figure below.



PIPESIM predicts the liquid surge rate using Cunliffe's Method. Cunliffe's Method predicts the liquid surge rate due to an overall gas rate change for condensate pipelines. This method is particularly useful for estimating liquid handling capacity for ramp-up (increasing gas rate) cases. As the gas rate increases, the total liquid holdup in the line will drop owing to less slippage between the gas and liquid phases. The liquid residing in the line is therefore accelerated to the equilibrium velocity at the final gas rate and thus expelled at a rate higher than the final equilibrium liquid rate for the duration of the transition period. The transition period is assumed to be equal to the residence time at the final gas rate, that is, the time it takes the liquid to travel from one end of the line to the other.

The average liquid rate during the transition period can be determined as follows:

$$q_{LT} = q_{Lf} + \frac{(H_{Li} - H_{Lf})}{t_r}$$

$$q_{Lt} = q_{Gi} (LGR_{out})$$

$$t_r = \frac{H_{Lf}}{q_{Lf}}$$

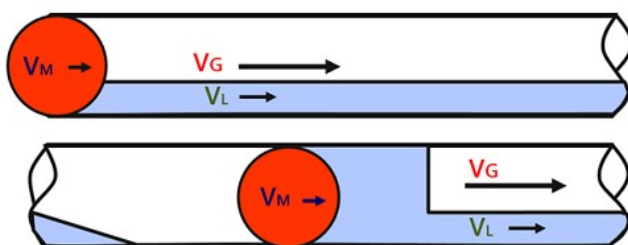
where:

q_{LT}	liquid rate during the transition period
q_{Lf}	final gas rate
H_{Li}	total liquid holdup volume in line - initial gas rate
H_{Lf}	total liquid holdup volume in line - final gas rate
LGR_{out}	liquid/gas ratio at outlet pressure (assumed constant)
t_r	liquid residence time (at final flowrate)

Note: The total liquid holdup volume in the line is provided in the summary output report. [Cunliffe](#) tested this method with field measurements for a 67 mi. 20 in. pipeline with an average operating pressure of 1300 psig and an LGR of 65 bbl/MMscf. He found that the change in condensate flow rate can be predicted to within 15% using this method.

Liquid by sphere (Sphere Generated Liquid Volume, SGLV)

During a pigging operation, a solid object of diameter slightly less than that of the pipeline is sent through the line to push out liquids and debris. As a pipeline is pigged (refer to the figure below), a volume of liquid builds up ahead of the pig and is expelled into the slug catcher as the pig approaches the exit.



PIPESIM considers that the pig travels at the mean fluid velocity. It uses the liquid holdup in the pipeline to calculate the volume of liquid that will be swept along in front of the pig as it moves. This calculation is reported as the sphere generated liquid volume (SGLV). Two approaches are available in PIPESIM for calculating SGLV:

1. SGLV Modified: This method was introduced in PIPESIM 2015 and is the new PIPESIM default. The SGLV Modified method is consistent with the method used in PIPEFLO and is the method recommended by Shell.
2. SGLV Original: This is the only method available in PIPESIM versions older than PIPESIM 2015.1 and PIPESIM 2012.3.

Calculations using the SGLV Modified method will result in SGLV values slightly less than those predicted using the SGLV Original method. The two

approaches PIPESIM uses for evaluating SGLV are steady-state approximations of pigging, which is a transient operation.

SGLV Modified (Default)

This method compares the steady-state liquid production when a pig is transiting a pipeline, with the liquid holdup volume or liquid inventory in the pipeline. If the steady state liquid production is less than the liquid holdup, liquid will accumulate in front of the pig. This difference between the liquid holdup in the pipe and the steady state liquid production while the pig is transiting the pipe, is the surge volume associated with the pig or the sphere generated liquid volume. It is evaluated with the equation below.

$$SGLV = H_L - T_{pig} Q_L$$

where:

$SGLV$ = Sphere generated liquid volume

H_L = Cumulative liquid holdup

T_{pig} = Cumulative pig/sphere transit time (Pig transit time = Pipe length/Fluid mean velocity)

Q_L = In-situ liquid flowrate

The modified SGLV method is the default in PIPESIM 2015.1 and 2012.3 and newer versions. However, the original SGLV method can be accessed using the [SGLV ORIGINAL](#) keyword. The sphere transit time and sphere dumping time can now also be requested as output variables.

SGLV Original

The liquid holdup throughout the pipe is divided into two notional fractions, the 'moving' and the 'static'. Since the liquid normally flows slower than the gas, the division will normally result in a positive value for both of these volumes. (If the pipe goes downhill the liquid often flows faster, so the 'static' will be negative in these sections, but this does not affect the equation.) If the fluid's phase split is assumed to be constant throughout the pipe, the size of the slug that issues when spheroid can be calculated using the following formula:

$$SGLV = \left(\frac{SLV}{TPV - MLV} \right) \times MLV + SLV \quad [\text{Eq. 1772.1}]$$

where:

$SGLV$ is Sphere Generated Liquid Volume

SLV is Static Liquid Volume in pipe

MLV is Moving Liquid Volume in pipe

TPV is Total Pipeline Volume

Note: $SLV + MLV$ = Total pipeline holdup, which PIPESIM calculates and writes to the summary output.

The slug of liquid starts to be produced from the pipe outlet when the pipe is full of liquid from its exit, back along to the position of the sphere. The liquid in the slug comprises 2 notional fractions: firstly, the entire SLV in the pipe, and secondly, the portion of the MLV that lies between the sphere and the outlet. Now, the maximum volume available for the SLV to occupy in the pipe is $TPV - MLV$. Dividing the actual SLV by this maximum value gives us the position of the sphere in the pipe as a value between 0 and 1, where 0 is the outlet. Multiplying the total MLV by the sphere position gives us the portion of the total MLV that is entrained in the slug, so adding this to the SLV gives the total slug volume or the total sphere generated liquid volume (SGLV).

The liquid holdup is calculated from the integration of the predicted holdup from the selected Multiphase Flow Correlation (MFC) along the entire pipeline length. The pipeline is simulated in segments, each of which has a length and cross sectional area, which multiplied together yields the segment volume. The MFC calculates a value for holdup in the range 0 to 1 for each segment, which when multiplied by the segment volume gives the holdup for each segment. The holdups for all the pipe segments are added together to determine the total holdup for the pipeline as reported in the summary file.

When a sphere is introduced into the pipeline, PIPESIM assumes it travels at the mean fluid velocity; as a result of this, a liquid slug will gather in front of the sphere made up of "all the liquid that is flowing slower than the mean fluid velocity in the pipeline at any given point". Thus the crucial value that determines Sphere Generated Liquid Volume (SGLV) is the Slip Ratio (SR) between the fluid phases, which is the average velocity of the fluid divided by the velocity of the liquid. If the liquid and gas move at the same speed, the slip ratio will be 1, that is there is 'no slip' between the phases. In this scenario, no liquid will accumulate in front of the sphere, so the SGLV will be zero. Normally the liquid flows slower than the gas, i.e. the slip ratio is greater than 1, so "some" of the liquid in the pipeline accumulates in front of the sphere to form the SGLV. The only way that "all" of the liquid in the pipeline accumulates to form the SGLV, is if the liquid velocity is zero, i.e. the slip ratio is infinite. This cannot happen in a steady-state reality, so the SGLV is always smaller than the total liquid holdup.

One complicating factor is that there will be a significant time lag between the time the slug of liquid swept up by the sphere begins to emerge from the pipe outlet and the time the sphere itself emerges. The slug will thus be composed of the liquid that accumulated in front of the sphere as it traveled along the pipeline, plus the normal liquid production of the system. This total volume is the value required to size the slug catcher, which is why we report it as "Volume by sphere".

To determine the sizes of terrain slugs or slugs from start-up, it is necessary to use a dynamic multiphase flow simulator such as OLGA.

Related links:

[SLUG Slug Calculation Options \(Optional\)](#)

Liquid loading

Critical unloading velocity

The critical unloading velocity is defined as the minimum gas velocity required to lift liquid droplets out of a gas well. Lower flowing gas velocities will result in liquid loading in the well. The critical unloading velocity is predicted by Turner's Equation.

$$V_t = \frac{N[\sigma(\rho_L - \rho_G)]^{0.25}}{(C_D^{25} \rho_G^{0.5})} \quad [\text{Eq. 1772.1}]$$

where

ρ_g	is the gas phase density	lb / ft ³
ρ_L	is the liquid phase density	lb / ft ³
σ	is the interfacial tension	dynes / cm
V_t	is the terminal velocity of liquid droplet	ft / s
θ	is pipe angle from vertical	°
C_D	is the drag coefficient	dimensionless
N	is a constant	dimensionless

The values of N and C_D are given in the following table for Turner's model and various others:

Model	N	C_D
Turner (1969)	1.56	0.44
Coleman (1991)	1.3	0.44
Nossier II (2000)	1.482	0.2
Li (2002)	0.724	1.0

Combining N and C_D , and discounting Turner's "built-in" 20% "correction factor" gives a constant of 1.593. The correction factor is split out into the E term below.

Turner's equation (general)

Turner's Equation (General Form):

$$V_t = \frac{1.593E[\sigma(\rho_L - \rho_G)]^{0.25}}{\rho_G^{0.5}} \quad [\text{Eq. 1772.2}]$$

Where E is the correction (efficiency) factor. The values of E for Turner's model and various others are given in the following table:

Model	E
Turner (1969)	1.2
Coleman (1991)	1.0
Nossier II (2000)	1.391
Li (2002)	0.454

Critical gas rate

The critical gas rate is the minimum gas rate required to prevent liquid loading.

Inflow performance relationships for vertical completions

Inflow performance relationships (IPRs) have been developed to model the flow of fluids from the reservoir, through the formation, and into the well. They are expressed in terms of the well static (or reservoir) pressure P_{ws} , the well flowing (or bottom hole) pressure P_{wf} , and flowrate Q . Typically, volume flow rates are proportional to the pressure drawdown:

$$Q_V \propto (P_{ws} - P_{wf}) \quad [\text{Eq. 440.1}]$$

For liquid IPRs the stock tank liquid rate is roughly proportional to the volume flow rate at well conditions, and this form of the equation is used:

$$Q_L \propto (P_{ws} - P_{wf}) \quad [\text{Eq. 440.2}]$$

For gas IPRs the stock tank flow rates are roughly proportional to the volume flow rate at reservoir conditions times the average reservoir pressure:

$$Q_G \propto Q_v \cdot \frac{(P_{ws} + P_{wf})}{2} \propto (P_{ws}^2 - P_{wf}^2) \quad [\text{Eq. 440.3}]$$

See also [Vertical Completion Options](#), [Multilayer Completions](#)

PIPESIM offers a comprehensive list of IPR options, for both oil and gas reservoirs, as follows:

IPR	Oil reservoirs	Gas and Gas Condensate Reservoirs	Multi-rate test
Backpressure Equation		Yes	Yes
Fetkovich	Yes		Yes
Hydraulically fractured	Yes	Yes	
IPR Table	Yes		
Jones / Forchheimer	Yes	Yes	Yes
Pseudo Steady State Equation / Darcy	Yes	Yes	
Transient	Yes	Yes	
Vogel	Yes		
Well PI (Productivity Index)	Yes	Yes	Yes

The [Well PI](#), [Pseudo Steady State](#) and [Transient](#) liquid IPRs can be combined with a [Vogel](#) IPR to model flow at pressures below the bubble point; see [bubble point correction](#).

Related links:

[Vertical completions overview](#)

Productivity index (PI)

PI is one of a number of methods that can be used to specify the [Inflow performance relationship](#) (IPR) for a completion. It can be regarded as a simplified version of the [Pseudo-steady state](#) or [Transient](#) IPRs.

Liquid PI

The (straight line) productivity index relationship for liquid reservoirs is perhaps the simplest and most widely used IPR equation. It states that rate is directly proportional to pressure drawdown between the bottom hole and the reservoir.

$$\boxed{\text{Equ}} \quad \text{Equ}$$

[Eq. 1773.1]

where:

$\boxed{\text{Equ}}$	is the stock-tank oil rate
$\boxed{\text{Equ}}$	is the well static (or reservoir) pressure
$\boxed{\text{Equ}}$	is the well flowing (or bottom hole) pressure
$\boxed{\text{Equ}}$	is the liquid productivity index.

Below bubble point correction

The liquid PI equation can be combined with a [Vogel equation](#) to model inflows when the bottom hole pressure is below the bubble point, see, [Bubble point correction](#).

Gas PI

For gas reservoirs a non-linear relationship is used:

$$\boxed{\text{Equ}} \quad \text{Equ}$$

[Eq. 1773.2]

where:

$\boxed{\text{Equ}}$	is the stock-tank gas rate
$\boxed{\text{Equ}}$	is the well static (or reservoir) pressure
$\boxed{\text{Equ}}$	is the well flowing (or bottom hole) pressure

 Equ | is the gas productivity index

Vogel's equation

[Vogel's \(1968\)](#) equation is one of a number of methods that can be used to specify the [Inflow Performance Relationship](#) (IPR) for a completion. It was developed to model saturated oil wells. Vogel's equation is a best-fit approximation of numerous simulated well performance calculations. Vogel's work considers only the effect of rock and fluid properties on saturated systems. The Vogel relation does not account for high-velocity-flow effects that may exist in high-rate wells, see the [Fetkovich equation](#).

Vogel's equation is:

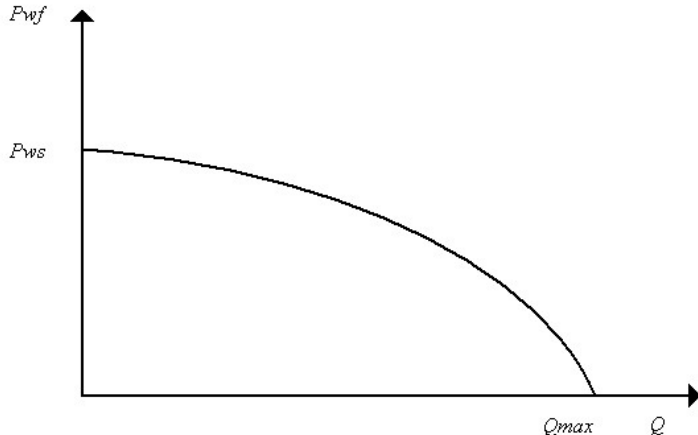
$$Q = Q_{\max} \left(1 - \left(1 - C \right) \left(\frac{P_{wf}}{P_{ws}} \right) - C \left(\frac{P_{wf}}{P_{ws}} \right)^2 \right) \quad [\text{Eq. 464.1}]$$

Where

Q	is the liquid flow rate (STB/D or m ³ /d)
Q_{\max}	is the absolute open hole flow potential, that is the liquid flow rate when the bottom hole pressure is zero
P_{wf}	is the well flowing (or bottom hole) pressure (psia or bara)
P_{ws}	is the well static (or reservoir) pressure (psia or bara)
C	is the Vogel coefficient.

The Vogel equation has the following properties:

$Q = Q_{\max}$	at $P_{wf} = 0$
$Q = 0$	at $P_{wf} = P_{ws}$
Productivity index $\frac{\partial Q}{\partial P_{wf}} = - \frac{Q_{\max} \cdot (1 + C)}{P_{ws}}$	at $P_{wf} = P_{ws}$



Related links:

[Vogel's reservoir properties](#)

Fetkovich's equation

Fetkovich's equation is one of a number of methods that can be used to specify the [Inflow Performance Relationship](#) (IPR) for a completion. The Fetkovich equation is a development of the [Vogel equation](#) to take account of high velocity effects.

$$Q = Q_{\max} \left(1 - \left(\frac{P_{wf}}{P_{ws}} \right)^2 \right)^n \quad [\text{Eq. 468.1}]$$

Where

Q	is the liquid flow rate (STB/D or m ³ /d)
Q_{\max}	is the absolute open hole flow potential, that is the liquid flow rate when the bottom hole pressure is zero
P_{wf}	is the well flowing (or bottom hole) pressure (psia or bara)
P_{ws}	is the well static (or reservoir) pressure (psia or bara)
n	is the Fetkovich exponent.

Related links:

[Fetkovich's reservoir properties](#)

Jones' equation

[Jones' equation](#) is one of a number of methods that can be used to specify the [Inflow performance relationship](#) (IPR) for a completion. It is similar to the [PI](#) method but contains an extra term to model turbulence.

Jones equation for gas inflow

The Jones equation for gas reservoirs is :

$$P_{ws}^2 - P_{wf}^2 = A Q_G^2 + B Q_G \quad [\text{Eq. 1773.1}]$$

where

Q_G	is the stock-tank gas rate
P_{ws}	is the well static (or reservoir) pressure
P_{wf}	is the well flowing (or bottom hole) pressure
$A \geq 0$	is the turbulence coefficient
$B \geq 0$	is the laminar coefficient

In the case when $A = 0$ the Jones equation is the same as the [gas PI](#) equation with productivity index $J_G = 1/B$. Values of $B > 0.05$ (psi²/MMscf/d) indicate low permeability or the presence of skin damage .

Jones equation for liquid inflow

Jones proposed the equation for gas flow, but it can also be used to model oil wells. However the [Fetkovich equation](#) can also be used for saturated oil wells and is the recommended method for IPRs in reservoirs producing below the bubble point.

The Jones equation for liquid reservoirs is :

$$P_{ws} - P_{wf} = A Q_L^2 + B Q_L \quad [\text{Eq. 1773.2}]$$

where

Q_L	is the stock-tank oil rate
-------	----------------------------

In the case when $A = 0$ the Jones equation is the same as the [Liquid PI](#) equation with productivity index $J_L = 1/B$

Forchheimer equation

[Forchheimer, 1901](#) gave an equation for non-Darcy flow in the reservoir, which is essentially the same as the [Jones equation](#) for liquid inflow.

Related links:

[Forchheimer's equation](#)

Back pressure equation

The Back Pressure Equation is one of a number of methods that can be used to specify the [Inflow performance relationship](#) (IPR) for a completion.

The Back Pressure Equation was developed by [Rawlins and Schellhardt \(1935\)](#) after testing 582 wells. The equation is typically applied to gas wells although its application to oil wells has also been proven. If correlations already exist for oil wells, use the Back Pressure Equation on gas wells only. The equation has the following form:

$$Q_G = C \cdot \left(P_{ws}^2 - P_{wf}^2 \right)^n \quad [\text{Eq. 474.1}]$$

where

Q_G	is the gas flow rate	(MMscf/d)	(m ³ /d),
P_{ws}	is the well static (or reservoir) pressure	(psia)	(bara)
P_{wf}	is the well flowing (or bottom hole) pressure	(psia)	(bara)
C	is the back pressure constant	(MMscf/d/(psia ²) ⁿ)	(m ³ /d/(bar ²) ⁿ)
n	is the dimensionless back pressure exponent		

The back pressure exponent, n , which ranges between 0.5 and 1.0, accounts for high velocity flow (turbulence). When $n = 1$ the back pressure equation is the same as the [gas P1](#) equation.

The back pressure constant, C , represents reservoir rock and fluid properties, flow geometry and transient effects.

The parameters C and n must be obtained by [multi-rate testing](#) of the well. Since

$$\log Q_G = \log C + n \cdot \log (P_{ws}^2 - P_{wf}^2) \quad [\text{Eq. 474.2}]$$

A plot of flow rate Q_G versus $P_{ws}^2 - P_{wf}^2$ on a log-log scale will give a line with slope n and intercept C . To avoid unit conversion problems when obtaining the parameters, check that the slope has a value between 0.5 and 1.0. If n is less than 0.5, this implies that the reservoir stabilization conditions are slow, or that liquid has accumulated in the wellbore (in gas condensate wells). The value of n can be greater than 1.0 if liquid is removed from the well during testing, or by removing drilling or stimulation fluids. Also, changes in well capacity during isochronal testing will cause a wider scatter of data points. This might be the result of liquid accumulation or cleaning of the wells.

Related links:

[Backpressure's reservoir properties](#)

Pseudo Steady State Equation / Darcy Equation

The pseudo steady state [IPR](#) equation (PSS), is derived from the equation for single phase Darcy flow into a well. A number of versions of the equation can be used (some require [keywords](#)):

- for liquid flow the PSS equation is written in terms of the [stock tank liquid](#) flow rate
 - this can be optionally combined with a Vogel formula for pressures [below the bubble point](#).
 - the liquid flow can be modelled using a two phase version of the radial flow equations for [oil and water](#)
- for gas flow the PSS is written in terms of the [stock tank gas](#) flow rate
 - a version using the [gas pseudo pressure](#) (more accurate for high pressure systems).
 - the PSS expressed in terms of [reservoir flow](#) rates can be used for either liquid or gas flow.
 - the liquid flow can be modelled using a two phase version of the reservoir flow equations for [oil and water](#)

Reservoir flow

The pseudo steady state equation, like the [transient IPR](#), is calculated by solving the radial, single phase, Darcy flow into a well. It applies for relatively long times, after the well has passed through the transient stage. The solution is given by [Dake 1978](#):

$$Q_{R\Phi} = M_\Phi \cdot T \cdot (P_{ws} - P_{wf}) \quad [\text{Eq. 1773.1}]$$

where the PSS transmissibility term is defined by:

$$T = \frac{2\pi kh}{C_l \left[\ln \left(\frac{r_e}{r_w} \right) - 0.75 + S \right]} \quad [\text{Eq. 1773.2}]$$

Where:

$Q_{R\Phi}$	is the volume flow rate at reservoir conditions of phase Φ	RB/d or MCF/d
M_Φ	is the mobility of phase Φ	$1/cp$
P_{ws}	is the average reservoir pressure	$psia$
P_{wf}	is the bottom hole pressure	$psia$
k	is the formation permeability	mD
h	is the formation thickness	ft
r_w	is the wellbore radius	ft
r_e	is the drainage radius	ft
S	is the skin	

C_1	is a conversion factor depending on the flow units	
$C_1 = \frac{14.7 \cdot 0.3048^2 \cdot 5.61458 \cdot 10^{-3}}{86400 \cdot 10^{-10}} = 2\pi \cdot 141.2$	If the flow is in RB/d	
$C_1 = \frac{14.7 \cdot 0.3048^2}{86400 \cdot 10^{-10}}$	If the flow is in MCF/d	

Note:

- The constant 0.75 comes from using the average reservoir pressure $P_{ws} = \bar{p}$. A similar formula can be derived using the pressure at the drainage radius $P_{ws} = p(r_c)$, but the value 0.75 is replaced by 0.5.
- The effective drainage radius may be explicitly specified or calculated based on the shape factor and the reservoir area.

The phase mobility is defined in terms of the phase relative permeability and viscosity:

$$M_\Phi = \frac{k_{r\Phi}}{\mu_\Phi}$$

$k_{r\Phi}$ = Relative permeability for phase Φ

μ_Φ = Viscosity for phase Φ at (for Production). For injection, this is the viscosity of the fluid at the average of the bottomhole flowing pressure and static reservoir pressure; and the bottomhole flowing temperature.

For single phase flow the relative permeability is $k_{r\Phi} = 1$, and the inflow equation simplifies to :

$$Q_{R\Phi} = \frac{1}{\mu_\Phi} \cdot T \cdot (P_{ws} - P_{wf}) \quad [\text{Eq. 1773.3}]$$

This version of the PSS IPR can be used for liquid or gas inflow.

For multiphase inflow, the total inflow can be written as the sum of the phase inflows:

$$Q_R = Q_{RO} + Q_{RW} + Q_{RG} \quad [\text{Eq. 1773.4}]$$

This can be rearranged to give:

$$Q_R = M \cdot T \cdot (P_{ws} - P_{wf}) \quad [\text{Eq. 1773.5}]$$

Where the total mobility is defined by

$$M = M_O + M_W + M_G \quad [\text{Eq. 1773.6}]$$

Oil and water flow

A two phase version of the multiphase inflow equation can be used to model liquid inflow.

$$Q_{RL} = \left(\frac{k_{rO}}{\mu_O} + \frac{k_{rW}}{\mu_W} \right) \cdot T \cdot (P_{ws} - P_{wf}) \quad [\text{Eq. 1773.7}]$$

The relative permeabilities can be determined from [permeability tables](#).

Injection

The reservoir injection flow equation is similar to the PSS production IPR:

$$Q_R = M_I \cdot T \cdot (P_{wf} - P_{ws}) \quad [\text{Eq. 1773.8}]$$

Here however, the mobility term represents the mobility of the fluid in the reservoir, rather than that of the injection fluid, and the properties of the fluid in the target reservoir must be specified in the fluid model assigned/mapped to the completion being injected into, if different from the injection fluid. In production, the fluid being produced is the same as that moving through the reservoir. In injection systems, the two fluids may be different and in this case, two fluids must be defined; the injection fluid mapped to the injection source, and the reservoir fluid mapped to the completion. In this scenario, we would expect different flow rates if gas is injected into a liquid filled reservoir versus a gas filled reservoir. If the injection fluid does differ from the reservoir fluid, then the injection mobility will change with time, as the reservoir fluid changes.

Note: For an injection well, the fluid properties used in the IPR equation (gas compressibility factor, viscosity, formation volume factor, etc.) are evaluated at the flowing bottomhole temperature (i.e. upstream of the flow into the completion) and the average of the static reservoir pressure and flowing bottomhole pressure.

Stock tank liquid flow

The pseudo steady state equation can be expressed in stock tank flow rates. For liquid flow, the stock tank flow rate $Q_L = Q_R / B_L$ is given by

$$Q_L = \frac{2\pi kh(p_{ws} - p_{wf})}{C_1 \mu_L B_L \left[\ln\left(\frac{r_e}{r_w}\right) - 0.75 + S \right]} \quad [\text{Eq. 1773.9}]$$

Q_L	is the liquid flowrate	STB/d
B_L	is the liquid volume formation factor	RB/STB
μ_L	is the liquid viscosity at reservoir conditions	cp

Below bubble point correction

The pseudo steady state equation can be combined with a [Vogel equation](#) to model inflows when the bottom hole pressure is below the bubble point, see, [Bubble point correction](#).

Oil and water flow

The [two phase version](#) of the reservoir liquid flow equation can also be written in terms of stock tank liquid flow rate:

$$Q_L = Q_R / B_L = Q_{RO} / B_L + Q_{RW} / B_L \quad [\text{Eq. 1773.10}]$$

Stock tank gas flow

This pseudo steady state equation can be expressed in stock tank flow rates. For gas flow, the formation volume factor can be expressed in terms of pressure and temperature $B_G = \frac{V}{V_s} = \frac{ZRT}{Z_s RT_s}$. The reservoir pressure is taken to be the average pressure in the reservoir: $P = \frac{P_{ws} + P_{wf}}{2}$, which gives a stock tank flow rate $Q_G = Q_R / B_G$:

$$Q_G = \frac{2\pi kh(p_{ws}^2 - p_{wf}^2)}{C_2 \mu_G TZ \left[\ln\left(\frac{r_e}{r_w}\right) - 0.75 + S + DQ_G \right]} \quad [\text{Eq. 1773.11}]$$

- The quadratic term in pressure arises from a combination of the pressure difference and the reservoir average pressure term

$$(p_{ws}^2 - p_{wf}^2) = (p_{ws} - p_{wf}) \cdot (p_{ws} + p_{wf}).$$

- The constant term arises from a combination of the conversion factor and stock tank properties

$$C_2 = \frac{2C_1 Z_s P_s}{T_s}.$$

- The skin has been modified to include a flow rate dependent term.

Q_G	is the gas flowrate	$MSCF/d$
B_G	is the gas volume formation factor	CF/SCF
μ_G	is the gas viscosity at reservoir conditions	cp
S	is the constant skin	
DQ	is the near wellbore turbulence factor or rate dependent skin	
T	is the reservoir temperature	$^{\circ}R$
Z	is the reservoir compressibility factor	
P_s	is the stock tank pressure	14.7 psi
T_s	is the stock tank temperature	$519.67 \text{ }^{\circ}R$

Z_s	is the stock tank compressibility factor	1
$C_2 = \frac{2 \cdot 14.7^2 \cdot 0.3048^2}{86400 \cdot 10^{-10} \cdot 519.67} = 2\pi \cdot 1422$	is a constant, arising from conversion factors and stock tank properties	

Gas pseudo pressure

Dake 1978 gives another version of the Pseudo steady state IPR for gas inflow, that is more accurate for large drawdowns, based on work by Al-Hussainy et al:

$$Q_G = \frac{2\pi kh[m(p_{ws}) - m(p_{wf})]}{C_2 T \left[\ln\left(\frac{r_e}{r_w}\right) - 0.75 + S + DQ_G \right]} \quad [\text{Eq. 1773.12}]$$

Here the gas pseudo pressure is given by:

$$m(p) = 2 \int \frac{p}{\mu_G Z} d p \quad [\text{Eq. 1773.13}]$$

Shape Factors for Pseudo Steady State Inflow

Geometry	CA	SA	Geometry	CA	SA
	31.62	0.000		10.84	0.535
	30.88	0.012		4.514	0.973
	31.60	0.000		2.077	1.362
	27.6	0.068		2.690	1.232
	27.1	0.077		0.232	2.458
	21.9	0.184		0.115	2.806
	21.84	0.185		3.335	1.125
	5.379	0.886		3.157	1.152
	2.361	1.298		0.581	1.998
	12.98	0.445		0.111	2.827
	4.513	0.973		0.098	2.888

Figure 1773.1. Shape Factors

See [Earlougher \(1977\)](#) for reference.

Transient IPR

The transient IPR equation, is derived from the equation for single phase Darcy flow into a well. A number of versions of the equation can be used (some require [keywords](#)):

- for liquid flow the transient IPR is written in terms of the [stock tank liquid](#) flow rate
 - this can be optionally combined with a Vogel formula for pressures [below the bubble point](#).
 - the liquid flow can be modelled using a two phase version of the radial flow equations for [oil and water](#)
- for gas flow the transient IPR is written in terms of the [stock tank gas](#) flow rate
 - a version using the [gas pseudo pressure](#) (more accurate for high pressure systems).
- the transient IPR expressed in terms of [reservoir flow](#) rates can be used for either liquid or gas flow.
 - the liquid flow can be modelled using a two phase version of the reservoir flow equations for [oil and water](#)

Reservoir flow

The transient IPR, like the [pseudo steady state IPR](#), is calculated by solving the radial, single phase, Darcy flow into the well. It applies for relatively small times, before the well has reached the pseudo steady state. A similarity solution is given by [Dake 1978](#):

$$Q_{R\Phi} = M_\Phi \cdot T \cdot (P_{ws} - P_{wf}) \quad [\text{Eq. 1773.1}]$$

where the transient IPR transmissibility is defined by:

$$T = \frac{2\pi kh}{C_1 \left[\frac{1}{2} \ln \left(\frac{4kt}{C_0 \gamma \theta \mu C r_w^2} \right) + S \right]} \quad [\text{Eq. 1773.2}]$$

$Q_{R\Phi}$	is the volume flow rate at reservoir conditions of phase Φ	RB/d or MCF/d
M_Φ	is the mobility of phase Φ	$1/cp$
P_{ws}	is the average reservoir pressure	$psia$
P_{wf}	is the bottom hole pressure	$psia$
t	time	$hours$
k	is the formation permeability	mD
h	is the formation thickness	ft
r_w	is the wellbore radius	ft
S	is the skin	
θ	is the reservoir porosity	
C	is the total compressibility of the reservoir and the reservoir fluids	$1/psi$
γ	is a constant equal to the exponential of Euler's constant	$\gamma = e^{0.5772} = 1.781$
C_0	is a conversion factor	$C_0 = \frac{14.7 \cdot 0.3048^2 \cdot 10^{-3}}{10^{-10} \cdot 3600}$
C_1	is a conversion factor depending on the flow units	
$C_1 = \frac{14.7 \cdot 0.3048^2 \cdot 5.61458 \cdot 10^{-3}}{86400 \cdot 10^{-10}} = 2\pi \cdot 141.2$	If the flow is in RB/d	
$C_1 = \frac{14.7 \cdot 0.3048^2}{86400 \cdot 10^{-10}}$	If the flow is in MCF/d	

The transient IPR equation can be written in similar terms to the [pseudo steady state IPR](#) by defining a radius

$$r^2 = \frac{4kt}{C_0 \gamma \theta \mu C} \quad [\text{Eq. 1773.3}]$$

$$T = \frac{2\pi kh}{C_1 \left[\ln \left(\frac{r}{r_w} \right) + S \right]} \quad [\text{Eq. 1773.4}]$$

The phase mobility is defined in terms of the phase relative permeability and viscosity:

$$M_\Phi = \frac{k_{r\Phi}}{\mu_\Phi} \quad [\text{Eq. 1773.5}]$$

$k_{r\Phi}$	is the relative permeability for phase Φ	
μ_Φ	is the viscosity of phase Φ at reservoir conditions	cp

For single phase flow the relative permeability is $k_{r\Phi} = 1$, and the inflow equation simplifies to :

$$Q_{R\Phi} = \frac{1}{\mu_\Phi} \cdot T \cdot (P_{ws} - P_{wf}) \quad [\text{Eq. 1773.6}]$$

This version of the transient IPR can be used for liquid or gas inflow.

For multiphase inflow, the total inflow can be written as the sum of the phase inflows:

$$Q_R = Q_{RO} + Q_{RW} + Q_{RG} \quad [\text{Eq. 1773.7}]$$

This can be rearranged to give:

$$Q_R = M \cdot T \cdot (P_{ws} - P_{wf}) \quad [\text{Eq. 1773.8}]$$

Where the total mobility is defined by

$$M = M_O + M_W + M_G \quad [\text{Eq. 1773.9}]$$

Oil and water flow

A two phase version of the multiphase inflow equation can be used to model liquid inflow.

$$Q_{RL} = \left(\frac{k_{rO}}{\mu_O} + \frac{k_{rW}}{\mu_W} \right) \cdot T \cdot (P_{ws} - P_{wf}) \quad [\text{Eq. 1773.10}]$$

The relative permeabilities can be determined from [permeability tables](#).

Stock tank liquid flow

This transient IPR equation can be expressed in stock tank flow rates. For liquid flow, the stock tank flow rate $Q_L = Q_R / B_L$ is given by

$$Q_L = \frac{2\pi kh(p_{ws} - p_{wf})}{C_1 \mu_L B_L \left[\frac{1}{2} \ln \left(\frac{4kt}{C_0 \gamma \theta \mu_L C r_w^2} \right) + S \right]} \quad [\text{Eq. 1773.11}]$$

Q_L	is the liquid flowrate	STB/d
B_L	is the liquid volume formation factor	RB/STB
μ_L	is the liquid viscosity	cp

The equation can be written using base 10 logarithms, since $\ln \frac{4x}{C_0 \gamma} = \ln 10 \cdot \log \frac{4x}{C_0 \gamma} = 2.302 \cdot (\log x + \log \frac{4}{C_0 \gamma}) = 2.302 \cdot (\log x - 3.23)$:

$$Q_L = \frac{2\pi kh(p_{ws} - p_{wf})}{1.151 \cdot C_1 \mu_L B_L \left[\log \left(\frac{kt}{C_0 \gamma \theta \mu_L C r_w^2} \right) - 3.23 + \frac{S}{1.151} \right]} \quad [\text{Eq. 1773.12}]$$

Below bubble point correction

The transient IPR equation can be combined with a [Vogel equation](#) to model inflows when the bottom hole pressure is below the bubble point, see, [Bubble point correction](#).

Oil and water flow

The [two phase version](#) of the reservoir liquid flow equation can also be written in terms of stock tank liquid flow rate:

$$Q_L = Q_R / B_L = Q_{RO} / B_L + Q_{RW} / B_L \quad [\text{Eq. 1773.13}]$$

Stock tank gas flow

This transient IPR equation can be expressed in stock tank f $B_G = \frac{V}{V_s} = \frac{ZRT}{P} \cdot \frac{P_s}{Z_s R T_s}$ low rates. For gas flow, the formation volume factor can be expressed in terms of pressure and temperature: . The reservoir pressure is taken to be the average pressure in the reservoir: $P = \frac{P_{ws} + P_{wf}}{2}$, which gives a stock tank flow rate $Q_G = Q_R / B_G$:

$$Q_G = \frac{2\pi kh(p_{ws}^2 - p_{wf}^2)}{C_2 \mu_G T Z \left[\frac{1}{2} \ln \left(\frac{4kt}{C_0 \gamma \theta \mu_G C r_w^2} \right) + S + DQ_G \right]} \quad [\text{Eq. 1773.14}]$$

- The quadratic term in pressure arises from a combination of the pressure difference and the average pressure term $(p_{ws}^2 - p_{wf}^2) = (p_{ws} - p_{wf}) \cdot (p_{ws} + p_{wf})$.
- The constant term arises from a combination of the conversion factor and stock tank properties $C_2 = \frac{2C_1 Z_s P_s}{T_s}$.
- The skin has been modified to include a flow rate dependent term.

Q_G	is the gas flowrate	$MSCF/d$
B_G	is the gas volume formation factor	CF/SCF
μ_G	is the gas viscosity	cp
S	is the constant skin	
DQ	is the near wellbore turbulence factor or rate dependent skin	
T	is the reservoir temperature	oR
Z	is the reservoir compressibility factor	
P_s	is the stock tank pressure	14.7 psi
T_s	is the stock tank temperature	519.67 ^oR
Z_s	is the stock tank compressibility factor	1
C_2	is a constant, arising from conversion factors and stock tank properties	For $MSCF/d :$ $C_2 = \frac{2 \cdot 14.7^2 \cdot 0.3048^2}{86400 \cdot 10^{-10} \cdot 519.67} = 2\pi \cdot 1422$

The equation can also be written using base 10 logarithms:

$$Q_G = \frac{2\pi kh(p_{ws}^2 - p_{wf}^2)}{1.151 \cdot C_2 \mu_G TZ \left[\log \left(\frac{kt}{\theta \mu_G Cr_w^2} \right) - 3.23 + \frac{S + DQ_G}{1.151} \right]} \quad [\text{Eq. 1773.15}]$$

Gas pseudo pressure

[Dake 1978](#) gives another version of the Pseudo steady state IPR for gas inflow, that is more accurate for large drawdowns, based on work by [Al-Hussainy et al](#):

$$Q_G = \frac{2\pi kh[m(p_{ws}) - m(p_{wf})]}{C_2 T \left[\frac{1}{2} \ln \left(\frac{4kt}{C_0 \gamma \theta \mu_G r_w^2} \right) + S + DQ_G \right]} \quad [\text{Eq. 1773.16}]$$

Here the gas pseudo pressure is given by:

$$m(p) = 2 \int \frac{p}{\mu_G Z} d p \quad [\text{Eq. 1773.17}]$$

Time to pseudo steady state solution

According to [Dake 1978](#), the solution to the well inflow equations changes from transient to [pseudo steady state](#) when the dimensionless time t_{DA} is given by

$$t_{DA} = \frac{kt}{C_0 \theta \mu CA} > 0.1 \quad [\text{Eq. 1773.18}]$$

Writing $A = \pi r_e^2$, where r_e is the drainage radius of the reservoir, the time when the [pseudo steady state](#) solution becomes applicable is

$$t_{pss} = (0.1 \cdot \pi \cdot C_0) \cdot \frac{\theta \mu C r_e^2}{k} \quad [\text{Eq. 1773.19}]$$

A warning will be issued if the time t exceeds this value.

Data File

Enter an IPR in table form (Flowrate versus Pressure) rather than using an [IPR](#) equation.

This feature is currently only available by using an [EKT](#) or in [expert mode](#).

Place the EKT (Spanner icon) between the completion and the tubing and enter the [IFPTAB](#) data.

Example:

```
! n liq pwf gor wcut
ifptab 0 0      3000 986  0
ifptab 0 1000   2990 986  2.0
ifptab 0 2699   2920 1096 2.2
ifptab 0 6329   2800 2540 2.8
ifptab 0 7288   2600 2980 3.9
ifptab 0 8082   2400 3370 5.6
ifptab 0 8805   2003 3770 8.0
ifptab execute
```

Note: The GOR and water cut values are optional.

All IPR data associated with the completion will be ignored.

Bubble Point Correction

The [Productivity index](#), [Pseudo steady state](#) and [Transient](#) IPRs for liquid inflow can be modified to use a form of [Vogel's equation](#) below the bubble point ($P_{wf} < P_{bp}$). This allows the effects of gas break-out to be modelled.

$$Q - Q_{bp} = Q_{\max} \left(1 - (1 - C) \left(\frac{P_{wf}}{P_{bp}} \right) - C \left(\frac{P_{wf}}{P_{bp}} \right)^2 \right) \quad [\text{Eq. 1773.1}]$$

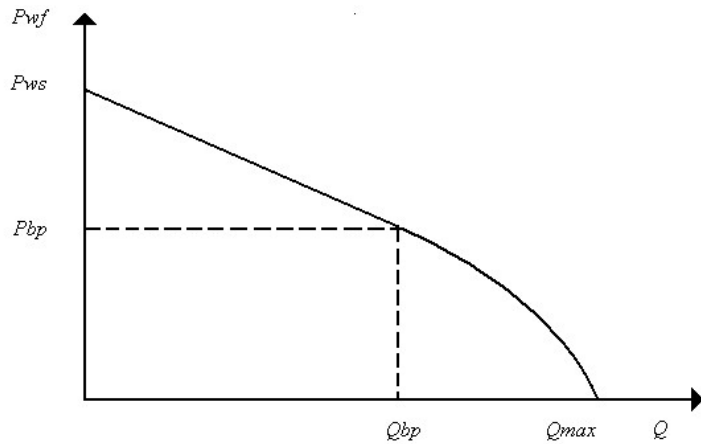
Where

Q	is the liquid flow rate (STB/D or m ³ /d)
Q_{bp}	is the flow at the bubble point flow
$Q_{\max} = \frac{Q_{bp}}{1 + C} \cdot \frac{P_{bp}}{P_{ws} - P_{bp}}$	is the absolute open hole flow potential, that is the liquid flow rate when the bottom hole pressure is zero
P_{bp}	is the bubble point pressure (psia or bara)
P_{wf}	is the well flowing (or bottom hole) pressure (psia or bara)
P_{ws}	is the well static (or reservoir) pressure (psia or bara)
C	is the Vogel coefficient.

The Vogel equation has been shifted to match a linear IPR above the bubble point:

$Q = Q_{bp}$	at $P_{wf} = P_{bp}$
Productivity index $\frac{\partial Q}{\partial P_{wf}} = - \frac{Q_{\max} \cdot (1 + C)}{P_{bp}} = - \frac{Q_{bp}}{P_{ws} - P_{bp}}$	at $P_{wf} = P_{bp}$

This correction only works if the bubble point pressure is less than the static (reservoir) pressure, $P_{bp} < P_{ws}$.



Vertical Well Skin Factor

The skin factor S is used in the [pseudo steady state](#) and [transient](#) IPRs to represent friction caused by damage to the formation close to the well (mechanical skin) and the effects of high flow (dynamic skin).

$$S = S_M + D \cdot Q \quad [\text{Eq. 508.1}]$$

Related links:

[Skin components](#)

[Vertical completion skin table](#)

[Skin options properties](#)

[Darcy's skin properties - openhole](#)

[Darcy's skin properties - openhole gravel packed](#)

[Darcy's skin properties - perforated](#)

[Darcy's skin properties - perforated and gravel packed](#)

[Darcy's skin properties - frac packed](#)

Mechanical skin factor

The [pseudo steady state](#) and [transient](#) IPRs are derived from Darcy's equation for a homogenous reservoir with a vertical completion. The mechanical skin can be used to represent friction terms arising from any departure from this idealized model. The mechanical skin has a number of separate components:

$$S_M = S_{pp} + S_\theta + S_d + S_g + S_p + S_f \quad [\text{Eq. 508.2}]$$

Different components are used in different completion types:

		Open hole	Open hole gravel pack	Perforated	Gravel Packed & Perforated	Frac Pack
S_{pp}	partial penetration	Yes	Yes	Yes	Yes	Yes
S_θ	deviation	Yes	Yes	Yes	Yes	Yes
S_d	damaged zone	Yes	Yes	Yes	Yes	Included in S_f
S_g	gravel pack		Yes		Yes	Included in S_f
S_p	perforated well			Yes	Yes	Included in S_f
S_f	frac pack					Yes

Related links:

[Skin components](#)

[Vertical completion skin table](#)

[Skin options properties](#)

[Darcy's skin properties - openhole](#)

[Darcy's skin properties - openhole gravel packed](#)

[Darcy's skin properties - perforated](#)

[Darcy's skin properties - perforated and gravel packed](#)

[Darcy's skin properties - frac packed](#)

Dynamic skin factor

The [pseudo steady state](#) and [transient](#) IPRs are derived from Darcy's equation for a homogenous reservoir with a vertical completion. The dynamic skin can be used to represent friction terms arising from turbulence in the flow entering the well. The dynamic skin has a number of separate components:

$$D = D_d + D_r + D_g + D_c + D_f \quad [\text{Eq. 508.3}]$$

Different components are used in different completion types:

		Open hole	Open hole gravel pack	Perforated	Gravel Packed & Perforated	Frac Pack
D_d	damaged zone	Yes	Yes	Yes	Yes	
D_r	reservoir	Yes	Yes	Yes	Yes	
D_s	gravel pack screen		Yes			
D_g	gravel pack				Yes	
D_c	crushed zone			Yes	Yes	
D_f	frac pack					Yes

Formulas for these skin components can be found in [Golan and Whitson \(1986\)](#). The damaged zone, reservoir and gravel pack screen dynamic skins all use the same formula D_G for gas flow and the same formula for liquid flow D_L :

$$D_d = \begin{cases} D_G(r_w, r_d, \beta_d) \\ D_L(r_w, r_d, \beta_d) \end{cases} \quad [\text{Eq. 508.4}]$$

$$D_r = \begin{cases} D_G(r_d, r_r, \beta_r) \\ D_L(r_d, r_r, \beta_r) \end{cases} \quad [\text{Eq. 508.5}]$$

$$D_s = \begin{cases} D_G(r_s, r_w, \beta_s) \\ D_L(r_s, r_w, \beta_s) \end{cases} \quad [\text{Eq. 508.6}]$$

The general gas flow dynamic skin term is given by:

$$D_G(r_{in}, r_{out}, \beta) = 2.222 \cdot 10^{-18} \cdot \beta \cdot \frac{k \cdot h \cdot \gamma_G}{h_c^2 \cdot \mu_G} \cdot \left(\frac{1}{r_{in}} - \frac{1}{r_{out}} \right) \quad [\text{Eq. 508.7}]$$

The general liquid flow dynamic skin term is given by:

$$D_L(r_{in}, r_{out}, \beta) = 1.635 \cdot 10^{-16} \cdot \beta \cdot \frac{k \cdot h \cdot \rho_L \cdot B_L}{h_c^2 \cdot \mu_L} \cdot \left(\frac{1}{r_{in}} - \frac{1}{r_{out}} \right) \quad [\text{Eq. 508.8}]$$

The gravel pack dynamic skin for gas flow is given by:

$$D_g = 2.45 \cdot 10^{-13} \cdot \beta_g \cdot \frac{k \cdot h \cdot \gamma_G \cdot L_{pack}}{(2r_p)^4 \cdot n_p^2 \cdot \mu_G} \quad [\text{Eq. 508.9}]$$

The gravel pack dynamic skin for liquid flow is given by:

$$D_g = 1.8 \cdot 10^{-11} \cdot \beta_g \cdot \frac{k \cdot h \cdot \rho_L \cdot B_L \cdot L_{pack}}{(2r_p)^4 \cdot n_p^2 \cdot \mu_L} \quad [\text{Eq. 508.10}]$$

The crushed zone dynamic skin for gas flow is given by:

$$D_c = 3.84 \cdot 10^{-15} \cdot \beta_c \cdot \frac{k \cdot h \cdot \gamma_G}{L_p^2 \cdot n_p^2 \cdot r_p \cdot \mu_G} \quad [\text{Eq. 508.11}]$$

The crushed zone dynamic skin for liquid flow is given by:

$$D_c = 0 \quad [\text{Eq. 508.12}]$$

The frac pack dynamic skin is given as the sum of the tunnel and annulus terms:

$$D_f = D_t + D_a \quad [\text{Eq. 508.13}]$$

The frac pack dynamic skin annulus term uses the same general formula as used for the damaged zone, reservoir and gravel pack screens:

$$D_a = \begin{cases} D_G(r_s, r_c, \beta_s) \\ D_L(r_s, r_c, \beta_s) \end{cases} \quad [\text{Eq. 508.14}]$$

The frac pack dynamic skin tunnel term for gas flow:

$$D_t = 2.222 \cdot 10^{-18} \cdot \beta_s \cdot 4 \cdot \frac{k \cdot h \cdot \gamma_G \cdot L_{tun}}{\left(\frac{r_p}{12}\right)^4 \cdot den_{shot}^2 \cdot \mu_G} \quad [\text{Eq. 508.15}]$$

The frac pack dynamic skin tunnel term for liquid flow:

$$D_t = 1.635 \cdot 10^{-16} \cdot \beta_s \cdot 4 \cdot \frac{k \cdot h \cdot \rho_L \cdot B_L \cdot L_{tun}}{\left(\frac{r_p}{12}\right)^4 \cdot den_{shot}^2 \cdot \mu_L} \quad [\text{Eq. 508.16}]$$

Related links:

[Skin components](#)

[Vertical completion skin table](#)

[Skin options properties](#)

[Darcy's skin properties - openhole](#)

[Darcy's skin properties - openhole gravel packed](#)

[Darcy's skin properties - perforated](#)

[Darcy's skin properties - perforated and gravel packed](#)

[Darcy's skin properties - frac packed](#)

Partial penetration skin

[Brons and Marting](#) (1961) (quoted in [Golan and Whitson](#)) expressed the effect of partial penetration and limited entry as a skin factor :

$$S_{pp} = \left(\frac{h}{L} - 1 \right) \left[\ln \left(\frac{h}{r_w} \sqrt{\frac{k_r}{k_z}} \right) - Y \right] \quad [\text{Eq. 514.1}]$$

with

$$Y = 2.948 - 7.363X + 11.45X^2 - 4.675X^3 \quad \text{and} \quad X = \frac{L}{h}$$

where:

h = Reservoir thickness in TVD

L = Length of open hole interval or perforated interval in TVD

r_w = Wellbore radius

k_r = Reservoir permeability

k_z = Vertical permeability

The skin factor is dimensionless. The equation for the skin factor involves ratios of permeability and ratios of length. It is assumed the same units (e.g. md) are used for all permeability terms, and the same units are used for all lengths (e.g. feet).

Related links:

[Skin components](#)

Deviation skin

[Cinco et al.](#) (1975) approximate the pseudo-skin factor caused by the slant of a well as :

$$S_\theta = - \left(\frac{\theta'}{41} \right)^{2.06} - \left(\frac{\theta'}{57} \right)^{1.865} \log_{10} \left(\frac{h}{100r_w} \sqrt{\frac{k_r}{k_z}} \right) \quad [\text{Eq. 1773.1}]$$

θ' is measured in degrees:

$$\tan(\theta') = \sqrt{\frac{k_z}{k_r}} \cdot \tan(\theta) \quad [\text{Eq. 1773.2}]$$

h	Reservoir Thickness
r_w	Wellbore Radius
k_r	Reservoir Permeability
k_z	Completion Vertical Permeability
$0 < \theta < 75^\circ$	deviation from vertical in degrees

The skin factor is dimensionless. The equation for the skin factor involves ratios of permeability and ratios of length. It is assumed the same units (e.g. md) are used for all permeability terms, and the same units are used for all lengths (e.g. feet).

Damaged zone skin

The effect of formation damage on productivity was treated analytically by [Muskat](#) (1937). [Hawkins](#) (1956) translated the Muskat Model of a near wellbore altered permeability into the following expression for the skin factor :

$$S_d = \left(\frac{k_r}{k_a} - 1 \right) \ln \left(\frac{d_a}{d_w} \right) \quad [\text{Eq. 1773.1}]$$

d_a	Damaged Zone Diameter
d_w	Wellbore Diameter
k_r	Reservoir Permeability
k_a	Damaged Zone Permeability

The skin factor is dimensionless. The equation for the skin factor involves ratios of permeability and ratios of length. It is assumed the same units (e.g. md) are used for all permeability terms, and the same units are used for all lengths (e.g. feet).

Gravel pack skin

Two different formula are used in PIPESIM. The skin factor is dimensionless. The equations for the skin factor involves ratios of permeability and ratios of length. It is assumed the same units (e.g. md) are used for all permeability terms, and the same units are used for all lengths (e.g. feet).

Open hole gravel pack skin

Assuming a radial flow through formation and gravel, the contribution to the skin is expressed as:

$$S_g = \frac{k_r}{k_g} \cdot \ln\left(\frac{r_e}{r_s}\right)$$

where:

r_e = Wellbore drainage radius

r_s = Screen radius

k_r = Reservoir permeability

k_g = Gravel pack proppant permeability

Compare this with the [Annulus skin](#) for a Frac Pack.

Gravel pack skin

Applying Darcy's law for linear flow in packed perforations for the steady state skin term due to gravel pack gives :

$$S_g = 2 \left(\frac{k_r}{k_g} \right) \left(\frac{h}{L} \right) \left(\frac{l'_t}{n \cdot r_p^2} \right)$$

where

$$l'_t = l_t + r_{ic} - r_s$$

k_r Reservoir permeability

k_g Gravel permeability

h Reservoir thickness

L Length of perforated interval

l_t Tunnel length

r_{ic} Casing internal radius

r_s Screen radius

n Number of perforations

r_p Perforation radius

Compare this with the [Gravel skin](#) for a Frac Pack.

Perforated well skin

McLeod model

[McLeod](#) (1983) used a model of a horizontal microwell with formation damage around it as an analogy to a perforation surrounded by a crushed zone. He quantified the effect of the crushed zone as the following skin factor:

Compacted or crushed zone skin, S_c ;

$$S_c = \frac{1}{n_p L} \cdot \frac{h}{l_p} \cdot \left(\frac{k_r}{k_c} - \frac{k_r}{k_d} \right) \cdot \ln \left(\frac{d_c}{d_p} \right)$$

where:

n_p = Perforation density

L = Length of open hole interval or perforated interval in MD

h = Reservoir thickness in TVD

l_p = Depth of penetration (or perforation length)

k_r = Reservoir permeability

k_c = Compacted or Crushed zone permeability

k_d = Damaged zone permeability

d_c = Compacted or Crushed zone diameter

d_p = Perforation diameter in the formation

Note: N = Total number of perforations = $n_p * L$

Karakas model

[Karakas and Tariq](#) (1991) have developed a semi analytical solution for the calculation of the perforation skin effect. Depending on the size of the damaged zone and the length of the perforation , the well radius and the perforation length, or their modified value are used in the model .

The thickness of the damaged zone is :

$$I_a = \frac{1}{2} (d_a - d_w) \quad [\text{Eq. 1773.1}]$$

For perforation sitting inside the damaged zone :

$$\begin{cases} r'_w = r_w \\ l'_p = l_p \end{cases} \text{ if } l_p \leq I_a$$

where:

r_w = Wellbore radius ($d_w/2$)

r'_w = Wellbore radius or modified wellbore radius

l'_p = Perforation length or modified perforation length

For perforations extending beyond the damaged zone

$$\begin{cases} r'_w = r_w + \left(1 - \frac{k_a}{k_r} \right) I_a \\ I'_p = I_p - \left(1 - \frac{k_a}{k_r} \right) I_a \end{cases} \text{ if } I_p > I_a \quad [\text{Eq. 1773.2}]$$

The perforation skin effect is divided into the following components :

Horizontal component of the skin

[Eq. 1773.3]

$$S_h = \ln \left(\frac{r'_w}{r'_{wc}} \right)$$

where

$$r'_{wc} = \alpha(\varphi) [r'_w + I'_p] \quad [\text{Eq. 1773.4}]$$

φ Phase Angle

$\alpha(\varphi)$ Function of phase angle φ (see table 1773.1)

Well bore skin

$$S_w = c_1 \exp \left[c_2 \frac{r'_w}{I'_p + r'_w} \right] \quad [\text{Eq. 1773.5}]$$

with

$c_1 = c_1(\varphi)$ and $c_2 = c_2(\varphi)$ Functions of the phase angle φ (see table 1773.1)

Vertical skin

$$S_v = 10^A H_n^{B-1} R_n^B \quad [\text{Eq. 1773.6}]$$

with

$$H_n = \frac{1}{n_p I_p} \sqrt{\frac{k_r}{k_z}}$$

$$R_n = \frac{n_p d_p}{4} \left(1 + \sqrt{\frac{k_z}{k_r}} \right)$$

$$A = a_1(\varphi) \times \log_{10} R_n + a_2(\varphi)$$

$$B = b_1(\varphi) R_n + b_2(\varphi)$$

$a_1(\varphi), a_2(\varphi), b_1(\varphi)$ and $b_2(\varphi)$ functions of phase angle φ (see table 1773.1)

The equation 1773.6 is valid for $H_n \leq 10$ and $R_n \geq 0.01$

Crushed zone effect

$$S_{ck} = \frac{1}{n_p I_p} \left(\frac{k_r}{k_c} - 1 \right) \ln \left(\frac{d_c}{d_p} \right) \quad [\text{Eq. 1773.7}]$$

The combined skin effect caused by perforations added to the crushed zone effects is given by :

$$S'_t = S_h + S_w + S_v + S_{ck} \quad [\text{Eq. 1773.8}]$$

If the perforations go beyond the damaged zone, the total perforation skin is the sum of these four contributions :

$$S_t = S'_t \quad \text{for } I_p > I_a \quad [\text{Eq. 1773.9}]$$

Damaged zone effect

For perforations within damaged zone, the skin caused by the combined effects of perforations and damage is :

[Eq. 1773.10]

$$S_t = \left(\frac{k_r}{k_a} - 1 \right) \ln \left(\frac{d_a}{d_w} \right) + \frac{k_r}{k_a} (S'_t + S_x) \quad \text{for } I_p \leq I_a$$

$$S_x = S_x(r) \quad \text{and} \quad r = \frac{d_a}{d_w + 2I_p}$$

r Ratio of the damaged zone diameter over the penetration zone diameter

$S_x(r)$ function of r (see table 1773.2)

Table 1. Karakas and Tariq Skin Correlation Coefficients

φ (degree)	45	60	90	120	180	360 (0)
α	0.860	0.813	0.726	0.648	0.500	0.250
a_1	-1.788	-1.898	-1.905	-2.018	-2.025	-2.091
a_2	0.2398	0.1023	0.1038	0.0634	0.0943	0.0453
b_1	1.1915	1.3654	1.5674	1.6136	3.0373	5.1313
b_2	1.6392	1.6490	1.6935	1.7770	1.8115	1.8672
c_1	4.6×10^{-5}	3.0×10^{-4}	1.9×10^{-3}	6.6×10^{-3}	2.6×10^{-2}	1.6×10^{-1}
c_2	8.791	7.509	6.155	5.320	4.532	2.675

Table 2. Skin caused by boundary effect, 180 degree phasing

$r = d_a / (d_w + 2I_p)$	S_x
18.0	0.000
10.0	-0.001
2.0	-0.002
1.5	-0.024
1.2	-0.085

Frac pack skin

The Frac Pack Skin is calculated only in association with a case hole gravel pack. If the gravel pack is not defined the Frac Pack Skin is 0.

[Pucknell and Mason](#) (1992) give a review of the contributions to the skin in a cased hole gravel pack completion.

$$S_f = S_{hf} + S_{ff} + S_{cf} + S_{an} + S_{tg}$$

S_{hf}	Hydraulic fracture
S_{ff}	Fracture face skin
S_{cf}	Choke fracture skin
S_{an}	Annulus skin
S_{tg}	Tunnel gravel skin

The skin factor is dimensionless. The equations for the skin factor involves ratios of permeability and ratios of length. It is assumed the same units (e.g. md) are used for all permeability terms, and the same units are used for all lengths (e.g. feet).

Hydraulic fracture

The following model is also applied in IPR Model "Hydraulic Fracture".

Hydraulic fracture is characterized by its length, capacity or conductivity and related equivalent skin effect. [Prats](#) (1961) introduced the concept of effective wellbore radius, providing pressure profiles in a fractured reservoir as functions of the fracture half-length and a relative capacity. He provided a graph relating the effective well radius and the capacity. [Cinco-Ley et al.](#) (1978, 1981a) (see also [Economides et al.](#) 1994) introduced the fracture conductivity instead, which is proportional to the inverse of the capacity, and provided an alternative graph relating the fracture conductivity to the skin. The following correlations are derived from Cinco-Ley and Samaniego graph.

Dimensionless fracture conductivity:

[Eq. 1773.1]

$$F_{cd} = \frac{k_p \cdot w_f}{k_r \cdot x_f}$$

Pseudo-skin factor for a well with a finite-conductivity vertical fracture

$$S'_{hf} = \begin{cases} -0.7205 * \ln(F_{cd}) + 1.6368 & \text{if } F_{cd} < 1 \\ 3.0386 - 2.349 \exp(-0.511 F_{cd}^{-0.909}) & \text{if } 1 \leq F_{cd} < 1000 \\ 0.692 & \text{if } F_{cd} \geq 1000 \end{cases} \quad [\text{Eq. 1773.2}]$$

and the hydraulic skin is given by:

$$S_{hf} = S'_{hf} - \ln\left(\frac{x_f}{r_w}\right) \quad [\text{Eq. 1773.3}]$$

x_f	Fracture Half Length
w_f	Fracture Width
k_r	Reservoir Permeability
k_p	Proppant Permeability
r_w	Wellbore Radius

Damaged hydraulic fracture performance can deviate substantially from undamaged fracture. Two types of damage are considered: [fracture face](#) and [choke fracture](#).

Fracture face skin

[Cinco-Ley and Samaniego](#) (1981b) quantified the damage that may develop on the fracture face, by a skin effect of the form

$$S_{ff} = \frac{\pi}{2} \cdot \frac{w_{af}}{x_f} \cdot \left(\frac{k_r}{k_{af}} - 1 \right) \quad [\text{Eq. 1773.4}]$$

w_{af}	Depth of Damage (normal to the fracture face) is very thin (0.2 ft or less)
k_{af}	Frac Face Damage Permeability

Choke fracture skin

Damage at the connection between the fracture and a well is referred to as a choke. Different to the fracture face skin, the damaged zone is within the fracture. [Romero et al.](#) (2002) express the extra pressure drop in the fracture in term of a skin effect:

$$S_{cf} = \pi \cdot \frac{x_{cf}}{x_f} \cdot \left(\frac{k_r}{k_{cf}} - \frac{k_r}{k_p} \right) \quad [\text{Eq. 1773.5}]$$

x_{cf}	Choke Length
k_{cf}	Frac Choke Permeability

Annulus skin

Between the casing internal radius and the screen outer radius, assuming a radial flow through the gravel the contribution to the skin is expressed as:

$$S_{an} = \frac{k_r}{k_g} \cdot \ln\left(\frac{d_{ic}}{d_s}\right) \quad [\text{Eq. 1773.6}]$$

d_{ic}	Casing Internal Diameter
d_s	Screen Diameter
k_g	Gravel Permeability

Gravel skin in tunnel

If a perforation is not defined, a default perforation diameter and a default perforation density are set (equal to 0.5 inches and 4 shots/ft respectively) for the calculation of the Frac Pack Skin. If the perforation tunnels through the casing and cement, where the most significant pressure drops usually occur, the skin component is:

$$S_{tg} = 2 \cdot \frac{k_r}{k_g} \cdot \frac{l_t}{n_p \cdot r_p^2} \quad [\text{Eq. 1773.7}]$$

l_t	Tunnel length
n_p	Perforation Density
r_p	Perforation radius

Inflow Performance Relationships for Horizontal Completions

Theory

The main purpose of drilling horizontal wells is to enhance production. There are also many circumstances that lead to drilling horizontal wells (Cooper, 1988):

Thin reservoirs

The increased area of contact of the horizontal well with the reservoir is reflected by the productivity index (PI). Typically, the PI for a horizontal well may be increased by a factor of 4 when compared to a vertical well penetrating the same reservoir.

Heterogeneous reservoirs

When irregular reservoirs exist, the horizontal well can effectively intersect isolated productive zones which might otherwise be missed. A horizontal well can also intersect vertical natural fractures in a reservoir.

Reduce water/gas coning

A horizontal well provides minimum pressure drawdown, which delays the onset of water/gas breakthrough. Even though the production per unit well length is small, the long well length provides high production rates.

Vertical permeability

If the ratio of vertical permeability to horizontal permeability is a high, a horizontal well may produce more economically than a vertical well.

Related links:

[Horizontal completion skin table](#)

[Skin options properties - horizontal distributed](#)

[Joshi & Babu and Odeh skin properties - perforated](#)

[Joshi & Babu and Odeh skin properties - perforated and gravel packed](#)

[Joshi & Babu and Odeh skin properties - openhole](#)

[Joshi & Babu and Odeh skin properties - open hole gravel packed](#)

Pressure drop

Effect of pressure drop on productivity

In many reservoir engineering calculations, the horizontal wellbore is treated as an infinite conductivity fracture, that is the pressure drop along the well length is negligible. However, in practice, there must be a pressure drop from the toe (tip-end) of the horizontal wellbore to the heel (producing-end) so as to maintain fluid flow within the wellbore (see Figure 1).

Dikken (1989), Folefac (1991) and Joshi (1991) have addressed the effect of wellbore pressure gradient on horizontal well production performance.

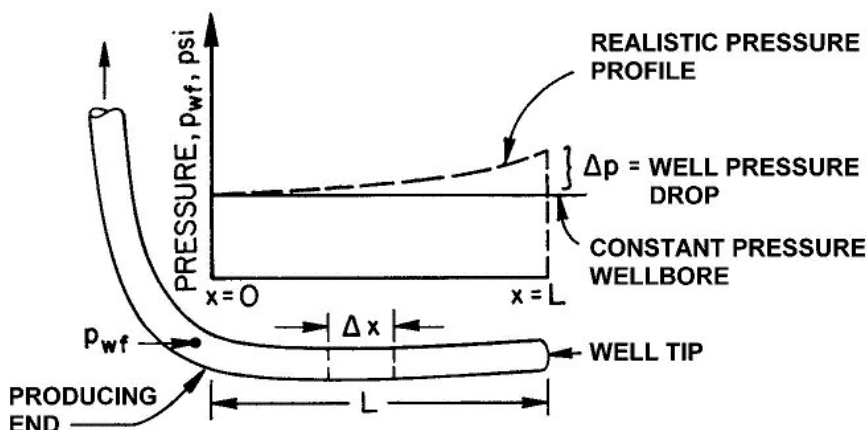


Figure 1773.1. Along-hole pressure gradient of a horizontal well (Joshi, 1991)

[Dikken](#) (1990) and [Folefac](#) (1991) contend that the assumption of constant pressure wellbore is reasonable for single phase laminar flow but is no longer valid when turbulent or multiphase flow occurs. Folefac (1991) showed that a typical well with the following properties: $\rho_o = 800 \text{ kg/m}^3$; $\mu = 1.0 \text{ cp}$; $d = 0.1968 \text{ m}$; and $Q = 5000 \text{ RB/d}$ gives a N_{RE} of 4000 which is well above the turbulence transition limit of 2000. In most practical situations, Dikken (1990) asserts that horizontal wells will exhibit non-laminar flow. In addition, the pressure drop will be even greater when multiphase flow exists.

[Joshi](#) (1991), thus, asked the question: What is the magnitude of the wellbore pressure drop as compared to pressure drop from the reservoir to the wellbore? If the wellbore pressure drop is significant as compared to the reservoir drawdown, then the reservoir drawdown, and consequently, the production rate along the well length will change. Thus, there is a strong interaction between the wellbore and the reservoir. The reservoir flow and wellbore equations must be solved simultaneously as shown in Figure 2.

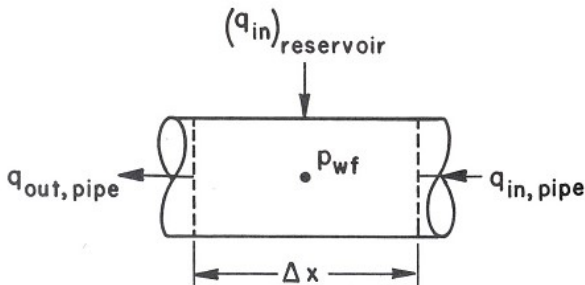


Figure 1773.2. Schematic of reservoir and flow relationship (Joshi, 1991)

The coupled equations were solved by Dikken (1990) analytically by simplified boundary conditions, notably, no inflow from the toe-end. Folefac (1991) used a Black Oil type model that involved a finite volume technique.

Folefac (1991) concluded that the well length, wellbore diameter and perforated interval had the most profound effect on the level of pressure drop in the wellbore. Folefac (1991) pointed out that the wellbore pressure profile is non-linear with respect to the well length. This is because the mixture momentum equation has a non-linear term in velocity, the friction force. This in turn will result in an uneven drawdown in the reservoir that is otherwise considered homogenous.

Furthermore, Folefac (1991) showed that as the wellbore radius increased from 64.5 mm (2.5") to 114.3 mm (4.5"), the rate at which pressure dropped along the wellbore became nearly constant. This is mainly due to the turbulent flow being converted to laminar flow by drilling a larger size hole.

Joshi (1991) mentions other situations where wellbore pressure drop is considerable:

- High flowrates of light oil (10,000 to 30,000 RB/d)
- High viscous crudes (heavy oils and tar sands)
- Long well lengths

The wellbore pressure drop effects well deliverability and in turn influences well completion and well profile design. The need to accurately calculate well flowrates and wellbore pressures is therefore, essential.

Joshi (1991) lists a few remedies to minimize high wellbore pressure drops:

- Drilling a larger diameter hole would dramatically reduce the pressure drop. The reason being that for single phase flow, $D \propto p^{1/d}$. For example, Joshi (1991), states "for a given production rate, by increasing the well diameter twofold, the pressure drop can be reduced at least thirty-two fold".
- Varying the shot density of a cemented hole or the slot size of a slotted liner would control production rates and minimize pressure drop along the wellbore
- Gravel packs are used in high permeability reservoirs. If the well is completed with a slotted liner, the slots should be placed as far apart as possible. Joshi (1991) states that "this will let the gravel pack act as a choke and facilitate maintaining minimum pressure drop across the well length".

Therefore, by selecting the appropriate well geometry, hole size and length, wellbore pressure drops can be minimized.

Single phase pressure drop

Assuming that the horizontal wellbore can be treated as a horizontal pipe, the single phase flow pressure drop calculation for oil flow can be written as follows:

$$\Delta p = (1.14644 \times 10^{-5}) f \rho q^2 \frac{L}{D^5} \quad [\text{Eq. 1773.1}]$$

where,

Δp is pressure drop, psia

f is Moody's friction factor, dimensionless

ρ fluid density, gm/cc

q is flowrate at reservoir conditions, RB/d

L is horizontal length, ft

D is internal diameter of pipe, inches

For gas flow, however, the pressure drop calculations are more complex. This is due to friction which could change the temperature of the gas as it travels through the wellbore. Moreover, density and viscosity are strong functions of gas pressure and temperature. This would result in a changing pressure drop per foot length of a well along the entire well length. The Weymouth equation for dry gas is the simplest equation to estimate pressure drop in a horizontal pipe

$$q_g = 15320 \sqrt{\frac{(P_1^2 - P_2^2) D^{16}}{\gamma_g T Z L}} \quad [\text{Eq. 1773.2}]$$

where

q_g is gas flowrate, scfd

P_1 is pipe inlet pressure, psia

P_2 is pipe outlet pressure, psia

L is pipe length, miles

T is average temperature, °R

Z is average gas compressibility factor

D is pipe diameter, in

γ_g gas specific gravity

Also, several multiphase correlations (Brill, 1988) are applicable for a single phase flow of either oil or gas.

Multiphase pressure drop

There is very little discussion on multiphase pressure drop in horizontal wells. Folefac (1991) studied the effect of two phase flow (hydrocarbon liquid and water are treated as one phase with identical velocity but averaged properties). The pressure drop along the horizontal wellbore was similar to that for single phase flow. However, the pressure drop was higher than for single phase flow for the same volume of fluid intake.

For a horizontal pipe, numerous multiphase flow correlations have been discussed by Brill (1988). Slip velocities between phases make these equations more complex than single phase flow equations. In general, Joshi (1991) states that, "different multiphase correlations may give different values of the pressure drop". The various correlations should be compared with actual pressure drop data. However, measuring the pressure at both ends of a horizontal well and calibrating the data is very difficult. There is a definite need for further study on multiphase flow in horizontal wells.

Inflow production profiles

Horizontal wellbore pressure drops also depend upon the type of fluid inflow profiles. Figure 3 shows some horizontal well fluid inflow profiles. On the basis of well boundary condition and reservoir heterogeneity, several profiles are possible. Joshi (1991) examined the effect of different fluid entry profiles on the wellbore pressure drop. Depending on the type of profile, Joshi concluded that the total pressure drop varied from 6 psi to 14.5 psi but it was not large enough to effect the wellhead pressure.

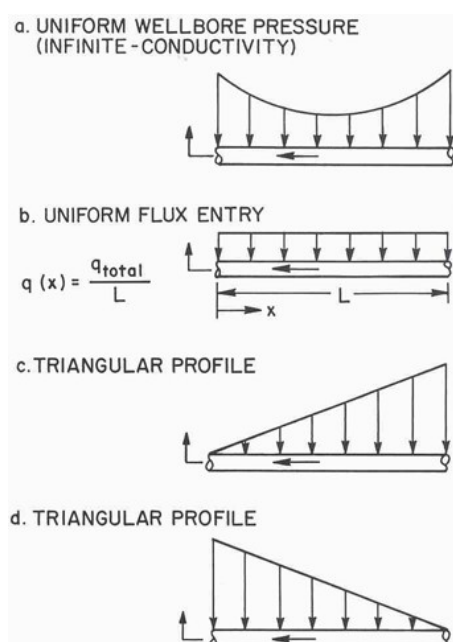


Figure 1773.1. Horizontal well inflow profiles (Joshi, 1991)

Steady-state productivity

The simplest form of horizontal well productivity calculations are the steady-state analytical solutions which assume that the pressure at any point in the reservoir is constant over time. According to Joshi (1991), even though very few reservoirs operate under steady-state conditions, steady state solutions are widely used because:

Analytical derivation is easy.

The concepts of expanding drainage boundary over time, effective wellbore radius and shape factors allows the conversion to either transient or pseudo-steady state results to be quite straightforward.

Steady-state mathematical results can be verified experimentally.

Giger (1984), Economides (1989), Mukherjee (1988) and numerous others have developed solutions to predict steady-state productivity. Most are similar in form to the equation given by Joshi (1988) who simplified the 3-D Laplace equation ($\Delta p=0$) by coupling two 2-D problems. This was based on the assumption that a horizontal well drains an ellipsoidal volume around the wellbore of length L as shown below.

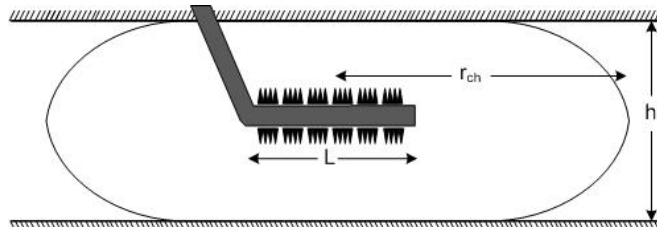


Figure 1773.1. Horizontal Well Drainage Pattern

For isotropic reservoirs $k_h = k_v$

$$q_h = \frac{k_h h \Delta p}{141.2 \mu_o B_o \left(\ln \left[\frac{a + \sqrt{a^2 - (L/2)^2}}{L/2} \right] + \left(\frac{h}{L} \right) \ln \left[\frac{h}{2r_w} \right] \right)} \quad [\text{Eq. 1773.1}]$$

and

$$a = \left(\frac{L}{2} \right) \left[0.5 + \sqrt{0.25 + \left(\frac{2r_{eh}}{L} \right)^4} \right]^{0.5} \quad [\text{Eq. 1773.2}]$$

where

q_h	is the flowrate	STB/d
a	is half the major axis of the drainage ellipse	ft
Δp	is the pressure drop	psi
L	is the horizontal well length	ft
h	is reservoir height	ft
r_w	is the wellbore radius	ft
r_{eh}	is the effective drainage radius of horizontal well	ft
μ_o	is the oil viscosity	cp
B_o	is the oil volume formation factor	RB/STB
k_h	is the horizontal permeability	mD

If the length of the horizontal well is significantly longer than the reservoir height, that is $L \gg h$, then the second term in the denominator of the [1773.1](#) equation is negligible and the solution simplifies to

$$q_h = \frac{k_h h \Delta p}{141.2 \mu_o B_o \ln \left[\frac{4r_{eh}}{L} \right]} \quad [\text{Eq. 1773.3}]$$

[Muskat](#) (1937) suggested a simple transformation to account for permeability anisotropy. An effective permeability, k_{eff} , is defined as

$$k_{eff} = \sqrt{k_v k_h} \quad [\text{Eq. 1773.4}]$$

To account for vertical anisotropy, the reservoir thickness can be modified as follows

$$h = h \sqrt{\frac{k_h}{k_v}} \quad [\text{Eq. 1773.5}]$$

In addition, the influence of well eccentricity (distance from the center of the reservoir in the vertical plane) was also implemented. Thus, equation [1773.1](#) was transformed as follows

$$q_h = \frac{k_h h \Delta p}{141.2 \mu_o B_o \left(\ln \left[\frac{a + \sqrt{a^2 - (L/2)^2}}{L/2} \right] + \beta^2 \frac{h}{L} \ln \left(\frac{h}{2r_w} \right) \right)} \quad [\text{Eq. 1773.6}]$$

where

$$\beta = \sqrt{\frac{k_h}{k_v}} \quad [\text{Eq. 1773.7}]$$

Productivity comparisons of a horizontal well to that of a vertical well can easily be made by using the [1773.6](#) equation. In converting the productivity of a horizontal well into that of an equivalent vertical well, an effective wellbore radius can be calculated, $r_{w,eff}$

$$r_{w,eff} = r_w \exp(-S) \quad [\text{Eq. 1773.8}]$$

The effective wellbore radius is defined as the theoretical well radius which will match the production rate. Joshi (1991) assumed equal drainage volumes, $r_{ch} = r_{cv}$, and equal productivity indices, $J_h = J_v$ to give the following for an anisotropic reservoir

$$r_{w,eff} = \frac{r \left(\frac{L}{2} \right)}{a \left[1 + \sqrt{1 - \left(\frac{L}{2a} \right)^2} \right] + \left[\frac{\beta h}{r_w} \right]^{\frac{\beta h}{L}}} \quad [\text{Eq. 1773.9}]$$

In this way, controlling parameters like well length, permeability and formation thickness can be used to screen potential candidates for further simulation studies.

[Renard](#) (1990) studied the effect of formation damage around the wellbore and modified the steady-state equation to include skin. Renard (1990) concluded that due to the lower productivity index per unit length in horizontal wells, the effect of skin damage is not as pronounced as it is in vertical wells. [Celia et al.](#) (1989) came to the same conclusion with respect to the effect of non-Darcy flow.

Pseudo-steady state productivity

It is often desirable to calculate productivity from a reservoir with unique boundary conditions, such as a gas cap or bottom water drive, finite drainage area, well location, and so on. In these instances pseudo-steady state equations are employed. Pseudo-steady state or depletion state begins when the pressure disturbance created by the well is felt at the boundary of the well drainage area

Pseudo-steady state productivity

[Dake](#) (1978) and [Golan](#) (1986) describe the pseudo-steady state flow of an ideal fluid (liquid) in a closed circular drainage area. Rearranging the equation gives the familiar vertical well productivity

$$q_v = \frac{k h \Delta p}{141.2 \mu_o B_o \left[\ln \left(\sqrt{\frac{2.2458 A}{C_A r_w^2}} \right) + S + S_m + D q_v \right]} \quad [\text{Eq. 1773.1}]$$

where

q_v	is the flowrate	STB/d
Δp	is the pressure drop between the reservoir and the wellbore	psi
S_m	is the mechanical skin factor due to drilling and completion related well damage	
S	is the skin due to perforations, partial penetration and stimulation	
C_A	is the shape factor	
	is the near wellbore turbulence factor or rate	

Dq_v	dependent skin	
μ_o	is the oil viscosity	cp
B_o	is the oil volume formation factor	RB / STB
k	is the formation permeability	mD
h	is the formation thickness	ft
A	is the drainage area	ft^2
r_w	is the wellbore radius	ft
r_{ch}	is the drainage radius	ft

The above equation can be reduced to the following single-phase pseudo-steady state equation for oil flow (assuming $S = 0$, $S_m = 0$ and $Dq_v = 0$),

$$q_v = \frac{kh\Delta p}{141.2\mu_o B_o \left[\ln \left(\frac{r_{ch}}{r_w} \right) - 0.75 \right]} \quad [\text{Eq. 1773.2}]$$

The equation is for a vertical well which is located in the center of a circular drainage area. [Fetkovich](#) (1985) wrote the shape factor in terms of an equivalent skin. This skin was expressed by choosing a reference shape factor of a well at the center of circular drainage area

$$S_{CA} = \ln \sqrt{\frac{C_{Aref}}{C_A}} \quad [\text{Eq. 1773.3}]$$

The horizontal well shape factor depends on the following:

- drainage area shape,
- well penetration.
- dimensionless well length, $L_D = \left(\frac{L}{2h} \right) \sqrt{\frac{k_v}{k_h}}$

L	is the length of the horizontal well	ft
h	is the formation thickness	ft
k_v	is the vertical permeability	mD
k_h	is the horizontal permeability	mD

[Joshi](#) (1991) explains that the well performance approaches a fully penetrating infinite-conductivity fracture when the horizontal well length is sufficiently long, i. e. $L_D > 10$.

[Babu](#) (1989), [Goode](#) (1989) and [Mutalik](#) (1988) have developed methods to calculate pseudo-steady state productivity for single phase flow in horizontal wells. Shape factors were used to arbitrarily locate the well within a rectangular bounded drainage area and the reservoir was bounded in all directions. Mutalik's model assumed the horizontal well as an infinite conductivity well (i.e. the wellbore pressure drop is negligible). Babu's model assumed uniform-flux boundary condition. Goode's model used an approximate infinite conductivity solution where the constant wellbore pressure is estimated by averaging the pressure values of the uniform-flux solution along the well length. Goode (1989) also considered the effects of completion type on productivity. Their model allowed for cased completion, selectively perforated completion, external casing packers to selectively isolate the wellbore and slotted liner completion with selectively isolating zones.

Babu (1989) developed a physical model consisting of a well drilled in a box-shaped drainage volume, parallel to the y direction (see figure [1773.1](#)).

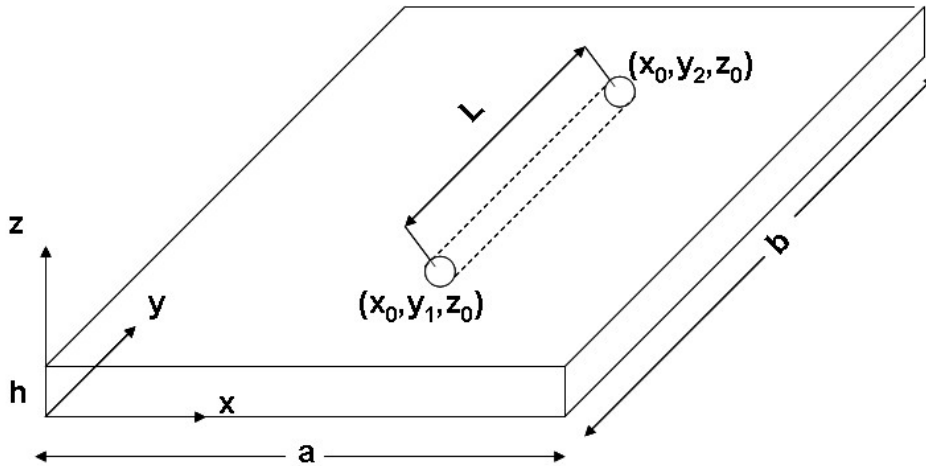


Figure 1773.1. Babu and Odeh physical model

The derived pseudo-steady productivity equation is

$$q_h = \frac{7.08 \times 10^{-3} b \sqrt{k_x k_z} \Delta p}{\mu_o B_o \left[\ln \left(\frac{\sqrt{A_l}}{r_w} \right) + \ln C_H - 0.75 + S_R \right]} \quad [\text{Eq. 1773.4}]$$

where

b	is extension of the drainage volume in the direction along the well axis Oy	ft
S_R	is the skin factor due to partial penetration	
C_H	is the geometric shape factor defined by Babu (1989)	
k_x	is the permeability along the x-axis	mD
k_z	is the permeability along the z-axis	mD
A_l	is the drainage area in the vertical plane	ft ²
r_w	is wellbore radius	ft

The validation rules for Babu and Odeh IPR model are:

- 1. Heel location (X position) must be from 0.0 to ReservoirXDim. In the original publication (see Babu and Odeh 1989), the requirement in the x-direction for the second case considered is that heel location (X position) must be from ReservoirXDim * 0.25 to ReservoirXDim * 0.75. While this requirement is not enforced in this product, user should take caution when operating outside of the requirement.
- 2. Heel location (Y position) + well length must be less than or equal to the reservoir Y dimension. Also, heel location (Y position) must be greater than or equal to zero.
- 3. Heel location (Z position) + well radius must be less than or equal to the reservoir thickness. Also, heel location (Z position) must be greater than or equal to well radius.

The equation 1773.4 is derived from a very complex general solution. It requires the calculation of C_H and S_R . The geometric shape factor accounts effect of permeability anisotropy, well location and relative dimensions of the drainage volume. The skin accounts for the restricted entry associated with the well length. Babu (1989) reported an error of less than 3% when compared to the more rigorous solution.

See [Earlougher \(1977\)](#) for reference.

Solution gas-drive IPR

Cheng (1990), Joshi (1991) and Bendakhlia (1989) have studied the inflow performance relationship (IPR) for solution gas-drive reservoirs. Bendakhlia followed the same approach used by Vogel for vertical wells and developed the following equation:

$$\frac{q_0}{q_{0,\max}} = \left[1 - V \left(\frac{P_{wf}}{P_R} \right) - 1 - V \left(\frac{P_{wf}}{P_R} \right)^2 \right]^n \quad [\text{Eq. 1773.1}]$$

The equation can be used under the assumptions of Vogel's original IPR correlation. The parameter V and n were correlated as a function of recovery factor.

Horizontal gas wells

The preceding sections have dealt with oil flow. However, horizontal wells are also appropriate for gas reservoirs. For example, in high-permeability gas reservoirs wellbore turbulence limits the deliverability of a vertical well. The most effective way, according to Joshi (1991), to reduce gas velocity around the wellbore is to reduce the amount of gas production per unit well length which can be accomplished by horizontal wells. Joshi (1991) describes two methods for the relationship between pressure and flowrate.

The gas flowrate is proportional to the pressure square terms.

[Al-Hussainy et al.](#) (1966) defined a pseudo-pressure $m(p)$. The gas flowrate is directly proportional to the pseudo-pressures which is defined as

$$m(p) = \int_{p_0}^p \frac{2pd\bar{p}}{\mu(p)Z(p)} \quad [\text{Eq. 1773.1}]$$

A comparison of the two methods was done by Joshi (1991). Below reservoir pressures of 2500 psia, either method can be employed. However, above 2500 psia, the pseudo-pressure should be used.

Steady state gas flow equation

The steady-state equation for gas flow is

$$q_h = \frac{7.027 \times 10^{-4} k_h h (p_e^2 - p_{wf}^2)}{\mu Z T \ln \left(\frac{r_{eh}}{r_w} \right)} \quad [\text{Eq. 1773.2}]$$

where

q_h	is the gas flowrate	mmscf/d
p_e	is the pressure at external radius	psia
p_{wf}	is the wellbore flowing pressure	psia
k_h	is the horizontal permeability	mD
h	is the reservoir height	ft
r_{eh}	is the drainage radius	ft
r_w'	is the effective wellbore radius	ft
μ	is the average viscosity	cp
Z	is the average compressibility factor	
T	is the reservoir temperature	$^{\circ}\text{R}$

Pseudo steady state gas flow equation

The pseudo-steady state gas flow equation can be written as follows (Joshi, 1991)

$$q_h = \frac{7.027 \times 10^{-4} k_h (p_e^2 - p_{wf}^2)}{\mu Z T \left[\ln \left(\frac{r_{eh}}{r_w} \right) - 0.75 + S + S_m + S_{ca} - C + D q_h \right]} \quad [\text{Eq. 1773.3}]$$

where

$$D = \frac{2.222 \times 10^{-15} (\gamma_G k_a h \beta)}{\mu_{pwf} r_w h_p^2} \quad [\text{Eq. 1773.4}]$$

In equation 1773.4, the high velocity flow coefficient is given by:

$$\beta = 2.73 \times 10^{10} k_a^{-1.1045} \quad [\text{Eq. 1773.5}]$$

where

q_h	is the gas flowrate	mmscf/d
-------	---------------------	------------------

P_r	is the average reservoir pressure	psia
P_{wf}	is the wellbore flowing pressure	psia
S	is the negative skin factor due to horizontal well (or well stimulation)	
S_m	is the mechanical skin damage	
S_{ca}	is the shape related skin factor	
C	is the shape factor conversion constant	
k	is the permeability	mD
h	is the reservoir height	ft
r_{ch}	is the drainage radius	ft
r_w	is the wellbore radius	ft
μ	is the average viscosity	cP
Z	is the average compressibility factor	
T	is the reservoir temperature	°R
μ_{pwf}	is the gas viscosity at well flowing conditions	cP
β	is the high velocity flow coefficient	1 / ft
γ_G	is the gas specific gravity	dimensionless
h_p	is the perforated interval	ft
k_a	is the permeability in the near wellbore region	mD

The equation [1773.3](#) is based upon circular drainage area as a reference area. In this equation, Dq_h is the turbulence term, also called turbulence skin, or rate dependent skin factor . (see [Joshi](#)(1991), [Brown](#) (1984) and [Golan and Whitson](#) (1986)). This term accounts for the extra pressure drop in the near wellbore region due to high gas velocity. This term was neglected when dealing with oil flow. In addition, the term makes the solution of [1773.3](#) iterative.

The equation [1773.5](#) is given in [Golan and Whitson](#) (1986)

Conclusions

The following can be concluded from this review:

The assumption of constant pressure drop in the wellbore is no longer valid, especially for long well lengths and when turbulent/multiphase flow occurs.

More realistic production geometries are being used in the existing models to calculate horizontal well productivity.

Existing models need to be verified and validated with actual field data. The absence of case studies in the literature is indicative of the 'tight-hole' status of most horizontal well projects.

Distributed productivity index method

for liquid reservoirs

$$Q = J(P_{ws} - P_{wf})L \quad [\text{Eq. 1773.1}]$$

for gas reservoirs

$$Q = J(P_{ws}^2 - P_{wf}^2)L \quad [\text{Eq. 1773.2}]$$

where J is the distributed productivity index.

Oil / water relative permeability tables

A table of oil and water relative permeabilities as functions of water saturation ($k_{ro}(S_{wat}), k_{rw}(S_{wat})$) can be defined in conjunction with the [Pseudo steady-state](#) or [Transient](#) liquid IPRs for vertical completions or the [Steady state](#) or [Pseudo-steady state](#) Liquid IPRs for horizontal completions.

If the reservoir water saturation is known, the water cut of the fluid flowing into the well can be calculated:

$$WCUT = 100 \cdot \frac{Q_w}{Q_o + Q_w} = 100 \cdot \frac{k_{rw}(S_{wat})/\mu_w}{k_{ro}(S_{wat})/\mu_o + k_{rw}(S_{wat})/\mu_w} \quad [\text{Eq. 1773.1}]$$

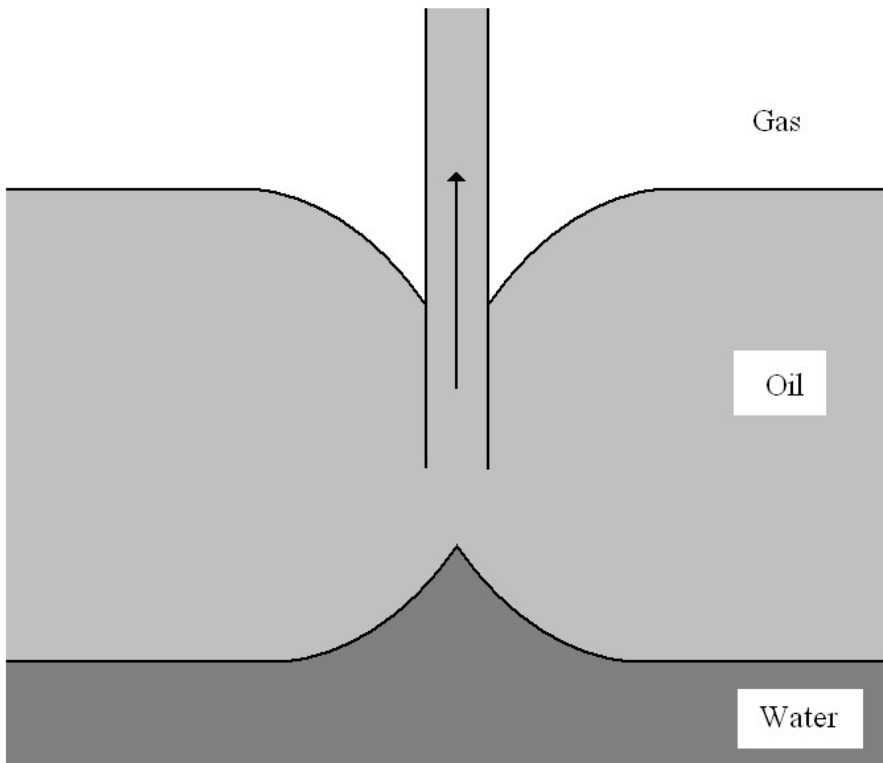
Alternatively, if the water cut is known, the water saturation can be found by solving the same equation for the water saturation, S_{wat} .

The oil and water inflows can then calculated separately using the relevant liquid IPR equation and summed to give the liquid flow rate.

Coning

In order to simulate gas and/or water breakthrough from the reservoir, flowrate-dependent values of GOR and watercut may be entered. In a homogeneous reservoir, analysis of the radial flow behavior of reservoir fluids moving towards a producing well shows that the rate dependent phenomenon of coning may be important. The effect of increasing fluid velocity and energy loss in the vicinity of a well leads to the local distortion of a gas-oil contact or a water-oil contact. The gas and water in the vicinity of the producing wellbore can therefore flow towards the perforation. The relative permeability to oil in the pore spaces around the wellbore decreases as gas and water saturation increase. The local saturations can be significantly different from the bulk average saturations (at distances such as a few hundred meters from the wellbore). The prediction of coning is important since it leads to decisions regarding:

- Preferred initial completions
- Estimation of cone arrival time at a producing well
- Prediction of fluid production rates after cone arrival
- Design of preferred well spacing



Choke

A choke is a mechanical device that limits the flow rate through the pipe. The fluid velocity increases through the constriction and for compressible fluids can reach the sonic velocity. As the pressure difference across the choke increases the flow velocity increases too. At the point the velocity becomes sonic, the flow is said to be critical, and is independent of the down stream pressure. See [Brill and Mukerjee \(1999\)](#) for a detailed description of flow through chokes and restrictions.

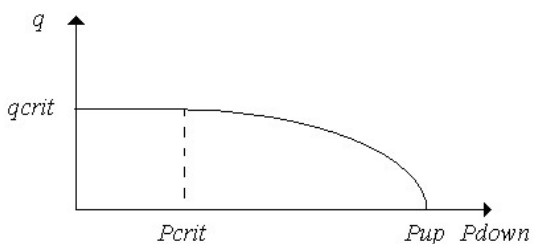


Figure 1774.1. Typical flow-pressure relationship for a choke

The choke is modeled by splitting the flow into two regimes:

flow is subcritical	$P_{crit} < P_{down} < P_{up}$	$q < q_{crit}$
flow is critical	$0 < P_{down} < P_{up}$	$q = q_{crit}$

where

P_{up}	is the upstream pressure	psi or lbf/in^2	N/m^2
P_{down}	is the downstream pressure	psi or lbf/in^2	N/m^2
P_{crit}	is the critical (downstream) pressure	psi or lbf/in^2	N/m^2
q	is the flow rate	lb/s	kg/s
q_{crit}	is the critical flow rate	lb/s	kg/s

The choke performance is determined by the following:

1. The choke geometry and fluid properties
2. The subcritical flow correlation
3. The critical pressure ratio
4. The critical flow correlation

Choke geometry

The main choke parameters are:

d_{up}	upstream diameter	in
d_{bean}	constriction (bean) diameter	in
c_v	flow coefficient (used in the Ashford & Pierce correlation)	
c_{vL}	liquid flow coefficient (used in the Mechanistic correlation)	
c_{vG}	gas flow coefficient (used in the Mechanistic correlation)	
c_d	discharge coefficient (used for calculating the flow coefficients)	

The flow coefficients can either be specified or calculated from the discharge coefficient:

$$c_v = \frac{c_d}{\sqrt{1 - \delta^4}} \quad [\text{Eq. 1774.1}]$$

where:

$\delta = \frac{d_{bean}}{d_{up}}$	is the diameter ratio	dimensionless
------------------------------------	-----------------------	---------------

Subcritical flow correlations

There are essentially two subcritical flow models used in PIPESIM, the [Mechanistic](#) correlation and [Ashford and Pierce](#) (1975) correlation. A third correlation [API-14B](#) is a modification of the Mechanistic correlation

Critical pressure ratio

For single phase liquids, the sonic velocity is high and flow is always subcritical. For single phase gas flow and multiphase flow, the critical pressure is given by

$$P_{crit} = C_{PR} \cdot P_{up} \quad [\text{Eq. 1774.2}]$$

The value of the critical pressure ratio C_{PR} can be set by the user or [calculated](#).

Critical flow correlations

A critical flow correlation can be used to set the critical flow rate q_{crit} . There is a danger that this will not match the subcritical flow at the critical pressure ratio. PIPESIM therefore adjusts the subcritical flow correlation to ensure the flow is correct at the critical pressure. To do this it first calculates the subcritical flow at the critical pressure:

$$q_{lim} = q_{sub}(P_{up}, P_{down}) \text{ evaluated at } P_{down} = P_{crit}$$

The choke downstream pressure is then calculated from the subcritical correlation using the upstream pressure and a scaled flow rate $(q_{lim}/q_{crit})q$. This matching can be turned off, in which case the critical flow correlation is ignored when calculating the pressure drop, although it is used for reporting purposes.

One of twelve correlations of four distinct types can be selected for the critical flow:

1. [Mechanistic](#), [API-14B](#)

2. [Ashford Pierce](#), A-P Tulsa, [Poettmann-Beck](#)
3. [Omaha](#)
4. [Achong](#), [Baxendale](#), [Gilbert](#), [Pilehvari](#), [Ros](#), [User defined](#)

Engine keywords

See [Choke keyword](#)

Choke subcritical flow correlations

Two subcritical flow correlations, [Ashford-Pierce](#) and [Mechanistic](#) are available. A third, [API 14B](#) is a version of the mechanistic correlation.

Ashford-Pierce

[Ashford-Pierce \(1975\)](#) give the following equation for oil flow rate through a choke:

$$q_o = \frac{c_1 c_v (64 d_{bean})^2}{\sqrt{c_2}} \cdot \sqrt{P_{up}} \cdot \frac{\sqrt{1 - \varepsilon + R_L (1 - \varepsilon^k) / k}}{1 + R_L \varepsilon^{-1/\gamma}} \cdot \frac{1}{\sqrt{B_o + F_{wo}}} \cdot \frac{\sqrt{\gamma_o + c_3 \gamma_G R_s + F_{wo} \gamma_w}}{\gamma_o + c_3 \gamma_G R + F_{wo} \gamma_w} \quad [\text{Eq. 1774.1}]$$

where

B_o	is the oil formation factor volume factor	bbl/STB
$c_1 = 3.51$	is a constant	
$c_2 = 198.6$	is a constant	
$c_3 = 0.000217$	is a constant	
c_v	is the flow coefficient	
d_{bean}	is the bean diameter	1/64 in
$k = \frac{\gamma - 1}{\gamma}$		dimensionless
F_{wo}	is the upstream water to oil ratio	
P_{up}	is the upstream pressure	
P_{down}	is the downstream pressure	
q_o	is the oil flow rate at standard conditions	bbl/d
R_s	is the upstream gas oil ratio	scf/STB
R	is the gas oil ratio at standard conditions	scf/STB
$R_L = \frac{T_{up} Z_{up} (R - R_s)}{198.6 P_{up}}$	is the upstream gas liquid ratio	dimensionless
$\varepsilon = \frac{P_{down}}{P_{up}}$	is the pressure ratio	dimensionless
$\gamma = \frac{C_p}{C_v}$	is the ratio of specific heats	dimensionless
γ_o	is the upstream oil specific gravity	dimensionless
γ_G	is the upstream gas specific gravity	dimensionless
γ_w	is the upstream water specific gravity	dimensionless

The Ashford and Pierce formula is based on the following assumptions:

- polytropic expansion of gas-liquid mixture
- equal gas and liquid velocities at the throat
- incompressible liquid phase
- liquid dispersed in a continuous gas phase
- negligible friction losses

Recommended values for the flow coefficient c_v are:

diameter in 1/64 in	d_{bean}	
8	0.125	1.2
12	0.1875	1.2

20	0.3125	0.976
24	0.375	0.96
32	0.5	0.95

Mechanistic correlation

The pressure drop across the choke is given by the weighted average of the liquid and gas phase pressure drops:

$$\Delta P = \lambda_L \cdot \Delta p_L + \lambda_G \cdot \Delta p_G \quad [\text{Eq. 1774.2}]$$

The liquid phase pressure drop is given by Bernoulli's equation:

$$\Delta p_L = \frac{\rho_n}{2 \cdot c} \left(\frac{v}{c_{vL} \cdot Z_L} \right)^2 \quad [\text{Eq. 1774.3}]$$

The gas phase pressure drop is given by Bernoulli's equation:

$$\Delta p_G = \frac{\rho_n}{2 \cdot c} \left(\frac{v}{c_{vG} \cdot Z_G} \right)^2 \quad [\text{Eq. 1774.4}]$$

$v = \frac{q}{A_{beam} \cdot \rho_n}$	is the mixture velocity through the choke	ft/s	m/s
q	is the mass flow rate	lb/s	kg/s
$A_{beam} = \frac{\pi \cdot d_{beam}^2}{4}$	is the choke area at the constriction	ft^2	m^2
$\rho_n = \lambda_L \cdot \rho_L + \lambda_G \cdot \rho_G$	is the no-slip density	lb/ft^3	kg/m^3
λ_L and λ_G	are the liquid and gas phase flowing fractions		
ρ_L and ρ_G	are the liquid and gas phase densities	lb/ft^3	kg/m^3
$Z_L = 1$ and $Z_G = 1 - \frac{0.41 + 0.35 \delta^4}{\gamma} \cdot \frac{\Delta P}{P_{up}}$	are the liquid and gas compressibilities		
c	is a conversion factor for engineering units	$c = 144 \cdot g \text{ lb}/(\text{ft} \cdot \text{s}^2)/\text{psi}$	$c = 1$

Total pressure drop for the two-phase system is therefore:

$$\Delta P = \frac{\rho_n \cdot v^2}{2 \cdot c} \cdot \left[\frac{\lambda_L}{(c_{vL} \cdot Z_L)^2} + \frac{\lambda_G}{(c_{vG} \cdot Z_G)^2} \right] \quad [\text{Eq. 1774.5}]$$

API 14-B formulation

The API 14-B formulation is similar to the mechanistic formulation, with the addition of the following assumptions:

- Liquid flow through the choke is incompressible. The discharge coefficient is constant with a value of $c_{vL} = 0.85$.
- Subcritical gas flow through the choke is adiabatic and compressible. The discharge coefficient is constant with a value of $c_{vG} = 0.9$.

Choke critical pressure ratio

The critical pressure ratio C_{PR} is used to determine the downstream pressure when critical flow occurs in the choke. You can set a value of C_{PR} or it can be calculated, either from the single-phase gas formula (used with the Mechanistic subcritical flow correlation) or using the Ashford and Pierce formula (used with the Ashford and Pierce subcritical flow correlation).

Single phase gas critical pressure ratio

For a single phase gas flow, the critical pressure is given as a function of the specific heat ratio:

$$C_{PR} = \left[\frac{2}{\gamma + 1} \right]^{\frac{\gamma}{\gamma - 1}} \quad [\text{Eq. 1774.1}]$$

The value of $\gamma = C_p / C_v$ is calculated by the program, but can be overridden by the user. For diatomic gases (for example air) $\gamma \approx 1.4$ and $C_{PR} = 0.53$

Ashford and Pierce critical pressure ratio

[Ashford-Pierce \(1975\)](#) give the critical flow condition $\frac{\partial q_o}{\partial \varepsilon} = 0$ at $\varepsilon = C_{PR}$. [1774.1](#) for q_o and simplifying gives:

$$\frac{\partial}{\partial \varepsilon} \left[\frac{\sqrt{1 - \varepsilon + R_L (1 - \varepsilon^k) / k}}{1 + R_L \varepsilon^{-1/\gamma}} \right] = 0 \quad [\text{Eq. 1774.2}]$$

This can be manipulated to give an equation for $\varepsilon = C_{PR}$:

$$(1 + R_L \varepsilon^{-1/\gamma})^2 = \frac{2R_L}{\gamma} \cdot \varepsilon^{-\frac{\gamma}{\gamma+1}} \cdot (1 - \varepsilon + R_L \cdot (1 - \varepsilon^k) / k) \quad [\text{Eq. 1774.3}]$$

Choke critical flow correlations

The following choke correlations are available:

Ashford and Pierce / Sachdeva / Poetmann-Beck

The [Ashford-Pierce \(1975\)](#) critical flow can be obtained by evaluating [1774.1](#) at $\varepsilon = C_{PR}$, determined from [1774.3](#). The stock tank critical oil flow rate takes the form:

$$q_o = \frac{c_1 c_v (64 d_{bean})^2}{\sqrt{c_2}} \cdot \sqrt{P_{up}} \cdot \frac{\sqrt{1 - \varepsilon + R_L (1 - \varepsilon^k) / k}}{1 + R_L \varepsilon^{-1/\gamma}} \cdot \frac{1}{\sqrt{B_o + F_{wo}}} \cdot \frac{\sqrt{\gamma_o + c_3 \gamma_g R_s + F_{wo} \gamma_w}}{\gamma_o + c_3 \gamma_g R + F_{wo} \gamma_w} \quad [\text{Eq. 1774.1}]$$

The [Sachdeva](#) critical flow correlation takes a similar form:

$$q_o = 0.858 c_v (64 d_{bean})^2 \cdot \sqrt{P_{up}} \cdot \frac{\sqrt{R_L + 0.76}}{R_L + 0.56} \cdot \frac{1}{\sqrt{B_o + F_{wo}}} \cdot \frac{1}{\sqrt{[(62.4(\gamma_o + c_3 \gamma_g R + F_{wo} \gamma_w))^2 + (62.4(\gamma_o + c_3 \gamma_g R_s + F_{wo} \gamma_w))^{-1}]} \quad [\text{Eq. 1774.2}]}$$

The [Poetmann-Beck](#) critical flow correlation takes a similar form:

$$q_o = 88992 \cdot \sqrt{9273.6} \cdot 0.4513 \cdot A_{bean} \cdot \sqrt{P_{up}} \cdot \frac{\sqrt{R_L + 0.766}}{R_L + 0.5663} \cdot \frac{1}{5.61 \rho_L + 0.0765 \gamma_G R} \cdot \frac{\rho_L + R_L \rho_G}{\sqrt{\frac{3}{2} \rho_L + R_L \rho_G}} \quad [\text{Eq. 1774.3}]$$

Mechanistic / API14B

The critical mass flow rate can be found by inverting the [1774.5](#) and evaluating it at the critical value of the pressure drop:

$$q = A_{bean} \sqrt{\frac{2g \cdot \rho_n \cdot \Delta P}{c_1 \cdot \left[\frac{\lambda_L}{(c_{vL} \cdot Z_L)^2} + \frac{\lambda_G}{(c_{vG} \cdot Z_G)^2} \right]}} \quad [\text{Eq. 1774.4}]$$

$$\Delta P = (1 - C_{PR}) P_{up} \quad [\text{Eq. 1774.5}]$$

The API14B critical flow uses the mechanistic critical flow formula, with $c_{vL} = 0.85$ and $c_{vG} = 0.9$

Omania correlation

The [Omania](#) correlation gives a formula for the stock tank critical liquid flow rate:

$$q_L = 1.953 \times 10^{-3} \cdot \sigma_L^{-1.245} \cdot \rho_L^{1.545} \cdot (1 + R_L)^{-0.657} \cdot d_{bean}^{1.8} \cdot \rho_G^{-3.49} \cdot P_{up}^{3.19} \quad [\text{Eq. 1774.6}]$$

where:

σ	surface tension at upstream conditions	(dynes/cm)
----------	--	------------

Gilbert, Ros, Baxendall, Achong, Pilehvari and user defined correlations

The equations proposed by Gilbert, Ros, Baxendall, Archong and Pilehvari ([Ghassan](#)) for stock tank critical liquid flow are all of the form:

$$q_L = \left[\frac{P_{up} \cdot (64d_{bean})^c}{a \cdot GLR^b} \right]^{1/e} \quad [\text{Eq. 1774.7}]$$

where

GLR - producing gas liquid ratio (scf/STB)

a, b, c - empirical coefficient given below

Correlation	a	b	c	e
Achong	3.82	0.650	1.88	1
Baxendall	9.56	0.546	1.93	1
Gilbert	10	0.546	1.89	1
Pilehvari	46.67	0.313	2.11	1
Ros	17.4	0.5	2.00	1

Users can also define their own parameters for this formula by using engine [keywords](#). For example:

```
CHOKE CCORR=USER a=0.1 b=0.546 c=1.89 e=1.0 ADJUSTSC dbean = 3
```

Keywords can be entered in the GUI by replacing the choke with an [Engine Keyword Tool](#).

Flow control valves mechanistic theory

PIPESIM's mechanistic choke equation is based on the theory for subcritical flow (see Brill and Mukherjee, 1969).

Subcritical flow

The mass flow rate is given in terms of the pressure drop as follows:

$$Q_{sc} = 12A_{bean} \sqrt{\frac{2g\rho_{ns}\Delta P}{\left[\frac{f_L}{(Z_L c_L)^2} + \frac{f_G}{(Z_G c_G)^2} \right]}} \quad [\text{Eq. 1774.1}]$$

where:

f_L and f_G	are the liquid and gas phase fraction
c_L and c_G	are the liquid and gas flow coefficient
A_{bean}	is the choke cross-section

ΔP is the pressure drop, which is given by:

$$\Delta P = f_L \Delta P_L + f_G \Delta P_G \quad [\text{Eq. 1774.2}]$$

and

$$\Delta P_L = \left(\frac{1}{2g\rho_{ns}} \right) \left[\frac{q}{(12Z_L c_L A_{bean})} \right]^2 \quad [\text{Eq. 1774.3}]$$

$$\Delta P_G = \left(\frac{1}{2g\rho_{ns}} \right) \left[\frac{q}{(12Z_L c_L A_{bean})} \right]^2 \quad [\text{Eq. 1774.4}]$$

where

$Z_L = 1$	is the liquid compressibility factor
$Z_G = Z_G(k, DP, P_{up})$	is the gas compressibility factor
$\rho_{ns} = f_L \rho_L + f_G \rho_G$	is the no slip density

Critical flow

The critical mass flow is given by the subcritical correlation evaluated at the critical pressure drop:

$$\Delta P_{crit} = P_{up} (1 - C_{PR}) \quad [\text{Eq. 1774.5}]$$

where C_{PR} is the critical pressure ratio.

Fittings

The pressure drop across a fitting is given by the [Crane Technical Paper 410](#):

$$\Delta P = K \cdot \frac{\rho \cdot v^2}{2 \cdot c} \quad [\text{Eq. 1774.1}]$$

K	is a dimensionless friction factor or resistance		
v	is the fluid velocity	ft/s	m/s
ρ	is the fluid density	lb/ft^3	kg/m^3
c	is a conversion factor for engineering units	$c = 144 \cdot g \text{ lb}/(\text{ft} \cdot \text{s}^2)/\text{psi}$	$c = 1$

The velocity of the fluid in the fitting depends on the internal diameter of the fitting where the velocity is measured. If the fitting has two internal diameters, d_1 and d_2 , the velocities are related by:

$$\frac{\rho_1 \cdot \pi \cdot d_1^2 \cdot v_1}{4} = \frac{\rho_2 \cdot \pi \cdot d_2^2 \cdot v_2}{4} = q \quad [\text{Eq. 1774.2}]$$

For incompressible fluids the density can be taken as constant and the velocities are inversely proportional to the square of the diameters. Therefore the pressure drop can be written in terms of either velocity:

$$\Delta P = K_1 \cdot \frac{\rho \cdot v_1^2}{2 \cdot c} = K_2 \cdot \frac{\rho \cdot v_2^2}{2 \cdot c} \quad [\text{Eq. 1774.3}]$$

The fitting resistances are related by:

$$K_2 = \frac{1}{\delta^4} \cdot K_1 \quad [\text{Eq. 1774.4}]$$

and $\delta = d_1 / d_2$ is the ratio of the internal diameters.

Comparison with the choke model

The fitting can be modeled as a [choke](#) using a mechanistic [sub-critical](#) liquid flow correlation. The choke diameter is taken as the minimum diameter of the fitting d_1 and the flow coefficient is calculated from the fitting resistance at d_1 :

$$c_v = \frac{1}{\sqrt{K_1}} \quad [\text{Eq. 1774.5}]$$

Resistance calculation

The fitting resistance K can be specified by the user. Since it is a function of the internal diameter, d , this value must also be specified to allow the velocity to be calculated correctly.

The fitting resistance can also be calculated by PIPESIM using formulae from the [Crane Technical Paper 410](#). The resistance is a function of the fitting type, the pipe nominal diameter, d_N the internal diameter, d_2 and the diameter of any constriction, d_1 . These [Crane Technical Paper 410](#) formula can be written as:

$$K_1 = a_1 \cdot f_T(d_N) + a_2 \cdot 0.5 \cdot (1 - \delta^2) + a_3 \cdot (1 - \delta^2)^2 \quad [\text{Eq. 1774.6}]$$

The first term $a_1 \cdot f_T$ represents friction due to the shape of the pipe fitting, the second term $a_2 \cdot 0.5 \cdot (1 - \delta^2)$ is the resistance due to sudden contraction through any constriction in the fitting and the third term $a_3 \cdot (1 - \delta^2)^2$ is the resistance due to sudden expansion after a constriction. The constants a_1 , a_2 and a_3 depend on the fitting type and are given by:

Fitting	a_1	a_2	a_3
Check Swing Valve Conventional	100	0	0
Check Swing Valve Clearway	50	0	0
Standard 90 degree Elbow	30	0	0
Standard 45 degree Elbow	16	0	0
Standard 90 degree Short Radius Elbow	14	0	0
Standard 90 degree Long Radius Elbow	12	0	0
Tee - Flow through run	20	0	0
Tee - Flow through branch	60	0	0
Check Lift Globe Valve	600	δ	δ
Globe Valve Conventional	340	δ	δ
Angle Valve Conventional	150	δ	δ
Globe Valve Y-Pattern	55	δ	δ
Check Lift Angle Valve	55	δ	δ
Gate Valve $\theta < 45^\circ$	8	$1.6 \cdot \sin \frac{\theta}{2}$	$2.6 \cdot \sin \frac{\theta}{2}$
Gate Valve $45^\circ < \theta < 180^\circ$	8	$\sqrt{\sin \frac{\theta}{2}}$	1
Ball Valve $\theta < 45^\circ$	3	$1.6 \cdot \sin \frac{\theta}{2}$	$2.6 \cdot \sin \frac{\theta}{2}$
Ball Valve $45^\circ < \theta < 180^\circ$	3	$\sqrt{\sin \frac{\theta}{2}}$	1

The friction factor f_T , depends on the nominal size of the pipe:

Nominal size d_N (inch)	f_T
1/2	.027
3/4	.025
1	.023
1 1/4	.022
1 1/2	.021
2	.019
2 1/12, 3	.018
4	.017
5	.016
6	.015
8 - 10	.014
12 - 16	.013

18 - 24 .012

Sudden expansions or contractions due to adjacent pipes of differing diameters

PIPESIM will by default calculate the pressure losses associated with sudden expansions or contractions associated with sudden pipe diameter changes if the pipes are separated by a junction.

When a change in pipe diameter occurs, the junction between the non-matching diameters are assumed to be straight-edged, and to cause pressure reduction due to turbulence effects. This approach is based on the method described by [Perry](#).

The pressure loss is calculated as:

$$\Delta P = \frac{KV_m^2 \rho_m}{144 * 2g_c}$$

Where for expansions,

$$K = \left(1 - \frac{a_1}{a_2}\right)^2$$

And for contractions,

$$K = .5357 - .5414 \left(\frac{a_2}{a_1}\right)$$

Where,

a_1 = pipe area of upstream segment (ft^2)

a_2 = pipe area of downstream segment (ft^2)

Note:

$$K = .5357 - .5414 \left(\frac{a_2}{a_1}\right)$$

- Equation is fitted to a straight line from data in Perry and is very close to [Crane](#) equation 2-10.
- The calculation is skipped for Reynolds numbers of less than 2000.

The results of this calculation are only reported in the output file if the pressure loss exceeds a specified limit. By default this limit is 10 psi, however this can be changed by entering the following single branch keyword in the Simulation » Advanced menu:

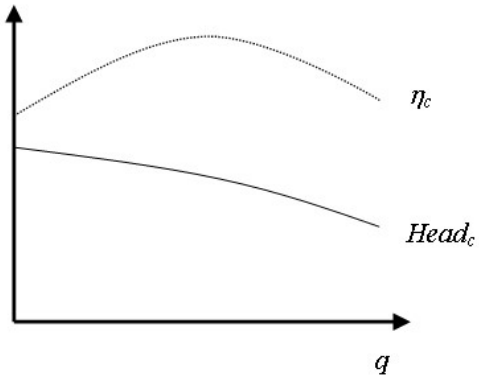
```
OPTIONS SEClim = X
```

Where X is the threshold (in psi units) below which SEC losses are not reported. When SEC losses are reported, they appear in the output file as shown in this example:

Dist. (feet)	Elev. (feet)	Horiz. Angle (deg)	Vert. Devn. (deg)	Pres. (psia)	Temp. (F)	Mean Vel. (ft/s)	Pressure Drop (psi)	Pressure Drop Elev. Frictn.	
Comp_Feed									
1	0.0000	0.0000	0.000	90.00	600.00	50.000	20.439	0.0000	0.0000
2	50.000	0.0000	0.000	90.00	599.82	49.986	20.446	0.0000	.18365
3	100.00	0.0000	0.000	90.00	599.63	49.973	20.452	0.0000	.18371
** SEC Loss : type = CONTRACTION DP = -3.913(psi) **									
Comp_Feedc									
4	0.0000	0.0000	0.000	90.00	595.72	49.707	145.84	0.0000	0.0000
5	50.000	0.0000	0.000	90.00	564.03	47.544	154.58	0.0000	31.029
6	100.00	0.0000	0.000	90.00	530.16	45.154	165.47	0.0000	33.081

Note: By default the engine output file is not shown. To display the engine output file, go to Workspace » Options » Advanced and select the option to Show Engine Output Files.

Centrifugal pumps and compressors



Centrifugal pumps and compressors are described by curves of head and efficiency as functions of the flow rate for a given speed:

$$Head(q, N_c) = Head_c(q) \quad [\text{Eq. 1774.1}]$$

$$\eta(q, N_c) = \eta_c(q) \quad [\text{Eq. 1774.2}]$$

where:

$Head$	is the head	$ft \cdot lbf / lb$	Nm / kg
η	is the efficiency, expressed as a fraction, $0 < \eta \leq 1$		
q	is the flow rate	lb / s	kg / s
N_c	is the compressor speed for the curve		

The fan laws can be used to determine the head and efficiency for speeds N that differ from the curve speed :

$$Head(q, N) = \left(\frac{N}{N_c} \right)^2 Head_c \left(\frac{q}{N/N_c} \right) \quad [\text{Eq. 1774.3}]$$

$$\eta(q, N) = \eta_c \left(\frac{q}{N/N_c} \right) \quad [\text{Eq. 1774.4}]$$

The change in pressure of the fluid and the power needed to run the pump or compressor can be determined from the head and efficiency:

$$\Delta P = P_{out} - P_{in} = c_1 \cdot Head \cdot \langle \rho \rangle \quad [\text{Eq. 1774.5}]$$

$$Power = \frac{c_2 \cdot q \cdot Head}{\eta} \quad [\text{Eq. 1774.6}]$$

where

$\langle \rho \rangle = \frac{[\rho(P_{in}, T_{in})] + [\rho(P_{out}, T_{out})]}{2}$	is the average density	lb / ft^3	kg / m^3
P_{in}	is the suction pressure	psi or lbf / in^2	N / m^2
P_{out}	is the discharge pressure	psi or lbf / in^2	N / m^2
T_{in}	is the suction temperature	$^{\circ}\mathcal{R}$	K
T_{out}	is the discharge temperature	$^{\circ}\mathcal{R}$	K
$Power$	is the power required by the pump or compressor	hp	W
c_1	is a conversion factor for engineering units	$\frac{1}{144} \left(\frac{in}{ft} \right)^2$	
c_2	is a conversion factor for engineering units	$\frac{1}{550} \frac{hp}{ft \cdot lbf / s}$	

The outlet temperature depends on how much of the pump energy is transferred to the fluid. Three different models can be used:

Adiabatic Route:	[Eq. 1774.7]
------------------	--------------

	$\Delta T = T_{out} - T_{in} = \frac{T_{in}}{\eta} \cdot \left(\left(\frac{P_{out}}{P_{in}} \right)^{\frac{\langle \gamma \rangle - 1}{\langle \gamma \rangle}} - 1 \right)$
Polytropic Route:	$\Delta T = T_{out} - T_{in} = T_{in} \cdot \left(\left(\frac{P_{out}}{P_{in}} \right)^{\frac{\langle n \rangle - 1}{\langle n \rangle}} - 1 \right) \quad [\text{Eq. 1774.8}]$
Mollier Route (Isentropic):	$S(P_{out}, T_{out}) = S(P_{in}, T_{in}) \quad [\text{Eq. 1774.9}]$

where

$\langle \gamma \rangle = \frac{[\gamma(P_{in}, T_{in})] + [\gamma(P_{out}, T_{out})]}{2}$	is the average value of γ		
$\gamma = \frac{C_p}{C_v}$	is the ratio of specific heats		
$\langle n \rangle = \frac{[n(P_{in}, T_{in})] + [n(P_{out}, T_{out})]}{2}$	is the average value of n		
$\frac{n}{n-1} = \eta \cdot \frac{\gamma}{\gamma-1}$	is the polytropic coefficient		
S	is the specific entropy	$\frac{BTU}{lb \cdot {}^{\circ}F}$	$\frac{J}{kg \cdot K}$

Note that:

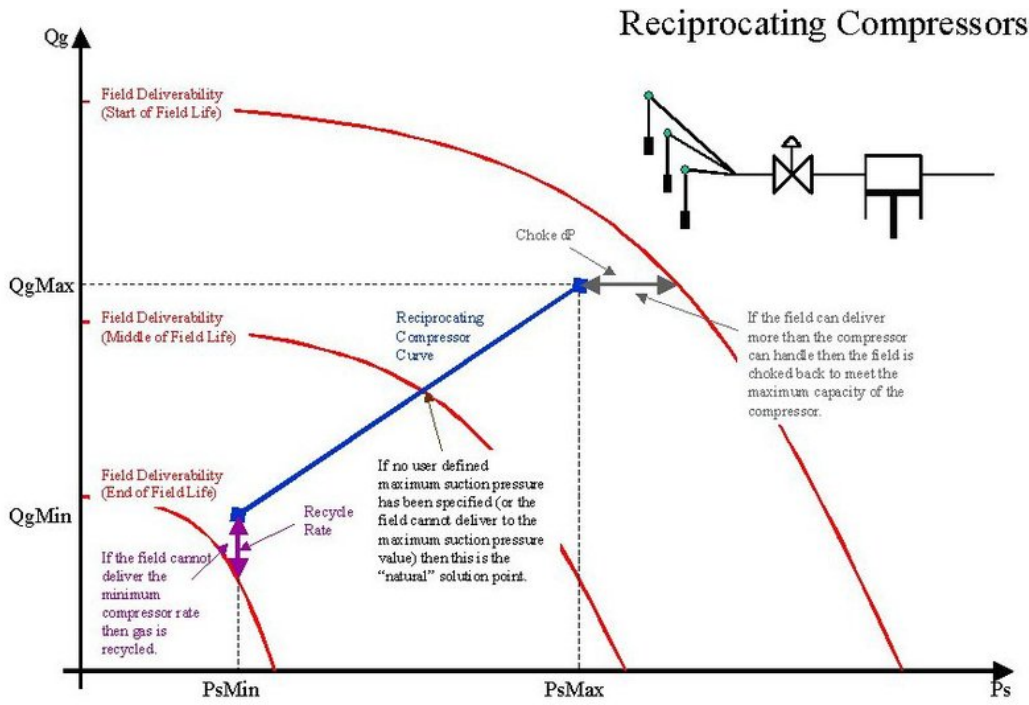
- Only a fraction η of the power is converted to head. When using the adiabatic route, the energy that is not converted to head is assumed to be converted to fluid heat. The usual adiabatic temperature increase is multiplied by a factor $1/\eta \geq 1$.
- The polytropic route $PV^n = \text{constant}$ can be used to model constant pressure ($n = 0$), constant temperature ($n = 1$), constant enthalpy ($n = \gamma$) and constant volume ($n = \infty$) changes as well as intermediate routes. PIPESIM uses a value of n that is a function of the efficiency (η) and the specific heat ratio (γ). This value can only be used when $\eta > (\gamma - 1)/\gamma$.
- In the special case when the efficiency $\eta = 1$, the polytropic coefficient equals the specific heat ratio $n = \gamma$ and the polytropic and adiabatic formulas are the same.
- The Mollier Route can only be used in compositional models, the PIPESIM blackoil model does not calculate entropy.

Engine keywords

See [compressor keywords](#).

Reciprocating compressor operation

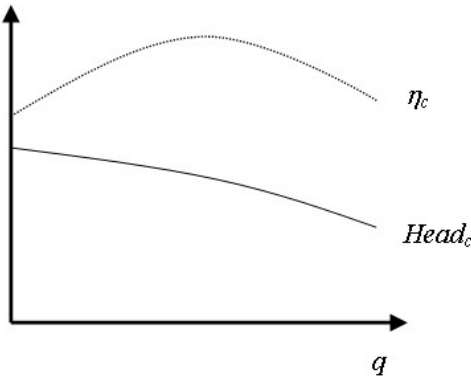
This graph shows how the reciprocating compressor will operate for various field deliverabilities:



Note the following:

1. If the field deliverability falls below the minimum compressor flowrate, recycle mode will be invoked. Due to the low pressure operation in this region, it may be necessary to add a reverse block to the branch containing the compressor.
2. If the field deliverability falls below the minimum suction pressure of the compressor, no solution is possible.
3. Always run the network model in **Wells Offline** mode, with no reverse blocks set.

Expanders



Expanders are modeled in a similar way to [centrifugal compressors](#), except they work in reverse. Fluid flows through the expander and power is extracted. As with compressors, expanders can be described by curves of head and efficiency as functions of the flow rate for a given speed:

$$Head(q, N_c) = Head_c(q) \quad [\text{Eq. 1774.1}]$$

$$\eta(q, N_c) = \eta_c(q) \quad [\text{Eq. 1774.2}]$$

where:

$Head$	is the head	$ft \cdot lbf / lb$	Nm / kg
η	is the efficiency, expressed as a fraction, $0 < \eta \leq 1$		
q	is the flow rate	lb / s	kg / s
N_c	is the expander speed for the curve		

The fan laws can be used to determine the head and efficiency for speeds N that differ from the curve speed :

[Eq. 1774.3]

$$\text{Head}(q, N) = \left(\frac{N}{N_c}\right)^2 \text{Head}_c\left(\frac{q}{N/N_c}\right)$$

$$\eta(q, N) = \eta_c\left(\frac{q}{N/N_c}\right)$$
[Eq. 1774.4]

The change in pressure of the fluid and the power needed to run the pump or compressor can be determined from the head and efficiency:

$$\Delta P = P_{in} - P_{out} = c_1 \cdot \text{Head} \cdot \langle \rho \rangle$$
[Eq. 1774.5]

$$\text{Power} = c_2 \cdot \eta \cdot q \cdot \text{Head}$$
[Eq. 1774.6]

where

$\langle \rho \rangle = \frac{[\rho(P_{in}, T_{in})] + [\rho(P_{out}, T_{out})]}{2}$	is the average density	lb/ft^3	kg/m^3
P_{in}	is the suction pressure	psi or lbf/in^2	N/m^2
P_{out}	is the discharge pressure	psi or lbf/in^2	N/m^2
T_{in}	is the suction temperature	$^{\circ}\text{R}$	K
T_{out}	is the discharge temperature	$^{\circ}\text{R}$	K
$Power$	is the power extracted by the expander	hp	W
c_1	is a conversion factor for engineering units	$\frac{1}{144} \left(\frac{in}{ft} \right)^2$	
c_2	is a conversion factor for engineering units	$\frac{1}{550} \frac{hp}{ft \cdot lbf/s}$	

The outlet temperature depends on how much of the energy is removed from the fluid. Three different models can be used:

Adiabatic Route:	$\Delta T = T_{out} - T_{in} = \eta \cdot T_{in} \cdot \left(\left(\frac{P_{out}}{P_{in}} \right)^{\frac{\langle \gamma \rangle - 1}{\langle \gamma \rangle}} - 1 \right)$	[Eq. 1774.7]
Polytropic Route:	$\Delta T = T_{out} - T_{in} = T_{in} \cdot \left(\left(\frac{P_{out}}{P_{in}} \right)^{\frac{\langle n \rangle - 1}{\langle n \rangle}} - 1 \right)$	[Eq. 1774.8]
Mollier Route (Isoentropic):	$S(P_{out}, T_{out}) = S(P_{in}, T_{in})$	[Eq. 1774.9]

where

$\langle \gamma \rangle = \frac{[\gamma(P_{in}, T_{in})] + [\gamma(P_{out}, T_{out})]}{2}$	is the average value of γ		
$\gamma = \frac{C_p}{C_v}$	is the ratio of specific heats		
$\langle n \rangle = \frac{[n(P_{in}, T_{in})] + [n(P_{out}, T_{out})]}{2}$	is the average value of n		
$\frac{n}{n-1} = \frac{1}{\eta} \cdot \frac{\gamma}{\gamma-1}$	is the polytropic coefficient		
S	is the specific entropy	$BTU/lb \cdot ^{\circ}\text{F}$	$J/kg \cdot K$

Notes:

- Only a fraction η of the head is converted to power. When using the adiabatic route, the energy that is not converted to power is assumed to be converted to fluid heat. The usual adiabatic temperature decrease is multiplied by a factor $\eta \leq 1$.
- The polytropic route $PV^n = \text{constant}$ can be used to model constant pressure ($n = 0$), constant temperature ($n = 1$), constant enthalpy ($n = \gamma$) and constant volume ($n = \infty$) changes as well as intermediate routes. PIPESIM uses a value of n that is a function of the efficiency (η) and the specific heat ratio (γ). This value can only be used when $\eta < \gamma/(\gamma-1)$.
- In the special case when the efficiency $\eta = 1$, the polytropic coefficient equals the specific heat ratio $n = \gamma$ and the polytropic and adiabatic formulas are the same.

- The Mollier Route can only be used in compositional models; the PIPESIM blackoil model does not calculate entropy.

Engine keywords

See [expander keywords](#)

Multiphase boosting technology

Multiphase boosting technology (also referred to as multiphase pumping technology) for the oil and gas industry has been in development since the early 1980s, and is now rapidly gaining acceptance as a tool to optimize multiphase production systems (Oxley, Ward and Derk 1999). Multiphase boosting has been recognized as a vital technology, preferable to the standard approach of separation, gas compression, liquid pumping and the use of dual flow lines back to the host facility. It is particularly beneficial for the development of satellite fields. Multiphase boosting enables the full (non-separated) well stream to be boosted in a single machine, thus greatly simplifying the production system, resulting in significant cost savings that in many scenarios, have made the development of marginal fields, economic.

Since 1990, thousands of multiphase boosters have been installed worldwide, with the vast majority of the installations based onshore or offshore topsides. Over the years, the development of multiphase boosting has led to two categories of commercial boosters:

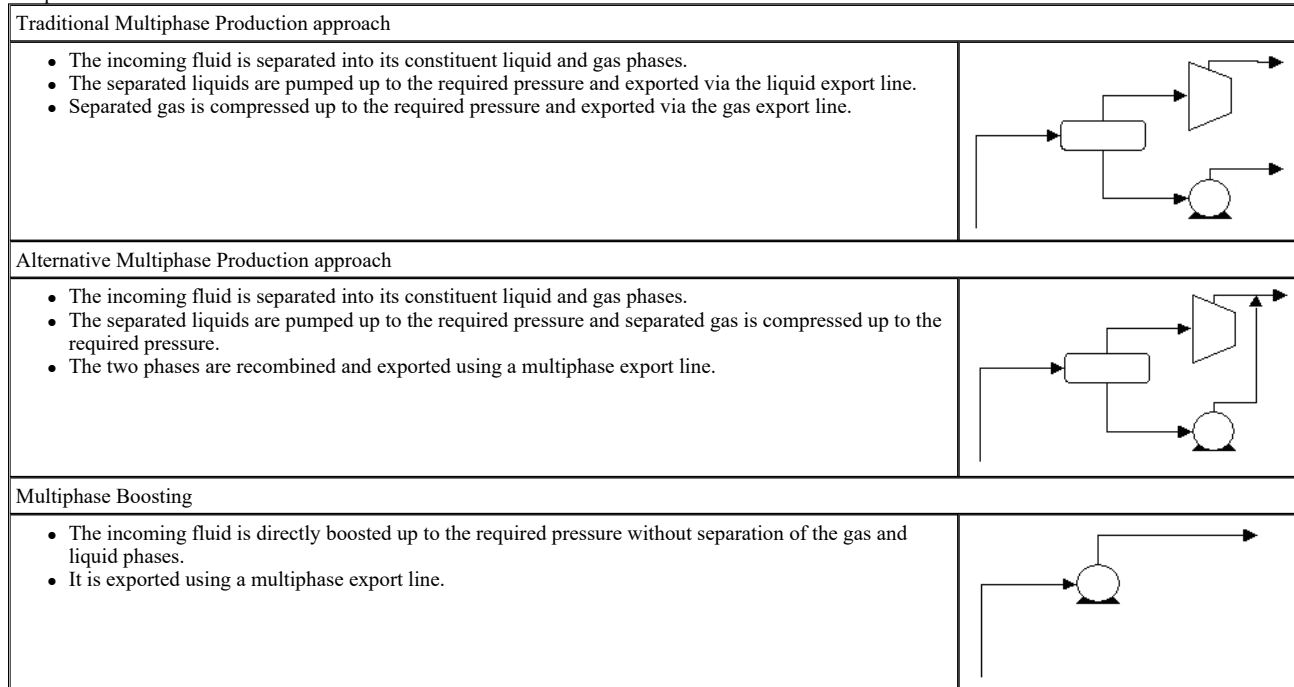
Positive Displacement

The most common types are the Twin screw type & Progressive cavity type multiphase boosters.

Rotodynamic

The most common type is the Helico-axial type multiphase booster.

The figure below depicts the difference between multiphase boosting technology and the more traditional technology of separation, pumping and compression.



Multiphase boosters are pumps/compressors that can accommodate fluids ranging from 100% liquid to 100% gas, and anywhere in between. Although commonly referred to as multiphase pumps, the terminology used in this document is 'multiphase booster' to recognize the fact that 100% gas can also be handled by this equipment (albeit with some restrictions, as outlined in later sections of this topic).

Multiphase boosters are used primarily for the following reasons:

Production Enhancement

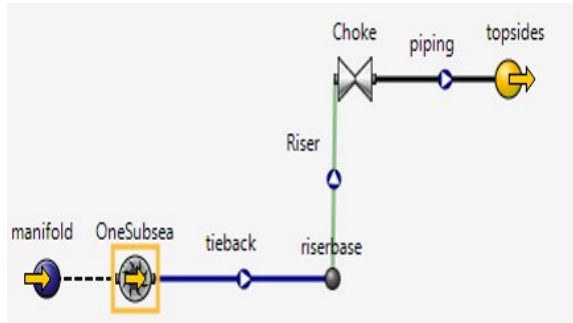
Multiphase boosting helps to accelerate and/or increase hydrocarbon production by lowering backpressure on wells.

Pressure Boosting

Multiphase boosting increases fluid pressure thus enabling the transportation of multiphase fluids over long distances. It also helps to move fluids from low pressure systems to higher pressure systems.

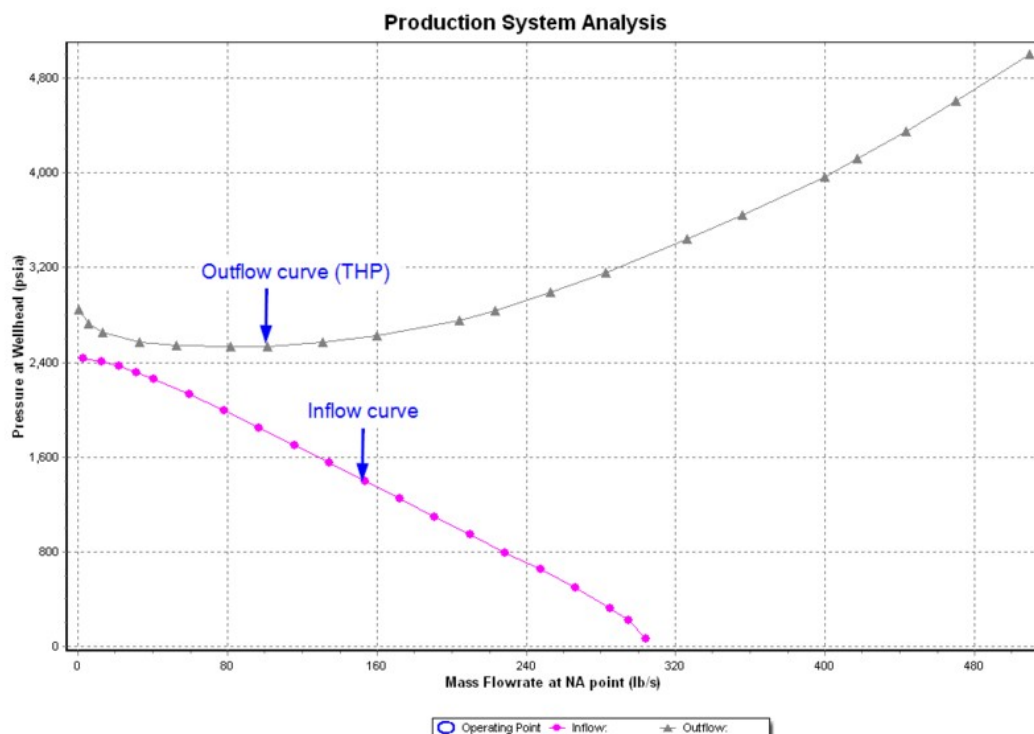
In many cases, Multiphase boosters will deliver the combined benefit of production enhancement and pressure boosting. For example, lowering the backpressure on a well by using a multiphase booster may increase the rate and simultaneously supply the fluid at a higher pressure at the flowline inlet.

To demonstrate the principle of multiphase boosting, take the example of a well which is connected using a flowline and riser to the inlet separator on the host facility, as in the following diagram.



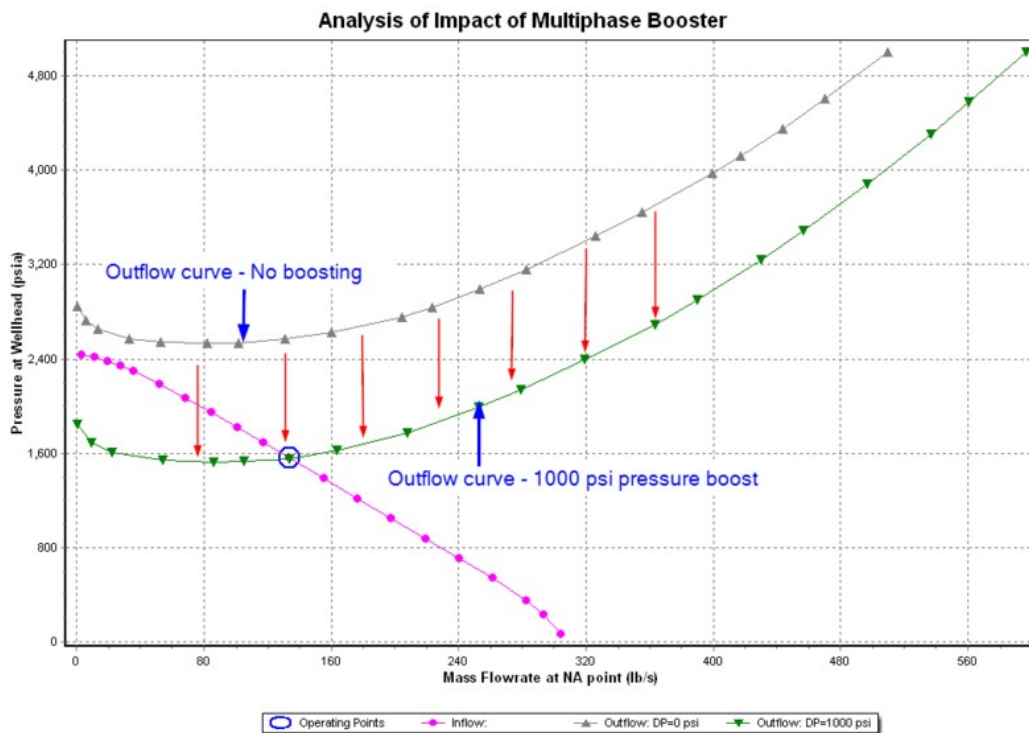
If the Wellhead is selected as the node, the inflow would represent the P-Q (pressure-flowrate) relationship from the reservoir up to the wellhead and the outflow would represent the P-Q relationship downstream of the wellhead, including the multiphase booster, flowline and riser. Both Inflow and Outflow are represented in the Systems plot. The point of intersection of the two curves is the system operating point, for example, the flowing wellhead pressure and production rate the system would operate at. In this example, there is no intersection point, which indicates that the system would not produce at these conditions.

Production system analysis: THP curve and outflow curve



For this example, you can see from the Production System Analysis graphic that the system is incapable of producing naturally. From the THP curve, it is clear that if the back pressure on the well could be lowered, production could be restored. Assuming that you could install a booster directly downstream of the wellhead, that would provide a pressure 'boost' of 1000 psi to the well fluids, the outflow curve could be lowered as shown in the figure below. The system would now produce 134 lb/s (32,412 stb/d of liquid) at a flowing wellhead pressure of 1554 psia. In this example, multiphase boosting has transformed a dead well to one that produces over 30,000 stb/d of fluid.

Production system analysis: the effect of multiphase boosting visualized



Through the type of analysis outlined above, the effect of multiphase boosting on a production system can be easily evaluated, and the requirements of the multiphase booster such as power requirement, speed, etc. can be determined.

Positive displacement multiphase pumps

Positive displacement type pumps work by transferring a definite amount of fluid through a pumping chamber operating at a particular speed. As the fluid is passed from the suction side to the discharge end, differential pressure is added hydrostatically rather than dynamically, which results in these pumps being less sensitive to fluid density than rotodynamic type pumps. This feature makes positive displacement type pumps more attractive for surface installations than rotodynamic type pumps. This is primarily because fluids at surface conditions are at lower pressures and temperatures and tend to have higher gas fractions and a greater tendency for density change than fluids at subsea conditions.

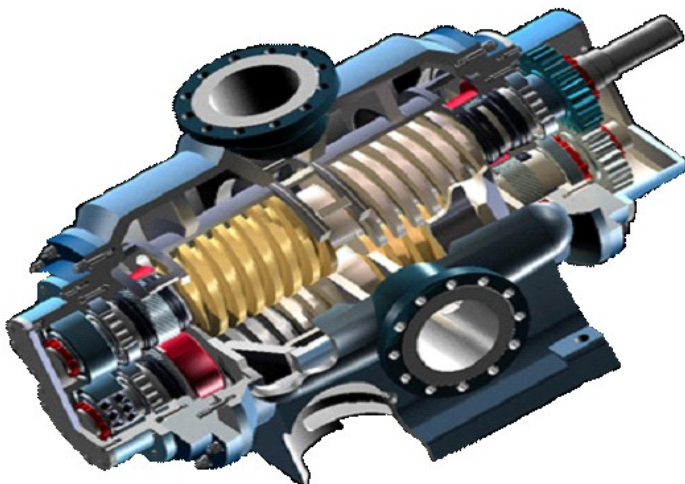
There are four (4) types of Positive displacement pumps: Twin Screw, Progressive Cavity (Single Screw), Piston & Diaphragm, but commercial development has focused mainly on the Twin Screw and Progressive Cavity types.

The majority of positive displacement type multiphase boosters on the market are of the Twin screw type, and they will be the primary focus of this topic.

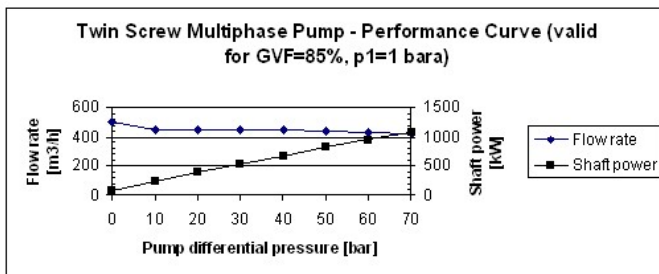
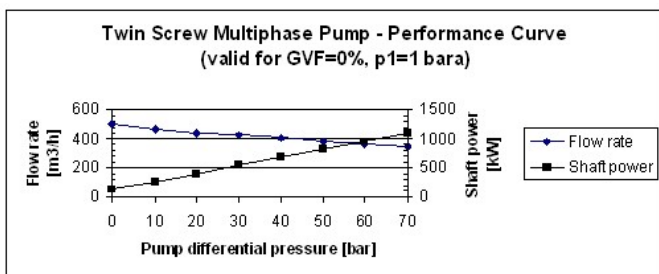
Twin screw type

The twin screw type booster, also referred to as two-spindle screw pump, works on the basis of fluid carried between the screw threads of two intermeshing feed screws and displaced axially as the screws rotate and mesh. The fluid is split into two inlets on opposite sides of the pumps. This equalizes stresses associated with slugging and better enables this type of pump to handle fluctuating inlet conditions. The fluid passes through a chamber created by the twin interlocking screws and moves along the length of the screws to the outlet at the top of the pump. The volumetric rate pumped depends on the screw pitch, diameter and rotational speed.

The following figure shows an example of a twin screw type pump.



It should be noted that, unlike screw type compressors, the volume of the chambers is not reduced from pump suction to pump discharge, for example, there is no in-built compression in the twin screw type multiphase boosters. Pressure buildup in the twin screw type multiphase booster is entirely based on the fact that a definite amount of fluid is delivered into the outlet system with every revolution of the feed screws, and the pressure developed at pump discharge is solely the result of resistance to flow in the outlet system. Additionally, as the fluid makes its way from suction to discharge, gas is compressed and liquid slips back, resulting in a reduction in the volumetric efficiency of the pump. This is due to the development of a pressure gradient across the moving chambers from pump discharge to suction, which causes an internal leakage in the pumping elements. This internal leakage/slip causes the pump net flow to be less than its theoretical capacity, as demonstrated in the pump performance curves shown below.



As can be seen from the typical pump performance curves above, pump flow rate is dependent on pump differential pressure: the higher the pump differential pressure, the higher the internal leakage, and thus the lower the pump flow rate.

The theoretical capacity of the pump, i.e. the flow rate if no internal leakage is present; is the flow rate at zero pump differential pressure. For the pump represented in the pump performance curves above, its theoretical capacity is 500 m³/h. The difference between the theoretical flow rate and the actual flow rate, is the internal leakage, also called 'pump slip'. As an example, for the pump represented in the GVF=0% pump performance curve, the actual flow rate for a pump differential pressure of 40 bar, would be 400 m³/h, and the pump slip would be 100 m³/h (for example, 500 - 400). Given the relative insensitivity of flow rate to differential pressure, especially at higher GVF's, the twin screw multiphase booster is sometimes referred to as a 'constant flow rate' pump. The twin screw pump is good for handling GVF's up to 98% at suction conditions and is the preferred technology for high viscosity fluids.

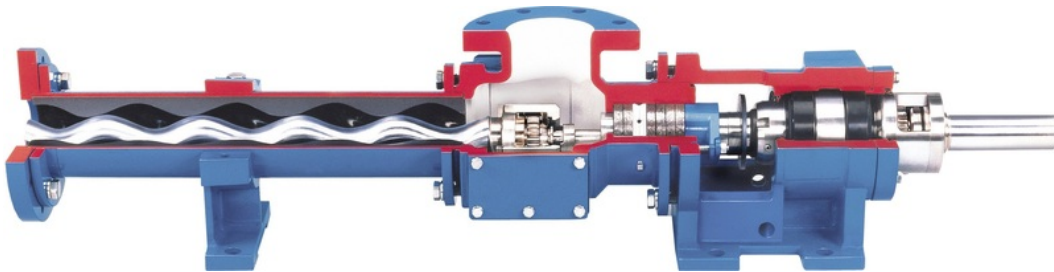
It can be seen from the pump performance curves that pump flow rate is dependent on GVF, but GVF has minimal impact on pump shaft power.

The pump performance curves may suggest that there is an unlimited variety of twin screw multiphase pumps available for an unlimited number of DP-Q (differential pressure - flow rate) combinations; however, in practice, there are several physical limitations that restrict pump options, as below:

- Pump differential pressure is typically limited to 70 bar to avoid excessive deflection of feed screws and possible contact between rotating screws and stator housing
- Pump flow rate (i.e. total volumetric flow rate at pump suction) is presently limited to approximately 2000 m³/h per pump
- Gas volume fraction at pump suction is typically limited to 95% maximum (for GVF > 95%, some form of liquid recirculation is typically required to maintain GVF at suction at 95% maximum)
- Pump inlet pressure and outlet pressures are restricted by casing design pressure and seal design pressure

Progressive cavity type

The progressive cavity type pump (also known as single-rotor screw pump) operates on the basis of an externally threaded screw, also called rotor, turning inside an internally threaded stator. It is the same artificial technology used in wells for production enhancement that was adapted for surface multiphase pumping.



As with the screw type pump, as the rotor rotates within the stator, chambers are formed and filled with fluid that progress from the suction side of the pump to the discharge side of the pump. The continuous seal line between the rotor and the stator helix keeps the fluid moving steadily at a fixed flow rate proportional to the pump rotational speed. Application of the progressive cavity type pump for multiphase boosting has been less widespread than the twin screw type multiphase booster, and flow rates and differential pressures are typically lower than those achievable with the twin screw type (< 30,000 bbl/d total volume).

An example of a progressive cavity type pump for multiphase applications is Moyno's R&M Tri-Phaze® System, which is considered one of the largest; capable of transferring multiphase flows up to 29,000 bbl/day (192 m³/h) at differential pressures up to 300 psi (20.7 bar). Progressive cavity pumps can tolerate high solids content and can be adapted to deliver higher flow rates and differential pressures by installing them in series or parallel arrangements, which increases the complexity (Mirza 1999).

Rotodynamic multiphase pumps

Rotodynamic type pumps work by adding kinetic energy to the fluid, which is then converted to pressure, thus boosting the fluid. The actual increase in pressure is directly proportional to the density of the pumped fluid, for example, the higher the fluid density, the higher the pressure increase. Because of this, dynamic type pumps are more sensitive to fluid density than positive displacement type pumps, and tend to be used in applications with lower maximum gas volume fractions; for example, in subsea applications.

The commercial development of dynamic type multiphase boosters has been focused on the helico-axial type, based on helico-axial hydraulics developed and licensed by Institute François du Pétrole (IFP). For very high gas volume fractions (GVF > 95%), the contra-rotating axial (CRA) machine was specially developed; originally by Framo Engineering AS (now OneSubsea) and Shell.

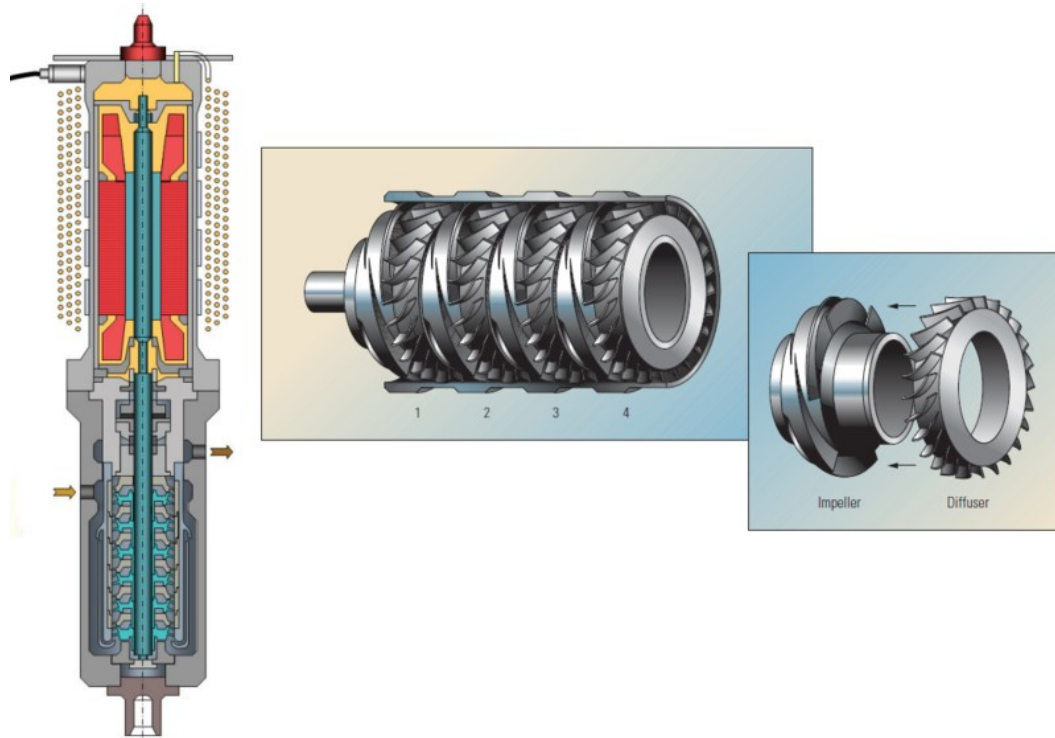
The design of the helico-axial type pump has also concentrated on its driver mechanism. For subsea use, there are electric motor driven units as well as hydraulic turbine driven units. For onshore or offshore topsides applications, other driver types can also be used.

Helico-axial type

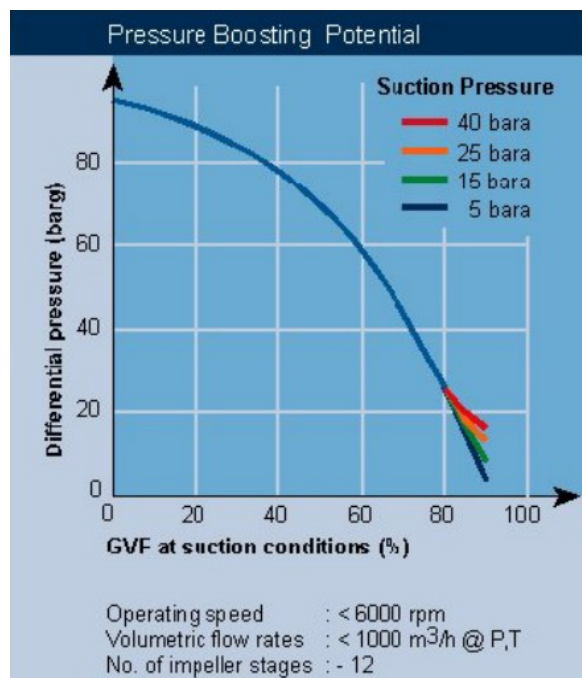
The helico-axial type multiphase booster features a number of individual booster stages, each consisting of an impeller mounted on a single rotating shaft, followed by a fixed diffuser. In essence, the impeller imparts kinetic energy to the fluid, which is converted to pressure in the diffuser. The diffuser homogenizes the fluid and redirects it to the next impeller stage. This interstage mixing prevents separation of the gas-oil mixture, enabling stable pressure-flow characteristics and increased overall efficiency. The impeller blades have a typical helical shape, and the profile of the open type impeller and diffuser blade arrangement are specifically designed to prevent the separation of the multiphase mixture inside the pump (de Marolles and de Salis, 1999).

Helico-axial pumps are able to pump large fluid volumes compared to positive displacement pumps, which is the reason they are installed in the majority of offshore and subsea applications. They can also handle limited amounts of sand but are more prone to stresses associated with slugging. They are good for handling GVF up to 95%.

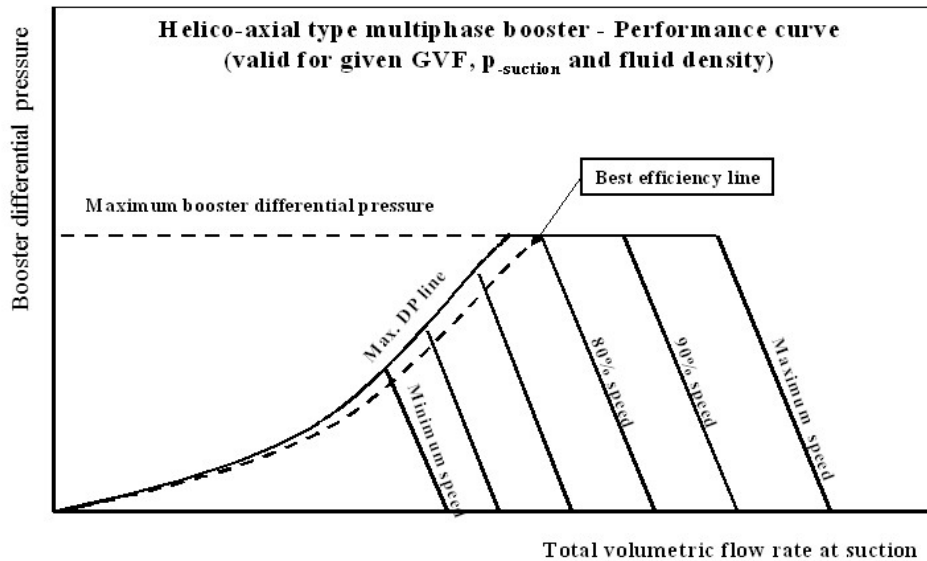
The following figure shows a vertically-configured helico-axial pump and a close-up of four individual stages.



The boosting capabilities of the helico-axial type pump are a function of GVF at suction, suction pressure, speed, number of impeller stages and impeller size.



As can be seen from the above figure, the pressure boosting capability drastically reduces with increasing GVF. Also, for lower speeds or a reduced number of stages, the pressure boosting capability will be less than the maximum shown in the figure. For a given pump with a given number of stages, speed and impeller diameter, pump performance curves can be provided as shown in the figure. These curves are valid for a given GVF at suction, suction pressure and fluid density only. New performance curves will have to be generated for conditions differing from those represented in a specific set of performance curves. See [OneSubsea multiphase booster](#)

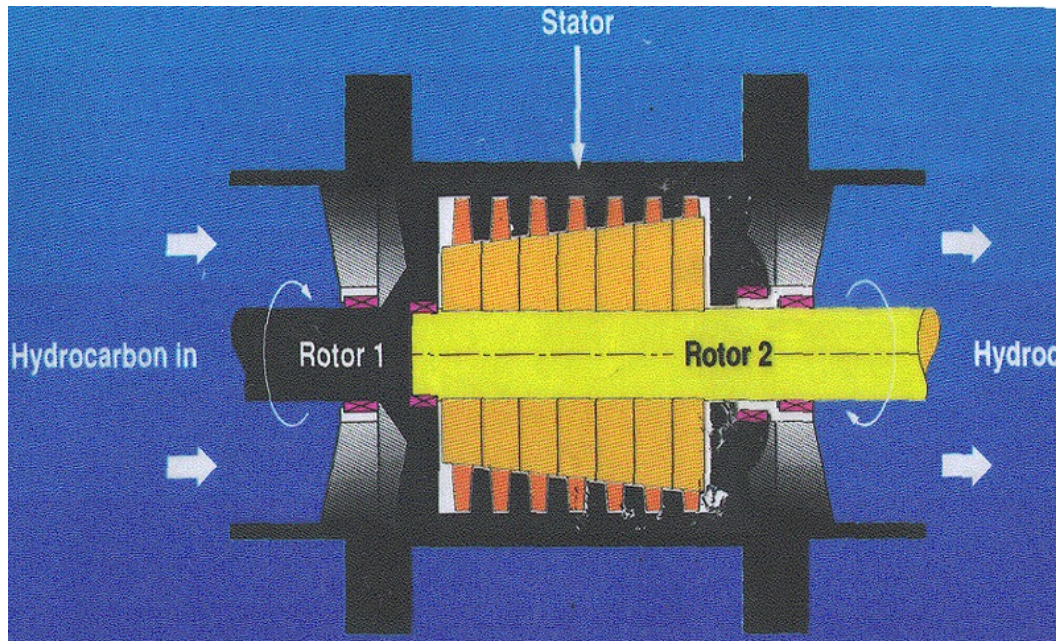


Practical operating limits of the helico-axial type multiphase booster are ([Siep-RTS 1998](#)):

- Pump differential pressure typically limited to 70 bar
- Pump flow rate (for example, total volumetric flow rate at pump suction) presently limited to approximately 1500 m³/h per pump
- Gas volume fraction at pump suction typically limited to 95% maximum
- Pump inlet pressure, 3.4 bara minimum
- Pump outlet pressure restricted by casing design pressure and seal design pressure

Contra-rotating axial type

The CRA operates on the basis of axial compressor theory, but rather than having one rotor and a set of stator vanes, the CRA employs two contra-rotating rotors. The inner rotor consists of several stages mounted on the outside of an inner cylinder. The outer rotor consists of several stages on the inside of a concentric, larger diameter cylinder.



The exact mechanism underlying pressure buildup inside the CRA compressor is not yet fully understood, nor are there sufficiently mature design rules available for the scale-up of CRA performance to larger flow rates.

CRA can handle flow rates of the same order of magnitude as the helico-axial type multiphase booster, however they can achieve significantly lower differential pressures (maximum 20 bar) and efficiencies (approximately 25%) than conventional boosting systems.

Given the wider operating range and greater popularity of helico-axial multiphase boosters in the oil and gas industry, PIPESIM currently focuses its modeling capabilities in the rotodynamic category of multiphase boosters, on the helico-axial type.

Alternative multiphase production approach

The alternative multiphase production approach described in the figure can also be modeled in PIPESIM. This is done using the generic booster option, which splits the fluid into liquid and gas; and pumps the liquid and compresses the gas. Efficiency values for the compressor have been obtained from field data and are available in the help system.

Wet gas compressors

Wet Gas Compressors are a special category of multiphase booster that are used for well streams with high gas volume fractions and small amounts of liquid. Multiphase pumps operating under these conditions are termed "wet gas compressors."

These well streams are often found in marginally economic fields where optimizing production and minimizing cost are critical targets.

The same guidelines that are used to design a multiphase pump, apply for wet gas compression service. But special attention must be paid to the design of the wet gas compression service, to ensure it can handle thermal expansion, quick temperature changes, as well as high equipment temperature due to compression heat generated.

Wet gas compressors can handle GVF's greater than 98% and small volumes of low viscosity fluids. The excessive heat generated by the compression of mostly gas in the well stream often necessitates the installation of a product cooler.



References

Subsea Development from Pore to Process, Oilfield Review, Volume 17, Issue 1, Publication Date: 3/1/2005, Amin Amin, Mark Riding, Randy Shepler, Eric Smedstad Schlumberger and John Ratulowski Shell.

Related links:

[Multiphase boosters](#)

[Generic multiphase booster](#)

[OneSubsea multiphase booster](#)

[OneSubsea wet gas compressor](#)

Guide to multiphase booster efficiencies

Tables 1 and 2 gives guidelines on the (pump and compressor) efficiencies to enter in the generic multiphase booster module, when the generic model is needed to simulate a [Helico-Axial Booster](#) or [Twin Screw Booster](#).

Related links:

[Generic multiphase booster](#)

Helico-axial

The following table gives guidelines on the efficiencies to enter in the generic multiphase booster module to simulate a Helico-Axial multiphase booster.

Table 1. Helico-Axial Multiphase Booster

FLUID GVF (%)	APPROXIMATE PUMP EFFICIENCY (%)	APPROXIMATE COMPRESSOR EFFICIENCY (%) (see 2)

0 (see 1)	10	10-100
10	50	20 -100
20	40	60-100
30	40	80-100
40	30-40	80-100
50	40(50) (see 3)	40 (20) (see 3)
60	40(50) (see 3)	30(20) (see 3)
70	30	60
80	30	50
90	20	70
100	10	100

Related links:

[Generic multiphase booster](#)

Twin screw

The following table gives guidelines on the efficiencies to enter in the generic multiphase booster module to simulate a Twin Screw multiphase booster.

Table 2. Twin Screw Multiphase Booster

FLUID GVF (%)	APPROXIMATE PUMP EFFICIENCY (%)	APPROXIMATE COMPRESSOR EFFICIENCY (%) (see 2)
0	5	20 -100
10	30	20 -100
20	30	70 -100
30	30	80 -100
40	30	90
50	40(50) (see 3)	40(20) (see 3)
60	40	50
70	30	70
80	20	60
90	10	30
100 (see 4)	10	100

Note:

1. Helico-Axial multiphase booster not recommended for pure liquid operations.
2. When using fluids with high liquid content the compressor efficiency has little effect as long as the compressor efficiency is within the range indicated.
3. Two sets of pump and compressor efficiencies are valid for fluids with these gas volume fractions.
4. Twin screw multiphase booster not recommended for pure gas operations

Related links:

[Generic multiphase booster](#)

Progressive cavity pump (PCP)

General

Progressive Cavity Pumps (PCP's) are a special type of rotary positive displacement pump sometimes referred to as "single-screw pumps". Unlike ESP's, PCP performance is based on the volume of fluid displaced and not on the pressure increase dynamically generated through the pump. PCP's are an increasingly common form of artificial lift for low- to moderate-rate wells, especially onshore and for heavy (solid laden) fluids.

Invented in the late 1920's by Rene Moineau, PCP's were not used in the oilfield until the late 1970's. Their use is becoming increasingly common for low- to moderate- rate onshore wells, particularly for heavy-oil and sand-laden fluids. (See [SPE Production Engineering Handbook](#).)

PCP systems have several advantages over other lift methods:

- Overall high energy efficiency (typically 55-75%)
- Ability to handle solids
- Ability to tolerate free gas
- No valves or reciprocating parts
- Good resistance to abrasion
- Low internal shear rates (limits fluid emulsification through agitation)
- Relatively lower power costs (prime mover capacity fully utilized)
- Relatively simple installation and operation (low maintenance)

- Low profile surface equipment and noise levels

Limitations of PCP systems include:

- Maximum production rates of approximately 5000 BPD
- The maximum installation depth is about 4,500 ft.
- Maximum operating temperature of approximately 300 °F.
- Corrosive fluids may damage elastomer and result in higher slippage
- Pump stator may sustain permanent damage if run dry even for short periods
- Rod sting and tubing wear can be problematic for directional and horizontal wells (though downhole drives can be used to avoid this)

Principle of operation

PCP's are most commonly driven by surface mounted electrical motors (Figure 407.1), although downhole electric and hydraulic drive systems are available.

A PCP is comprised of two helical gears, a steel rotating gear called the rotor ("internal gear") and a stationary gear called the stator ("external gear"), which is commonly made of elastomer but may be steel as well. The rotor is positioned inside the stator and rotates along the longitudinal axis (Figure 407.1):

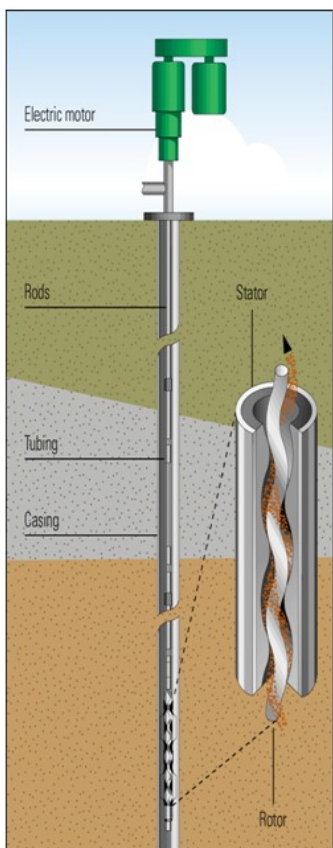


Figure 407.1. PCP Pump Illustration

The volume between the stator and rotor forms a sealed cavity that traps the fluid and as the rotor turns this cavity "progresses" the fluid from the inlet to the outlet of the pump. The volume of the cavity and the rotational speed (N) determine the flow rate achieved by the pump.

The volume of the cavity may be calculated based on geometric parameters. The volume of the cavity is defined by the diameter of the rotor (D_r) times the stator pitch length (L_s) times the eccentricity (e). The eccentricity is defined as the distance between the centerlines of the major and minor diameters of the rotor.

Therefore, the flow rate through the pump can be expressed as:

$$Q = 4eD_rL_sN$$

In field units, P_s , e and D are in feet and N in revolutions per-minute to give a rate in ft³/min. Multiply by 256.46 to convert to BPD. (See [Bellarby](#).) The geometric parameters required for this calculation vary considerably among vendors and are generally not published.

Hydraulic power can then be calculated by:

$$Hhp = 1.7 \times 10^{-5} \Delta PQ$$

Where ΔP is the pressure differential across the pump (psi) and Q is rate (BPD).

In practice, the clearance between the rotor and stator are not perfect due mainly to deformation of the elastomeric stator as a function of pressure, temperature, and wear. This causes some of the fluid to slip back into preceding cavities. Slip increases with increasing pressure and number of stages.

Higher viscosity fluids exhibit less slip.

For simulation purposes, PCP performance curves are generally used. While the format of performance curves varies by vendor, PIPESIM has adopted the format suggested by [ISO 15136-1 \(2009\)](#). PIPESIM provides performance curves from several vendors based on reference conditions (generally water at standard conditions). While catalog performance curves for rotodynamic-type pumps (such as ESP's) are generally consistent with field performance, PCP performance curves vary considerably based on the operating conditions (pressure and temperature) as well as the fluid properties. Therefore, the catalog curves available from within PIPESIM should only be used for preliminary analysis. It is common for PCP's to undergo "bench tests" to generate performance curves for specific pumps at intended operating conditions. It is therefore recommended that these curves be used for more detailed simulation studies.

Viscosity effects

PIPESIM has the option to apply a viscosity correction to reduce slippage effects for higher viscosity fluids. The method of [Karassik et al.](#) is used.

$$\frac{q_{v2}}{q_{v1}} = \sqrt{\frac{v_1}{v_2}} \quad [\text{Eq. 407.1}] \quad (1)$$

Where v = the kinematic viscosity, SSU (Saybold Seconds Universal)

q = the slippage, (BPD)

The range of kinematic viscosity is 100 to 10,000 SSU for this viscosity correction. If the reference fluid is water with kinematic viscosity of about 32 SSU, the equation reduces to:

$$q_{s(v2)} = \sqrt{\frac{32}{v_2} q_{s(\text{curve})}} \quad [\text{Eq. 407.2}] \quad (2)$$

Note: SSU is a viscosity unit that is equal to the measure of the time that 60 cm³ of oil takes to flow through a calibrated tube at a controlled temperature. This should not be confused with the dynamic (absolute) viscosity, unit of cp or Pa·s.

Related links:

[PCP properties](#)

Electrical submersible pumps (ESP)

General

The electric submersible pump (ESP) is perhaps the most versatile of the artificial lift methods. The ESP comprises a down hole pump, electric power cable, motor and surface controls. In a typical application, the down hole pump is suspended on a tubing string hung on the wellhead and is submerged in the well fluid. The pump is close-coupled to a submersible electric motor that receives power through the power cable and surface controls.

ESPs are used to produce a variety of fluids and the gas, chemicals and contaminants commonly found in these fluids. Aggressive fluids can be produced with special materials and coatings. Sand and similar abrasive contaminants can be produced with acceptable pump life by using modified pumps and operation procedures.

ESPs usually do not require storage enclosures, foundation pads, or guard fences. An ESP can be operated in a deviated or directionally drilled well, although the recommended operating position is in a vertical section of the well.

The ESP has the broadest producing range of any artificial lift method ranging from 100 b/d of total fluid up to 90,000 b/d.

ESPs are currently operated in wells with bottom hole temperatures up to 350 degree Fahrenheit. Operation at elevated ambient temperatures require special components in the motor and power cables of sustained operation at high temperatures, and have efficiently lifted fluids in wells deeper than 12,000 ft. System efficiency ranges from 18 to 68%, depending on fluid volume, net lift and pump type.

ESP system components: motor

The ESP system's prime mover is the submersible motor. The motor is a two-pole, three-phase, squirrel-cage induction type. Motors run at a nominal speed of 3,500 rev/min in 60-Hz operation. Motors are filled with a highly refined mineral oil that provides dielectrical strength, bearing lubrication and thermal conductivity. The design and operation voltage of these motors can be as low as 230 volt or as high as 4,000 volt. Amperage requirement may be from 17 to 110 amps. The required horsepower is achieved by simply increasing the length of the motor section. The motor is made up of rotors, usually about 12 to 18 inches (300-460 mm) in length that are mounted on a shaft and located in the electrical field (stator) mounted within the steel housing. The larger single motor assemblies will approach 33 feet (10 m) in length and will be rated up to 400 horsepower, while tandem motors will approach 90 feet (27.5 m) in length and will have a rating up to 750 horsepower. The rotor is also composed of a group of electromagnets in a cylinder with the poles facing the stator poles. The speed at which the stator field rotates is the synchronous speed, and can be computed from the equation:

$$v = \frac{120 f}{M} \quad [\text{Eq. 1774.1}]$$

Where: v is speed in rev/min, f is frequency in cycles/sec and M is number of magnetic poles.

The number of poles the stator contains is determined by the manufacturer. Therefore to change the speed of the stator magnetic field, the frequency will have to change.

Heat generated by the motor is transferred to the well fluid as it flows past the motor housing. Because the motor relies on the flow of well fluid for cooling, a standard ESP should never be set at or below the well perforations or producing interval, unless the motor is shrouded.

Motors are manufactured in four different diameters (series) 3.75, 4.56, 5.40 and 7.8 in. Thus motors can be used in casing as small as 4.5 in. 60-Hz horsepower capabilities range from a low of 7.5 hp in 3.75-in series to a high of 1,000 hp in the 7.38-in series.

Motor construction may be single section or several "tandems" bolted together to reach a specific horsepower. Motors are selected on the basis of the maximum diameter that can be run easily in a given casing size.

ESP system components: pumps

The ESP is a multistage centrifugal pump. Each stage of a submersible pump consists of a rotating impeller and a stationary diffuser. The pressure-energy change is accomplished as the liquid being pumped surrounds the impeller. As the impeller rotates it imparts two rotating motion components to the liquid: one is in a radial direction outward from the center of the impeller (centrifugal force), the other motion moves in a direction tangential to the outside diameter of the impeller. The resultant of these two components is the actual direction of flow. The type of stage used determines the rate of fluid production. The number of stages determines the total design head generated and the motor horsepower required. The design falls into one of two general categories: the smaller flow pumps are generally of radial flow design. As the pumps reach design flows of approximately 1,900 B/D, the design changes to a mixed flow.

The impellers are of a fully enclosed curved vane design, whose maximum efficiency is a function of the impeller design and type and whose operating efficiency is a function of the percent of design capacity at which the pump is operated. The mathematical relationship between head, capacity, efficiency and brake horse power is expressed as:

$$\text{Power} = \frac{q_v H \gamma}{\eta} \quad [\text{Eq. 1774.2}]$$

Where: q_v is the volume flow rate, H is the head, γ is the fluid specific gravity and η is the pump efficiency

The discharge rate of a submersible centrifugal pump depends on the rotational speed (rpm), size of the impeller, impeller design, number of stages, the dynamic head against which the pump is operating and the physical properties of the fluid being pumped. The total dynamic head of the pump is the product of the number of stages and the head generated by each stage.

"Bolt-on" design makes it possible to vary the capacity and total head of a pump by using more than one pump section. However, large-capacity pumps typically have integrated head and bases.

Pump design data

Design Production rate

Desired flowrate through the pump in stock-tank units. The actual flowing quantity will be computed.

Design Outlet Pressure

the required outlet pressure of the PIPESIM model when the pump is installed. It is recommended to only model the well, and no associated flowline or riser, while designing the ESP system. In this case the outlet pressure would then be the wellhead pressure

Static Reservoir Pressure

If you entered a value previously, that value is preserved. However, if this field is empty, the value is taken from the PIPESIM model.

Water cut

If you entered a value previously, that value is preserved. However, if this field is empty, the value is taken from the PIPESIM model.

GOR (or GLR)

If you entered a value previously, that value is preserved. However, if this field is empty, the value is taken from the PIPESIM model.

Pump Depth

The depth at which the pump is to be installed. This is taken from the PIPESIM model if a pump is already installed or can be entered.

Casing ID

The casing size that the pump has to fit into. Usually 3.38 to 11.25 in.

Design Frequency

The frequency/speed that the pump is expected to run at.

Gas Separator Efficiency

The efficiency of the gas separator if installed.

Head factor

Allows the pump efficiency to be factored (default = 1).

Viscosity Correction

All pump performance curves are based on water systems, this option will correct for oil viscosity.

Select Pump

Will use the available data to select suitable pumps from the database. The pump intake conditions will first be computed. The resulting pump list can be sorted by efficiency or Maximum flowrate by selecting the column header. The Manufacturers to select from can be filtered.

Pump parameters

Calculate

Calculate pump performance at the conditions specified.

Stage-by-stage

Perform the stage calculations on a stage-by-stage basis. Default = stage-by-stage.

Selected Pump

The pump selected, by the user, from the design data

No. of Stages required

The computed number of stages for this pump under these conditions.

Pump efficiency @ Design rate

The efficiency of the pump at the design production rate

Pump power required

The power required for this pump to deliver the required flowrate.

Pump intake pressure

The computed pump intake pressure.

Pump discharge pressure

The computed pump discharge pressure.

Head required

The computed pump head required
Liquid density
The computed liquid density at the pump intake
Free gas fraction at inlet conditions
The computed gas fraction.
Pump performance plot
plot performance curves at different speeds
Pump curves
plot standard performance curves
Install pump
Install the pump into the tubing of model. This will replace any existing ESP but not gas lift valves.

ESP database

To simulate an ESP, PIPESIM maintains a database of manufacturers and models from which the user can select. For each model the diameter, minimum and maximum flowrate and base speed are provided. A plot of the ESP's performance is also available. If the required ESP is not in the database, you can easily enter the basic data required for it into the database using the ESP catalog.

Selection

When modeling an ESP, it is important that the correct size (expected design flowrate and physical size) ESP is used. A search facility is available, based on these two parameters, to select the appropriate ESP from the database. The search can, if required, be restricted to a particular manufacturer. Pumps that meet the design criteria will be listed.

Stage-by-stage modeling

Stage-by-stage modeling is selected by selecting the check box next to the calculate button. Alternatively by inserting Engine Keywords ([PUMP STAGECALCS](#)) into the model, using the [EKT](#).

Install a pump

Once the ESP [manufacturer and model](#) has been selected from the [database of common ESP's](#) some parameters can be altered. The performance curves for each model are (normally) based on a Speed of 60Hz and 1 stage.

Design data

Speed

The actual operating speed of the ESP

Stages

The actual number of stages of the ESP

Head factor

Allows the efficiency to be factored (default = 1)

Calculation options

Viscosity Correction

Allow a viscosity correction factor to be applied to take account of changes to the fluid viscosity by the pressure and temperature.

Gas Separator present

Allow a gas separator to be added (automatically) with an efficiency: Separator efficiency - efficiency of an installed gas separator (default = 100% if installed)

Performance table

The data used to predict the performance of the ESP

Standard Curves

The standard performance curves for the ESP - can be printed/exported

Variable Speed Curves

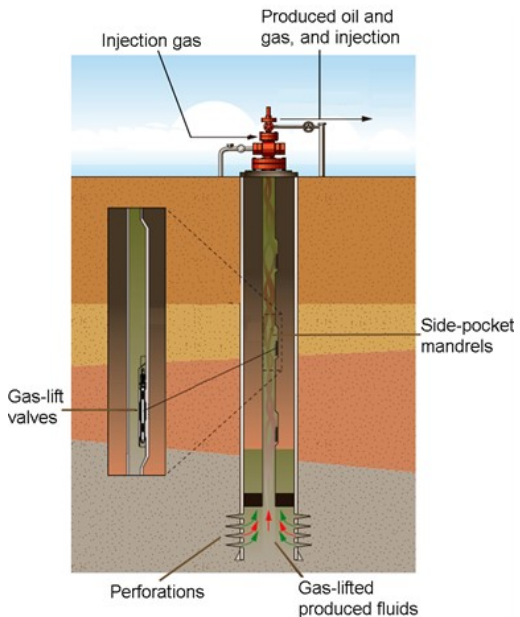
Variable speed curves at 30 - 90 Hz.- can be printed/exported

See also [Design an ESP](#)

Gas lift

The operation of a continuously lifted gas lift well is very similar to that of a naturally flowing well. Gas is continuously injected into the tubing through a gas lift valve at a fixed depth. The only difference between this type of operation and a naturally flowing well is that the gas-liquid ratio changes at some point in the tubing for the gas lift well.

The following image shows a gas lifted well and the related downhole equipment.



Related links:

[Run gas lift tasks](#)

Gas lift injection

The basic goal behind gas lift injection in oil wells is to lower the density of the produced fluid in the tubing. This results in a reduction of the elevational component of the pressure gradient above the point of injection and a lower bottomhole pressure. Lowering the bottomhole pressure increases reservoir drawdown and, thus, the production rate.

The depth at which the operating gas lift valve can be located depends on the available gas injection pressure; the more pressure available, the deeper the injection point. Also, as the depth of the injection gas increases, less injection gas is required to achieve the same bottomhole pressure.

The figure below (*Pressure profile of a gas lifted well*) illustrates the concept of a continuous gas lift well in terms of the pressure values, pressure gradients, well depth, and depth of injection. With the available flowing bottomhole pressure and the natural flowing gradient $(dp/dz)b$, the reservoir fluids ascend only to the point indicated by the projection of the pressure profile in the well. This leaves a partially filled wellbore.

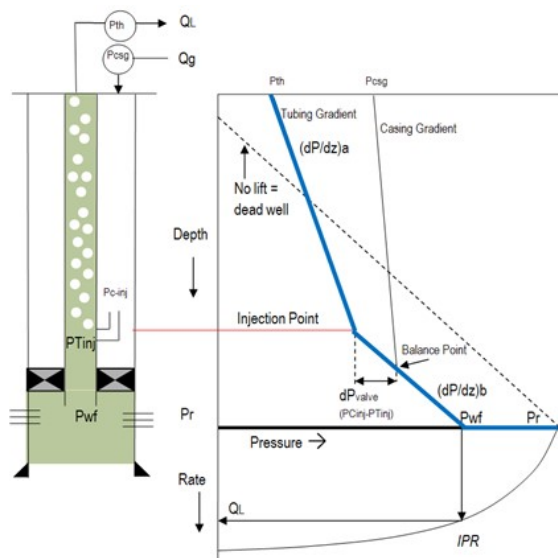


Figure 1774.1. Pressure profile of a gas lifted well

Addition of gas at the injection point reduces the pressure gradient $(dP/dz)a$, allowing the fluids to be lifted to the surface. The intersection of the casing pressure gradient with the lower tubing pressure gradient $(dP/dz)b$ is shown as the *Balance Point*. However, due to the pressure loss across the lift valve, the valve must be located at an injection depth higher than the balance point.

The flow rate is shown at the intersection of the bottomhole flowing pressure and the (sideways projected) IPR curve.

Other valves are required above the working valve to unload the well.

In terms of the overall pressure gradient, the trade-off to the increased presence of gas is an increased frictional pressure gradient. As shown in the figure below (*Gas lift vs. liquid production*), as the rate of injection gas increases, a point is reached where the benefits of reducing the elevational gradient

equals the drawback of increasing the frictional gradient.

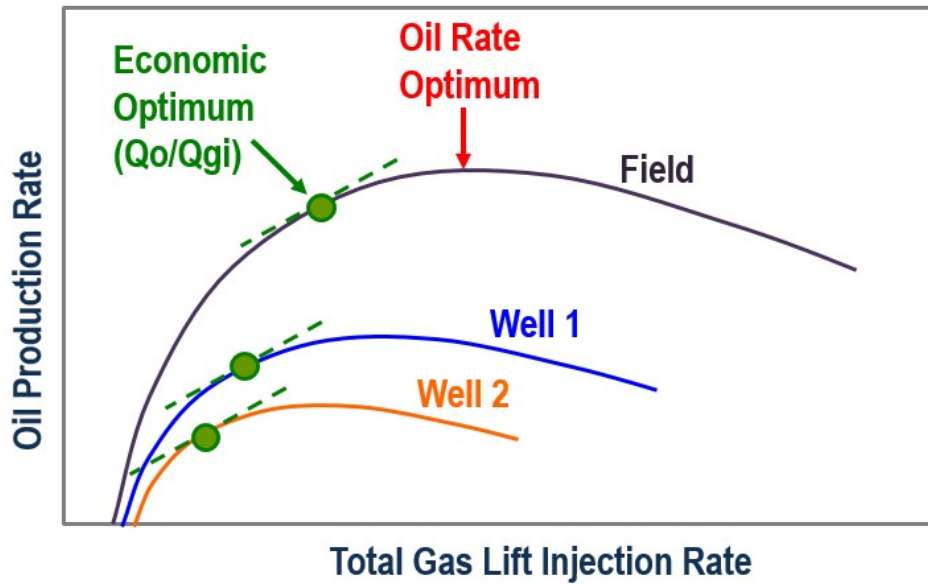


Figure 1774.2. Gas lift vs. liquid production

A further increase of injection gas has a detrimental effect on the overall production rate. This point is called the *optimal unconstrained gas-lift injection rate* and, for individual wells, is relatively easy to calculate.

If a long horizontal flowline is used to connect the wellhead to the delivery point, the frictional effects of the gas are more pronounced, resulting in a lower optimal gas lift value.

Gas lift design

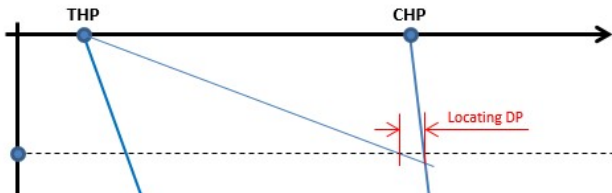
PIPESIM provides three tasks for gas lift design simulations: two design methods for wells with IPO valves, and one design method for wells with PPO valves.

IPO surface close

When you enter data in the Gas lift design dialog box and run a gas lift design simulation using the IPO surface close method, PIPESIM calculates Mandrel spacing and valve sizing. The IPO surface close method uses a user-specified fixed surface close (injection) pressure drop between valves.

PIPESIM performs the following steps.

1. As the starting point for the spacing calculation, PIPESIM calculates the Deepest point of Injection (DIP) and gets results that it uses as the starting point for the spacing calculation.



2. PIPESIM locates the top valve using an unloading gradient line from the wellhead to the point where the line meets the casing pressure line.
3. PIPESIM reads the depth of valve 1 (the top valve).
4. PIPESIM calculates the required gas to unload a section of the tubing above valve 1.
5. Based on the calculated gas rate, PIPESIM computes the required port size using the Thornhill-Craver equation.

$$Q_{gi} = \frac{155.5 C_d (A) P_1 \sqrt{2(g) \left(\frac{k}{k-1} \right) \left[(F_{du})^{\frac{2}{k}} - (F_{du})^{\frac{k+1}{k}} \right]}}{\sqrt{\gamma_g(T_1)}}$$

where

Q_{gi} = gas flowrate at standard conditions, Mscf/D^{-1}
 C_d = discharge coefficient
 A = area of orifice or choke open to gas flow, in^2
 P_1 = gas pressure upstream of an orifice or choke, psia
 P_2 = gas pressure downstream of an orifice or choke, psia
 g = acceleration because of gravity, ft/sec^{-2}
 k = ratio of specific heat C_p/C_v
 T_1 = gas temperature upstream of an orifice or choke, psia
 F_{du} = pressure ratio, P_2/P_1 , absolute units

$$F_{cf} = \left(\frac{2}{k-1} \right)^{\frac{k}{k-1}} = \text{critical flow pressure ratio}$$

6. PIPESIM performs the following pressure calculations at the top valve depth:

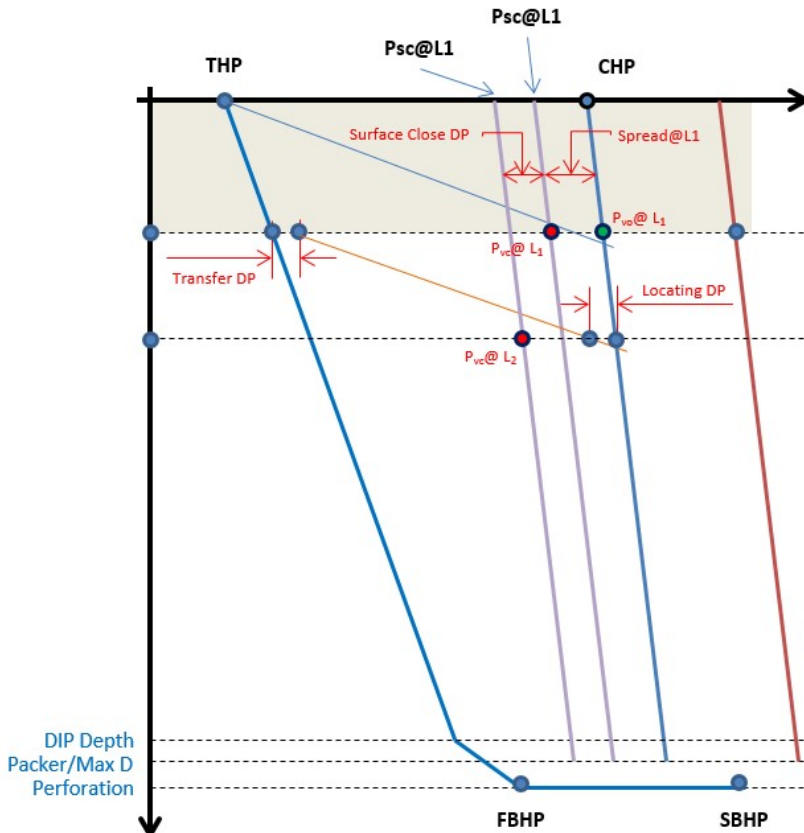
- Opening pressure
- Dome pressure
- Closing pressure
- Spread

Note: The opening pressure for the top valve is equal to the casing pressure at the valve depth.

7. PIPESIM draws a line parallel to the *CHP* line from the wellhead to the packer.

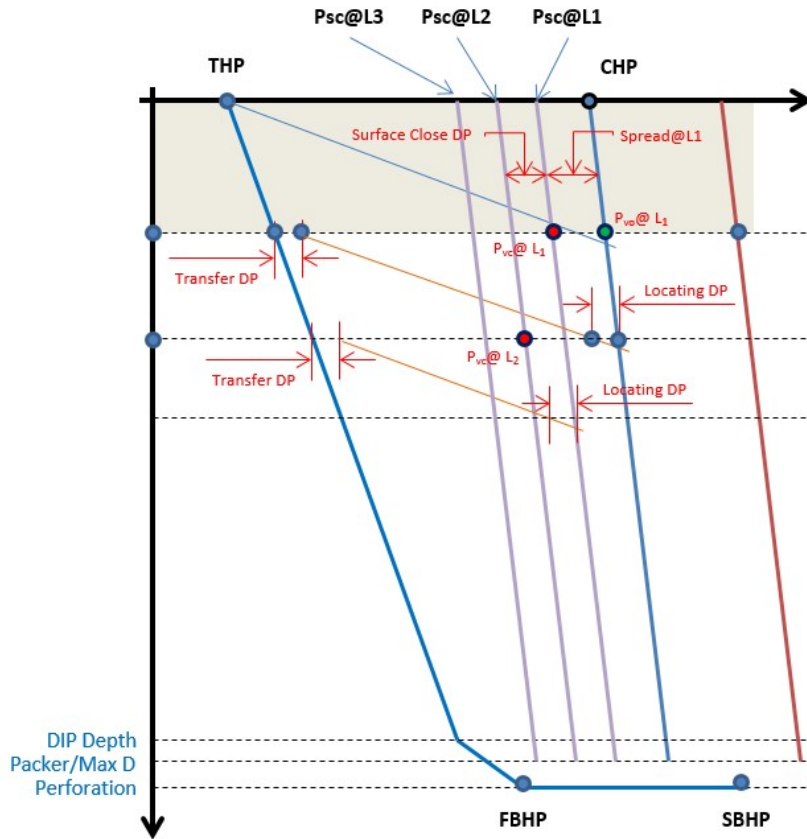
This line passes through the closing pressure location for valve 1.

8. PIPESIM locates the second valve based on the gradient line starting from the transfer point at the top valve depth underneath the *CHP* line within the *Locating DP* margin.



9. PIPESIM draws a line parallel to the surface close location for valve 1 by using the known surface closing pressure DP (*Surface Close DP*).

10. PIPESIM draws a line at the second valve depth that goes to the surface close pressure for valve 1.



11. PIPESIM repeats spacing for other valves in the same way until the maximum depth is reached.

Note: Maximum depth is determined by the deepest injection point computation performed at the starting point of the design.

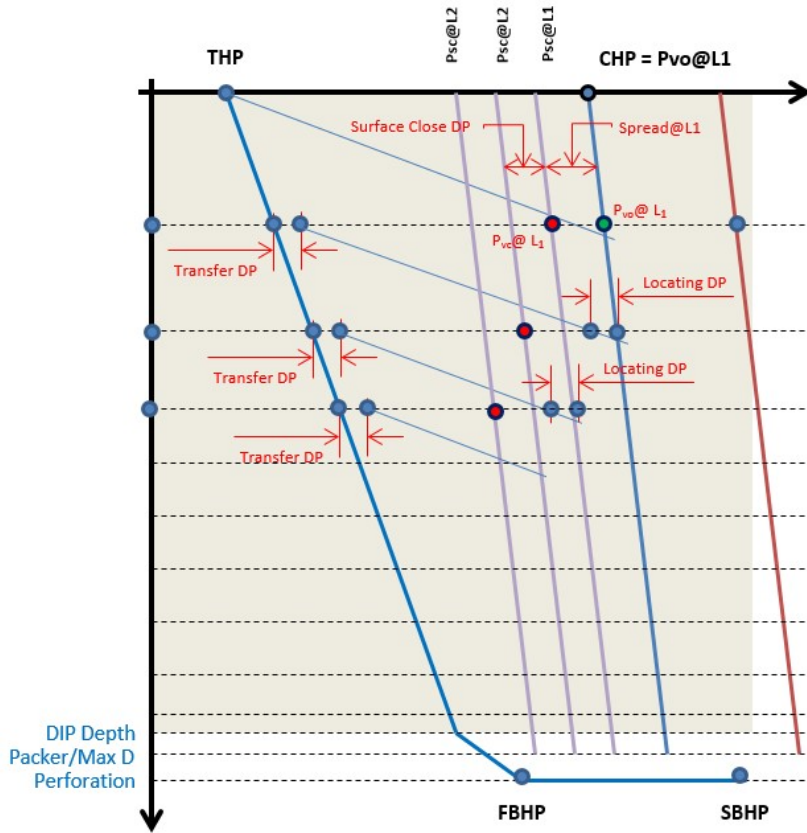
At each valve location, PIPESIM computes the gas rate to unload the section of the tubing above the valve, computes the port size using the Thornhill-Craver equation, and selects the valve from the gas lift valve DP in PIPESIM.

12. After selecting each valve, the PIPESIM performs the following pressure computations at the valve depth:

- Opening pressure
- Dome pressure
- Closing pressure
- Spread

Note:

- While performing pressure calculations for the top valve, PIPESIM uses the known valve opening pressure to compute the remaining pressures.
- For the remaining valves, PIPESIM uses the known closing pressure to calculate the dome and opening pressure at each valve depth.
- For IPO surface close design, the surface closing pressure drops between valves are fixed according to the user-entered value in the gas lift design task (value entered in the Surface close DP field in the Design Bias group in the Gas lift design dialog box).



For information on how PIPESIM calculates valve pressures, refer to [Pressure computations for IPO valves](#).

Related links:

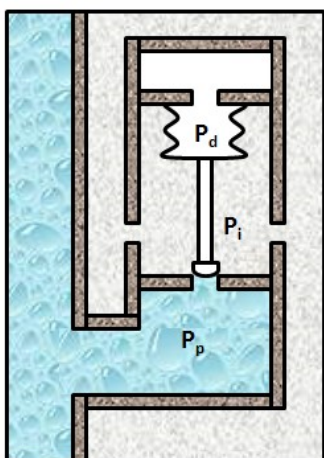
[Run gas lift design](#)

Pressure computations for IPO valves

PIPESIM uses mathematical equations to compute the opening, dome, and closing pressures for the IPO valves used in gas lift design simulations.

Opening, dome, and close pressures

PIPESIM calculates the pressures for the IPO valves.



- Opening pressure (P_v) – pressure in the casing at the instance before the valve opens from its closed position

Force balance results in a closed valve condition.

PIPESIM uses the following equation to calculate the opening pressure:

$$P_{vo} = \frac{P_d - P_p R}{1 - R}$$

- Dome pressure (P_d) – pressure exerted on the bellow due to the nitrogen charge in the dome of the valve

PIPESIM uses the following equation to calculate the dome pressure:

$$P_d = P_{vo}(1 - R) + P_p R$$

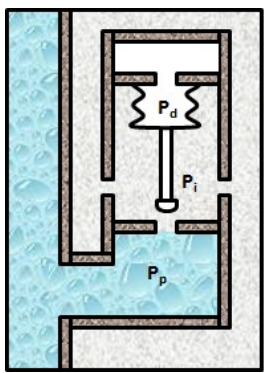
$$P_d @ L_n = P_{vo} @ L_n (1 - R @ L_n) + P_p @ L_n R$$

- Closing pressure (P_{vc}) – pressure at the instance the valve is about to close from its open position

Force balance results in an open valve condition.

$$P_{vc} = P_d$$

$$P_{vc} @ L_n = P_d @ L_n$$



- Spread – difference between the opening pressure and the closing pressure at the valve location

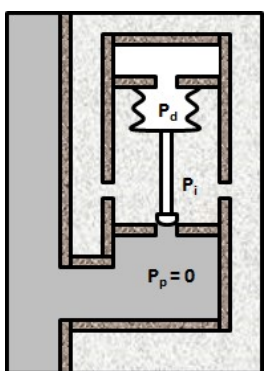
$$\text{Spread (DP)} = P_{vo} - P_{vc}$$

Ptrd

PIPESIM calculates the Ptrd and spread for the IPO valves.

- Ptrd is the valve dome pressure at the test rack condition entered by the user in the Gas lift design dialog box.

PIPESIM can derive Ptrd for each valve by using the dome pressure and temperature at the valve depth as well as the test rack temperature.



$$P_{tro} = \frac{P_{trd}}{(1 - R)}$$

IPO surface close kickoff pressure handling

The kickoff pressure is the maximum possible injection pressure to kick off the well.

You can use the following information to determine the value to enter for the top valve placement.

Valve #	Without KOP	With KOP	Comparison
Top	Top valve location is at the intersection of the CHP line with the static gradient by locating DP margin CHP line is set as the Pso@L1 line	Top valve location is at the intersection of the KOP line with the static gradient by locating DP margin CHP line is the Pso@l line	Valve is placed at a different location (Pso@L1 remains the same)
2	Second valve location is also at the intersection of the CHP line with the static gradient by locating DP margin	Second valve location is also at the intersection of the CHP line with the static gradient by locating DP margin	Same location
3	Third valve located DP is as per the Psc@L1 line	Third valve located DP is as per the Psc@L1 line	Same location
4	Forth valve located DP is as per the Psc@L2 line Note: The Psc@L2 line is shifted left of Psc@L1 by a fixed surface close pressure drop between valves.	Forth valve located DP is as per the Psc@L2 line Note: The Psc@L2 line is shifted left of Psc@L1 by a fixed surface close pressure drop between valves.	Same location
5	Follows the sequence as defined in the preceding valves	Follows the sequence as defined in the preceding valves	Same location

Surface piping and equipment handling

PIPESIM calculates the IPO design based on surface equipment location.

Valve computation	No surface equipment (branch ends at wellhead)	With surface equipment (branch ends beyond wellhead)
DIP computation	DIP computation takes full flow-path from reservoir to wellhead	DIP computation takes full flow-path from reservoir to the end of surface equipment
Top valve spacing starting point calculation	THP point = Production Outlet Pressure Top valve spacing gradient starts at THP	THP Point \neq Production Outlet Pressure THP point on the gas lift plot is computed as follows: The following computations are derived from the DIP result: <ul style="list-style-type: none"> • Pout • THP at the wellhead node • Surface ΔP_t (Pout-THP) • Surface ΔP_f (friction component) E (delta elevation between wellhead and outlet) • ΔE (delta elevation between wellhead and outlet) • Unloading elevation ΔP ($UE\Delta P$) for surface section $\rightarrow UE\Delta P = \Delta E$ Unloading gradient (kill fluid gradient) • Total shift = $\Delta P_t + UE\Delta P$ Spacing gradient starts at THP + Total shift
Plot	Design Plot starts at wellhead	Design Plot starts at wellhead
Flow-path for gas rate computation	Consider partial flow-path from valve depth to wellhead	Consider partial flow-path from valve depth to end of surface equipment

Known valve spacing handling

PIPESIM determines valve spacing differently if you entered a value in the Current field on the Gas lift design dialog box.

Valve computation	Spacing not known	Spacing known
DIP computation	Compute DIP for optimum valve depths	Compute DIP for known valve depths
Spacing for valves	Perform spacing calculation as explained Draw horizontal depth line at the valve depth	Skip spacing calculation Draw horizontal depth line at the known depth
Static gradient line display	Draw downward and display as follows: <ul style="list-style-type: none"> • Start: Wellhead (or previous valve depth shifted right of Pp by transfer DP) 	Draw upward and display as follows: <ul style="list-style-type: none"> • Start: Note the intersection of the appropriate injection pressure line and the known depth line. Then, shift left by locating DP.

- | | | |
|--|--|--|
| | <ul style="list-style-type: none"> • End: Appropriate injection pressure line with locating DP margin | <ul style="list-style-type: none"> • End: At the intersection of the gradient line and the depth line of the previous valve (wellhead depth line for the top valve), if the gradient line meets the Y-axis before reaching the depth line, it terminates there. |
|--|--|--|

Note: The pressure and port size computations are based on the standard methods for both cases.

Minimum valve spacing handling

PIPESIM determines the minimum distance for valve spacing (TVD) differently if you entered a value in the Minimum valve spacing field on the Gas lift design dialog box.

Valve computation	Computed Valve \geq Minimum Spacing	Computed Valve $<$ Minimum Spacing
Spacing for valves (except for the last valve)	Perform spacing calculation based on the selected design method If Δ TVD (current TVD - last TVD) \geq minimum spacing, continue with spacing as computed.	Perform spacing calculation based on the selected design method If Δ TVD (current TVD - last TVD) $<$ minimum spacing, ignore the computed spacing by placing the valve at a location that makes Δ TVD equal to the minimum spacing.
Spacing for the last valve (i.e. the operating valve)	Not applicable	Ignore minimum spacing and use one of the following guidelines to place the last operating valve <ul style="list-style-type: none"> • Place the valve at the deepest injection point (DIP) if the DIP is below the last valve by at least 50 ft. • Make the previous valve the operating valve

Note: The pressure and port size computations are based on the standard methods for both cases.

Liquid level condition handling

PIPESIM calculates the top valve location based on the location of the liquid relative to the surface.

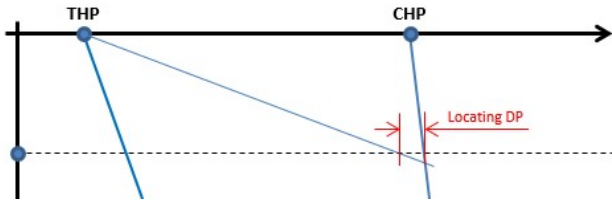
Valve computation	Assume liquid to surface	Assume liquid is not at surface
Compute actual liquid level top	Liquid level top TVD is computed as follows: $TVD = \frac{\text{Reservoir pressure}}{\text{Unloading fluid gradient}}$	If the computed top extends above the wellhead, PIPESIM sets the liquid level top at the wellhead depth. Note: PIPESIM computes the liquid level top even if the user selects the Liquid level top option Assume liquid to surface or Specify liquid level on the Gas lift design dialog box.
Draw liquid level gradient line	PIPESIM draws a straight line using the kill fluid gradient beginning at the mid perforation depth (TVD) at the reservoir pressure and ending at the pressure or depth axis, depending on which axis comes first	
Top valve locating unloading gradient	Starts from the THP location	<ul style="list-style-type: none"> • If the user specified a liquid level, PIPESIM starts the locating gradient for the top valve at the depth axis (0 pressure, specified liquid level TVD) • If the user did not specify a liquid level, PIPESIM uses one of the following methods to determine the starting point of the locating gradient: <ul style="list-style-type: none"> ◦ Liquid level top if it is below the wellhead ◦ THP if the liquid level is at or above the wellhead
Gas rate computation at valve location		<ul style="list-style-type: none"> • If the liquid level top is below the partial flow-path for the valve location, the gas rate is set at 0 • If the liquid level top is at or above the partial flow-path, PIPESIM computes the gas rate
Port size computation		<ul style="list-style-type: none"> • If the required gas rate is 0, PIPESIM selects the lowest port size based on the filter criteria that the user entered under the Valve Selection Filter group on the Gas lift design dialog box

IPO PT min/max

When you enter data in the Gas lift design dialog box and run a gas lift design simulation using the IPO PT Min/Max Design spacing method option, PIPESIM calculates Mandrel spacing and valve sizing. The IPO PT Min/max method uses a calculated surface close (injection) pressure drop between valves (with a user-specified minimum).

PIPESIM performs the following steps.

- As the starting point for the spacing calculation, PIPESIM calculates the Deepest point of Injection (DIP) and gets results that it uses as the starting point for the spacing calculation.



2. PIPESIM locates the top valve using an unloading gradient line from the wellhead to the point where the line meets the casing pressure line.
3. PIPESIM reads the depth of valve 1 (the top valve).
4. PIPESIM calculates the required gas to unload a section of the tubing above valve 1.
5. Based on the calculated gas rate, PIPESIM computes the required port size using the Thornhill-Craver equation.

$$Q_{gi} = \frac{155.5 C_d(A) P_1 \sqrt{2(g) \left(\frac{k}{k-1} \right) \left[(F_{du})^{\frac{2}{k}} - (F_{du})^{\frac{k+1}{k}} \right]}}{\sqrt{\gamma_g(T_1)}}$$

where

Q_{gi} = gas flowrate at standard conditions, Mscf/D^{-1}
 C_d = discharge coefficient
 A = area of orifice or choke open to gas flow, in^2
 P_1 = gas pressure upstream of an orifice or choke, psia
 P_2 = gas pressure downstream of an orifice or choke, psia
 g = acceleration because of gravity, ft/sec^{-2}
 k = ratio of specific heat C_p/C_v
 T_1 = gas temperature upstream of an orifice or choke, psia
 F_{du} = pressure ratio, P_2/P_1 , absolute units

$$F_{cf} = \left(\frac{2}{k-1} \right)^{\frac{k}{k-1}} = \text{critical flow pressure ratio}$$

6. PIPESIM performs the following pressure calculations at the top valve depth:

- o Opening pressure
- o Dome pressure
- o Closing pressure
- o Spread

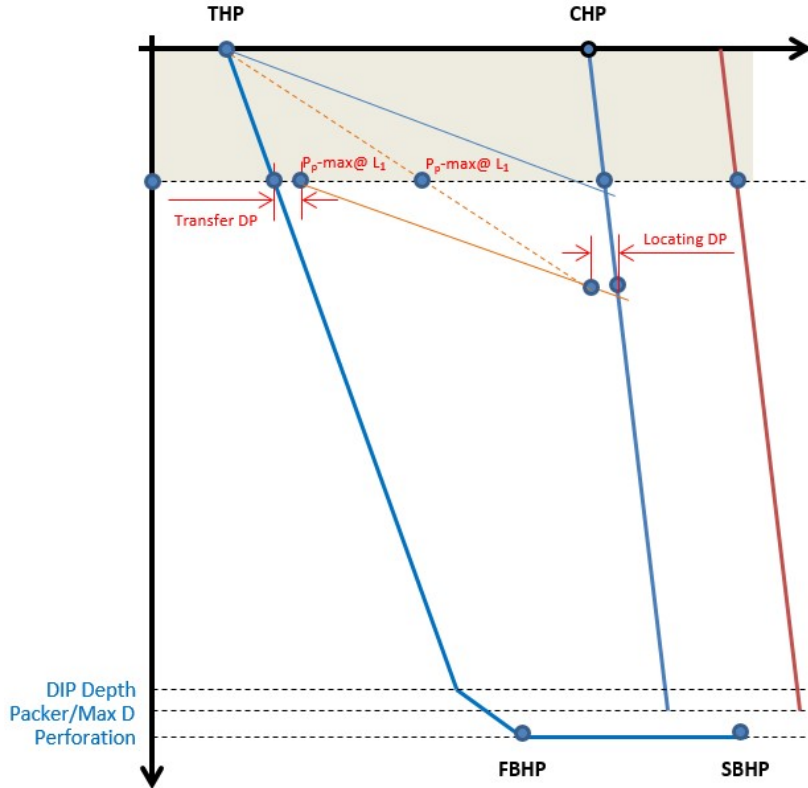
Note: The opening pressure for the top valve is equal to the casing pressure at the valve depth.

7. In order to locate the second valve, PIPESIM determines the transfer point that is to the right of the tubing pressure at the valve 1 location by the P_{pmin} margin. This is called P_{pmax} at the top valve location.
 - a. From this point, PIPESIM draws a static gradient line that crosses the injection pressure line. A Locating DP margin is set to identify the location on the static gradient line to the left of the injection pressure line.
 - b. From this point, a dotted line is drawn that connects the THP and the intersection of this dotted line with the depth line of the top valve. This is identified as P_{pmax} at the top valve location.
 - c. Based on P_{pmin} and P_{pmax} at the top valve location, PIPESIM calculates the production pressure effect (PPE) using the following three equations:

$$TPE@L_1 = (P_{pmax}@L_1 - P_{pmin}@L_1)(TPEF@L_1)$$

$$TPEF@L_1 = \left(\frac{R}{1-R} \right) @ L_1$$

$$R = \left(\frac{A_p}{A_b} \right) @ L_1$$



8. PIPESIM computes the surface opening pressure for valve 2 using the following equations:

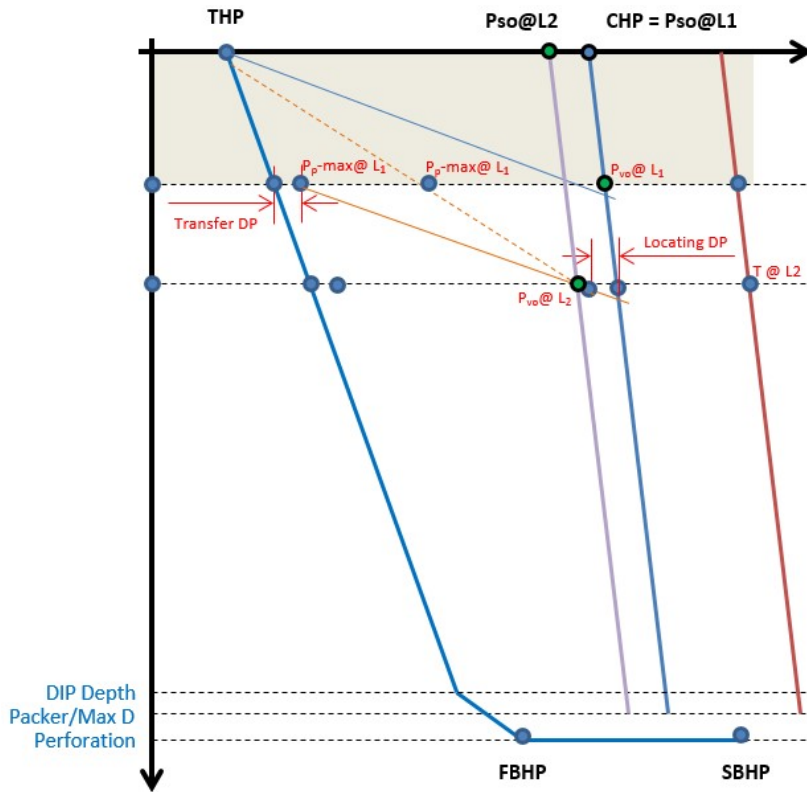
$$P_{so}@L_2 = P_{so}@L_1 - TPE@L_1$$

$$P_{so}@L_1 = CHP$$

Note:

- o The surface opening pressure $P_{so} @ L1$ for valve 1 is the same as CHP.
- o The *Locating DP* intersecting static gradient line is not the valve depth.

9. Once the P_{so} at valve 2 is known, PIPESIM draws a line parallel to the *CHP* line as shown in the image. The point where the $P_{so} @ L2$ line crosses the static gradient line, PIPESIM draws a static gradient line that crosses the injection pressure line. A *Locating DP* margin is set to identify the location on the static gradient line to the left of the injection pressure line. This location is identified as the depth for valve 2. This intersection point is also the opening pressure for valve 2.



10. PIPESIM then calculates the operating pressure at the valve 2 location by using the following formula:

$$P_o@L_2 = P_i@L_2 - TPE@L_1$$

Note: PIPESIM uses the following equation to calculate the operating pressure for all subsequent valves.

$$P_o@L_n = P_i@L_n - TPE@L_{(n-1)}$$

- a. PIPESIM calculates the required gas to unload a section of the tubing above valve 2.
- b. Based on the calculated gas rate, PIPESIM computes the required port size.

11. PIPESIM repeats Step 7 – Step 10 to locate and size valve 3 and all remaining valves until the maximum depth is reached.

Note:

- o While PIPESIM used the CHP line as a reference for Locating DP for valves 1 and 2, PIPESIM uses the $P_{so}@L_2$ line as the reference point for locating valve 3. For the valve 4 location, PIPESIM uses $P_{so}@L_3$ as the reference point. PIPESIM uses this process for the remaining valves.
- o PIPESIM uses the following equations:

$$TPE@L_{n-1} = (P_{p\max}@L_{n-1} - P_{p\min}@L_{n-1})(TPEF@L_{n-1})$$

$$TPEF@L_{n-1} = \left(\frac{R}{1-R} \right) @ L_{n-1}$$

$$R = \left(\frac{A_p}{A_b} \right) @ L_{n-1}$$

- o PIPESIM computes the $P_{so}@L_3$ line using the same formula used to calculate $P_{so}@L_2$. PIPESIM continues this computation for all remaining valves.

$$P_{so}@L_3 = P_{so}@L_2 - TPE@L_2$$

12. After selecting each valve, PIPESIM performs the following pressure computations at the valve depth:

- o Opening pressure
- o Dome pressure
- o Closing pressure
- o Spread

Note:

- While performing pressure calculations for a valve, PIPESIM uses the known valve opening pressure to compute the remaining pressures.
- For the IPO PT Min/max design, PIPESIM calculates the surface closing pressure drops between valves during the design. However, you can control this by specifying the minimum value in the Gas lift design dialog box Design Bias group Minimum Surface open DP field.

Related links:

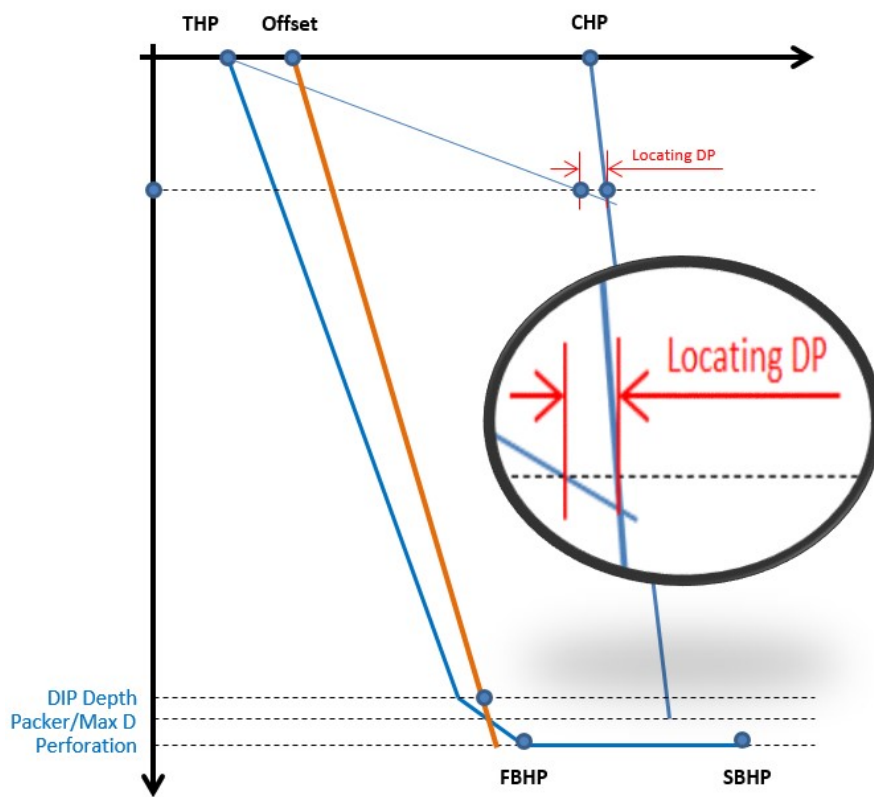
[Run gas lift design](#)

PPO design

When you enter data in the Gas lift design dialog box and run a gas lift design simulation using the PPO design method, PIPESIM calculates Mandrel spacing and valve sizing. The PPO method uses a transfer gradient line as the design production pressure line. This method is normally used for gas lift designs with production pressure operated (PPO) valves.

PIPESIM performs the following steps.

1. As the starting point for the spacing calculation, PIPESIM calculates the Deepest point of Injection (DIP) and gets results that it uses as the starting point for the spacing calculation. PIPESIM locates the top valve using an unloading gradient line from the wellhead to the point where the line meets the casing pressure line.
2. PIPESIM draws the transfer gradient line starting from the surface *Offset* to the operating valve DP.
3. PIPESIM locates the top valve using an unloading gradient line from the wellhead to the point where the line meets the casing pressure line.



4. PIPESIM reads the depth of valve 1 (the top valve).
5. PIPESIM calculates the required gas to unload a section of the tubing above valve 1.
6. Based on the calculated gas rate, PIPESIM computes the required port size using the Thornhill-Craver equation.

$$Q_{gi} = \frac{155.5 C_d (A) P_1 \sqrt{2(g) \left(\frac{k}{k-1} \right) \left[(F_{du})^{\frac{2}{k}} - (F_{du})^{\frac{k+1}{k}} \right]}}{\sqrt{\gamma_g(T_1)}}$$

where

- Q_{gi} = gas flowrate at standard conditions, Mscf/D^{-1}
- C_d = discharge coefficient
- A = area of orifice or choke open to gas flow, in^2
- P_1 = gas pressure upstream of an orifice or choke, psia
- P_2 = gas pressure downstream of an orifice or choke, psia
- g = acceleration because of gravity, ft/sec^{-2}
- k = ratio of specific heat C_p/C_v
- T_1 = gas temperature upstream of an orifice or choke, psia
- F_{du} = pressure ratio, P_2/P_1 , absolute units

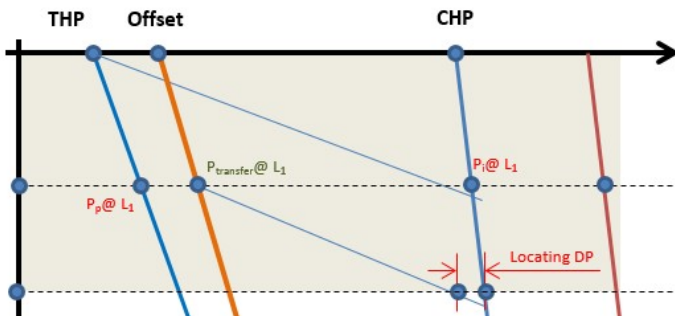
$$F_{cf} = \left(\frac{2}{k-1} \right)^{\frac{k}{k-1}} = \text{critical flow pressure ratio}$$

7. PIPESIM performs the following pressure calculations at the top valve depth:

- Opening pressure
- Dome pressure
- Closing pressure
- Spread

Note: The opening pressure for the top valve is equal to the casing pressure at the valve depth.

8. PIPESIM locates the second valve based on the gradient line starting from the transfer point at the intersection of the top valve depth with the transfer gradient line and locates the valve where the gradient line meets the CHP line within the *Locating DP* margin.



9. PIPESIM repeats spacing for other valves in the same way until the maximum depth is reached.

Note: Maximum depth is determined by the deepest injection point computation performed at the starting point of the design.

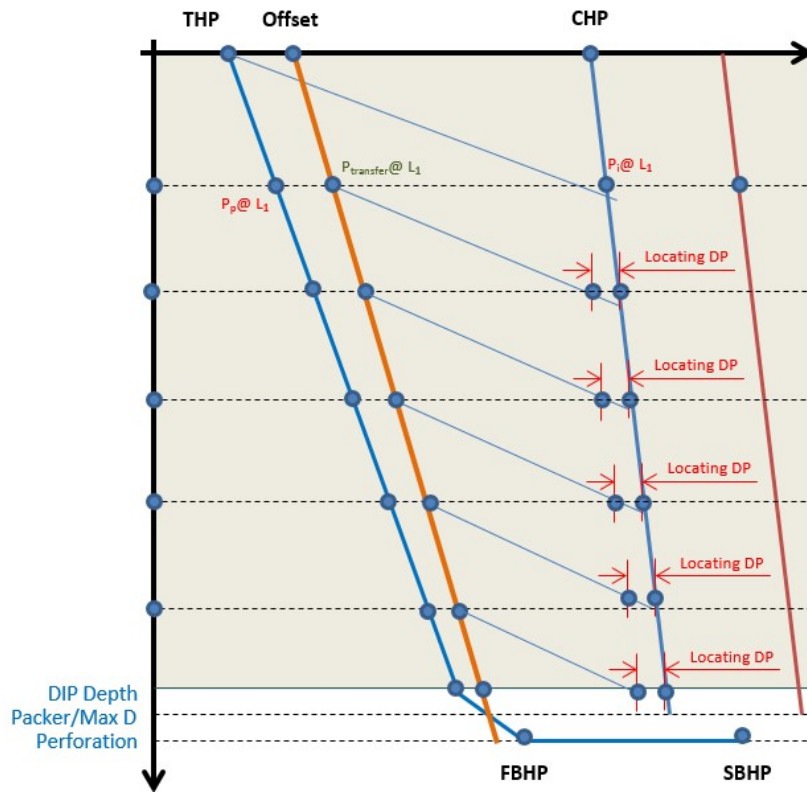
At each valve location, PIPESIM computes the gas rate to unload the section of the tubing above the valve, computes the port size, using the Thornhill-Craver equation, and selects the valve from the gas lift valve DP.

10. After selecting each valve, PIPESIM performs the following pressure computations at the valve depth:

- Opening pressure
- Dome pressure
- Closing pressure
- Spread

Note:

- While performing pressure calculations for the valves, PIPESIM uses the transfer line pressure at the valve location as the valve opening pressure at the valve depth.
- Based on the opening pressure, PIPESIM calculates the dome and closing pressure at each valve depth.



For information on how PIPESIM calculates valve pressures, refer to [Pressure computations for PPO valves](#).

Related links:

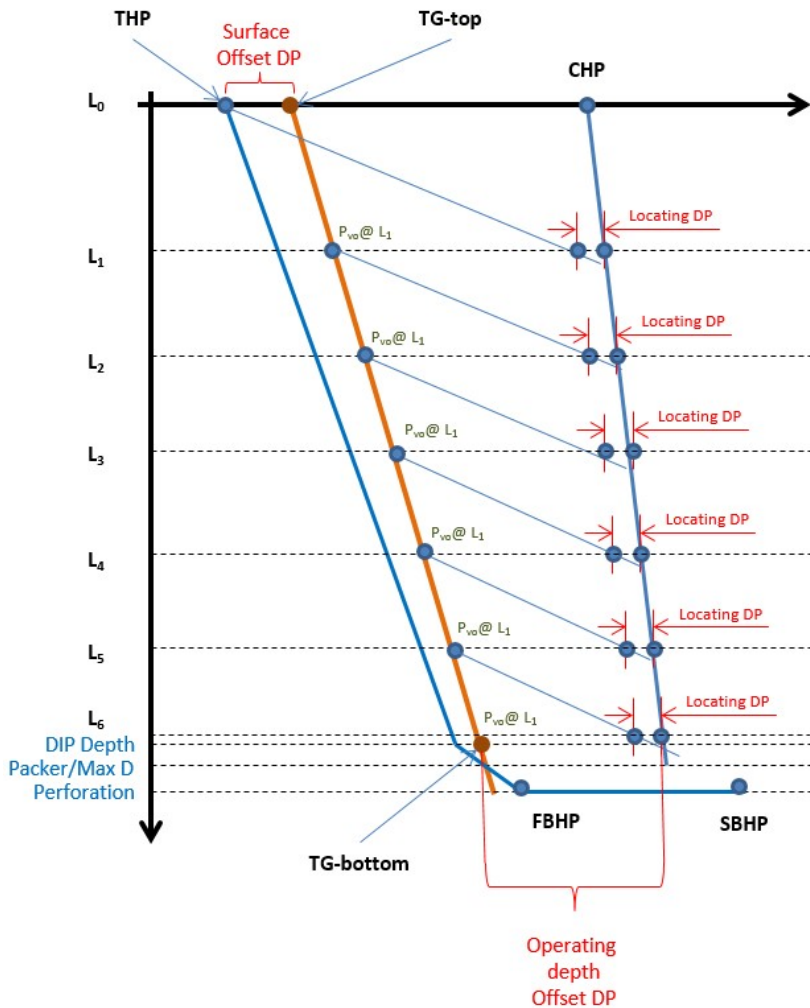
[Run gas lift design](#)

Pressure computations for PPO valves

PIPESIM uses mathematical equations to compute the opening, dome, and closing pressures for the PPO valves used in gas lift design simulations.

Transfer gradient

The transfer gradient line is also referred to as the design production line.



PIPESIM calculates the transfer gradient top and bottom locations and the slope of the line using the following three equations. This gradient line is used for PPO design spacing calculations.

- Transfer gradient top – wellhead location of the transfer gradient line

$$TG\ Top = THP + Surface\ Offset\ DP$$

- Transfer gradient bottom – operating valve location of the transfer gradient line

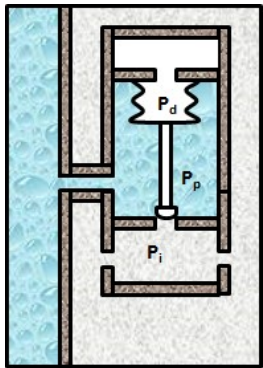
$$TG\ Bottom = Pi@DIP - Operating\ depth\ Offset\ DP$$

- Transfer gradient slope – slope of the transfer gradient line

$$TG\ Slope = \frac{(TG\ Top - TG\ Bottom)}{(DIP_{tvd} - Wellhead_{TVD})}$$

Opening, dome and close pressures

PIPESIM calculates the pressures for the PPO valves.



- Opening pressure (P_v) – pressure in the tubing at the instance before the valve opens from its closed position

Force balance results in a closed valve condition. Opening pressure is taken directly from the transfer gradient line. PIPESIM uses the following equation to calculate the opening pressure:

$$P_{vo}@L_n = TG\ Top + (TG\ Slope)(Valve_{tvd} - Wellhead_{tvd})$$

- Dome pressure (P_d) – pressure exerted on the bellow due to the nitrogen charge in the dome of the valve

PIPESIM uses the following equation to calculate the dome pressure:

$$P_d = P_{vo}(1 - R) + P_iR$$

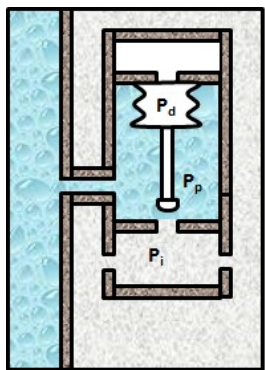
$$P_d@L_n = P_{vo}@L_n(1 - R@L_n) + P_i@L_n$$

- Closing pressure (P_{vc}) – tubing pressure at the instance the valve is about to close from its open position

Force balance results in an open valve condition.

$$P_{vc} = P_d$$

$$P_{vc}@L_n = P_d@L_n$$



- Spread – difference between the opening pressure and the closing pressure at the valve location

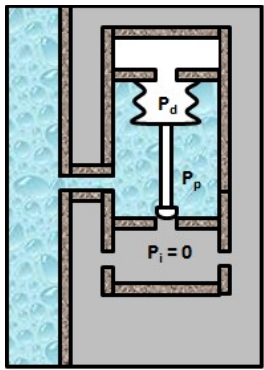
$$Spread (DP) = P_{vo} - P_{vc}$$

Ptrd

PIPESIM calculates Ptrd for the PPO valves.

- Ptrd is the valve dome pressure at the test rack condition entered by the user in the Gas lift design dialog box.

PIPESIM can derive Ptrd for each valve by using the dome pressure and temperature at the valve depth as well as the test rack temperature.



PIPESIM calculates P_{trd} based on the Winkler-Eads equation for nitrogen temperature correction.

$$P_{trd} = P_d - M(T_v - T_{tr})$$

where

For $P_{trd} < 1238$ psia:

$$M = -0.00226 + 0.001934 P_{trd} + 3.054 * 10^{-7} P_{trd}^2$$

For $1238 \text{ psia} \leq P_{trd} < 3000 \text{ psia}$:

$$M = -0.267 + 0.002298 P_{trd} + 1.84 * 10^{-7} P_{trd}^2$$

T_v = valve temperature at operating condition

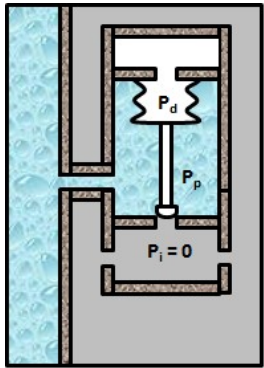
By default, this is the production temperature. However, you can run the Gas lift design task to change this option for top and lower valves

T_{tr} = test rack temperature

Ptro

PIPESIM calculates Ptro for the PPO valves.

- Ptro is the opening pressure required to open the valve at the test rack condition. Force balance results in a closed valve at the test rack condition.



$$P_{tro} @ L_n = \frac{P_{trd} @ L_n}{(1 - R) @ L_n}$$

Gas lift instability

Unstable operational conditions may occur in a continuous gas lift well because the characteristics of the system mean that small perturbations can degenerate into huge oscillations in the flow parameters. Therefore, a clearly defined mechanism is required to show the relative importance of the different factors involved, to help to assure stable flow conditions at the design phase, or to decide what to do to stabilize an unstable gas lift well.

Unified instability criteria were developed by Alhanati et al. (1993) for continuous gas lift wells to overcome drawbacks in previous developments. The unified criteria can be used for all possible flow regimes for the gas-lift valve and surface gas injection choke. The unified criteria were developed using a number of simplifying assumptions, so are not highly accurate or applicable to every type of instability experienced in a gas lift installation. However, they cover a number of common cases encountered in the industry and certainly indicate what can be done to improve operating instability.

For the Alhanati factors to be computed, the well model must have the following:

- Well IPR modeled by the PI method
- Casing inside diameter is set. The simple or detailed tubing model can be used.
- Valve port diameter set. The operating Gas Lift Valve Port (Orifice) Diameter.
- Surface injection pressure set. This is the gas lift injection surface pressure, upstream of the surface injection choke (which must be set higher than the internally calculated casing head pressure).
- To ensure accurate results from the Alhanati instability check, the model should be developed only to the well head.

Note: The factors will not be computed if data is missing or incorrect.

From this data the well model automatically calculates the steady state casing and tubing pressures. The Gas Lift performance curve should then be developed as normal; the Alhanati factors C1 and C2 are automatically generated. For stable gas lift operations, both these factors must be greater than zero.

To view the Alhanati factors (C1 and C2) graphically (using the system plot), select:

- X-axis: Total Injection Gas
- Left Y-axis: Alhanati Criterion 1
- Right Y-axis: Alhanati Criterion 2. For stable gas lift operations, both these factors must be greater than zero

If the graphical display is empty, this implies that one or more of the above data items is missing/incorrect.

Related links:

[Add a gas lift injection port](#)

Assumptions of the alhanati model

The model assumes:

- Constant pressure at the gas injection manifold, which is upstream of the surface injection choke
- Adiabatic flow through the choke.

In the unified criteria, two sets of criteria were defined, namely C1 and C2, and both must be greater than zero for stable gas lift operation.

$$C_2 = \left(F_1 \frac{\gamma_v}{\mu_v} \right) + \frac{\gamma_v}{F_c} \quad [\text{Eq. 1774.1}]$$

where

$$F_3 = \frac{(q_{fo} + q_{Go}) \cdot A_t}{(P_f - P_G) \cdot g} \cdot \frac{P_{co}}{q_{fo}} \quad [\text{Eq. 1774.2}]$$

$$\mu_{ch} = \frac{(ZT)_c}{(ZT)_m} \quad [\text{Eq. 1774.3}]$$

Nomenclature

A_t	Cross sectional area of tubing	in^2
g	Acceleration due to gravity	ft^2/s
P_{co}	Steady state casing pressure	psia
P_g		
P_f		
q_{fo}	Steady state reservoir fluids flow rate	stbd
q_{Go}	Steady state injected gas flow rate	mmscf
γ	Gas expansion factor	
T	Temperature	${}^\circ \text{F}$
Z	gas compressibility factor	

subscripts

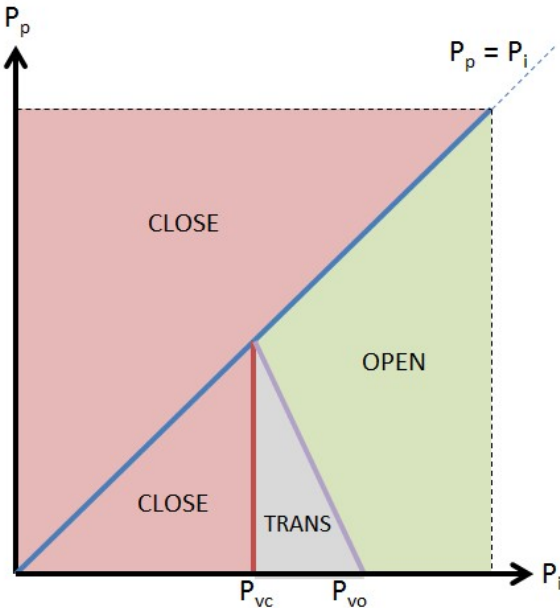
v	gas lift valve
ch	gas injection choke
t	tubing
c	casing
m	manifold

Valve status

When you run a gas lift design or gas lift diagnostics task, the PIPESIM engine calculates the valve status (open or closed) for IPO valves, PPO nitrogen-charged valves, and PPO spring-loaded valves.

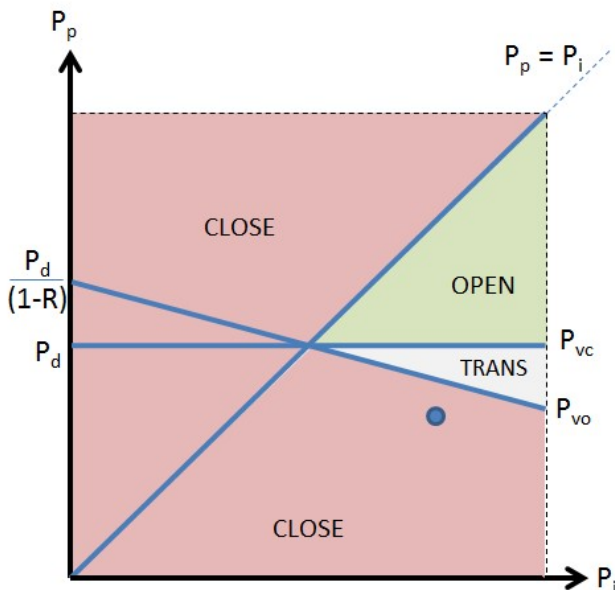
IPO valves

For IPO bellow-operated valves, the engine determines the valve status as shown in the image below. As displayed in the upper left pink shaded area of the graph, the valve remains closed if the production pressure (P_p) is higher than the injection pressure (P_i). For the region on the graph where $P_i > P_p$, as P_i increases beyond P_{vo} , the valve opens (as shown in the green shaded area on the graph). In the transition region (*TRANS*), displayed in the grey color, the valve is assumed to be closed.



PPO nitrogen-charged valves

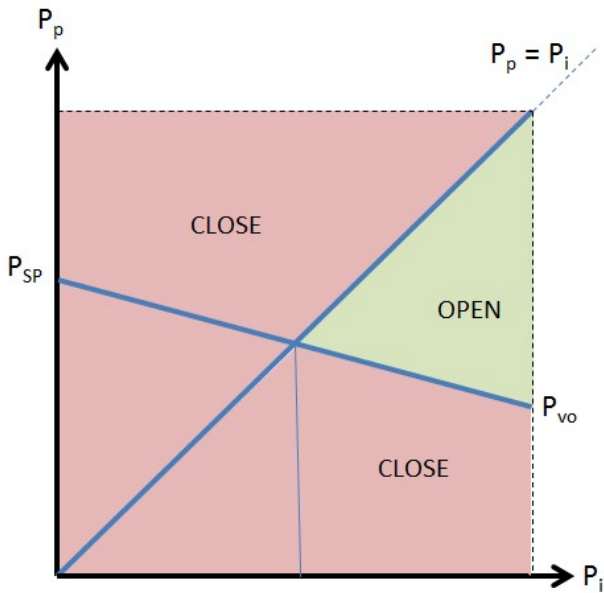
For PPO nitrogen-charged valves, the engine determines the valve status as shown in the image below. As displayed in the upper left pink shaded area of the graph, the valve remains closed if the production pressure (P_p) is higher than the injection pressure (P_i). For the region on the graph where $P_i > P_p$, as P_p increases beyond P_{vo} , the valve opens (as shown in the green shaded area on the graph). In the transition region (*TRANSITION*), displayed in the grey color, the valve is assumed to be open. The graph also shows a horizontal line at $P_p = (1-R)P_d$ and another at $P_p = P_d$.



PPO spring-loaded valves

For PPO spring-loaded valves, the engine determines the valve status as shown in the image below. As displayed in the upper left pink shaded area of the graph, the valve remains closed if the production pressure (P_p) is higher than the injection pressure (P_i). For the region on the graph where $P_i > P_p$, as P_p

increases beyond P_{vo} , the valve opens (as shown in the green shaded area on the graph).



Energy equation for steady-state flow

PIPESIM uses the **first law of thermodynamics** to perform a rigorous heat transfer balance on each pipe segment. The first law of thermodynamics is the mathematical formulation of the principle of conservation of energy applied to a process occurring in a closed system (a system of constant mass m). It equates the total energy change of the system to the sum of the heat added to the system and the work done by the system. For steady-state flow, it connects the change in properties between the streams flowing into and out of an arbitrary control volume (pipe segment) with the heat and work quantities across the boundaries of the control volume (pipe segment). For a multiphase fluid in steady-state flow, the energy equation is given by:

$$\Delta \left[\left(H + \frac{1}{2} v_m^2 + gz \right) dm \right] = \sum \delta Q - \delta W_s \quad [\text{Eq. 1775.1}]$$

where the specific enthalpy:

$$H = U + PV \quad [\text{Eq. 1775.2}]$$

is a state property of the system since the internal energy U the pressure P and the volume V are state properties of the system.

It is clear from the left-hand side of equation 1775.1, that the change in total energy is the sum of the change in enthalpy energy,

$$\Delta [Hdm] = \Delta [(U + PV)dm] \quad [\text{Eq. 1775.3}]$$

the change in gravitational potential energy:

$$\Delta E_P = \Delta [(gz)dm] \quad [\text{Eq. 1775.4}]$$

and the change in total kinetic energy (based on the mixture velocity v_m)

$$\Delta E_K = \Delta \left[\left(\frac{1}{2} v_m^2 \right) dm \right] \approx 0 \quad [\text{Eq. 1775.5}]$$

which is assumed to be negligible.

On the right-hand side of equation 1775.1, $\sum \delta Q$ includes all the heat transferred to the control volume (pipe segment) and δW_s represents the shaft work, that is work transmitted across the boundaries of the control volume (pipe segment) by a rotating or reciprocating shaft.

Overall heat transfer coefficient

Steady state heat transfer between the fluid inside a pipe (flowline, riser or tubing) and its surroundings occurs due to the difference between the bulk fluid temperature T_b and the ambient temperature T_a . In the case of a flowline or riser, the ambient temperature is the temperature of the ambient fluid (air or water) moving above the mud line. In the case of a tubing, the ambient temperature is the ground temperature at a distance far from the well, given by the geothermal gradient at the tubing depth. The rate at which heat is transferred depends on various thermal resistances such as:

- Inside fluid film (which is used to model heat transfer between a moving fluid and the pipe wall)
- Wax layers on the inside of the pipe wall
- Pipe wall and surrounding layers (for example coatings, fluid-filled annuli)
- Ground and surrounding medium (air or sea)

The heat transfer Q can be expressed as:

$$Q = UA(T_b - T_a)$$

where U = Overall heat transfer coefficient

A = Heat loss area ($= \pi D_o$ for a circular pipe. The reference area is based on the pipe outside diameter)

T_b = Bulk fluid temperature

T_a = Ambient temperature

Resistances in series

For resistances in series, (for example pipe coatings, see Fig 1775.1) the temperature difference can be written as the sum of the temperature differences across each resistance:

$$T_a - T_b = \sum_i \Delta T_i \quad [\text{Eq. 1775.1}]$$

Therefore

$$\frac{1}{U} = -\frac{A}{Q} \sum_i \Delta T_i = \sum_i \frac{1}{h_i} \quad [\text{Eq. 1775.2}]$$

Here h_i is the heat transfer coefficient for resistance i given by:

$$\frac{1}{h_i} = -\frac{A}{Q} \Delta T_i \quad [\text{Eq. 1775.3}]$$

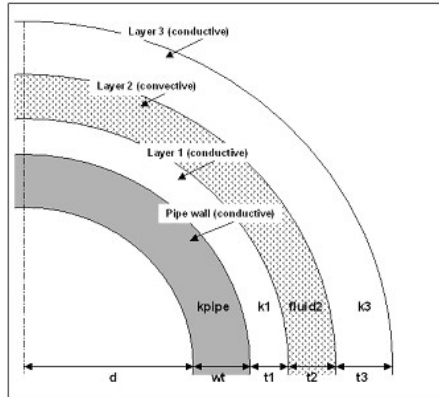


Figure 1775.1. Pipeline and Layers

Resistances in parallel

For resistances in parallel, (for example partially buried pipes, see Fig 1775.2) the overall heat transfer can be written as the sum of the heat transfer through each resistance:

$$Q = \sum_i Q_i = \sum_i U_i A (T_b - T_a) \quad [\text{Eq. 1775.4}]$$

Therefore the overall heat transfer coefficient can be found by summing the heat transfer coefficients for each resistance in parallel:

$$U = \sum_i U_i \quad [\text{Eq. 1775.5}]$$

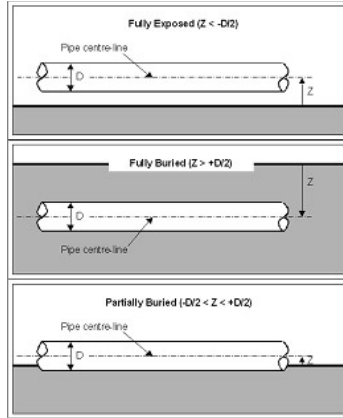


Figure 1775.2. Burial configurations

Heat transfer models

Heat transfer models are required for:

- radial heat transfer between a moving fluid and the pipe wall, see [Inside film coefficient](#).
- radial heat transfer through a [conductive layer](#), such as internal wax layers, the pipe wall and insulation.
- radial heat transfer through a [convective layer](#), such as a fluid-filled annulus.
- heat transfer through the ground
 - between the pipe and the surface for buried and partially buried [horizontal flowlines](#)
 - radially, between the pipe and the far field geothermal temperature gradient for [vertical wells](#)
- heat transfer through the ambient fluid
 - between the ground and the ambient fluid for buried and partially buried horizontal flowlines
 - between the pipe and the ambient fluid for partially buried and fully exposed horizontal flowlines
 - between the pipe and the ambient fluid for fully exposed vertical risers

Reference diameter for overall heat transfer coefficient

By default in PIPESIM, all Heat Transfer Coefficients (including local Inside, Outside, and Wall Coefficients, as well as the Overall Heat Transfer Coefficient) are referenced to the pipe outside diameter (and outside area), in keeping with the industry standard for heat exchanger design. However, the default reference diameter can be changed from the pipe outside diameter to a user-specified diameter using the [HEAT HTCRD](#) keyword, which can either be entered in the [Engine Keyword Tool](#) section or using an Engine Keyword Tool (EKT). This will override the default basis for all the reported heat transfer coefficients to the user-specified diameter, for all pipes in the workspace. This can be useful for direct comparison with Heat Transfer Coefficients which are reported by some other flow assurance software on an inside diameter and area basis (for example, OLGA, PIPEFLO).

Related links:

[HEAT](#)

[Engine Keyword Tool](#)

[Inside fluid film heat transfer coefficient](#)

[Conductive heat transfer coefficients](#)

[Annulus and outside convective heat transfer coefficients](#)

[Heat transfer between a horizontal flowline and the ground surface](#)

[Heat transfer between a vertical well and the surrounding rock](#)

Inside fluid film heat transfer coefficient

This inside film heat transfer coefficient accounts for resistance to heat flow between the bulk of the fluid and the inside of the pipe wall. It is one component of the Overall Heat Transfer Coefficient (U), which is used to calculate the heat transfer rate, Q . The inside fluid film heat transfer coefficient consists of convection from the fluid to the pipe wall. There are 3 types of convection mechanism depending on the nature of the flow; forced, free/natural and mixed convection, as described below. Usually, one convection mechanism will dominate, which is determined by the Reynolds number and Grashof number. However, in some instances, mixed convection may occur.

Reynolds Number

The Reynolds number is a dimensionless number calculated as the ratio of the inertial forces to the viscous forces acting on the fluid.

$$Re = \frac{\rho v d}{\mu}$$

where Re = Reynolds number

ρ = Fluid density

v = Fluid velocity

d = Pipe inside diameter

μ = Dynamic viscosity of fluid

Grashof Number

The Grashof number is a dimensionless number calculated as the ratio of the buoyancy forces to the viscous forces acting on a fluid.

$$Gr = \frac{g\beta(T_s - T_\infty)D^3}{v^2}$$

where Gr = Grashof Number

g = Acceleration due to Earth's gravity

β = Volumetric thermal expansion coefficient of the fluid

T_s = Surface temperature of pipe wall

T_∞ = Bulk temperature of fluid flowing inside pipe

v = Kinematic viscosity = $\frac{\mu}{\rho}$

μ = Dynamic viscosity of fluid

ρ = Fluid density

Forced Convection

Fluid flow, and subsequent convective heat transfer, is caused by external means such as a fan or pump or differential pressure. It is correlated with the Reynold's number. Forced convection dominates when $Gr/Re^2 \ll 1$ i.e. inertial forces on the fluid are much greater than buoyancy forces. The [Forced Convection Nusselt number](#) is thus a function of Reynold's number and Prandtl number. PIPESIM has two models for calculating the forced convection heat transfer coefficient; Kreith and Kaminsky. For each model, there are different forms of the Nusselt number correlation that are used depending on the type of flow; laminar, transition or turbulent flow for both the Kreith and Kaminsky models, and the ratio of the pipe length to diameter i.e. short duct, medium duct and long duct, specifically for the Kreith model.

Free/Natural Convection

Fluid flow, and subsequent convective heat transfer, is induced by buoyancy forces which are due to density differences caused by temperature differences in the fluid. Free convection can occur even when fluids are at rest. It is correlated with the Grashof number. Free convection dominates when $Gr/Re^2 \gg 1$ i.e. buoyancy forces on the fluid are much greater than inertial forces. The [Natural Convection Nusselt number](#) is thus a function of Grashof's number and Prandtl number.

Mixed Convection

This is a combination of forced and free convection where the fluid is in motion and forced convection is either aiding or opposing natural convection. The combined effects of free and forced convection (i.e. mixed convection) should be considered when $Gr/Re^2 \approx 1$.

The type of convection mechanism is important because it determines which Nusselt number correlation PIPESIM will use to calculate the inside film heat transfer coefficient. PIPESIM considers that only one convection mechanism will dominate at one time; forced or natural i.e. it does not account for the mixed convection scenario.

For most PIPESIM cases, forced convection will dominate internal heat transfer and a Nusselt number correlation will be selected as described above; the exact equation used will depend on whether the Kreith or Kaminsky model is selected, and whether the forced flow is laminar, turbulent or in the transition region. For the Kreith model specifically, the Nusselt number correlation is selected based on an additional parameter; the ratio of the pipe length to the pipe diameter.

For the less common PIPESIM cases where inside natural convection may dominate internal convective heat transfer, an inside film natural convection Nusselt number is also computed. In these cases, PIPESIM compares these two competing convection mechanisms; Forced and Natural convection, and then sets the Inside Fluid Film Heat Transfer Coefficient equal to the higher of these values.

Related links:

[Inside forced convection](#)

[Inside natural convection](#)

[HEAT](#)

[Conductive heat transfer coefficients](#)

[Annulus and outside convective heat transfer coefficients](#)

[Heat transfer between a horizontal flowline and the ground surface](#)

Heat transfer between a vertical well and the surrounding rock

Inside forced convection

Forced convection heat transfer inside a pipe occurs when the fluid flow is induced by external means such as a fan or pump or differential pressure. It is correlated with the Reynold's number. Forced convection dominates when $\text{Gr}/\text{Re}^2 \ll 1$ i.e. inertial forces on the fluid are much greater than buoyancy forces.

A number of inside film coefficient (IFC) correlations for forced convection were added over time to the legacy PIPESIM engine. Several of those legacy correlations are no longer used. However, these may still be accessed using the [HEAT](#) keyword for compatibility with historic work.

PIPESIM has two models for computing the Inside Forced Convective Heat Transfer Coefficient:

- [Kreith method](#) (Default method. Uses mixture values for the multiphase properties to evaluate Reynolds number, etc.)
- [Kaminsky method](#) (Recommended for cases with a stratified multiphase flow regime, because of enhanced prediction of the Inside Fluid Film Forced Convective Heat Transfer Coefficient)

PIPESIM will calculate the Inside Film Forced and Inside Film Natural Convective heat transfer coefficients and will set its Inside Fluid Film Heat Transfer Coefficient to the higher of these two values.

Related links:

[Inside fluid film heat transfer coefficient](#)

[Inside natural convection](#)

[HEAT](#)

[Conductive heat transfer coefficients](#)

[Annulus and outside convective heat transfer coefficients](#)

[Heat transfer between a horizontal flowline and the ground surface](#)

[Heat transfer between a vertical well and the surrounding rock](#)

Kreith

This is the default method in PIPESIM.

Kreith (averaged) mixture properties

For cases with multiphase flow, the Kreith method uses mixture properties for a pseudo single-phase, based on the local (slip-flow) liquid holdup. These properties are calculated as follows.

First, liquid and gas Reynolds numbers are calculated based on the superficial velocities V_{SL} and V_{SG} :

$$\text{Re}_{SL} = \frac{\rho_L V_{SL} D}{\mu_L} \quad [\text{Eq. 1775.1}]$$

$$\text{Re}_{SG} = \frac{\rho_G V_{SG} D}{\mu_G} \quad [\text{Eq. 1775.2}]$$

where ρ is the density, μ the viscosity, D the pipe diameter and the subscripts L and G refer to the liquid and gas phase properties.

A total Reynolds number is then obtained:

$$\text{Re}_{TOTAL} = \text{Re}_{SL} + \text{Re}_{SG} \quad [\text{Eq. 1775.3}]$$

A Prandtl number is then calculated using fluid mixture properties:

$$\text{Pr}_m = \frac{\mu_m c_p m}{k_m} \quad [\text{Eq. 1775.4}]$$

where c_p is the specific heat capacity, k the thermal conductivity, and M the viscosity, and the subscript m refers to the mixture.

The mixture thermal conductivity is given by:

$$[\text{Eq. 1775.5}]$$

$$k_m = \frac{1}{\frac{H_L}{k_L} + \frac{(1 - H_L)}{k_g}}$$

and the mixture heat capacity:

$$C_{p_m} = H_L C_{p_L} + (1 - H_L) C_{p_G} \quad [\text{Eq. 1775.6}]$$

where H is the holdup.

Kreith single-phase nusselt number relations

In both single-phase and multiphase cases, PIPESIM's Kreith inside fluid film coefficient is based on the following methods for prediction of the inside film Nusselt Number.

For turbulent flow ($\text{Re}_{TOTAL} \geq 6000$):

Kreith recommends the McAdams enhancement to the respected Dittus-Boelter equation for turbulent inside Nusselt Number (Nu). McAdams fixes the Pr exponent at 0.33 - in agreement with the other respected Sieder-Tate equation for turbulent inside Nu. McAdams also applies a 'short-pipe' entrance effect (D/L) multiplier to Dittus-Boelter's turbulent inside Nu method, similar to the entrance effects found in all laminar forced-flow Nu methods.

$$Nu_{1P_{Turb}} = 0.023 \text{Re}_{TOTAL}^{0.8} \text{Pr}^{0.33} \left(1 + \left(\frac{D}{L} \right)^{0.7} \right) \quad [\text{Eq. 1775.7}]$$

For laminar flow ($\text{Re}_{TOTAL} \leq 2000$):

$$\begin{aligned} Nu_{1P_{Lam}}^{SD} &\equiv \frac{RePrD}{4L} \ln \left[\frac{1}{1 - \left(\frac{2.654}{Pr^{0.167}} \right) \left(\frac{RePrD}{L} \right)^{-0.5}} \right]; \frac{L}{D} \leq 10 \\ Nu_{1P_{Lam}}^{MD} &\equiv - \left[1 - \frac{\left(\frac{D}{L} - 10 \right)}{30 - 10} \right] Nu_{1P_{Lam}}^{SD} + \left[\frac{\left(\frac{D}{L} - 10 \right)}{30 - 10} \right] Nu_{1P_{Lam}}^{LD}; 10 < \frac{L}{D} \leq 30 \\ Nu_{1P_{Lam}}^{LD} &\equiv 1.86 \left[Re_{total} Pr \left(\frac{D}{L} \right) \right]^{\frac{1}{3}}; \frac{L}{D} > 30 \end{aligned}$$

where the superscripts SD, MD and LD stand for short duct, medium duct and long duct, respectively.

For transition flow ($2000 \leq \text{Re}_{TOTAL} \leq 6000$):

$$Nu_{1P} = Nu_{1P_{Lam}} \left[\frac{Re_{total}}{2000} \right]^{\left(\frac{\ln(Nu_{1P_{Turb}}) - \ln(Nu_{1P_{Lam}})}{\ln(Re_{max}) - \ln(Re_{min})} \right)}$$

Note: As the Reynolds number decreases, the laminar flow Nusselt number is approaches 4. So if the Reynolds number is less than 2000, then PIPESIM limits the Reynolds number to a minimum of 4.

Reference: [Kreith](#)

Kreith multiphase inside fluid film coefficient

If the flow is multiphase then the void fraction is given by

$$\phi = \frac{Av_G}{Av_G + Av_L} \quad [\text{Eq. 1775.8}]$$

where the cross-sectional area of the pipe:

$$A = \frac{\pi D^2}{4} \quad [\text{Eq. 1775.9}]$$

The gas-weighted two phase fluid thermal conductivity is defined as:

$$k_{2P} = \phi k_G + (1 - \phi)k_L \quad [\text{Eq. 1775.10}]$$

The two phase inside film coefficient for the correlations below (unless otherwise stated) is defined as:

$$h_{i_{2P}} = \frac{Nu_{2P} k_{2P}}{D} \quad [\text{Eq. 1775.11}]$$

Note: Nu_{2P} in this equation is computed by applying the Kreith (averaged) mixture properties to the Kreith Single-Phase Nusselt Number relations.

Kaminsky

The Kaminsky method may give enhanced prediction for cases where multiphase stratified-flow heat transfer effects will strongly affect the Overall Heat Transfer Coefficient (as one of its largest series resistances).

Kaminsky (regime-dependent) film phase and dimensionless parameters

If the flow regime is mist, single gas phase or froth then the Kaminsky method's fluid film at the inside wall is considered to be a single-phase gas and the base superficial Reynolds number is:

$$\text{Re}_S = \text{Re}_{SG} = \frac{\rho_G v_{SG} D}{\mu_G} \quad [\text{Eq. 1775.1}]$$

and the Prandtl number is:

$$\text{Pr} = \text{Pr}_G = \frac{\mu_G c_{pG}}{k_G} \quad [\text{Eq. 1775.2}]$$

where ρ is the density, μ the viscosity, v the velocity, c_p the specific heat capacity, k the thermal conductivity, D the pipe diameter and the subscript SG refers to the superficial gas phase properties.

For all other flow regimes, the Kaminsky method's fluid film at the inside wall is considered to be a single-phase liquid and the base superficial Reynolds number is:

$$\text{Re}_S = \text{Re}_{SL} = \frac{\rho_L v_{SL} D}{\mu_L} \quad [\text{Eq. 1775.3}]$$

and the Prandtl number is:

$$\text{Pr} = \text{Pr}_L = \frac{\mu_L c_{pL}}{k_L} \quad [\text{Eq. 1775.4}]$$

where the subscript SL refers to the superficial liquid phase properties.

The following minimum and maximum superficial Reynolds numbers are defined as boundaries of the laminar-turbulent transition region:

$$\text{Re}_{S_{\min}} = 2000 \quad [\text{Eq. 1775.5}]$$

$$\text{Re}_{S_{\max}} = 6000 \quad [\text{Eq. 1775.6}]$$

Kaminsky base single-phase film nusselt number

The following minimum and maximum superficial Reynolds numbers are defined as boundaries of the laminar-turbulent transition region:
 $\text{Re}_{S_{\min}} = 2000$

$$\text{Re}_{S_{\max}} = 6000$$

The Kaminsky method bases its single-phase Nusselt Number on the Sieder and Tate equations for turbulent and laminar flows of the film phase, as follows.

For turbulent Kaminsky Film Phase ($\text{Re}_S > \text{Re}_{S_{\max}}$):

$$[\text{Eq. 1775.7}]$$

$$Nu_{1PTurb} = 0.023 Re_S^{4/5} Pr^{1/3} \left(\frac{\mu}{\mu_W} \right)^{0.14}$$

For laminar Kaminsky Film Phase ($Re \leq Re_{S_{max}}$):

$$Nu_{1PLam} = [1.86 Re_S \Pr \left(\frac{D}{L} \right)^{1/3}] \left(\frac{\mu}{\mu_W} \right)^{0.14} \quad [\text{Eq. 1775.8}]$$

where L is the length of the pipe and the subscript W refers to wall properties. The viscosity μ is either the liquid or gas viscosity depending on the flow regime (as described above).

Throughout the transition region ($2000 \leq Re \leq 6000$), PIPESIM prorates the Kaminsky Nu_{1P} by applying

$$Nu_{1PTurb} \quad [\text{Eq. 1775.9}]$$

from Kaminsky Film Equation 1081.16 and

$$Nu_{1PLam} \quad [\text{Eq. 1775.10}]$$

from Kaminsky Film Equation 1081.17 to the same

$$Nu_{1P} \quad [\text{Eq. 1775.11}]$$

Interpolation Method listed above as Kreith Equation 1081.9.

Reference: [Sieder and Tate](#)

Kaminsky single-phase inside fluid film coefficient

If the flow regime is mist, single gas phase or froth, this PIPESIM method regards the entire inside bulk fluid as a single-phase gas and the Inside Film Coefficient is:

$$h_{i_{1P}} = \frac{k_G Nu_{1P}}{D} \quad [\text{Eq. 1775.12}]$$

Similarly, for the case of a single-phase bulk liquid flow the inside film coefficient reduces to:

$$h_{i_{1P}} = \frac{k_L Nu_{1P}}{D} \quad [\text{Eq. 1775.13}]$$

Kaminsky multiphase inside fluid film coefficient

For all other (multiphase) flow regimes, with a turbulent liquid film ($Re \geq 2300$):

$$h_{i_{2P}} = h_{i_{1P_{SL}}} \sqrt{S \frac{\Delta P_{2Pf}}{\Delta P_{1Pf}}} \quad [\text{Eq. 1775.14}]$$

Its required input of the single-phase turbulent heat transfer film coefficient h_{1P} , must first be computed by the Sieder-Tate correlation. This Multiphase Pressure-Drop/Heat-Transfer Analogy Method also implicitly requires that both the Superficial Liquid Pressure Drop and the Multiphase Pressure Drop be pre-calculated as additional inputs, before its h_{1P} can be computed.

For horizontal (for example, if the pipe angle $|\beta| < \beta_{swap}$) stratified flow, the wetting of the pipe wall is calculated from

$$S = \pi D \theta \quad [\text{Eq. 1775.15}]$$

where θ is the wetted wall fraction given by [Grolman's correlation](#):

$$\theta = \theta_0 \left(\frac{\sigma_W}{\sigma} \right)^{0.15} + \frac{\rho_G}{\rho_L + \rho_G} \frac{1}{\cos(\beta)} \left\{ \frac{\rho_L u_{LS} D}{\sigma} \right\}^{0.25} \left\{ \frac{u_{GS}^2}{(1 - H_L)^2 g D} \right\}^{0.8} \quad [\text{Eq. 1775.16}]$$

in which the minimum wetted wall fraction θ_0 is approximated by:

$$[\text{Eq. 1775.17}]$$

$$\theta_0 \approx 0.624 H_L^{0.374}$$

For all other types of flow, heat transfer it is reasonable to assume that heat transfer is circumferentially uniform (i.e. $S = 1$).

For laminar flow ($Re < 2300$):

$$h_{i_{2P}} = \frac{(2 - H_L) h_{i_{1PSL}}}{H_L^{\frac{2}{3}}} \quad [\text{Eq. 1775.18}]$$

The single-phase laminar heat transfer is estimated by the Sieder-Tate correlation.

Reference: [Kaminsky](#)

Inside natural/free convection

Natural convection heat transfer inside a pipe occurs when the fluid flow is induced by buoyancy forces which are due to density differences caused by temperature differences in the fluid. Natural convection can occur even when fluids are at rest. It is correlated with the [Grashof number](#). Natural convection dominates when $Gr/Re^2 \gg 1$ i.e. buoyancy forces on the fluid are much greater than inertial forces.

Whenever fluid temperature may be significantly influenced by Natural Convection heat transfer (typically laminar flow), PIPESIM checks for the possible influence of Natural Convection inside the pipe. PIPESIM always computes the inside film natural convection heat transfer coefficient for laminar flow, and additionally for transition and turbulent flow with a Reynold's number $< 10,000$ using the Nusselt number equation below.

$$Nu_{NC} = \max \left[3.66, 0.184 (GrPr)^{\frac{1}{3}} \right]$$

Where Gr = Grashof number

$$Pr = \text{Prandtl number} = \frac{C_p \mu}{k}$$

C_p = Specific heat capacity of the fluid

μ = Fluid viscosity

K = Thermal conductivity of the fluid

This equation is a simple, computationally-inexpensive, and numerically stable way to compute the inside film natural convection heat transfer coefficient. PIPESIM compares the value calculated from the correlation above, to the theoretical minimum value for the Natural Convection Nusselt number which occurs when the heat transfer mechanism is as a result of conduction only (can be theoretically derived to be 3.66, see Incropera reference below). This Nusselt number value of 3.66 is the conduction-only limiting minimum Nusselt number for a circular pipe. PIPESIM sets Nu_{NC} to be equal to the maximum of these 2 values.

Finally, after calculating the inside film forced (Nu_{FC}) and inside film natural convective (Nu_{NC}) heat transfer coefficients, PIPESIM will determine the higher of the two values and set the Inside Fluid Film Heat Transfer Coefficient equal to this value.

References

Fundamentals of Heat and Mass Transfer, 7th Edition, Frank P. Incropera and David P. Dewitt, Pg. 539

Related links:

[Inside fluid film heat transfer coefficient](#)

[Inside forced convection](#)

[Grashof number](#)

[HEAT](#)

[Conductive heat transfer coefficients](#)

[Annulus and outside convective heat transfer coefficients](#)

[Heat transfer between a horizontal flowline and the ground surface](#)

[Heat transfer between a vertical well and the surrounding rock](#)

Conductive heat transfer coefficients

[Brill and Mukherjee](#) give a formula for radial heat transfer Q per unit length of pipe through a conductive layer:

$$\Delta T = T_o - T_i = - \frac{Q \ln(r_o/r_i)}{2 \pi k} \quad [\text{Eq. 1775.1}]$$

where

k	is the conductivity of the layer.
r_i	is the inner radius of the layer
r_o	is the outer radius of the layer
T_i	is the temperatures at the inside edge of the layer
T_o	is the temperatures at outside edge of the layer

This equation can be used to calculate the heat transfer coefficient for a conductive layer:

$$\frac{1}{h} = -\frac{A}{Q}\Delta T = \frac{A}{2\pi} \cdot \frac{\ln(r_o/r_i)}{k} \quad [\text{Eq. 1775.2}]$$

where

$\frac{A}{2\pi} = \frac{D_o}{2}$	is the radius of the reference area (normally the pipe outside radius)
----------------------------------	--

Wax heat transfer coefficient

[1775.2](#) can be used for heat transfer through a wax layer on the inside wall of the pipe, where

$k = k_{wax}$	is the conductivity of the wax layer.
$r_i = \frac{D_i}{2} - r_{wax}$	is the inner radius of the wax layer (equal to the pipe inner radius minus the wax thickness)
$r_o = \frac{D_i}{2}$	is the outer radius of the wax layer (equal to the pipe inner radius)

Pipe wall heat transfer coefficient

[1775.2](#) can be used for heat transfer through the pipe wall, where

$k = k_{pipe}$	is the conductivity of the pipe wall.
$r_i = \frac{D_i}{2}$	is the inner radius of the pipe
$r_o = \frac{D_o}{2}$	is the outer radius of the pipe

Conductive layer heat transfer coefficient

[1775.2](#) can be used for heat transfer through conductive layers, such as foam insulation or cement, where

$k = k_n$	is the conductivity of the n th layer
$r_i = \frac{D_{ni}}{2}$	is the inner radius of the n th layer
$r_o = \frac{D_{no}}{2}$	is the outer radius of the n th layer

Annulus and outside convective heat transfer coefficients

Convective heat transfer can occur in a number of places in a well and surface network, across a fluid filled annulus; between a pipe or surface and the air or sea. Free (or natural) convection occurs when the bulk fluid is at rest and convection is driven by buoyancy effects alone. Forced convection occurs when the fluid is moving, which will increase the rate at which heat is transferred.

The heat transfer coefficient for free convection at a wall is given in terms of the Nusselt number (Nu), the fluid conductivity (k) and a length scale (L):

$$h = \frac{k \cdot Nu}{L} \quad [\text{Eq. 1775.1}]$$

The Nusselt number can be found experimentally, depending on the geometry of the convective surfaces. It also depends on the fluid properties, which are encapsulated in two dimensionless numbers, the Prandtl number (Pr) representing the ratio of velocity and temperature gradients:

$$Pr = \frac{c_p M}{k} \quad [\text{Eq. 1775.2}]$$

and the Grashof number representing the ratio of buoyancy to viscous forces:

$$Gr = \frac{L^3 P^2 B g \Delta T}{\mu^2} \quad [\text{Eq. 1775.3}]$$

β	Fluid thermal expansion coefficient	K^{-1}
μ	Fluid dynamic viscosity	$kg \cdot m^{-1} \cdot s^{-1}$
ρ	Fluid density	$kg \cdot m^{-3}$
c_p	Fluid heat capacity	$W \cdot kg^{-1}$
k	Fluid thermal conductivity	$W \cdot m^{-1} \cdot s^{-1}$

Fluid properties are calculated at a film temperature T_{film} half way between the wall temperature and the bulk fluid temperature:

$$T_{film} = (T_{wall} + T_f)/2 \quad [\text{Eq. 1775.4}]$$

The wall temperature and bulk fluid temperature are used to calculate the temperature difference in the formula for the Grashof number:

$$\Delta T = |T_f - T_{wall}| \quad [\text{Eq. 1775.5}]$$

Because the fluid properties and Grashof numbers are functions of the wall temperatures, the heat transfer coefficient is also a function of the wall temperatures. The heat loss calculation therefore needs to be solved iteratively.

Convection in a fluid filled vertical annulus

PIPESIM can model the heat transfer in a fluid filled annulus by free convection. The heat transfer coefficient can be determined from the heat transfer coefficients at the inner and outer walls:

$$\frac{1}{h_{annulus}} = \frac{1}{h_{inner}} + \frac{1}{h_{outer}} \quad [\text{Eq. 1775.6}]$$

For vertical pipes ($\text{angle} \geq 45^\circ$), the Nusselt number is given by [Eckert and Jackson \(1950\)](#) (quoted in [Kreith and Bohn\(1997\)](#)) in terms of the Rayleigh number (Ra):

$$Nu = 0.555 Ra^{0.25} \quad \text{for } Ra \leq 10^9 \quad [\text{Eq. 1775.7}]$$

$$Nu = 0.021 Ra^{0.4} \quad \text{for } Ra > 10^9 \quad [\text{Eq. 1775.8}]$$

where

$$Ra = \Pr \cdot Gr \quad [\text{Eq. 1775.9}]$$

The bulk fluid temperature is assumed to be the average of the annulus wall temperatures:

$$T_f = (T_{inner} + T_{outer})/2 \quad [\text{Eq. 1775.10}]$$

Convective Heat transfer through fluid-filled annuli can be modeled by the use of the [EKT](#). Refer to the Expert Mode Keyword Reference section on [fluid coats](#).

Convection in a fluid-filled horizontal annulus

PIPESIM uses the same equations to calculate the heat transfer for a horizontal fluid annulus as for a vertical annulus, except that the Nusslet number is given by:

$$Nu = 0.53 Ra^{0.25} \quad [\text{Eq. 1775.11}]$$

Fully exposed pipe

For a flowline or riser exposed to the sea or the air, the “ambient” heat transfer coefficient can be calculated by summing the free and forced convection heat transfer coefficients:

$$h_a = h_{forced} + h_{free} \quad [\text{Eq. 1775.12}]$$

For forced convection, the heat transfer coefficient depends on the Reynolds number of the flow

$$Nu_{forced} = (0.4Re^{0.5} + 0.06Re^{0.67})\Pr^{0.4} \quad [\text{Eq. 1775.13}]$$

Heat transfer between a horizontal flowline and the ground surface

Fully buried ground heat transfer coefficient

The fully buried heat transfer coefficient for a flowline is evaluated by determining a conduction shape factor to account for the geometrical and thermal

effects of the burial configuration. Once the shape factor is known, the ground heat transfer coefficient is calculated from the following equations, depending on the burial method chosen:

2009 method

$$h_g = \frac{k_g S}{R}$$

where R is the chosen reference length and is taken to be the outer radius of the pipe for the 2009 burial method.

2000 and 1983 methods

$$h_g = \frac{k_g S}{\pi D}$$

where πD is the chosen reference length and is taken to be the outer circumference of the pipe for the 2000 and 1983 burial methods.

The shape factor used differs depending on the partial burial option that is selected.

A pseudo film coefficient is then added in series in order to model the ambient fluid moving above ground level:

$$\frac{1}{h_{ext}} = \frac{1}{h_g} + \frac{1}{h_a} \quad [\text{Eq. 1775.1}]$$

2009 method

The conduction shape factor is obtained from a solution to the steady-state heat conduction equation (the Laplace equation) with convective boundary conditions on the pipe inside wall and ground surfaces:

$$S = \frac{B_p a_{bur}}{\left[\left(\cosh \alpha_0 - B_p a_{bur} \alpha_0 + \frac{B_p}{B_g} \right)^2 - \left(1 + \frac{B_p}{B_g} \right)^2 \right]^{\frac{1}{2}}} \quad [\text{Eq. 1775.2}]$$

where

$$\alpha_0 = -\cosh^{-1} \left(-\frac{Z}{R} \right) \quad [\text{Eq. 1775.3}]$$

is a auxiliary geometrical quantity and

$$a_{bur} = -\sinh \alpha_0 = \sqrt{\left(\frac{Z}{R} \right)^2 - 1} \quad [\text{Eq. 1775.4}]$$

is a scale factor for bicylindrical coordinates and

$$B_p = \frac{U_{ipc} R}{k_g} \quad [\text{Eq. 1775.5}]$$

is the Biot number of the pipe and

$$B_p = \frac{h_a R}{k_g} \quad [\text{Eq. 1775.6}]$$

is the Biot number of the ground. U_{ipc} is the combined heat transfer coefficient of the inside film, pipe, coatings (and wax)

$$\frac{1}{U_{ipc}} = \frac{1}{h_i} + \frac{1}{h_{wax}} + \frac{1}{h_{pipe\&layers}} \quad [\text{Eq. 1775.7}]$$

Equation 1775.2 is not valid when the pipe&layers surface is just touching the ground surface ($Z/R=1$). In such a case, the shape factor is calculated from the following asymptotic expression

$$S \sim \frac{B_p}{\left[\left(1 + \frac{B_p}{B_g} \right) \left(1 + 2B_p \right) \right]^{\frac{1}{2}}} \quad [\text{Eq. 1775.8}]$$

We obtain the ground heat transfer coefficient from:

$$h_g = \frac{k_g S}{R}$$

Note: This is the default method in PIPESIM. The shape factor above is accurate to within 2.5% of the numerical simulation studies given by [Schneider](#). For information about how the results of the 2009 method compare to Schneider's, see [Ouworrie](#).

1983 & 2000 methods

The conduction shape factor is obtained from a solution to the steady-state heat conduction equation (the Laplace equation) with isothermal boundary conditions on the pipe inside wall and ground surfaces:

$$S = \frac{2\pi}{\cosh^{-1}\left(\frac{Z}{R_{\text{pipe\&layers}}}\right)} \quad [\text{Eq. 1775.9}]$$

Reference: [Kreith](#)

Partially buried ground heat transfer coefficient

To calculate the overall heat transfer coefficient for a partially buried pipeline, buried and exposed heat transfer coefficients must be calculated and combined in parallel. The method of combination and the ground conduction shape factors used differ depending on the partial burial option that is selected.

2009 method

1. A fully exposed pseudo pipe of the same diameter is created and an overall heat transfer coefficient (U_{exp}) is calculated using the methods described in the sections above.
2. A partially buried conduction shape factor is calculated using the methods described in the sections above. The shape factor is computed from

$$S = \begin{cases} \frac{2B_p a_{\text{part}} \tan^{-1}\left(\sqrt{\frac{1-A_{\text{part}}}{1+A_{\text{part}}}}\right)}{\pi\left(1+\frac{B_p}{B_g}\right)\sqrt{1-A_{\text{part}}^2}}; & -1 < A_{\text{part}} < 1 \\ \frac{B_p a_{\text{part}}}{\pi\left(1+\frac{B_p}{B_g}\right)}; & A_{\text{part}} = 1 \end{cases} \quad [\text{Eq. 1775.10}]$$

where

$$A_{\text{part}} = \left(1 + \frac{B_p}{B_g}\right)^{-1} \left(\cos \beta_0 + B_p a_{\text{part}} \left(\pi + \beta_0 \right) - \frac{B_p}{B_g} \right) \quad [\text{Eq. 1775.11}]$$

is an auxiliary geometrical quantity and

$$a_{\text{part}} = -\sin \beta_0 = \sqrt{1 - \left(\frac{Z}{R}\right)^2} \quad [\text{Eq. 1775.12}]$$

is a scale factor for bicylindrical coordinates.

3. The fully buried and fully exposed heat transfer coefficients are then combined in parallel (according to the fraction of pipe exposed and the fraction of pipe buried) using equation [1775.13](#) to give the overall heat transfer coefficient:

Note: This is the default method in PIPESIM. For more information, see [Ouworrie](#).

2000 method

1. A fully exposed pseudo pipe of the same diameter is created and an overall heat transfer coefficient (U_{bur}) is calculated using the methods described in the sections above.
2. A fully buried pseudo pipe ($Z=+R$) of the same diameter is created and an overall heat transfer coefficient (U_{exp}) is calculated using the methods described in the sections above.
3. The fully buried and fully exposed heat transfer coefficients are then combined in parallel (according to the fraction of pipe exposed and buried) to give the overall heat transfer coefficient:

$$U = \left(1 + \frac{\beta_0}{\pi}\right) U_{\text{exp}} - \frac{\beta_0}{\pi} U_{\text{bur}} \quad [\text{Eq. 1775.13}]$$

where the negative of half of the angle of the exposed arc:

$$\beta_0 = -\cos^{-1}\left(-\frac{Z}{R}\right) \quad [\text{Eq. 1775.14}]$$

1983 method

1. A fully exposed pseudo pipe with diameter corresponding to the exposed surface area is created and an overall heat transfer coefficient (U_{exp}) is calculated using the methods described in the sections above.
2. A fully buried pseudo pipe with diameter corresponding to the buried surface area is created and an overall heat transfer coefficient (U_{bur}) is calculated using the methods described in the sections above.
3. The fully buried and fully exposed heat transfer coefficients are then combined in parallel (according to the surface areas of pipe exposed and buried) to give the overall heat transfer coefficient:

$$U = \frac{A_{\text{exp}}}{A} U_{\text{exp}} + \frac{A_{\text{bur}}}{A} U_{\text{bur}} \quad [\text{Eq. 1775.15}]$$

where the total surface area of the buried pipe:

$$A = 2\pi R \quad [\text{Eq. 1775.16}]$$

The surface area of the exposed portion of the pipe is:

$$A_{\text{exp}} = \pi R \left(1 - \frac{\theta_{\text{bur}}}{2\pi}\right) \quad [\text{Eq. 1775.17}]$$

where the angle of the buried arc:

$$\theta_{\text{bur}} = \sin^{-1}\left(\frac{Z}{R}\right) \quad [\text{Eq. 1775.18}]$$

The surface area of the buried portion of the pipe is:

$$A_{\text{bur}} = A - A_{\text{exp}} \quad [\text{Eq. 1775.19}]$$

Heat transfer between a vertical well and the surrounding rock

Ramey model

Heat transfer between a well and its surroundings varies with time: the well exchanges energy with the formation, heating it up (or cooling it down), until the formation is at the same temperature as the well.

The [Ramey \(1962\)](#) model is an analytical method for determining the ground heat transfer coefficient, h_g , given the length of time t a well has been operating. The model assumes that heat transfer in the wellbore is steady-state, whilst heat transfer to the formation is by transient radial conduction. In his paper, Ramey quotes various solutions for different boundary conditions. He observed that the solutions eventually converge after about a week. He concluded that a line source with constant heat flux gives a good asymptotic solution for long times (times greater than one week).

The wellbore (ground) heat transfer coefficient is given by:

$$h_g = \frac{2k_g}{D f(t)} \quad [\text{Eq. 1775.1}]$$

where the time function:

$$f(t) = \frac{1}{2} E_1\left(\frac{D^2}{4\alpha T}\right) \exp\left(\frac{D^2}{4\alpha T}\right) \quad [\text{Eq. 1775.2}]$$

The exponential integral is given by:

$$E_1\left(\frac{D^2}{4\alpha t}\right) = \int_0^{\frac{D^2}{4\alpha t}} \frac{1 - \exp(-r)}{r} dr - \ln\left(\frac{D^2}{4\alpha t}\right) - \gamma \quad [\text{Eq. 1775.3}]$$

For large values of time t , Ramey uses a series expansion for the exponential integral, which to leading order gives:

$$f(t) \approx -\ln\left(\frac{D_{co}}{4\sqrt{\alpha t}}\right) - \frac{\gamma}{2} \quad [\text{Eq. 1775.4}]$$

k_g	ground thermal resistance	$\text{W m}^{-1} \text{K}^{-1}$
D	outside diameter of pipe	m
D_{co}	outside diameter of pipe and thermal coatings	m
$\alpha = \frac{k_g}{\rho_g c_g}$	ground thermal diffusivity	$\text{m}^2 \text{s}^{-1}$
c_g	ground specific heat capacity	$\text{J kg}^{-1} \text{K}^{-1}$
ρ_g	ground density	kg m^{-3}
r	radial distance from the centre of the well	m
$\gamma \approx 0.577$	Euler-Mascheroni gamma constant	dimensionless

In the case of a tubing we see that:

$$\frac{1}{h_{ext}} = \frac{1}{h_g} \quad [\text{Eq. 1775.5}]$$

and the ambient temperature used in equation [1775.1](#) is given by the geothermal temperature at some radial distance far from the centre of the well.

Note: To compute a geothermal gradient and hence a geothermal temperature at a particular well depth, PIPESIM requires knowledge of at least two ambient temperatures at two corresponding measured depths (MD) or true vertical depth (TVD) — usually these are the ambient temperatures at top and bottom of the tubing.

Reference: ["Wellbore Heat Transmission", H.J. Ramey](#)

Fluid Models

A number of fluid and solid phases may be present in oil and gas pipeline. These include:

- Fluids
 - Vapour hydrocarbon and water (gas)
 - Liquid hydrocarbon (oil)
 - Liquid water
 - Other liquids (e.g. liquid CO₂)
- Solids
 - Hydrate I
 - Hydrate II
 - Wax
 - Asphaltene
 - Ice
 - Scale

PIPESIM simulates flow of only three fluid phases, oil, gas and water. In fact some flow models only consider two phases, liquid and gas. Liquid properties are determined by combining the oil and water properties.

PIPESIM can be used to model wax precipitation and deposition. Other solid phases cannot be modelled, although the appearance of hydrates, asphaltene and ice can be predicted. PIPESIM can model scale prediction.

Fluid models are used to determine the phase state (e.g. single phase oil, single phase gas, two phase oil and gas etc) and the phase thermodynamic and transport properties needed for simulation (e.g. density, enthalpy and viscosity). PIPESIM allows three different types of fluid description:

- **Black oil** Three phases are allowed, oil, gas and water. The hydrocarbon fluid is made up of oil and gas. Simple correlations are used to determine how much gas can dissolve in oil and the phase properties.
- **Compositional** The number of phases allowed depends on the flash package. Fluid is made up of components, such as methane, ethane, water etc. Phase state is determined by minimizing Gibbs energy of the system (the flash). This can be a complicated calculation and is therefore significantly slower than black oil. PIPESIM can use a number of different flash packages.
- **Fluid Property Table Files** Two phase (liquid and gas) properties can be output from compositional packages in a tabular form that PIPESIM can read.

Steam modelling

For steam systems (production and injection) PIPESIM uses "ASTEM97 - IAPWS IF97 Properties of Water and Steam for Industrial Use," Copyright Edward D. Throm (C) 2005.

When modeling steam systems the pressure and quality or temperature are required. If the quality is not provided, superheated (quality =100%) or sub-cooled (quality=0%) then the temperature is required.

Steam systems can be modeled in both single branch and network models using **engine keywords**. These can be specified from the Pipesim GUI as described below. However:

Notes:

- Because the GUI does not understand steam as a fluid model choice, it will require you to specify a valid fluid model, either as Black Oil, or Compositional. The steam keywords will override this, so the choice is not really relevant when the model is working.
- PIPESIM requires a Fluid Model defined and mapped to each source. The current configuration recognize either a Black Oil or Compositional Fluid and the same is linked to validation mechanism. For a special case of Steam Modelling which the underlying PIPESIM Engine is capable a handle, user must present the Steam definition using keywords as detailed above and ensure there is no other fluid (Black Oil or Compositional) is present. This can only be done by skipping the validation mechanism.

The steam case study CSW_113_Steam Injection Well.pips is available for reference in the Case Studies » Well Models installation directory.

Single branch steam

- To model steam in a single branch PIPESIM model, in the single branch view of the steam source branch, on the Home tab, in the Data group, click Simulation settings, click the Advanced tab, and specify the following keywords, for example:

```
STEAM
INLET QUALITY = 0.5
```

The inlet steam quality needs to be specified, if not, the engine will assume it to be either 0.0 or 1.0 depending on the pressure and temperature at the inlet.

- To sensitize on steam quality, you may specify the following keywords, for example:

```
STEAM
MULTICASE ?GAMMA = (0.5,0.7,0.9)
INLET QUALITY = ?GAMMA
```

- Make sure you have a black oil fluid specified, with a GLR of zero and a watercut of 100% correctly.
- Mass flow rates must be used with steam. Any operation that specifies a flowrate, or sets a flowrate limit, must do so with a mass rate, not a gas or liquid rate.

When steam quality is provided, it will be used with the Inlet pressure to calculate the resulting steam temperature and enthalpy; Any inlet temperature you specify will be ignored.

If quality is not provided, enthalpy will be used instead. If Enthalpy is not provided, the system will be flashed at the specified inlet pressure and temperature, and as a result will be 100% liquid or 100% vapour at the system inlet.

Network model steam

- To model steam sources in a network model, in the network view, on the Home tab, in the Data group, click Simulation settings, click the Advanced tab, and enter the following data for example in the lower section of the window:

```
SETUP COMP = STEAM
SOURCE NAME = SS1 QUALITY = 0.8
```

- Enter the quality for all the steam sources. If the quality is not entered, it will be determined from the temperature and pressure given for that source. If it is entered the source will be considered saturated at that pressure and the temperature will be adjusted accordingly.

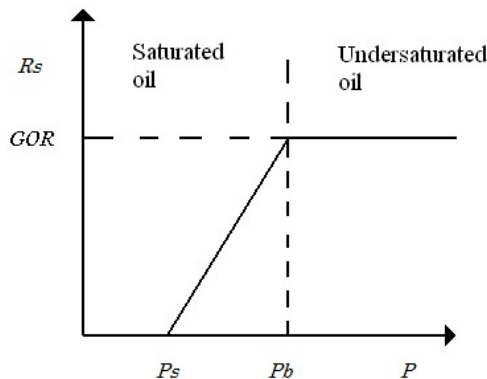
Note: Steam is considered as a third thermodynamic model (after blackoil and compositional). At present only one thermodynamic model is allowed per network, so steam systems have to be modeled as a separate network from the hydrocarbon production or injection networks.

Black oil fluid modeling

Black oil fluids are modelled as three phases, oil, gas and water. The amount of each phase is defined at stock tank conditions, by specifying two ratios, typically the gas oil ratio (GOR) and the water cut (WCUT). Properties at pressures and temperatures other than stock tank are determined by [correlations](#). Water is assumed to remain in the water phase. The key property for determining the phase behaviour of the hydrocarbons is the [solution gas—oil ratio](#), $R_s(P, T)$, which is used to calculate the amount of the gas dissolved in the oil at a given pressure and temperature:

$$\frac{\text{Stock tank volume of gas dissolved in oil: } R_s \cdot V_O}{\text{Stock tank volume of free gas: } V_G = (GOR - R_s) \cdot V_O}$$

At stock tank conditions $R_s = 0$. The [bubble point pressure](#) $P_b(T)$ can be found by calculating the pressure at which all the gas is dissolved in the oil $R_s(P_b, T) = GOR$



For pressures below the bubble point the oil is **saturated** (no more gas can dissolve in it at that pressure and temperature). For pressures above the bubble point, there is no vapour phase and the oil is **undersaturated**, since more gas could be dissolved in it if it were available. Above stock tank pressure $P > P_s$ the oil contains dissolved gas, and is known as **live oil**. Oil at stock tank pressure (or oil with $GOR=0$) is known as **dead oil**. Different correlations apply for dead oil, saturated live oil, and unsaturated live oil properties.

[Correlations](#) are needed for the fluid properties needed for simulation:

- the [oil formation volume factor](#) (which is used to determine oil density),
- the [gas compressibility](#) (to determine the gas density)
- the water density
- the [oil viscosity](#)
- the [gas viscosity](#)
- the water viscosity
- the [fluid enthalpy](#)
- the [oil-gas surface tension](#)
- the [water-gas surface tension](#)

[Liquid properties](#) are calculated by combining the oil and water properties.

Black oil correlations

The following black oil correlations are available:

Solution gas and bubble point pressure	Lasater , Standing , Vasquez and Beggs , Kartoatmodjo and Schmidt , Glasø , De Ghetto et al or Petrosky and Farshad .
Oil formation volume factor of saturated systems	Standing , Vasquez and Beggs , Kartoatmodjo and Schmidt
Oil formation volume factor of undersaturated systems	Vasquez and Beggs
Dead oil viscosity	Beggs and Robinson, Glasø, Kartatmodjo, De Ghetto, Hossain, Petrosky, Elsharkawy or Users data.
Live oil viscosity of saturated systems	Chew and Connally, Kartatmodjo, Khan, De Ghetto, Hossain, Petrosky, Elsharkawy, or Beggs and Robinson.
Live oil viscosity of undersaturated systems	Vasquez and Beggs, Kouzel, Kartatmodjo, Khan, De Ghetto, Hossain, Petrosky, Elsharkawy, Bergman or None.
Viscosity of oil/water mixtures	Inversion, Volume Ratio, or Woelflin.
Gas viscosity	Lee et al.
Gas compressibility	Standing, Hall and Yarborough, or Robinson et al.
Oil-gas surface tension	
Water-gas surface tension	

Correlation data

The data points spanned the following ranges :

		Lasater	Standing	Vasquez and Beggs	Kartoatmodjo and Schmidt
Data		Correlation was developed in 1958 from 158 experimental data points	Correlation was based on 105 experimentally determined bubble point pressure of California oil systems.	Correlations use data from more than 600 oil systems. Approximately 6,000 measured data points were collected.	740 different crude oil samples with 5392 data points from South East Asia, North America, the

					Middle East, and Latin America are used.
P_b	bubble point pressure (psia)	48 to 5,780	130 to 7,000	50 to 5,250	24.7 to 4764.7
T	temperature (°F)	82 to 272	100 to 258	70 to 295	75 to 320
API	API gravity (°API)	17.9 to 51.1	16.5 to 63.8	16 to 58	14.4 to 59.0
γ_G	gas specific gravity	0.574 to 1.223	0.59 to 0.95	0.56 to 1.18	0.4824 to 1.668
R_{sb}	solution gas at bubble point pressure (scf/STB)	3 to 2,905	20 to 1,425	20 to 2,070	0 to 2890
			Beggs and Robinson	Chew and Connally	
Data			Data from 600 oil systems were used to develop correlations for dead and live oil viscosity. 460 dead oil observations and 2,073 live oil observations were used.	Data from 457 oil systems was used to develop correlation for live oil viscosity	
P_b	bubble point pressure (psia)	50 to 5,250	132 to 5,645		
T	temperature (°F)	70 to 295	72 to 292		
API	API gravity (°API)	16 to 58			
γ_G	gas specific gravity				
R_{sb}	solution gas at bubble point pressure (scf/STB)	20 to 2,070	51 to 3,544		

[Glaso](#) developed PVT correlations from analysis of crude oil from the following North Sea Fields:- Ekofisk Stratfjord Forties Valhall COD 30/7-2A.

Solution gas-oil ratio

The solution gas-oil ratio, R_s (scf/STB), can be determined using one of a number of correlations:

- [De Ghetto et al](#)
- [Glaso](#)
- [Kartoatmodjo and Schmidt](#)
- [Lasater](#)
- [Petrosky and Farshad](#)
- [Standing](#)
- [Vasquez and Beggs](#)

The correlations depend on:

P	pressure (psia)
T	temperature (°F)
API	API gravity (°API)
γ_G	gas specific gravity

De ghetto et al.

De Ghetto *et al.* give different correlations for the solution gas-oil ratio and the bubble point pressure. In PIPESIM it is important to use related formula for these two properties to ensure consistency. The PIPESIM implementation of the solution gas-oil ratio is therefore derived from the De Ghetto *et al* equations for the bubble point pressure.

Extra heavy oil, API < 10

For extra heavy oil the De Ghetto formula is a modified version of the [Standing](#) formula:

$$R_s(P, T) = C \cdot \gamma_G \cdot \left[\frac{P}{10.7025 \cdot A(T)} \right]^{1.1128} \quad [\text{Eq. 1780.1}]$$

Here A is a function of the fluid temperature and the oil API density:

$$\log_{10} A = 0.002 \cdot T - 0.0142 \cdot API \quad [\text{Eq. 1780.2}]$$

C is a [calibration](#) constant.

Heavy oil, 10 < API < 22.3

For heavy oil the De Ghetto formula is a modified version of the [Standing](#) formula:

$$R_s(P, T) = C \cdot \gamma_G \cdot \left[\frac{P}{15.7286 \cdot A(T)} \right]^{1/0.7885} \quad [\text{Eq. 1780.3}]$$

Here A is a function of the fluid temperature and the oil API density:

$$\log_{10} A = 0.002 \cdot T - 0.0142 \cdot API \quad [\text{Eq. 1780.4}]$$

C is a [calibration](#) constant.

Medium oil, $22.3 < API < 31.1$

For medium oil the De Ghetto formula is a modified version of the [Kartoatmojo and Schmidt](#) formula:

$$R_s = C \cdot C_1 \cdot \left[\gamma_G \cdot (1 + g_{corr}) \right]^{C_2} \cdot A(T) \cdot P^{C_4} \quad [\text{Eq. 1780.5}]$$

Here A is a function of the fluid temperature and the oil API density:

$$\log_{10} A = C_3 \cdot \frac{API}{T + 460} \quad [\text{Eq. 1780.6}]$$

If the separator pressure and temperatures are known then a non-zero gas specific gravity correction factor is used:

$$g_{corr} = 0.1595 \cdot API^{0.4078} \cdot T_{sep}^{-0.2466} \cdot \log_{10} \left(\frac{P_{sep}}{114.7} \right) \quad [\text{Eq. 1780.7}]$$

C is a [calibration](#) constant.

The constants C_1, C_2, C_3 and C_4 :

C_1	C_2	C_3	C_4
0.10084	0.2556	7.4576	0.9868

Light oil, $31.1 < API$

For light oil the De Ghetto formula is a modified version of the [Standing](#) formula:

$$R_s(P, T) = C \cdot \gamma_G \cdot \left[\frac{P}{31.7648 \cdot A(T)} \right]^{1/0.7885} \quad [\text{Eq. 1780.8}]$$

Here A is a function of the fluid temperature and the oil API density:

$$\log_{10} A = 0.0009 \cdot T - 0.0148 \cdot API \quad [\text{Eq. 1780.9}]$$

C is a [calibration](#) constant.

Glasø

The Glasø formula for the solution gas-oil ratio is:

$$R_s = \gamma_G \cdot [f(P)]^{1.22549} \cdot API^{1.212009} \cdot T^{-0.210784} \quad [\text{Eq. 1780.10}]$$

Here:

$$\log_{10} f(P) = 2.887 \cdot \left[1 - \sqrt{1 - 0.397 \cdot (\log_{10} P - C)} \right] \quad [\text{Eq. 1780.11}]$$

C is a [calibration](#) constant.

Kartoatmodjo and Schmidt

The Kartootmodjo and Schmidt formula for the solution gas-oil ratio:

$$R_s = C \cdot C_1 \cdot \left[\gamma_G \cdot (1 + g_{corr}) \right]^{C_2} \cdot A(T) \cdot P^{C_4} \quad [\text{Eq. 1780.12}]$$

Here A is a function of the fluid temperature and the oil API density:

$$\log_{10} A = C_3 \cdot \frac{API}{T + 460} \quad [\text{Eq. 1780.13}]$$

If the separator pressure and temperatures are known then a non-zero gas specific gravity correction factor is used:

$$g_{corr} = 0.1595 \cdot API^{0.4078} \cdot T_{sep}^{-0.2466} \cdot \log_{10} \left(\frac{P_{sep}}{114.7} \right) \quad [\text{Eq. 1780.14}]$$

C is a [calibration](#) constant.

The constants C_1, C_2, C_3 and C_4 depend on the oil API density:

	C_1	C_2	C_3	C_4
$API < 30$	0.05958	0.7972	13.1405	1.0014
$API > 30$	0.0315	0.7587	11.2895	1.0937

Lasater

The Lasater formula for the solution gas-oil ratio:

$$R_s(P, T) = C \cdot 132755 \cdot \frac{Y_G}{(1 - Y_G)} \cdot \frac{\gamma_O}{MW_O} \quad [\text{Eq. 1780.15}]$$

$$Y_G = 0.08729793 + 0.37912718 \cdot \ln \left(\frac{P \cdot \gamma_G}{T + 460} + 0.769066 \right) \quad [\text{Eq. 1780.16}]$$

The oil molecular weight is given by

$$MW_O = 677.3893 - 13.2161 \cdot API + 0.024775 \cdot API^2 + 0.00067851 \cdot API^3 \quad [\text{Eq. 1780.17}]$$

The oil specific gravity is given by

$$\gamma_O = \frac{141.5}{API + 131.5} \quad [\text{Eq. 1780.18}]$$

C is a [calibration](#) constant.

Petrosky and Farshad

The Petrosky and Farshad formula for the solution gas-oil ratio is

$$R_s(P, T) = C \cdot \left[\left(\frac{P}{112.727} + 12.34 \right) \cdot \frac{\gamma_G^{0.8439}}{A(T)} \right]^{\frac{1}{0.5774}} \quad [\text{Eq. 1780.19}]$$

Here A is a function of the fluid temperature and the oil API density:

$$A(T) = 4.561 \cdot 10^{-5} \cdot T^{1.3911} - 7.916 \cdot 10^{-4} \cdot API^{1.541} \quad [\text{Eq. 1780.20}]$$

C is a [calibration](#) constant.

Standing

The Standing formula for the solution gas-oil ratio used in PIPESIM is:

$$R_s(P, T) = C \cdot \gamma_G \cdot \left[\frac{P}{A(T) \cdot 18} \right]^{1/0.83} \quad [\text{Eq. 1780.21}]$$

Here A is a function of the fluid temperature and the oil API density:

$$\log_{10} A = 0.00091 \cdot T - 0.0125 \cdot API \quad [\text{Eq. 1780.22}]$$

C is a [calibration](#) constant.

Vasquez and Beggs

The Vasquez and Beggs formula for the solution gas-oil ratio used in PIPESIM is:

$$R_s(P, T) = \frac{C}{C_1} \cdot \gamma_g \cdot (P - 14.7)^{C_2} \cdot A(T) \quad [\text{Eq. 1780.23}]$$

Here A is a function of the fluid temperature and the oil API density:

$$\log_{10} A = \frac{C_3 \cdot \text{API}}{T + 460} \quad [\text{Eq. 1780.24}]$$

C is a [calibration](#) constant.

The constants C_1 , C_2 and C_3 depend on the oil API density:

	C_1	C_2	C_3
$\text{API} < 30$	11.172	1.0937	11.172
$\text{API} > 30$	10.393	1.187	10.393

Calibration

If a calibration data point is provided, $R_{scal} = R_s(P_{cal}, T_{cal})$, then the calibration term C is calculated to ensure the calibration point is a solution of the relevant solution gas-oil ratio equation. For example, for the [Vasquez and Beggs](#) equation, the calibration term will be given by

$$R_{scal} = \frac{C}{C_1} \cdot \gamma_g \cdot (P_{cal} - 14.7)^{C_2} \cdot A(T_{cal}) \quad [\text{Eq. 1780.25}]$$

Hence the [Vasquez and Beggs](#) equation for the solution gas oil ratio can be re-written as:

$$R_s(P, T) = R_{scal} \cdot \left(\frac{P - 14.7}{P_{cal} - 14.7} \right)^{C_2} \cdot \frac{A(T)}{A(T_{cal})} \quad [\text{Eq. 1780.26}]$$

It is assumed that the calibration point is a [bubble point](#), although this will in fact only be the case if the calibration solution gas-oil ratio R_{scal} is equal to the fluid GOR.

If no calibration data is provided, PIPESIM uses $C = 1$.

Bubble point pressure

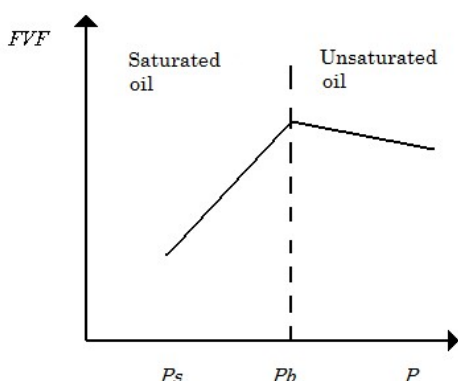
The bubble point pressure $P_b(T)$ is the pressure at which all the free gas is dissolved, i.e. when the solution gas-oil ratio is equal to the fluid GOR:

$$R_s(P_b, T) = R_{sb} \quad [\text{Eq. 1780.27}]$$

The bubble point can therefore be determined by solving the relevant [solution gas-oil ratio](#) equation.

Oil formation volume factor

The oil formation volume factor (FVF) is the ratio of the oil volume (at a given pressure and temperature) to the stock tank oil volume. As pressure increases, two competing processes take place: gas is dissolved in oil which increases the volume, and the oil is compressed, which decreases the volume. Below the bubble point, the effect of gas dissolving in oil dominates and the saturated oil FVF increases with pressure. However at the bubble point pressure, all the available gas has dissolved in the oil. Therefore above the bubble point pressure the only effect is compressibility and the undersaturated oil FVF increases with pressure.



Separate correlations are available for the [saturated oil FVF](#) and [undersaturated oil FVF](#).

Related links:

[Calibration properties](#)

Oil formation volume factor for saturated systems

For saturated systems $P < P_b$ the oil formation volume factor B_{ob} (bbl/STB) depends on the solution gas-oil ratio R_s and the temperature T .

Standing

The saturated oil formation volume factor is given by:

$$B_{ob} = 0.972 + 0.000147F^{1.175} \quad [\text{Eq. 1782.1}]$$

where the correlating factor is calculated using :

$$F = R_s \left(\frac{\gamma_g}{\gamma_o} \right)^{0.5} + 1.25T \quad [\text{Eq. 1782.2}]$$

[Data used to develop correlation](#)

Vasquez and Beggs

The saturated oil formation volume factor is given by:

$$B_{ob} = 1 + C_1 R_s + C_2 (T - 60) \left(\frac{API}{\gamma_G} \right) + C_3 R_s (T - 60) \left(\frac{API}{\gamma_G} \right)^2 \quad [\text{Eq. 1782.3}]$$

	C_1	C_2	C_3
$API < 30$	$4.677 \cdot 10^{-4}$	$1.751 \cdot 10^{-5}$	$-1.81 \cdot 10^{-8}$
$API > 30$	$4.67 \cdot 10^{-4}$	1.100×10^{-5}	1.337×10^{-9}

[Data used to develop correlation](#)

Kartoatmodjo and Schmidt

The saturated oil formation volume factor is given by:

$$B_{ob} = 0.98496 + 0.0001F^{1.50} \quad [\text{Eq. 1782.4}]$$

Where the correlating factor

$$F = R_s^{0.755} \gamma_g^{0.25} \gamma_o^{-1.50} + 0.45T \quad [\text{Eq. 1782.5}]$$

Oil formation volume factor for undersaturated systems

The oil formation volume factor B_o (bbl/STB) for pressures above the bubble point is given by a simple compressibility law:

$$B_o = B_{ob}(R_{sb}) \cdot \exp \left[\lambda Z_o(p_b - p) \right] \quad [\text{Eq. 1783.1}]$$

where Z_o is the oil compressibility and λ is a calibration factor (used in mixing different fluids).

Vasquez and Beggs

The Vasquez and Beggs correlation for the oil compressibility is

$$Z_o = 10^{-5} \cdot \frac{5 \cdot R_{sb} + 17.2 \cdot T - 1180 \cdot \gamma_G + 12.61 \cdot API - 1433}{P} \quad [\text{Eq. 1783.2}]$$

[Data used to develop correlation](#)

TURZO method

The performance of a rotodynamic (centrifugal or vertical) pump on a viscous liquid differs from the performance on water, which is the basis for most published curves. Typically, head and rate of flow decrease as viscosity increases, while power and the net positive suction head required (NPSHR) increases. Starting torque could be affected.

The following formula is the TURZO equation for viscosity correction:

$$\text{Power} = \frac{Q \cdot H}{E} \quad [\text{Eq. 1784.1}]$$

where

P is power.

Q is the rate.

H is the head.

E is the efficiency.

$$Q_v = Q \cdot f_Q \quad [\text{Eq. 1784.2}]$$

$$H_v = H \cdot f_H \quad [\text{Eq. 1784.3}]$$

$$E_v = E \cdot f_E \quad [\text{Eq. 1784.4}]$$

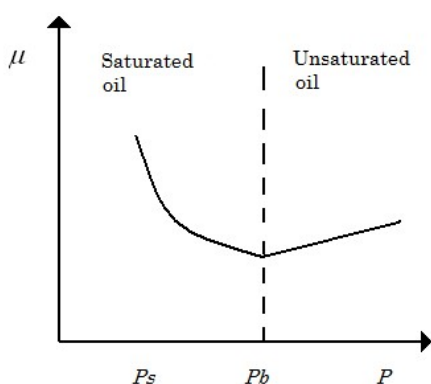
where the value of each equation is less than 1.

The viscosity correction is calculated as follows:

$$\frac{P_v}{P} = \frac{f_Q \cdot f_H}{f_E} \quad [\text{Eq. 1784.5}]$$

Oil viscosity

As pressure increases, two competing processes take place: gas is dissolved in oil which lightens the oil, reducing its viscosity, and the oil is compressed, which increases the viscosity. Below the bubble point, the effect of gas dissolving in oil dominates and the saturated viscosity decreases with pressure. However at the bubble point pressure, all the available gas has dissolved in the oil. Therefore above the bubble point pressure the only effect is compressibility and the undersaturated viscosity increases with pressure.



Three sets of correlations are used to determine the oil viscosity:

- At stock tank pressure the oil viscosity is given by [dead oil viscosity correlations](#) as a function of the flowing fluid temperature $\mu_o(P_s, T) = \mu_{od}(T)$.
- At pressures below the bubble point the oil viscosity is given by [live oil viscosity correlations](#) as a function of the dead oil viscosity and the solution gas-oil ratio $\mu_o(P, T) = \mu_{ob}(\mu_{od}, R_s)$.
- At pressures above the bubble point the oil viscosity is given by [undersaturated oil viscosity correlations](#), as a function of the bubble point viscosity and the pressure $\mu_o(P, T) = \mu_{ou}(\mu_{ob}, P)$.

Dead oil viscosity

The correlations available for calculating dead oil viscosity are:

Beggs and Robinson

Dead oil viscosity is calculated as follows :

$$\mu_{od} = 10^x - 1 \quad [\text{Eq. 1786.1}]$$

where $x = yT^{-1.163}$

and $y = 10^z$ and $z = 3.0324 - 0.02023 \cdot g_{API}$

Data used to develop correlation

The Beggs-Robinson dead oil viscosity correlation was developed using temperature data above 70F. The Beggs-Robinson correlation, when applied to lower temperatures tends to overpredict viscosity and may display asymptotic behavior which worsens with decreasing API gravity and temperature. To address this, extrapolation to temperatures lower than 70F are performed by tuning the [Users Data](#) equation using Beggs and Robinson calculations at 70F and 80F.

However, as a best practice user data should be used to calibrate dead oil viscosity, especially for low API oils are modeled at temperatures lower than 70F.

[Data used to develop correlation](#)

Glasø

Dead oil viscosity is calculated as follows :

$$\mu_{od} = c[\log_{10}(g_{API})]^d \quad [\text{Eq. 1786.2}]$$

where

$$c = 3.141 \cdot 10^{10} \cdot T^{-3.444} \text{ and } d = 10.313 \cdot \log_{10}(T) - 36.447$$

Kartoatmodjo and Schmidt

Dead oil viscosity is calculated as follows :

$$\mu_{od} = c[\log_{10}(g_{API})]^d \quad [\text{Eq. 1786.3}]$$

where

$$c = 16 \cdot 10^8 \cdot T^{-2.8177} \text{ and } d = 5.7526 \cdot \log_{10}(T) - 26.9718$$

De Ghetto et al

De Ghetto et al. use a combination of four correlations to compute the dead oil viscosity depending on the value of the API.

For API < 10 (extra heavy oils) the following correlation is used:

$$\mu_{od} = 10^x - 1 \quad [\text{Eq. 1786.4}]$$

where $x = 10^y$ and $y = 1.90296 - 0.012619 \cdot g_{API} - 0.61748 \cdot \log_{10}(T)$

For 10 < API < 22.3 (heavy oils) the following correlation is used:

$$\mu_{od} = 10^x - 1 \quad [\text{Eq. 1786.5}]$$

where $x = 10^y$ and $y = 2.06492 - 0.0179 \cdot g_{API} - 0.70226 \cdot \log_{10}(T)$

For 22.3 < API < 31.1 (medium oils) the following correlation is used:

$$\mu_{od} = c[\log_{10}(g_{API})]^d \quad [\text{Eq. 1786.6}]$$

where $c = 220.15 \cdot 10^9 \cdot T^{-3.556}$ and $d = 12.5428 \cdot \log_{10}(T) - 45.7874$

For API > 31.1 (light oils) the following correlation is used

$$\mu_{od} = 10^x - 1 \quad [\text{Eq. 1786.7}]$$

where $x = 10^y$ and $y = 1.67083 - 0.017628 \cdot g_{API} - 0.61304 \cdot \log_{10}(T)$

Petrosky and Farshad

Dead oil viscosity is calculated as follows:

$$\mu_{od} = c \left[\log_{10}(g_{API}) \right]^d \quad [\text{Eq. 1786.8}]$$

where $c = 2.3511 \cdot 10^7 \cdot T^{-2.10255}$ and $d = 4.59388 \cdot \log_{10}(T) - 22.82792$

Hossain et al

Hossain et al. correlation for dead oil viscosity is only valid for heavy oils ($10 < \text{API} < 22.3$) and it is given as follows:

$$\mu_{od} = 10^A \cdot T^B \quad [\text{Eq. 1786.9}]$$

where $A = -0.71523 \cdot g_{API} + 22.13766$ and $B = 0.269024 \cdot g_{API} - 8.268047$

Elsharkawy and Alikhan

Elsharkawy and Alikhan dead oil viscosity is only valid in the API range 20-48 and is calculated as follows:

$$\mu_{od} = 10^x - 1 \quad [\text{Eq. 1786.10}]$$

where $x = 10^y$ and $y = 2.16924 - 0.02525 \cdot g_{API} - 0.68875 \cdot \log_{10}(T)$

User's data

If user's data is selected for the dead oil viscosity method, then a curve is fitted through the two supplied data points (μ_1, T_1) and (μ_2, T_2) based on the functional form of the [Beal correlation](#):

$$\log(\mu_{od}) = \log(B) - C \log(T) \quad [\text{Eq. 1786.11}]$$

where

$$C = \frac{\log\left(\frac{\mu_1}{\mu_2}\right)}{\log\left(\frac{T_2}{T_1}\right)} \quad [\text{Eq. 1786.12}]$$

and

$$B = \mu_1 T_1^C = \mu_2 T_2^C \quad [\text{Eq. 1786.13}]$$

Live oil viscosity correlations

Many of the correlations available for calculating live oil viscosity are of the form

$$\mu_{ob} = A \cdot \mu_{od}^B \quad [\text{Eq. 1787.1}]$$

where A and B are functions of the Solution gas-oil ratio R_s :

Correlation		A	B
Chew and Connally	Data used to develop correlation	$0.2 + \left(\frac{0.8}{10^{0.000852 R_s}} \right)$	$0.482 + \left(\frac{0.518}{10^{0.000777 R_s}} \right)$
Beggs and Robinson	Data used to develop correlation	$10.715 \cdot (R_s + 100)^{-0.515}$	$5.44 \cdot (R_s + 150)^{-0.338}$
Elsharkawy and Alikhan		$1241.932 \cdot (R_s + 641.026)^{-1.12410}$	$1768.841 \cdot (R_s + 1180.335)^{-1.06622}$
Hossain et al		$1 - 1.7188311 \cdot 10^{-3} \cdot R_s + 1.58031 \cdot 10^{-6} \cdot R_s^2$	$1 - 2.052461 \cdot 10^{-3} \cdot R_s + 3.47559 \cdot 10^{-6} \cdot R_s^2$
Petrosky and Farshad		$0.1651 + 0.6165 \times 10^{-6.0866 \times 10^{-4} \times R_s}$	$0.5131 + 0.5109 \times 10^{-1.1831 \times 10^{-3} \times R_s}$

Other authors use more complicated formulas:

Kartoatmodjo and Schmidt

Live oil viscosity is calculated as follows:

$$\mu_{ob} = -0.06821 + 0.9824F + 0.0004034F^2 \quad [\text{Eq. 1787.2}]$$

where

$$F = A \cdot \mu_{od}^{0.43+0.5165 \cdot B} \quad [\text{Eq. 1787.3}]$$

and

$$A = 0.2001 + 0.8428 \left[10^{-0.000845 R_s} \right] \quad [\text{Eq. 1787.4}]$$

and

$$B = 10^{-0.00081 R_s} \quad [\text{Eq. 1787.5}]$$

Khan

Live oil viscosity calculated by Khan is a function of the gas and oil specific gravities (γ_G, γ_O), the solution gas-oil ratio (R_s), the bubble pressure (P_b), and the flowing pressure (P). It is given as follows:

$$\mu_{ob} = A \cdot e^y \quad [\text{Eq. 1787.6}]$$

where

$$y = \ln(0.09) + 0.5 \cdot \ln(\gamma_G) - \frac{1}{3} \cdot \ln(R_s) - 4.5 \cdot \ln\left(\frac{T}{460}\right) - 3 \cdot \ln(1 - \gamma_O) \quad [\text{Eq. 1787.7}]$$

and

$$A = \left(\frac{P}{P_b} \right)^{-0.14} \cdot e^{-2.5 \times 10^{-4}(P - P_b)} \quad [\text{Eq. 1787.8}]$$

De Ghetto et al

De Ghetto et al. expression of the live oil viscosity is a combination of 4 correlations depending on the value of oil API.

		F	A	B
For API < 10 (extra heavy oils)	$\mu_{ob} = 2.3945 + 0.8927F + +0.01567F^2$	$A \cdot \mu_{od}^{0.5798+0.3432B}$	$-0.0335 + +1.0875 \left[10^{-0.000845 \cdot R_s} \right]$	$10^{-0.00081 \cdot R_s}$
For $10 < \text{API} < 22.3$ (heavy oils)	$\mu_{ob} = -0.6311 + 1.078F - -0.003653F^2$	$A \cdot \mu_{od}^{0.4731+0.5664B}$	$0.2478 + +0.6114 \left[10^{-0.000845 \cdot R_s} \right]$	$10^{-0.00081 \cdot R_s}$
For $22.3 < \text{API} < 31.1$ (medium oils)	$\mu_{ob} = 0.0132 + 0.9821F - -0.005215F^2$	$A \cdot \mu_{od}^{0.3855+0.5664B}$	$0.2038 + +0.8591 \left[10^{-0.000845 \cdot R_s} \right]$	$10^{-0.00081 \cdot R_s}$
For $\text{API} > 31.1$ (light oils)	$\mu_{ob} = A \cdot \mu_{od}^B$		$25.1921 \cdot (R_s + 100)^{-0.6487}$	$2.7516 \cdot (R_s + 150)^{-0.2135}$

Undersaturated oil viscosity

The correlations available for calculating undersaturated oil viscosity are:

Vasquez and Beggs

Undersaturated oil viscosity is calculated as follows:

$$\mu_{ou} = \mu_{ob} \left(\frac{p}{p_b} \right)^A \quad [\text{Eq. 1788.1}]$$

where $A = 2.6p^{1.187} \exp(-8.98 \times 10^{-5}p - 11.513)$

[Data used to develop correlation](#)

Kouzel

Undersaturated oil viscosity is derived from the equation:

$$\mu_{ou} = \mu_{ob} \cdot \frac{10^{F(p)}}{10^{F(p_b)}} \quad [\text{Eq. 1788.2}]$$

$$F(p) = \frac{p - 14.7}{1000 \left(A + B\mu_{od}^{0.278} \right)} \quad [\text{Eq. 1788.3}]$$

Where A and B are parameters entered by the user. Suggested values for A and B are 0.0239 and 0.01638 respectively.

Kartoatmodjo and Schmidt

Undersaturated oil viscosity is calculated as follows:

$$\mu_{ou} = 1.00081\mu_{ob} + 0.001127A(p - p_b) \quad [\text{Eq. 1788.4}]$$

$$A = -0.006517\left(\mu_{ob}^{1.8148}\right) + 0.038\left(\mu_{ob}^{1.59}\right)$$

Khan

Undersaturated oil viscosity is calculated as follows:

$$\mu_{ou} = \mu_{ob} \exp[9.65e^{-5}(p - p_b)] \quad [\text{Eq. 1788.5}]$$

De Ghetto et al

De Ghetto et al. expression of the undersaturated oil viscosity is a combination of 3 correlations depending on the value of oil API.

For API < 10 (extra heavy oils) the following correlation is used:

$$\mu_{ou} = \mu_{ob} - \left(1 - \frac{p}{p_b}\right) \left(\frac{A}{B} \right) \quad [\text{Eq. 1788.6}]$$

$$\text{where } A = 10^{-2.19} \left(\mu_{od}^{1.055} \right) \left(p_b^{0.3132} \right) \text{ and } B = 10^{(0.0099g_{API})}$$

For 10 < API < 22.3 (heavy oils) the following correlation is used:

$$\mu_{ou} = 0.9886\mu_{ob} + 0.002763A(p - p_b) \quad [\text{Eq. 1788.7}]$$

$$\text{where } A = -0.01153\left(\mu_{ob}^{1.7933}\right) + 0.03610\left(\mu_{ob}^{1.5939}\right)$$

For API > 22.3 (medium and light oils) the following correlation is used:

$$\mu_{ou} = \mu_{ob} - \left(1 - \frac{p}{p_b}\right) \frac{A}{B} \quad [\text{Eq. 1788.8}]$$

$$\text{where } A = 10^{-2.19} \left(\mu_{od}^{1.055} \right) \left(p_b^{0.3132} \right) \text{ and } B = 10^{(-0.00288g_{API})}$$

Hossain et al

Undersaturated oil viscosity is calculated as follows:

$$\mu_{ou} = \mu_{ob} + 0.004481(p - p_b)(A - B) \quad [\text{Eq. 1788.9}]$$

where $A = 0.555955(\mu_{ob})^{1.068099}$ and $B = 0.527737(\mu_{ob})^{1.063547}$

Petrosky and Farshad

Undersaturated oil viscosity is calculated as follows:

$$\mu_{ou} = \mu_{ob} + 1.3449E^{-3}(p - p_b)(10^A) \quad [\text{Eq. 1788.10}]$$

where $A = -1.0146 + 1.3322X - 0.4876X^2 - 1.15036X^3$ and $X = \log_{10}(\mu_{ob})$

Elsharkawy and Alikhan

Undersaturated oil viscosity is calculated as follows:

$$\mu_{ou} = \mu_{ob} + A[10^{-2.0771}](p - p_b) \quad [\text{Eq. 1788.11}]$$

where $A = [\mu_{od}]^{1.19279} \cdot [\mu_{ob}]^{-0.40712} \cdot [p_b]^{-0.7941}$

Bergman and Sutton

Undersaturated oil viscosity is calculated as follows:

$$\mu_{ou} = \mu_{ob} \exp[A(p - p_b)^B] \quad [\text{Eq. 1788.12}]$$

where $A = 2.278877 \cdot 10^{-4} - 1.48211 \cdot 10^{-5} \cdot X + 6.5698 \cdot 10^{-7} \cdot X^2$, $B = 0.873204 + 2.24623 \cdot 10^{-2} \cdot X$ and $X = \log_{10}(\mu_{ob})$

Disabling the calculation of undersaturated oil viscosity

If you select **None** as the undersaturated oil viscosity method, then the undersaturated oil viscosity is assumed to be the same as the saturated live oil viscosity at the same temperature and pressure.

Gas compressibility

The real gas law is given by $pV = ZRT$ where

P	pressure
V	volume
R	universal gas constant
T	absolute temperature
Z	gas compressibility factor

Numerous equations of state have been proposed to predict this Z-factor. Standing and Katz presented a generalized Z-factor chart for predicting the volumetric behavior of natural gases. To employ this chart, we require knowledge of the critical properties of the gas (namely, critical pressure and critical temperature) as a function of the specific gravity. These are given in the black oil model by Standing (1977) for natural gas and gas-condensate systems:

Gas systems

$$T_c = 168 + 325 \gamma_G - 12.5 \gamma_G^2 \quad [\text{Eq. 1789.1}]$$

Gas-condensate systems

$$T_c = 187 + 330 \gamma_G - 71.5 \gamma_G^2 \quad [\text{Eq. 1789.2}]$$

$$p_c = 706 - 51.7 \gamma_G - 11.1 \gamma_G^2 \quad [\text{Eq. 1789.3}]$$

where



T_c	critical temperature
p_c	critical pressure
γ_G	specific gravity of the gas mixture

This allows us to calculate the reduced temperature and reduced pressure, defined respectively as:

$$T_c = \frac{T}{T_c} \quad [\text{Eq. 1789.4}]$$

$$p_c = \frac{P}{p_c} \quad [\text{Eq. 1789.5}]$$

Various correlations have been proposed for curve fitting this reduced pressure-reduced temperature Z-factor chart and are available in PIPESIM:

[Hall-Yarborough Z-Factor Correlation](#)

[Standing Z-Factor Correlation](#)

[Robinson et al. Z-Factor Correlation](#)

Hall-Yarborough Z-factor correlation

Gas compressibility (Z-factor) is calculated as follows:

$$Z = \left(\frac{0.06125 p_R T_R}{\rho_R} \right) e^{x \left[-1.2(1-T_R)^2 \right]} \quad [\text{Eq. 1789.6}]$$

where the reduced density is a root of the following equation:

$$F(\rho_R) = 0.06125 p_R T_R \left[-1.2(1-T_R)^2 \right] + \frac{\left(\rho_R^2 + \rho_R^3 + \rho_R^4 - \rho_R^5 \right)}{\left((1-\rho_R)^3 - \left(14.67 T_R^2 - 9.76 T_R^2 4.85 T_R^3 \right) \rho_R \right)^2} + \left(90.7 T_R - 242.2 T_R^2 + 42.4 T_R^3 \right) \rho_R = 0 \quad [\text{Eq. 1789.7}]$$

where

where ρ_R	reduced density
p_R	reduced pressure
T_R	reciprocal of the reduced temperature

The method is not recommended for use within a pressure range $p_R = [0, 1]$.

Standing Z-factor correlation

Gas compressibility (Z-factor) is calculated as follows:

$$Z = \frac{A + (1-A)}{e^x B + F p_r^G} \quad [\text{Eq. 1789.8}]$$

where the coefficients A to G are given by:

$A = 1.39(T_r - 0.92)^{0.5} - 0.36 T_R - 0.101$
$B = (0.62 - 0.23 T_r) p_R + \left[\frac{0.666}{(T_r - 0.86)} - 0.037 \right] p_R^2 + \frac{0.32 p_R^6}{10^9 (T_r - 1)}$
$C = (0.132 - 0.32 \log(T_R))$
$D = 10^{\left(0.3016 - 0.49 T_R + 0.1824 T_R^2 \right)}$

The method is not valid for $T_R < 0.92$.

Robinson et al. Z-factor correlation

Gas compressibility (Z-factor) is calculated as follows:

$$Z = 1 + \left[A_1 + \left(\frac{A_2}{T_R} \right) + \left(\frac{A_3}{T_R^3} \right) \right] \rho_R + \left[A_4 + \left(\frac{A_5}{T_D} \right) \right] \rho_R^2 + \left[\frac{A_6 A_7}{\rho_R} \right] D_R^5 \\ + \left[\frac{A_7}{T_r^3} \right] \rho_R^2 \left(1 + A_8 \rho_R^2 \right) e^{x(-A_8 \rho_R^2)} \quad [\text{Eq. 1789.9}]$$

where

$D = \frac{0.27 p_R}{T_R}$
$A_1 = 0.310506237$
$A_2 = -1.4067099$
$A_3 = -0.57832729$
$A_4 = 0.53530771$
$A_5 = -0.61232032$
$A_6 = -0.10488813$
$A_7 = 0.68157001$
$A_8 = 0.68446549$

The method is valid within a temperature and pressure range of $T_r = [1.05, 3.0]$ and $p_r = [0.2, 3.0]$.

Gas viscosity

Gas viscosity is calculated using the [Lee et al](#) correlation as follows:

$$\mu_g = K \cdot \exp \left[X \cdot \rho_g^Y \right] \quad [\text{Eq. 1008.1}]$$

where

$$K = \frac{(7.77 + 0.183 \cdot \gamma_G) \cdot (T + 460)^{1.5}}{(122.4 + 373.6 \cdot \gamma_G + T + 460)} \cdot 10^{-4}$$

$$X = 2.57 + \frac{1914.5}{T} + 0.275 \gamma_g$$

$$Y = 1.11 + 0.04X$$

μ_g	is the gas viscosity (cp)
γ_g	is the gas specific gravity
ρ_g	is the gas density (g/cc)
T	is the temperature ($^{\circ}\text{F}$)

Related links:

[Calibration properties](#)

Surface tension

Oil-gas surface tension

The oil-gas surface tension is given by [Baker and Swerdloff](#):

$$\sigma_O = [37.7 - 0.05 \cdot (T - 100) - 0.26 \cdot API] \cdot$$

$$\cdot [1 - 7.1 \cdot 10^{-4} \cdot P + 2.1 \cdot 10^{-7} \cdot P^2 + 2.37 \cdot 10^{-11} \cdot P^3]$$

[Eq. 1791.1]

σ_O	is the surface tension between the oil and the gas	(dynes/cm)
P	is the pressure	(psia)
T	is the temperature	(°F)
API	is the oil API gravity	

Water-gas surface tension

The water-gas surface tension is given by Katz:

$$\sigma_W = 70 - 0.1 \cdot (T - 74) - 0.002 \cdot P$$

[Eq. 1791.2]

σ_W	is the surface tension between the water and the gas	(dynes/cm)
P	is the pressure	(psia)
T	is the temperature	(°F)

Black oil enthalpy

Black oil fluid enthalpy model

The black oil fluid model makes some approximations in the entropy balance based upon the thermodynamic behavior of typical hydrocarbon fluids. The black oil model is suitable for light, medium and heavy oil based fluids, particularly if significant quantities of water are present. The black oil model is fast, simple to use and easy to calibrate. It is also suitable for gas and gas/condensate screening studies.

There are currently two black oil enthalpy calculation methods available in PIPESIM.

2009 method

The enthalpy of the gas phase is given by:

$$H_g = c_{p_g} T - \eta_g c_{p_g} P + \Delta H_{vap}$$

[Eq. 1792.1]

The enthalpy of the oil phase is given by:

$$H_o = c_{p_o} T - \eta_o c_{p_o} P$$

[Eq. 1792.2]

The enthalpy of the water phase is given by:

$$H_w = c_{p_w} T - \eta_w c_{p_w} P$$

[Eq. 1792.3]

where the gas, oil and water Joule Thomson coefficients are approximated by (Ref: [Alves, Alhanati and Shoham](#):

$$\eta_g = \frac{1}{\rho_g c_{p_g}} \left[\frac{T}{Z} \frac{\partial Z}{\partial T} \right] \Bigg| 5.40395$$

[Eq. 1792.4]

$$\eta_o = - \frac{1}{\rho_o c_{p_o}} \Bigg| 5.40395$$

[Eq. 1792.5]

$$\eta_w = - \frac{1}{\rho_w c_{p_w}} \Bigg| 5.40395$$

[Eq. 1792.6]

The total enthalpy of the fluid is given by:

$$H = H_g w_g + H_o w_o + H_w w_w$$

[Eq. 1792.7]

where:

H	is the specific enthalpy	BTU/lb
T	is the flowing temperature	$^{\circ}F$
P	is the flowing pressure	$psia$
c_p	is the specific heat capacity at constant pressure	$BTU/lb^{\circ}F$
η	is the Joule Thomson coefficient	$^{\circ}F/psia$
ρ	is the flowing density	lb/ft^3
Z	is the gas compressibility factor	dimensionless
w	is the flowing mass fraction	dimensionless
ΔH_{vap}	is the latent heat of vaporization	BTU/lb

$$1BTU/\text{ft}^3 = 5.40395 psia$$

1983 method

The enthalpy of the gas phase is given by:

$$H_g = c_{p_g} T + P \left[(1.619 \times 10^{-10} P + 1.412 \times 10^{-6})P - 0.02734 \right] \quad [\text{Eq. 1792.8}]$$

The enthalpy of the oil phase is given by:

$$H_o = c_{p_o} T + 3.36449 \times 10^{-3} P \quad [\text{Eq. 1792.9}]$$

The enthalpy of the water phase is given by:

$$H_w = c_{p_w} T + \left(\frac{2.9641 \times 10^{-3}}{\gamma_w} \right) P \quad [\text{Eq. 1792.10}]$$

The total enthalpy of the fluid is given by:

$$H = H_g m_g + H_o m_o + H_w m_w \quad [\text{Eq. 1792.11}]$$

where:

m	is the stock tank mass fraction	dimensionless
γ	is the stock tank specific gravity	dimensionless

Black oil mixing

Introduction

Mixing occurs in network models, when two or more streams meet at a junction and in single branch models where injected fluid, or fluids from multiple completions mix with fluid already in the branch. The fluid properties of the mixed stream need to be determined.

Stock tank oil properties

Phase ratios (gas oil ratio / water cut)

The phase ratios for a mixed stream are calculated by adding the individual phase rates of each stream and then calculating the ratio of the phases. The calculations are at stock tank conditions.

$$GOR_{mix} = \frac{Q_{vg,mix}}{Q_{vo,mix}} \quad [\text{Eq. 1793.1}]$$

$$WCUT_{mix} = \frac{Q_{vw,mix}}{Q_{vw,mix} + Q_{vo,mix}} \quad [\text{Eq. 1793.2}]$$

Here:

GOR_{mix}	is the gas oil ratio of the mixture
$WCUT_{mix}$	is the water cut of the mixture

$Q_{vo,mix} = \sum_{i=1}^n Q_{vo,i}$	is the stock tank oil volume rate of the combined stream
$Q_{vw,mix} = \sum_{i=1}^n Q_{vw,i}$	is the stock tank water volume rate of the mixture
$Q_{vg,mix} = \sum_{i=1}^n Q_{vg,i}$	is the stock tank gas volume rate of the mixture
$Q_{vo,i} = Q_{vL,i} \times (1 - WCUT_i)$	is the stock tank oil volume rate of stream i
$Q_{vw,i} = Q_{vL,i} \times WCUT_i$	is the water volume rate of stream i
$Q_{vg,i} = Q_{vL,i} \times GOR_i$	is the stock tank gas volume rate of stream i
$Q_{vL,i} = Q_{vo,i} + Q_{vw,i}$	is the stock tank liquid volume rate of stream i
$WCUT_i$	is the water cut of stream i
GOR_i	is the gas oil ratio of stream i
n	is the number of streams in the mixture

Phase densities

The phase densities (and specific gravities) are determined as a volumetric average of the input stream densities:

$$DOD_{mix} = \frac{\sum DOD_i \times Q_{vo,i}}{Q_{vo,mix}} \quad [\text{Eq. 1793.3}]$$

$$GSG_{mix} = \frac{\sum GSG_i \times Q_{vg,i}}{Q_{vg,mix}} \quad [\text{Eq. 1793.4}]$$

$$WSG_{mix} = \frac{\sum WSG_i \times Q_{vw,i}}{Q_{vw,mix}} \quad [\text{Eq. 1793.5}]$$

Here:

DOD_{mix}	is the dead oil density of the mixture
GSG_{mix}	is the gas specific gravity of the mixture
WSG_{mix}	is the water specific gravity of the mixture
DOD_i	is the dead oil density of stream i
GSG_i	is the gas specific gravity of stream i
WSG_i	is the water specific gravity of stream i

Contaminants

The mole fractions of contaminants for the mixed stream is determined using a gas phase volumetric average of the individual stream mole fractions:

$$Z_{j,mix} = \frac{\sum Z_{j,i} \times Q_{vg,i}}{Q_{vg,mix}} \quad [\text{Eq. 1793.6}]$$

Here:

$Z_{j,mix}$	is the mole fraction of contaminant j in the mixture
$Z_{j,i}$	is the mole fraction of contaminant j in stream i

Thermal data (heat capacity and thermal conductivity)

The phase thermal properties of mixed streams are calculated using mass averages of the phase properties of the input streams:

$$CP_{\varphi,mix} = \frac{\sum CP_{\varphi,i} \times Q_{\varphi,i}}{Q_{\varphi,mix}} \quad [\text{Eq. 1793.7}]$$

$$K_{\varphi,mix} = \frac{\sum K_{\varphi,i} \times Q_{\varphi,i}}{Q_{\varphi,mix}} \quad [\text{Eq. 1793.8}]$$

$$\Delta H_{vap,mix} = \frac{\sum \Delta H_{vap,i} \times Q_{g,i}}{Q_{g,mix}} \quad [\text{Eq. 1793.9}]$$

Here:

φ	is the phase, oil $\varphi = O$, vapor (gas) $\varphi = G$, or water $\varphi = W$
$CP_{\varphi,mix}$	is the heat capacity of phase φ in the mixture
$K_{\varphi,mix}$	is the thermal conductivity of phase φ in the mixture
$\Delta H_{vap,mix}$	is the latent heat of vaporization of the gaseous phase g in the mixture
$CP_{\varphi,i}$	is the heat capacity of phase φ in stream i
$K_{\varphi,i}$	is the thermal conductivity of phase φ in stream i
$\Delta H_{vap,i}$	is the latent heat of vaporization of the gaseous phase g in stream i
$Q_{\varphi,mix} = \sum_{i=1}^n Q_{\varphi,i}$	is the mass flow rate of phase φ of the mixture
$Q_{\varphi,i}$	is the mass flow rate of phase φ of stream i

Correlations

Unlike other properties, the choice of correlations used for the combined fluid can not be decided by averaging. Instead, the selected correlation for the mixed stream is chosen as the one which has the highest flow rate associated with it for the relevant phase. For example the correlation for mixture Oil Viscosity is set to be the correlation that has maximum stock tank rate associated with it.

While deciding the correlation for the mixed stream, we have to consider following rules:

- All properties are independent of each other. For example the choice for mixture dead Oil viscosity correlation has nothing to do with mixture live Oil viscosity
- Resultant mixture correlation is decided based on associated phase rate (for example, oil if we are deciding Oil property) ; not based on number of streams using that correlation
- Stock tank flow rates are used at the point of mixing.

Example 1

For an example assume we are mixing 7 flow streams which have different sets of correlations as tabulated below:

Stream	Flow rate (STB/day)	Dead Oil Viscosity	Live Oil Viscosity	Under-saturated Oil Viscosity
1	5000	Hossain	Kartoatmodjo	Vasquez and Beggs
2	2000	Glasso	Khan	Kouzel
3	4000	Petrosky-Farshad	Chew and Connally	Kouzel
4	3000	Beggs and Robinson	Khan	Kouzel
5	6000	Beggs and Robinson	Kartoatmodjo	Bergman and Sutton
6	8000	Glasso	Hossain	Bergman and Sutton
7	2000	Beggs and Robinson	Elsharkawy	Kouzel

The total oil flow for each correlation, and the correlations selected for the combined fluid are tabulated below:

Stream	Flow rate (STB/day)	Dead Oil Viscosity
4,5,7	11000	Beggs and Robinson
2,6	10000	Glasso
1	5000	Hossain
3	4000	Petrosky-Farshad
combined	30000	Beggs and Robinson

Stream	Flow rate (STB/day)	Live Oil Viscosity
1,5	11000	Kartoatmodjo
6	8000	Hossain
2,4	5000	Khan
3	4000	Chew and Connally
7	2000	Elsharkawy
combined	30000	Kartoatmodjo

Stream	Flow rate (STB/day)	Under-saturated Oil Viscosity
5,6	14000	Bergman and Sutton

2,3,4,7	11000	Kouzel
1	5000	Vasquez and Beggs
combined	30000	Bergman and Sutton

Example 2

Mixing of fluids that use different correlations may produce unexpected results. In the above example, a 51%-49% mixture of streams 1 and 2 will use the same correlations as stream 1, but a 49%-51% mixture will use the same correlations as stream 2. So, even though these two mixtures are similar, their properties may be modelled completely differently. Therefore it is important to select compatible correlations when modelling networks.

Calibration data

A number of correlations are calibrated using user supplied data. This section describes how streams with different calibration data are mixed.

Dead oil viscosity

[Dead oil viscosity](#) can be specified using no calibration data; 2-point $\{(T_1, \mu_1), (T_2, \mu_2)\}$ calibration data; or as a **User Supplied Table** with multipoint calibration data $\{(T_1, \mu_1), \dots, (T_n, \mu_n)\}$. If none of the streams in a mixture use calibration data, then the mixing is done by simply determining the mixture correlation, as outlined in [Correlations](#). If however, at least one of the input streams uses dead oil viscosity with calibration data then a **User Supplied Table** is used for the mixture deadoil viscosity. The table entries are calculated in three steps:

1. The number and value of the temperature points $\{T_x\}$ in the table are determined:
 - o If the inlet streams use multipoint calibration, then the mixed stream will use multipoint calibration. PIPESIM will try to include all the input temperatures in the mixture table, up to a maximum of 40 points.
 - o If the inlet streams only use 2-point calibration data, then the mixed stream will use only two points. The Temperature will be set to the minimum and maximum temperatures of the input stream calibration temperatures.
2. The viscosity of each inlet stream $\mu_i(T_x)$ is calculated at each temperature in the mixed stream table.
3. The mixture viscosity is calculated at each point in the stream using the Kendall and Monroe cubic mixing rule:

$$\mu_{comb}(T_x) = \left(\sum_{i=1}^n \frac{Q_{vo,i}}{Q_{vo,mix}} \cdot (\mu_i(T_x))^{1/3} \right)^3 \quad [\text{Eq. 1793.10}]$$

Example 3

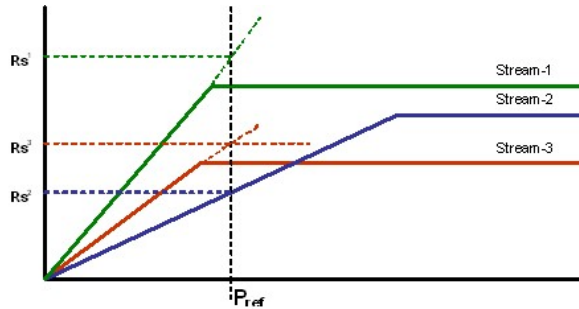
Streams 1–3, defined in the table below, mix at a junction. All streams use dead oil correlations without data, so the mixed stream, stream 4, uses the dead oil correlation with the biggest flow, in this case Beggs and Robinson. Stream 4 then mixes with stream 5 at another junction. Stream 5 uses a correlation with calibration data. Even though stream 5 has less flow than stream 4, the mixture, stream 6, will use a User Supplied Table to define its dead oil correlation.

Stream	Flow rate (STB/day)	Dead Oil Viscosity
1	2000	Beggs and Robinson
2	2500	Chew and Connally
3	1000	Beggs and Robinson
4= 1+2+3	5500	Beggs and Robinson
5	2500	Any correlation with 2-point data, or a User Supplied Table
6 = 4+5	8000	User Supplied Table

Solution gas Rs

If one or more of the input streams has a single point calibration data, $R_{si}(P_{ref,i}, T_{ref,i})$, then the mixed stream solution gas will also be calibrated using a single point:

1. Determine the [correlation](#) for the mixed stream.
2. Determine reference pressure and temperature values $(P_{ref,mix}, T_{ref,mix})$ for calibrating the mixed stream viscosity. These are calculated as the mass flow rate average of the input stream reference pressures and temperatures — for those input streams with calibration data.
3. Determine the solution gas of each stream at the reference pressure and temperature for the mixed stream $R_{si}(P_{ref,mix}, T_{ref,mix})$. For those streams that are undersaturated at $(P_{ref,mix}, T_{ref,mix})$ the “potential” solution gas is determined by extrapolation.



4. The solution gas for the mixed stream is determined as a volume average of all the input stream solution gas (or potential solution gas) values.

Live oil viscosity

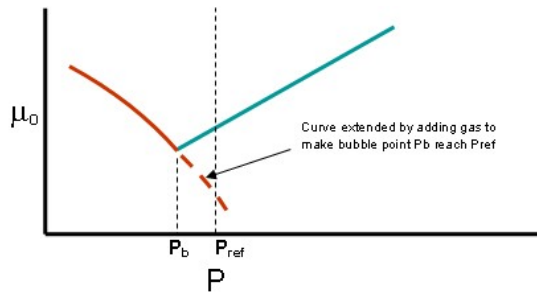
A number of steps are needed to determine the live oil viscosity of a mixture:

1. Determine the [correlation](#) for the mixed stream.
2. Determine reference pressure and temperature values ($P_{ref,mix}$, $T_{ref,mix}$) for calibrating the mixed stream viscosity. These are calculated as the mass flow rate average of the input stream reference pressures and temperatures, for those input streams with calibration data. If the mixed stream is not saturated at the calculated reference pressure and temperature, the reference pressure is reduced to the saturation pressure

$$T_{ref,mix} = \sum_{i=1}^n \frac{Q_{o,i}}{Q_{o,mix}} T_{ref,i}$$

$$P_{ref,mix} = \text{MIN} \left[\sum_{i=1}^n \frac{Q_{o,i}}{Q_{o,mix}} P_{ref,i}, P_{sat,mix}(T_{ref,mix}) \right]$$

3. Determine the input stream viscosities at the mixture reference pressure and temperature $\mu_{o,i}(P_{ref,mix}, T_{ref,mix})$. If an input stream is undersaturated at $(P_{ref,mix}, T_{ref,mix})$ then its viscosity is calculated by first adding more gas so that the stream is saturated. The added gas has a specific gravity equal to that of the mixture.



4. The live oil viscosity of the mixture is calculated at $(P_{ref,mix}, T_{ref,mix})$ using the [1793.10](#) equation.

5. The live oil correlation can then be calibrated using $\mu_{o,mix}(P_{ref,mix}, T_{ref,mix})$

Compositional fluid modeling

In compositional fluid models the user can specify a number of components that make up the fluid. These can be real molecules, such as methane, ethane or water, known as library components or pseudo components that represent the properties of several molecules, known as petroleum fractions. The phase behaviour and thermodynamic properties are determined by an equation of state (EOS). This equation of state is either a [cubic equation](#) (this is a modified form of the Van der Waals equation) or a [non-cubic equation](#). The number of phases that can be modelled depends on the flash package:

- **Two phase flash.** Water is removed from the fluid and the remaining hydrocarbons are flashed to determine the amount of oil and vapour. This method is used for most compositional flash packages (and for black oil models). This means that water only appears in the water phase and does not appear in the vapour phase.
- **Three phase flash.** If the Multiflash compositional package is used, then a three phase flash is performed. This means that there is a possibility that water will appear in the vapour phase, and some components (e.g. water, methanol) will appear in the aqueous phase.

The three phase flash gives a more accurate model of water behaviour than the two phase flash. However, there can be problems when the flash produces two non-aqueous liquids — one of these may be mis-identified as water.

- **Multiphase flash.** The Multiflash compositional standalone package can be used to model vapour and three liquid phases as well as solid phases. Within PIPESIM flow simulations, Multiflash is only ever used to model two liquid phases. However, it can be used within PIPESIM to plot phase envelopes and to predict whether solid phases (asphaltene, hydrates, wax and ice) would be present.

Cubic equations of state

Equations of state (EoS) describe the pressure, volume and temperature (PVT) behavior of pure components and mixtures. The phase state and most thermodynamic properties (e.g. density, enthalpy, entropy) are derived from the equation of state. Separate models are used for transport properties, such as [Viscosity](#), thermal conductivity and surface tension. PIPESIM can use both cubic and [non-cubic](#) Equations of State.

Volume shift (three-parameter) and acentric factor corrections, if available, are recommended for the cubic equations of state.

The cubic equation of state can be written as:

$$P = \frac{nRT}{V - b} + \frac{a}{(V + m_1 \cdot b) \cdot (V + m_2 \cdot b)} \quad [\text{Eq. 1795.1}]$$

Where:

P	is the pressure of the fluid
V	is the total volume of the container containing the fluid
a	is a measure of the attraction between particles
b	is the volume excluded from V by a particle
n	is the number of moles
T	is the temperature
R	is the gas constant
m₁, m₂	constants: for the Peng-Robinson EOS $(m_1, m_2) = (1 + \sqrt{2}, 1 - \sqrt{2})$ for the Soave—Redlich—Kwong EOS $(m_1, m_2) = (1, 0)$

The EoS is a cubic equation for the volume, as a function of the pressure, temperature and EoS parameters. It is often written in terms of the compressibility:

$$Z = \frac{PV}{nRT} \quad [\text{Eq. 1795.2}]$$

In the special case $(m_1, m_2) = (0, 0)$ the cubic EoS reduces to van der Waals equation, and in the special case when $a = b = 0$ the cubic EoS reduces to the ideal gas equation.

The parameters **a** and **b** are in fact functions of the pressure, temperature, composition, component properties and the mixing rules. If there is more than one phase present, the composition of each phase differs and hence each phase has different equation of state parameters. Assuming a quadratic mixing rule for **a** and a linear mixing rule for **b** the parameters for phase φ are given by

$$a_\varphi = \frac{n^2 \cdot R^2 \cdot T^2}{P} \cdot \sum \sum (A_i \cdot A_j)^{1/2} \cdot (1 - \delta_{ij}) \cdot x_{\varphi i} \cdot x_{\varphi j} \quad [\text{Eq. 1795.3}]$$

$$b_\varphi = \frac{n \cdot R \cdot T}{P} \cdot \sum B_i \cdot x_{\varphi i} \quad [\text{Eq. 1795.4}]$$

Where:

$x_{\varphi i}$	is the mole fraction of component <i>i</i> in phase φ
A_i	is a function of the temperature T , the component critical pressure P_{ci} , critical temperature T_{ci} and acentric factor ω_i
B_i	is a function of the component critical pressure P_{ci} and critical temperature T_{ci}
δ_{ij}	is the Binary Interaction Parameter between component <i>i</i> and component <i>j</i>

Thermodynamic properties

Thermodynamic properties can be calculated from the equation of state. The method may vary between flash packages. The following equations are used in E300 flash.

The fugacity coefficient $\Phi_{\varphi i}$ for each component in each phase is used to determine the phase state and phase split. It is given by:

$$\ln \Phi_{\varphi i} = \frac{-1}{RT} \int_V^\infty \left[\frac{RT}{V} - \left(\frac{\partial P}{\partial n_i} \right)_{T, V, n_j} \right] dV - \ln \frac{PV}{RT} \quad [\text{Eq. 1795.5}]$$

The phase density can be found from the phase volume. For a two parameter Equation of State, this is found by solving the cubic equation. However, this can give poor prediction of the liquid density. For a three parameter Equation of State, the phase volume is modified by subtracting a volume shift term:

$$V_\varphi = V_\varphi^{eos} - \sum x_{\varphi i} \cdot V_{si} \quad [\text{Eq. 1795.6}]$$

The phase enthalpy H_φ is calculated from the ideal gas enthalpy: H_φ^o :

$$H_\varphi = H_\varphi^o - \int_V^\infty \left[T \left(\frac{\partial P}{\partial T} \right)_V - P \right] dV - RT + PV \quad [\text{Eq. 1795.7}]$$

The phase entropy S_φ is calculated from the ideal gas entropy: S_φ^o :

$$S_\varphi = S_\varphi^o - \int_V^\infty \left[\left(\frac{\partial P}{\partial T} \right)_V - \frac{R}{V} \right] dV + R \cdot \ln \frac{PV}{RT} \quad [\text{Eq. 1795.8}]$$

The ideal gas enthalpy and entropy are determined from the ideal gas specific heat C_{pq}^o :

$$\begin{aligned} H_\varphi^o &= \int_{T_{ref}}^T C_{pq}^o dT & [\text{Eq. 1795.9}] \\ S_\varphi^o &= \int_{T_{ref}}^T \frac{C_{pq}^o}{T} dT - R \cdot \ln \frac{P}{P_{ref}} - R \cdot \sum (x_{\varphi i} \cdot \ln x_{\varphi i}) & [\text{Eq. 1795.10}] \end{aligned}$$

The ideal gas specific heat is calculated by summing the component specific heats

$$C_{pq}^o = \sum C_{pi}^o \cdot x_{\varphi i} \quad [\text{Eq. 1795.11}]$$

For library components, the component specific heat C_{pi}^o is a known function of temperature. For user defined petroleum fractions, the component specific heat is calculated as a function of temperature and the component molecular weight MW_i , boiling point temperature T_{Bi} , specific gravity γ_i and acentric factor ω_i .

E300 flash

The ECLIPSE version of the Peng Robinson EoS has an option correction for the A_i term for large acentric factors (ECLIPSE PRCORR keyword).

E300 flash name	Peneloux Volume Shift Correction	Peng Robinson 1978 Acentric Factor Correction
Peng-Robinson		
Peng-Robinson		Yes
Peng-Robinson	Yes	
Peng-Robinson	Yes	Yes
SRK	Yes	
SRK		

Multiflash

The Multiflash Implementation in PIPESIM has the cubic Equations of State, Peng-Robinson and RKS, along with the Cubic Plus Association (CPA) model, which is an extension of the RKS (advanced) cubic EoS to handle polar and hydrogen bonding components. The Multiflash implementation also includes [non-cubic EoS](#).

EoS names differ from those in the Multiflash GUI.

PIPESIM GUI name	Multiflash GUI name	Peneloux Volume Shift Correction	Peng Robinson 1978 Acentric Factor Correction
Peng-Robinson	PR (Advanced)	Yes	
NOT CURRENTLY AVAILABLE	PR78 (Advanced)		Yes
SRK	RKS (Advanced)	Yes	
Association (CPA)	Association (CPA-Infochem)	Yes	

Versions of the Peng-Robinson and SRK equations of state without the volume shift correction are available, but are not recommended. Liquid densities predicted by these equations of state can be poor. In particular the liquid water density is out by about 15%. This causes problems in PIPESIM, since it can predict water being lighter than oil. This particular problem does not arise in two phase flashes, where the water properties are not determined by the equation of state. It does occur in 3 phase flashes, such as Multiflash.

PIPESIM GUI name	Multiflash GUI name	Volume Shift Correction	Peng Robinson 1978 Acentric Factor Correction
Standard Peng-Robinson	PR		

NOT CURRENTLY AVAILABLE	PR78		Yes
Standard SRK	RKS		

Non-cubic equations of state

Equations of state (EoS) describe the pressure, volume and temperature (PVT) behavior of pure components and mixtures. The phase state and most thermodynamic properties (e.g. density, enthalpy, entropy) are derived from the equation of state. Separate models are used for transport properties, such as viscosity, conductivity and surface tension.

PIPESIM can use both [cubic](#) and non-cubic and Equations of State.

Multiflash

BWRS

The BWRS is an 11-parameter non-cubic equation. The BWRS equation gives much more accurate volumetric and thermal property predictions for light gases and hydrocarbons. It should give reasonable vapor-liquid phase equilibrium predictions, but owing to its complexity, it requires more computing time than the cubic EOS (e.g SRK or Peng-Robinson). The EoS is similar to a virial expansion in density:

$$P = \frac{RT}{V} \cdot \left[n + \frac{B}{V} + \frac{C}{V^2} + \frac{D}{V^5} + \frac{C'}{V^5} \cdot \left(1 + \frac{\gamma^2}{V^2} \right) \cdot \exp \left(\frac{-\gamma^2}{V^2} \right) \right] \quad [\text{Eq. 1796.1}]$$

The BWRS EoS can be used with most of the [components that can be used with the cubic EoS](#).

Note: It does not work with the Hydrogen component or with aqueous components.

CSMA

CSMA is the Multiflash multi-reference fluid corresponding states model. The CSMA model is based on a collection of very accurate equations of state for a number of common substances. The density, thermal properties and VLE of each substance are generally reproduced to within the accuracy of experimental measurements. The properties of mixtures can be estimated from a model that reduces to the (accurate) pure component values as the mixture composition approaches each pure component limit.

An important application is mixtures containing CO₂, H₂S and light hydrocarbons. It can only be used with a limited selection of [components](#).

Note: It can only be used via an MFL file.

CPA

The CPA (cubic-plus-association) model extends the capabilities of industry-standard cubic equations of state to polar and hydrogen-bonding components. It is applicable to a wide variety of systems of importance to the upstream oil industry such as hydrocarbons, gases, water and hydrate inhibitors (alcohols and glycols).

The Multiflash CPA model is based on the Infochem RKSA (advanced Redlich-Kwong-Soave) equation of state. It has the advantage for non-polar substances, because it reduces the RKSA eos so that all the characterization methods and parameters for standard oil and gas mixtures can be used. Extra terms in the equation describe polar and associating compounds. The main application in Multiflash is representing the fluid phases when modeling hydrates and hydrate inhibition. CPA shows improvements over standard cubic eos for other systems such as acid gases and water.

Note: Salt components are not supported.

The CPA model is the subject of an active research program that is extending its applicability to many other systems of industrial importance.

Reference fluid thermodynamic and transport properties — REFPROP

REFPROP is an acronym for REference fluid PROPERTIES. The flash package provides thermodynamic and transport properties of industrially important fluids and their mixtures with an emphasis on refrigerants and hydrocarbons, especially natural gas systems. It is developed by the National Institute of Standards and Technology (NIST).

REFPROP is based on highly accurate single component and mixture models based on the Helmholtz energy.

NIST recommendation for pure fluids / mixture

For single components, REFPROP has a recommended set of equations of state explicit in Helmholtz energy. That is, for each single component, a specific equation of state explicit in Helmholtz energy is chosen. e.g. for carbon dioxide this is [Span and Wagner \(1996\)](#). Mixture calculations employ a model that applies mixing rules to the Helmholtz energy of the mixture components; it uses a departure function to account for the departure from ideal mixing.

GERG

Introduction

GERG is an acronym for Groupe Européen de Recherches Gazières, which is supported by the European natural-gas companies. The European natural-gas companies include E.ON Ruhrgas (Germany), Enagás (Spain), Gasunie (The Netherlands), Gaz de France (France), Snam Rete Gas (Italy) and Statoil (Norway).

The flash package, developed at Ruhr-Universität Bochum, provides thermodynamic and transport properties of industrially important gases and other

mixtures with an emphasis on hydrocarbons and further components. Lehrstuhl fuer Thermodynamik (Department of Thermodynamics) of Ruhr-Universitat Bochum, Germany have developed a wide-range equation of state (EOS) for natural gases and other mixtures that meets the requirements of standard and advanced natural gas applications.

The first published equation of state by Ruhr-Universitat Bochum covers mixtures consisting of up to 18 components as listed below:



Annotations:

Yellow – natural gas main components

Red – further hydrocarbons

Blue – further components

In 2004, the new equation of state was evaluated by the GERG group and then adopted under the name GERG-2004 equation of state (or GERG-2004 for short) as an international reference equation of state for natural gases and similar mixtures (GERG standard).

GERG-2008

In 2008, Ruhr-Universitat Bochum further extended GERG-2004 by including three additional components *n-nonane*, *n-decane* and *hydrogen sulfide*, making its component list up to 21 components. This expanded equation of state was called GERG-2004 XT08, where "XT08" meant "eXTension 2008". In 2010, upon the request of the ISO Working Group (ISO TC193 SC1 WG13), Ruhr-Universitat Bochum simplified the name of GERG-2004 XT08 to GERG-2008, the current version of GERG.

The GERG-2008 equation of state has been adopted as an ISO Standard (ISO 20765-2 and ISO 20765-3) for natural gases. The ISO group ISO TC 193/SC 1/WG 13 is working on this matter.

Reference fluid thermodynamic and transport properties — REFPROP

For thermodynamic and transport properties, REFPROP is used.

REFPROP is an acronym for REFerence fluid PROPERTIES. The flash package provides thermodynamic and transport properties of industrially important fluids and their mixtures with an emphasis on refrigerants and hydrocarbons, especially natural gas systems. It is developed by the National Institute of Standards and Technology (NIST).

REFPROP is based on highly accurate single component and mixture models based on the Helmholtz energy.

NIST recommendation for pure fluids / mixture

For single components, REFPROP has a recommended set of equations of state explicit in Helmholtz energy. That is, for each single component, a specific equation of state explicit in Helmholtz energy is chosen. e.g. for carbon dioxide this is [Span and Wagner \(1996\)](#). Mixture calculations employ a model that applies mixing rules to the Helmholtz energy of the mixture components; it uses a departure function to account for the departure from ideal mixing.

Description

Structure

The GERG equation of state is based on a multi-fluid approximation, which is explicit in the reduced Helmholtz energy $\alpha = \alpha(RT)$ [α = Alpha in the figures] dependent on the density ρ , the temperature T and the composition x (mole fractions) of the mixture. The structure of the equations of state is shown in the following figure:



Figure 1797.1. The basic structure of the equations of state GERG-2004 ($N = 18$) and GERG-2008 ($N = 21$) for natural gases and other mixtures.

Three elements are necessary to set up a multi-fluid approximation:

- Pure substance equations of state for all components
- Reducing functions for density and temperature
- Departure function

The reducing functions as well as the departure function were developed to describe the behaviour of the mixture and contain substance and mixture specific parameters. From the reducing functions, the reducing values ρ_r and T_r for the density and the temperature of the mixture are calculated. They only depend on the mixture composition and turn into the critical properties ρ_c and T_c , respectively, for the pure components. The departure function depends on the reduced density δ , the inversely reduced temperature τ ($\tau = \text{Tau}$ in the figures), and the composition x of the mixture. It contains the sum of binary specific and generalized departure functions, which can be developed for single binary mixtures (binary specific) or for a group of binary mixtures (generalized). The following equation illustrates this summation:



Figure 1797.2. The departure function for the mixture in a multi-fluid approximation as a double summation over all binary specific and generalized departure functions developed for the binary subsystems; GERG-2004: $N = 18$; GERG-2008: $N = 21$.

The mathematical structure of the part of the binary specific and generalized departure functions that depends on δ and τ is similar to the structure of pure substance equations of state and is determined by our method for optimizing the structure of equations of state. Furthermore, the departure functions contain a factor that only depends on the composition of the mixture. For further details, see the references given at the end of this description.

In order to obtain a reference equation of state that yields accurate results for various types of natural gases and other multi-component mixtures over wide ranges of composition, the reducing and departure functions were developed using only data for binary mixtures. The 18 pure components covered by GERG-2004 form 153 different binary mixtures, and the 21 pure components covered by GERG-2008 result in 210 possible binary mixture combinations. Departure functions $\Delta\alpha_{ij}(\delta, t, x)$ were developed only for such binary mixtures for which accurate experimental data existed. For binary mixtures with limited or poor data, no departure functions were developed, and only the parameters of the reducing functions $p_r(x)$ und $T_r(x)$ were fitted; in case of very poor data, simplified reducing functions without any fitting were used.

The multi-fluid approximation used enables a simple inclusion of additional components in future developments. This means that, for example, fitted parameters of the existing equation of state do not have to be refitted when incorporating new components. This also holds for the departure function with its optimized structure, which remains unchanged when expanding the model.

Range of validity and accuracy

The entire range of validity of GERG-2008 covers the following temperatures and pressures:

- Normal range: $90 \text{ K} \leq T \leq 450 \text{ K}$, $p \leq 35 \text{ MPa}$
- Extended range: $60 \text{ K} \leq T \leq 700 \text{ K}$, $p \leq 70 \text{ MPa}$

Moreover, the equation can be reasonably extrapolated beyond the extended range, and each component can basically cover the entire composition range, i.e. (0-100)%.

GERG-2008 represents most of the experimental data, including the most accurate measurements available, to within their uncertainties. The uncertainty values given in the following correspond to the uncertainties of the most accurate experimental data.

In the gas region, the uncertainties in density and speed of sound are 0.1%, in enthalpy differences (0.2-0.5)% and in heat capacities (1-2)%. In the liquid region, the uncertainty in density is (0.1-0.5)%, in enthalpy differences (0.5-1)% and in heat capacities (1-2)%. In the two-phase region, vapour pressures are calculated with a total uncertainty of (1-3)%, which corresponds to the uncertainties of the experimental VLE data. For mixtures with limited or poor data, the uncertainty values stated above can be somewhat higher.

These accuracy statements are based on the fact that GERG-2008 represents the corresponding experimental data to within their experimental uncertainties (with very few exceptions).

References

The comprehensive descriptions of GERG (with the entire numerical information, experimental data used, quality, range of validity, etc.) are retrievable from the following reference:

Kunz, O., Klimeck, R., Wagner, W., Jaeschke, M. The GERG-2004 wide-range equation of state for natural gases and other mixtures. GERG TM15 2007. Fortschr.-Ber. VDI, Reihe 6, Nr. 557, VDI Verlag, Düsseldorf, 2007; also available as GERG Technical Monograph 15 (2007).

Kunz, O., Wagner, W. The GERG-2008 wide-range equation of state for natural gases and other mixtures: An expansion of GERG-2004. To be submitted to J. Chem. Eng. Data (2011).

Note: This GERG Monograph is available for download from the website of GERG - <http://www.gerg.eu/publications/tm.htm>

Components for cubic equations of state

For the [cubic equations of state](#), non-aqueous components can either be selected from a [library](#), or user-defined components ([petroleum fractions](#)) can be selected by defining their properties.

For two phase flashes, water can be selected, but it is treated differently from the other components. It is removed from the flash calculations, and the water phase properties are calculated separately. For three phase flashes (Multiflash), [aqueous components](#) can be selected from the component library. User-defined aqueous components are not allowed.

Non-aqueous library components

Different library components are available for each package. When converting from one package to another, if a library component is not available in the new package, it will be converted into a [petroleum fraction](#). Default molecular weight and boiling point temperature are used to define the petroleum fraction — data for pure components are taken from [Poling et al.](#).

The non-aqueous library components can be divided into three types

1. [Pure hydrocarbon components](#)
2. [Non-hydrocarbon components](#)
3. [Pseudo-components](#)

Pure hydrocarbon components

The following pure library components can be selected:

Formula	Multiflash	E300 flash	MW (g/gmol)	Tbp (K)
CH4	Methane	C1	16.043	111.66
C2H4	Ethylene		28.054	169.42
C2H6	Ethane	C2	30.070	184.55
C3H4			40.065	238.77
C3H6			42.081	225.46

C3H6			42.081	240.34
C3H8	Propane	C3	44.097	231.02
C4H6			54.092	268.62
C4H6			54.092	269.00
C4H8			56.108	266.24
C4H8			56.108	266.92
C4H8			56.108	274.03
C4H8			56.108	276.87
C4H10	Isobutane	IC4	58.123	261.34
C4H10	N-Butane	NC4	58.123	272.66
C5H10			70.134	322.38
C5H10	Cyclopentane		70.134	303.11
C5H12	2,2-Dimethylpropane		72.150	282.65
C5H12	Isopentane		72.150	300.99
C5H12	N-Pentane		72.150	309.22
C6H6	Benzene	BEN	78.114	353.24
C6H12			84.161	336.63
C6H12	Methylcyclopentane		84.161	344.98
C6H12	Cyclohexane		84.161	353.93
C6H14	N-Hexane		86.177	341.88
C7H8	Toluene	TOL	92.141	383.79
C7H14			98.188	366.79
C7H14	Methylcyclohexane		98.188	374.09
C7H16	3-Methyl Hexane		100.204	365.00
C7H16	N-Heptane		100.204	371.57
C7H16	3-Methyl Hexane		100.204	365.00
C8H10	Ethylbenzene		106.167	409.36
C8H10	P-Xylene		106.167	411.53
C8H10	M-Xylene		106.167	412.34
C8H10	O-Xylene		106.167	417.59
C8H16			112.215	394.44
C8H16	Ethylcyclohexane		112.215	404.00
C8H18	N-Octane		114.231	398.82
C9H12			120.194	442.49
C9H12	Cumene		120.194	425.52
C9H20	N-Nonane		128.258	423.97
C10H14	1,2-Diethylbenzene		134.22	456
C10H22	N-Decane		142.285	447.30
C11H24	N-Undecane		156.312	469.08
C12H26	N-Dodecane		170.338	489.48
C13H28	N-Tridecane		184.365	508.63
C14H10			178.233	611.55
C14H30	N-Tetradecane		198.392	526.76
C15H32	N-Pentadecane		212.419	543.83
C16H34	N-Hexadecane		226.446	559.98
C17H36	N-Heptadecane		240.473	574.56
C18H38	N-Octadecane		254.500	588.30
C19H40	N-Nonadecane		268.527	602.34
C20H42	N-Eicosane		282.554	616.84
C21H44	N-Heneicosane			
C22H46	N-Docosane			
C23H48	N-Tricosane			
C24H50	N-Tetracosane			

C25H52	N-Pentacosane				
C26H54	N-Hexacosane				
C28H58	N-Octacosane				
C29H60	N-Nonacosane				
C30H62	N-Triacontane				
C32H66	N-Dotriacontane				
C36H74	N-Hexatriacontane				

Non-hydrocarbons

The following pure library components can be selected:

Formula	Multiflash	E300 flash	MW (g/gmol)	Tbp (K)
H2	Hydrogen	H2	2.016	20.38
He	Helium		4.003	4.30
N2	Nitrogen	N2	28.014	77.35
O2	Oxygen		31.999	90.17
Ar	Argon		39.948	87.27
Kr			83.800	119.74
Xe			131.290	165.01
NH3	Ammonia		17.031	239.81
H2S	Hydrogen Sulphide	H2S	34.082	212.84
CO	Carbon Monoxide	CO	28.010	81.66
CO2	Carbon Dioxide	CO2	44.010	
SF6			146.06	209.00

Pseudo-hydrocarbon components

Some packages contain pseudo components, essentially pre-defined [petroleum fractions](#), that can be used to represent the heavy end of the oil.

Formula	Multiflash	E300 flash	MW (g/gmol)	Tbp (K)
		C4	58.124	268.9
		C5	72.151	305.9
		C6	84.00	341.9
		C7	96.00	371.6
C8H10			106.167	411.9
		C8	107.00	398.8
		C9	121.00	424.0
		C10	134.00	447.0
		C11	147.00	469.0
		C12	161.00	489.0
		C13	175.00	508.0
		C14	190.00	527.0
		C15	206.00	544.0
		C16	222.0	560.0
		C17	237.00	575.0
		C18	251.00	589.0
		C19	263.00	603.0
		C20		
		C21		
		C22		
		C23		
		C24		
		C25		
		C26		
		C27		

	C28		
	C29		
	C30		
	C31		
	C32		
	C33		
	C34		
	C35		
	C36		
	C37		
	C38		
	C39		
	C40		
	C41		
	C42		
	C43		
	C44		
	C45		
		544.00	773.2

Aqueous library components

Aqueous components are defined as those that will distribute mainly in the second liquid phase. These are water and the hydrate suppressants methanol, ethylene glycol, diethylene glycol and triethylene glycol. The calculation in of the amount of aqueous components to add corresponds to an agreed definition. The water phase is added as a proportion of the DRY gas at stock tank conditions (15 degrees C, 1bar). The discrepancy between hand calculations and software is because the software makes a correction for the amount of aqueous components that will partition to the gas phase. That is, it aims to add the amount of aqueous components requested as a separate aqueous phase. There will also be some loss to the hydrocarbon liquid phase but this will not be significant unless the aqueous phase contains a lot of methanol. The amount lost to the vapor phase will be significant if there is a large amount of gas present relative to other phases.

Formula	Multiflash
H ₂ O	Water
CH ₃ -OH	Methanol
C ₂ H ₅ -OH	Ethanol
C ₂ H ₆ O ₂	Ethylene Glycol (MEG)
C ₄ H ₁₀ O ₃	Diethylene Glycol (DEG)
C ₆ H ₁₄ O ₄	Triethylene Glycol (TEG)
NaCl	Salt Component

Petroleum fractions

User-defined components can be created by defining key properties: molecular weight MW_i , critical pressure P_{ci} , critical temperature T_{ci} , boiling point temperature T_{Bi} , specific gravity γ_i and acentric factor ω_i . It is not always necessary to supply values for all these properties — the flash packages can use correlations to determine unspecified properties from those that are specified. Minimum data required is shown in the table below:

	Multiflash	E300 flash
MW_i, γ_i	yes	
MW_i, T_{Bi}	yes	
T_{Bi}, γ_i	yes	
MW_i		yes
P_{ci}, T_{ci}, ω_i	yes	

Note: The Multiflash routines that calculate the petroleum fraction properties assume the molecular weight of petroleum fractions exceed 72.

Components for non-cubic equations of state

Only library components can be used for the CSMA, NIST recommendation for pure fluid/mixture and GERG-2008 [non-cubic equations of states](#).

Formula	Multiflash (CSMA)	REFPROP (NIST recommendation for pure fluid/mixture)	GERG-2008 (GERG-2008)

CH4	Methane	methane	Methane
C2H6	Ethane	ethane	Ethane
C3H8	Propane	propane	Propane
i-C4H10	Isobutane	isobutane	Isobutane
n-C4H10	Butane	butane	n-Butane
i-C5H12	Isopentane	isopentane	Isopentane
n-C5H12	Pentane	pentane	n-Pentane
n-C6H14	Hexane	hexane	n-Hexane
n-C7H16	Heptane	heptane	n-Heptane
n-C8H18	Octane	octane	n-Octane
n-C9H20		nonane	n-Nonane
n-C10H22		decane	n-Decane
C2H2	Ethylene		
C6H12	Cyclohexane		
C7H8	Toluene		
H2	Hydrogen	hydrogen (normal)	Hydrogen
He	Helium	helium	Helium
N2	Nitrogen	nitrogen	Nitrogen
O2	Oxygen	oxygen	Oxygen
Ar	Argon	argon	Argon
H2S	Hydrogen Sulphide	hydrogen sulfide	Hydrogen sulphide
CO	Carbon Monoxide	carbon monoxide	Carbon monoxide
CO2	Carbon Dioxide	carbon dioxide	Carbon dioxide
NH3	Ammonia		

Multiflash is a 3-phase flash and allows aqueous components. REFPROP and GERG-2008 allow water, but are two phase flashes. The water component is therefore removed before the flash calculation, and water properties are calculated outside the flash.

Formula	Multiflash (CSMA)	NIST-REFPROP	GERG-2008
H2O	Water	water	Water
C2H5-OH	Ethanol		

REFPROP and GERG–2008 component restrictions

In the REFPROP flash [Binary interaction parameters \(BIPs\)](#) are not available for all pairs of components. The REFPROP flash will not work if the fluid contains any component pair with a missing BIP. The problem only occurs with fluids containing Hydrogen Sulphide, Nonane or Decane. Pairs of components that are not allowed are marked with an 'X' in the table below. (Note that the water component is allowed in the simulation, but is not used in the flash).

Note: The GERG-2008 flash is a pure flash package. However transport properties are also required for PIPESIM simulation purposes. As a result, the implementation of GERG-2008 within the PVT Toolbox framework uses REFPROP for transport properties calculations. As such, the same component restrictions listed below also apply to GERG-2008 for the corresponding components.

REFPROP (NIST recommendation for pure fluid/mixture)	GERG-2008	Hydrogen Sulphide [Hydrogen sulphide]	Nonane	Decane
water	Water			
methane	Methane		X	X
ethane	Ethane		X	X
propane	Propane		X	X
isobutane	Isobutane		X	X
butane	n-Butane		X	X
isopentane	Isopentane		X	X
pentane	n-Pentane			
hexane	n-Hexane			
heptane	n-Heptane			
octane	n-Octane		X	
nonane	n-Nonane			
decane	n-Decane			
hydrogen (normal)	Hydrogen	X	X	X

helium	Helium	X	X	X
nitrogen	Nitrogen		X	X
oxygen	Oxygen	X	X	X
argon	Argon		X	X
hydrogen sulfide	Hydrogen sulphide			
carbon monoxide	Carbon monoxide		X	X
carbon dioxide	Carbon dioxide		X	X

Viscosity models for compositional fluids

Select Setup » Compositional, then on the **Property Models** tab, select one of the following models for determining viscosity:

- Pedersen (the default)
- LBC (Lohrenz-Bray-Clark)
- Pedersen Twu
- SuperTRAPP
- Aasberg-Petersen (only available for E300)
- NIST recommendation for pure fluids / mixture (only available for REFPROP and GERG-2008)

The Pedersen model is a predictive corresponding states model, originally developed for oil and gas systems. It is based on accurate correlations for the viscosity and density of the reference substance, which is methane. The model is applicable to both gas and liquid phases.

The LBC model is a predictive model which relates gas and liquid densities to a fourth degree polynomial in reduced density. It is recommended for fluids that contain the standard components found in oil and gas processing.

The Twu model is a predictive model suitable for oils. It is based on a correlation of the API monograph for kinematic viscosity, plus a mixing rule for blending oils. It is only applicable to liquids.

The SuperTRAPP model is a predictive, extended corresponding states model that uses propane as a reference fluid. It can predict the viscosity of petroleum fluids and well-defined components, over the entire phase range from dilute gas to the dense fluid. It is recommended for petroleum fluids and well-defined components over the entire phase range from the dilute gas to the dense fluid and is the default for the Multiflash standalone application.

Overall, the SuperTRAPP method is the most versatile method for viscosity predictions and its performance is generally better than the other methods. However, PIPESIM currently uses the Pedersen method as the default, because it also is widely applicable and accurate for oil and gas viscosity predictions.

The results for different components for some of the models above, are as follows:

Lower Alkanes

Predicted liquid viscosities using LBC and Pedersen methods have been compared to experimental data for Methane and Octane as a function of both temperature and pressure and for Pentane as a function of temperature. For both Methane and Pentane the Pedersen method predictions show close agreement with experimental data. For Octane, the Pedersen and LBC methods give comparable results. For the aromatic compound, Ethyl Benzene, the Pedersen method is not as good as LBC.

Higher Alkanes

The results for higher alkanes Eicosane and Triacontane are mixed: the Pedersen method is adequate for Eicosane whereas LBC is slightly better than Pedersen for Triacontane. For Triacontane both the LBC and Pedersen methods are inadequate. However, in the majority of cases the higher hydrocarbons should be treated as petroleum fractions rather than as single named components.

Petroleum Fractions

The LBC method describes viscosity as a function of the fluid critical parameters, acentric factor and density. The LBC model is therefore very sensitive to both density and the characterization of the petroleum fractions.

Water

The Pedersen method suffers the same drawback as LBC in that it is unable to predict the temperature dependence of water, a polar molecule. To overcome this problem, the Pedersen method has been modified especially for water so that it now accurately models the viscosity of water in the liquid phase. This was achieved by the introduction of a temperature-dependent correction factor. However the prediction of the viscosity of the gas phase is also affected, though in only a minor way.

Methanol

Neither the LBC nor Pedersen method can deal with polar components, with the Pedersen method slightly worse than LBC. This is not surprising, as both methods were developed for non-polar components and mixtures. The Pedersen method works best with light alkanes and petroleum mixtures in the liquid phase. It performs as well or better than the LBC method in nearly all situations.

The choice of the equation of state has a large effect on the viscosities predicted by both methods. The LBC method is more sensitive to the equation of state effects than is the Pedersen method.

See also: [Package](#), [Binary Interaction Parameters](#), [Emulsions](#), [Equation of State](#)

Asphaltene prediction

ONLY AVAILABLE WITH MFL FILES

Asphaltene formation line is displayed automatically on the phase envelope to enable the determination of the conditions (temperature and pressure) at which asphaltene appears

Hydrates

Only available with Multiflash.

Requires additional licensing option.

Hydrate lines are displayed automatically on the [Phase Envelope](#) if water is in the component list and hydrates will form. The amount of water may influence the results of the calculations, particularly when inhibitors or water-soluble gases are present.

Background

Natural gas hydrates are solid ice-like compounds of water and light components of natural gas. The phase behavior of the systems involving hydrates can be very complex because up to six phases must normally be considered. The behavior is particularly complex if there is significant mutual solubility between phases.

The Multiflash hydrate model uses a modification of the SRK equation of state for the fluid phases plus the van der Waals and Platteeuw model for the hydrate phases. The model can explicitly represent all the effects of the presence of inhibitors.

Hydrate inhibitors

Hydrate inhibitors decrease the hydrate formation temperature or increase the hydrate formation pressure in a given gas mixture. The model includes parameters for the commonly used inhibitors such as Methanol, and the glycols MEG, DEG and TEG.

A new mixing rule has been developed for the SRK equation of state to model the inhibitors' effects on the fluid phases. The treatment of hydrate inhibition has the following features. The model can represent explicitly all the effects of inhibitors, including the depression of hydrate formation temperature, the depression of the freezing point of water, the reduction in the vapor pressure of water (i.e. the dehydrating effect) and the partitioning of water and inhibitor into the oil, gas and aqueous phases. The model has been developed using all available data for mixtures of water with Methanol, MEG, DEG and TEG. This involves simultaneously representing hydrate dissociation temperatures, depression of freezing point data and vapor-liquid equilibrium data. The solubilities of hydrocarbons and light gases in water/inhibitor mixtures have also been represented. There is no fundamental difference between calculations with and without inhibitors. To investigate the effect of an inhibitor it must be added to the list of components in the mixture and the amount must be specified just as for any other component. It is not possible to specify the amount of inhibitor in a particular phase, only the total amount in the mixture. This is because the inhibitor will be split among the different phases present at equilibrium with the amount in a particular phase depending on the ambient conditions and the amounts of other components present in that phase. This is exactly what happens in reality. The amount of inhibitor typically needed would be approximately 35% by mass of inhibitor relative to water.

Model features

The main features of the model are:

- The description of the hydrate phase behavior uses a thermodynamically consistent set of models for all phases.
- The vapor pressures of pure water are reproduced. The following natural gas hydrate formers are included: METHANE, ETHANE, PROPANE, ISOBUTANE, BUTANE, NITROGEN, CO₂ AND H₂S.
- The thermal properties (enthalpies and entropies) of the hydrates are included, permitting flashes involving these phases.
- The properties of the hydrates have been fixed by investigating data for natural gas components in both simple and mixed hydrates to obtain reliable predictions of both structure I and structure II hydrates.
- The properties of the empty hydrate lattices have been investigated and the most reliable recent values have been adopted.
- Proper allowance has been made for the solubilities of the gases in water so that the model parameters are not distorted by this effect. This is particularly important for Carbon Dioxide and Hydrogen Sulphide, which are relatively soluble in water.
- Correct thermodynamic calculations of the most stable hydrate structure have been made. The model has been tested on a wide selection of open literature and proprietary experimental data. In most cases the hydrate dissociation temperature is predicted to within 1 degree Kelvin.

To ensure that reliable results are obtained, it is particularly important to use the correct set of models and phase descriptors. The hydrate model set contains a complete set of model and phase specifications.

Hydrate model details

The hydrate model set has the following definitions:

FLUID PHASE MODEL

The recommended fluid phase model is the advanced SRK equation of state with a parameter fitted to the pure component vapor pressure, the Peneloux density correction and the INFOCHEM mixing rule. The required binary interaction parameters (BIP) for hydrocarbons, light gases, water and inhibitors are available from the OILGAS2 BIP data set.

HYDRATE MODELS

The hydrate model consists of lattice parameters for the empty hydrate and parameters interaction of gas molecules with water in the hydrate. There are different parameter values for each hydrate structure, HYDRATE I and II. In addition, the hydrate must be associated with a liquid phase model that is used to obtain the properties of water. It is important that this is the same model that is used for water as a fluid phase.

PHASES

In most cases, six phase descriptors are required: gas, hydrocarbon liquid, aqueous liquid, hydrate I, hydrate II and ice. At high pressures and/or low temperatures the 'gas' phase may become liquid-like and a second non-aqueous liquid PD is needed. This is also the case if there is a significant amount of CO₂ or H₂S present. In most practical cases, the gas contains propane and has a hydrate II stable hydrate structure. Key components are defined to distinguish between the hydrocarbon and aqueous liquid phases. In principle, hydrate calculations and phase envelope plotting with Multiflash are no different from flash calculations and envelope plotting for the fluid phases alone. Multiflash treats fluid and solid phases the same. It can carry out a full range of flashes for streams with hydrates.

Ice prediction

Only available with Multiflash Flash.

Ice is treated as a pure solid phase. The ice formation line is displayed automatically on the phase envelope if water is in the component list and ice will form.

Wax prediction

ONLY AVAILABLE WITH MFL FILES

Waxes are complex mixtures of solid hydrocarbons that freeze (solidify) out of crude oils if the temperature is low enough - below the critical wax deposition temperature. They are mainly formed from normal paraffins or if isoparaffins and naphthenes are present. The wax formation line is displayed automatically on the phase envelope to enable the determination of the conditions (temperature and pressure) at which wax could deposit.

[Wax deposition](#) can also be modelled.

Fluid property table files

Fluid properties can be pre-calculated for a range of pressure and temperature values and stored in a table. PIPESIM reads the table and can interpolate it to get properties for any pressure and temperature. Tables in a format that can be read by PIPESIM can be generated by a range of Compositional Fluid Packages, including PIPESIM itself. Table files representing different fluids cannot be mixed. They are therefore useful in single branch models, but less so in network models, unless the entire network contains only a single fluid.

The tables contain liquid and gas properties:

Property		
Pressure	<i>psia</i>	<i>kPa</i>
Temperature	<i>F</i>	<i>K</i>
Liquid Volume Fraction	<i>%</i>	<i>%</i>
Water cut	<i>%</i>	<i>%</i>
Liquid Density	<i>lb / ft³</i>	<i>kg / m³</i>
Gas Density	<i>lb / ft³</i>	<i>kg / m³</i>
Gas Compressibility		
Gas Molecular Weight	<i>lb / lbmol</i>	<i>kg / kgmol</i>
Liquid Viscosity	<i>cP</i>	<i>cP</i>
Gas Viscosity	<i>cP</i>	<i>cP</i>
Total Enthalpy	<i>BTU / lbmol</i>	<i>kJ / kgmol</i>
Total Entropy	<i>BTU / (lbmol · F)</i>	<i>kJ / (kgmol · K)</i>
Liquid Heat Capacity	<i>BTU / (lbmol · F)</i>	<i>kJ / (kgmol · K)</i>
Gas Heat Capacity	<i>BTU / (lbmol · F)</i>	<i>kJ / (kgmol · K)</i>
Liquid Surface Tension	<i>dyne / cm</i>	<i>dyne / cm</i>
Gas Thermal Conductivity	<i>BTU / (hr · ft · F)</i>	<i>W / (m · K)</i>
Oil Thermal Conductivity	<i>BTU / (hr · ft · F)</i>	<i>W / (m · K)</i>
Water Thermal Conductivity	<i>BTU / (hr · ft · F)</i>	<i>W / (m · K)</i>

The number of phases and the phase volume fractions, can be determined from the liquid fraction and water cut. However, since only liquid and gas properties are available, these tables are only suitable for use with two-phase flow models.

The table files also contain the total molecular weight of the fluid, which is independent of the pressure and temperature. This allows PIPESIM to calculate the liquid molecular weight from the other table properties. The total molecular weight, liquid molecular weight and gas molecular weight are then used to convert the molar quantities (enthalpy, entropy and heat capacities) to mass based quantities.

Table files may also contain compositional data. In this case the table data may be ignored and PIPESIM may use normal compositional flashing.

Internal fluid property tables

PIPESIM can also use property tables to store fluid data in compositional runs. Properties are interpolated from the table properties and as the simulation progresses, tables values are filled in when necessary. This can speed up compositional simulations, although it requires more memory to store the data. These tables can be used in network simulations with multiple fluids — a new mixture can be created by mixing the fluid components and a new internal table created for the new fluid.

Liquid mixture properties

Two phase flow correlations model flow of a liquid and a gas phase. When there are two liquid phases, such as oil and water, the two liquid phases need to be combined and modelled as a single liquid phase. The oil and water will flow at the same velocity. The liquid density can be simply averaged. However more complicated models are used for [liquid viscosity](#) and [liquid-gas surface tension](#).

Liquid viscosity and oil/water emulsions

An **emulsion** is a mixture of two immiscible liquid phases. One phase (the dispersed phase) is carried as droplets in the other (the continuous phase). In Oil/Water systems at low watercuts, oil is usually the continuous phase. As watercut is increased there comes a point where **phase inversion** occurs, and water becomes the continuous phase. This is the **Critical Watercut of Phase Inversion**, otherwise called the **cutoff**. It occurs typically between 55% and 70% watercut. The viscosity of the mixture is usually highest at and just below the cutoff. Emulsion viscosities can be many times higher than the viscosity of either phase alone.

Related links:

[Viscosity properties](#)

[Viscosity properties](#)

Correlations and methods

The methods available for calculating the oil/water mixture viscosity are:

- Inversion
- Volume Ratio
- User-supplied Table

In addition a number of emulsion correlations are available:

- Woelflin
- Brinkman
- Vand
- Richardson
- Leviton and Leighton

The cutoff can be entered as a watercut, or calculated using the Brauner and Ullman correlation. The cutoff is used by all the emulsion correlations and methods, except for the Volume ratio method.

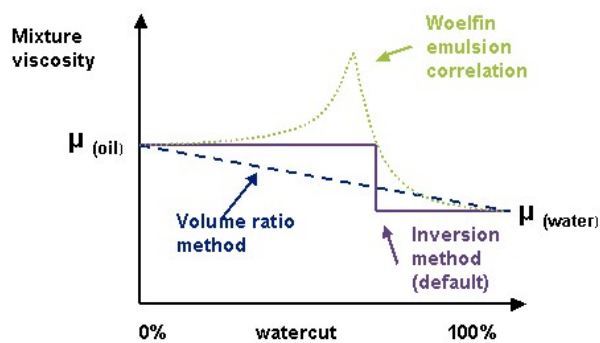


Figure 1000.1. Viscosity of oil/water mixtures

Related links:

[Viscosity properties](#)

[Viscosity properties](#)

Inversion

The inversion method sets the liquid viscosity to the viscosity of the continuous phase. This means that, at a watercut below or equal to the cutoff, water droplets are carried by a continuous oil phase, and the mixture assumes the viscosity of the oil. At a watercut above the cut-off value, oil droplets are carried by a continuous water phase, and the mixture assumes the viscosity of the water.

Related links:

[Viscosity properties](#)

[Viscosity properties](#)

Volume ratio

The Volume ratio method calculates mixture viscosity as follows:

$$\mu_m = \mu_o \varphi_o + \mu_w \varphi_w \quad [\text{Eq. 1000.1}]$$

where

μ_o	is oil viscosity
φ_o	is the volume fraction of oil
μ_w	is the water viscosity
φ_w	is the volume fraction of water

Related links:

[Viscosity properties](#)

[Viscosity properties](#)

User-supplied table

This method uses a user-supplied table of viscosity multipliers against flowing (in situ) watercut. The table is entered in the dialog revealed by pressing the **Setup** button. The first watercut value in the table must be zero.

The table is applied to watercuts from zero up to the supplied watercut cutoff value; above this, the liquid viscosity is set to the water viscosity using a transition region.

Related links:

[Viscosity properties](#)

[Viscosity properties](#)

Woelflin

The Woelflin correlations assume that the continuous phase changes from oil to water at a given watercut cutoff point. This means that, at a watercut below or equal to the cutoff value, a water-in-oil emulsion forms, and the emulsion viscosity is given by the Woelflin correlation. At a watercut above the cutoff value, oil droplets are carried by a continuous water phase, and the mixture assumes the viscosity of the water, using a transition region.

In his 1942 paper, Woelflin described 3 types of water-in-oil emulsions, which he labeled **loose**, **medium** and **tight**. The paper provides tables of viscosity multiplication factors as a function of watercut for the 3 types, and a chart showing curves to fit the data. The PIPESIM implementation is a digitization of the curves.

The viscosity of all 3 emulsion types increases with watercut up to the specified cutoff value, above which it falls and assumes the value of the water viscosity. It should be noted that all 3 emulsion types can yield **emulsion viscosities many times greater than the oil viscosity**. In the case of the tight emulsion, multiplier values in the region of 100 are readily obtained. In his experiments on tight emulsions, Woelflin reported that the viscosity of a 60% watercut emulsion could not be determined, because the mixture was too viscous to flow through the viscometer.

Versions of PIPESIM prior to the 2007.1 release implemented only the loose emulsion correlation, using a curve-fit as follows:

$$\mu_m = \mu_o \left(1 + 0.00123 V_w^{2.2} \right) \quad [\text{Eq. 1000.2}]$$

where μ_o is oil viscosity, and V_w is volume fraction of water. This option is retained for backwards compatibility and is called **Pipesim Original Woelflin**. It gives very similar answers to the new loose emulsion option up to a watercut of 60%, but diverges above this.

Related links:

[Viscosity properties](#)

[Viscosity properties](#)

Brinkman

The Brinkman correlation calculates elevated emulsion viscosities on either side of the cutoff, using the formula

$$\mu_L = \mu_c (1 - \varphi_d)^{-2.5} \quad [\text{Eq. 1000.3}]$$

where μ_c is the viscosity of the continuous phase and φ_d is the volume fraction of the discontinuous phase.

Related links:

[Viscosity properties](#)

[Viscosity properties](#)

Vand

The Vand correlations calculate elevated emulsion viscosities on either side of the cutoff, using the formula

$$\mu_L = \mu_c e^{\left[\frac{(k_1 \varphi_d)}{(1-k_2 \varphi_d)} \right]} \quad [\text{Eq. 1000.4}]$$

where μ_c is the viscosity of the continuous phase,

φ_d is the volume fraction of the discontinuous phase,

and the coefficients k_1 and k_2 are selected as follows. The Vand coefficients are 2.5 and 0.609; Barnea and Mizrahi are 2.66 and 1.0; the user-supplied coefficients are entered in the accompanying data entry boxes.

Related links:

[Viscosity properties](#)

[Viscosity properties](#)

Richardson

The Richardson correlation calculates elevated emulsion viscosities on either side of the cutoff, using the formula

$$\mu_L = \mu_c (k \varphi_d)^e \quad [\text{Eq. 1000.5}]$$

where μ_c is the viscosity of the continuous phase,

φ_d is the volume fraction of the discontinuous phase,

and k is a user-supplied constant. Separate values of k can be provided for oil-in-water and water-in-oil conditions, the default values are 3.8 and 6.6.

Related links:

[Viscosity properties](#)

[Viscosity properties](#)

Leviton and leighton

The Leviton and Leighton correlation calculates elevated emulsion viscosities either side of the cutoff, using the formula

$$\mu_L = \mu_c \left[\frac{2.5(\mu_d + 0.4\mu_c)}{(\mu_d + \mu_c)(\varphi_d + \varphi_d^{1.66} + \varphi_d^{3.66})} \right]^e \quad [\text{Eq. 1000.6}]$$

where μ_d and μ_c are the viscosities of the discontinuous and continuous phases, and φ_d is the volume fraction of the discontinuous phase.

Related links:

[Viscosity properties](#)

[Viscosity properties](#)

Brauner and ullman

The Brauner and Ullman correlation can be used to calculate the watercut cutoff value. It uses the formula

$$c = 1 - \left(\frac{\rho t^{0.6} \mu_t^{0.4}}{(1 + \rho t^{0.6} \mu_t^{0.4})} \right) \quad [\text{Eq. 1000.7}]$$

where

c	is the cutoff/100
$\mu_t = \frac{\mu_o}{\mu_w}$	
μ_o	is the oil viscosity (in cP)
μ_w	is the water viscosity (in cP)
$\rho_t = \frac{\rho_o}{\rho_w}$	
ρ_o	is the oil density (in lb/ft ³)
ρ_w	is the water density (in lb/ft ³)

See also: [Inversion](#) and [Volume Ratio](#).

Related links:

[Viscosity properties](#)

[Viscosity properties](#)

Limits and safety factors

Emulsion correlations and methods have the potential to cause difficulty for the calculation engine. Extremely large viscosities can be predicted, this can cause convergence failure. The discontinuous behavior around the inversion point (cutoff) can also cause problems, particularly in a network model. As a result, a number of limits and safety factors have been introduced, as described below. All of these are **properties of the model**: only one value is held, and it is applied to all fluids in the model.

Related links:

[Viscosity properties](#)

[Viscosity properties](#)

Maximum cutoff

A typical value for the cutoff is between 55% to 70%, and the default is 60%. The Woelflin correlations are particularly sensitive to high cutoff values, so there is a maximum limit of 70%, which will be applied silently. The limit may be extended using the keyword [MAXCUTOFF](#) =.

Related links:

[Viscosity properties](#)

[Viscosity properties](#)

Transition region above the cutoff

The Woelflin and user-supplied table methods exhibit pronounced discontinuity about the cutoff. For these methods therefore, the discontinuity about the cutoff is smoothed with a transition region, extending from the cutoff value in the direction of increasing watercut. By default this is 5% wide. Predicted viscosities in this region are interpolated between the value predicted at the cutoff (the maximum emulsion viscosity point, with oil the continuous phase) and the value at cutoff plus transition region width (the viscosity predicted from a continuous water phase). The size of the transition region can be controlled with the keyword [SMOOTHCUTOFF](#) =.

Related links:

[Viscosity properties](#)

[Viscosity properties](#)

Maximum emulsion table multiplier

The user-supplied and Woelflin correlations are subject to a maximum multiplier limit, default value 100. This can be controlled with the keyword [MAXEMULSION](#) =.

Related links:

[Viscosity properties](#)

[Viscosity properties](#)

Maximum liquid viscosity

As viscosity increases, the resistance to fluid flow also increases. There comes a point where viscosity is so high that the term 'fluid' ceases to be appropriate, and the prediction of pressure drops due to fluid flow can be regarded as non physical. The maximum liquid viscosity is by default 1.0E+7 (ten million) cP, this can be controlled by the keyword [MAXLIQVISC](#) =.

Related links:

[Viscosity properties](#)

[Viscosity properties](#)

Liquid-gas surface tension

The surface tension between the liquid and gas phase is used in two phase flow correlations, for example to calculate bubble velocity. If there are two liquid phases present, the surface tension will depend on the oil-gas surface tension, the water-gas surface tension, and the water cut.

In **black oil models**, when there is sufficient oil, it is assumed that the liquid is segregated with the water below the oil. The gas is therefore only in contact with the oil, and the surface tension is given by:

$$\sigma_L = \sigma_O \mid WCUT < 60$$

If water dominates the liquid then the surface tension is taken as an average of the oil-gas and water-gas surface tensions:

$\sigma_L = \sigma_O \cdot \left(1 - \frac{WCUT}{100}\right) + \sigma_O \cdot \frac{WCUT}{100} \mid WCUT > 60$	
σ_L	is the surface tension between the oil and the gas (dynes/cm)
σ_O	is the surface tension between the oil and the gas (dynes/cm)
σ_W	is the surface tension between the water and the gas (dynes/cm)
$WCUT$	is the water cut (%)

Stock tank and flowing conditions

Stock tank conditions

Stock tank conditions are defined as:

Pressure	Temperature
14.7 psia	60° F
1 bara	15.5° C

Flowing conditions

Flowing conditions are defined at the actual in-situ flowing pressure (P) and temperature (T).

Examples:

Flowing gas flowrate

The gas flowrate at stock-tank conditions (mmscf/d), this rate does not include the dissolved gas and therefore its value increases along the flow path due to pressure losses. If the outlet pressure is set to 14.7 psia, then the profile will eventually converge to the stock-tank gas rate.

Flowing gas volume flowrate

The gas volume flowrate at in-situ flowing pressure (P) and temperature (T) (mmcf/d). This rate has lower values than those of flowing gas flowrate.

Stock tank gas flowrate

The gas flowrate at stock-tank conditions (mmscf/d), this is the total gas (free + dissolved) which remains constant throughout the flow path.

Limits

The following limitations apply to PIPESIM.

General

- Maximum number of components in a stream: 50

Well Performance

- Maximum number of completions: 10
- Maximum number of sinks: 1
- Maximum number of tubing strings: Detailed model = 20, Simple model = 4

Network

- Maximum number of wells / branches: Unlimited.
- Maximum number of nodes: Unlimited.
- Maximum number of PVT files: 500
- Maximum number of compositions: 1,000
- Maximum number of Black Oil fluids: 1,024
- Maximum number of PQ data points: 30

Note: Although the maximum number of wells, and so on, is unlimited practical limits may apply depending upon the configuration of the PC used. The limiting factors [for large models] will be memory and processor speed. Schlumberger tests network models up to 10,000 wells. Please see the License and Installation Guide for your version of PIPESIM for recommendations on memory.

Typical values

Related links:

[Flowline/riser catalog properties](#)

Fluid properties

The table below gives typical values for properties, in Engineering units and data for various oil locations worldwide.

	Default	Min	Max	North Sea	North America	South America	Middle East	Far East	Australia
Black Oil Properties									
Water cut	0	0	100						
GOR	required				340 -1,100	600-20,000			
Gas s.g.	0.64				0.64 - 0.81	0.65 - 0.8			
Water s.g.	1.02				1.01 - 1.03	1.01 - 1.05			
API	30			38	13 - 56	7-45	32-44	34	

Solution Gas Correlation	Lasater			Glaso	Lasater			
Viscosity Data								
Dead Oil viscosity	Beggs and Robinson				Beggs and Robinson			
Viscosity @ 200F	2.247				0.4 -11	5 - 10,000		
Viscosity @ 60F	117.8				3.8 - 82,000	120 - 10,000		
Heat capacities								
Oil	0.45							
Gas	0.55							
Water	1.0							

Default values can be changed - click the relevant link.

Related links:

[Flowline/riser catalog properties](#)

Roughness

Material	ft.	in
Drawn tubing (brass, lead, glass, and the like)	0.000005	0.00006
Commercial steel or wrought iron	0.00015	0.0018
Asphalted cast iron	0.0004	0.0048
Galvanized iron	0.0005	0.006
Cast iron	0.00085	0.010
Wood stave	0.0006-0.003	0.0072-0.036
Concrete	0.001-0.01	0.012-0.12
Riveted steel	0.003-0.03	0.036-0.36

Related links:

[Flowline/riser catalog properties](#)

Thermal Conductivities

Material	Density (kg/m ³)	Thermal Conductivity Btu/hr/ft/F	Thermal Conductivity (W/m/K)
Anhydrite		0.75	
Carbon Steel	7900	28.9	50
Concrete Weight Coat	2000 - 3000	0.81 - 1.15	1.4 - 2.0
Corrosion Coat (Bitumen)	-	0.19	0.33
Corrosion Coat (Epoxy)	-	0.17	0.30
Corrosion Coat (Polyurathane)	-	0.12	0.20
Dolomite		1.0	
Ground (Earth)		0.37 - 1.5	
Gypsum		0.75	
Halite		2.8	
Ice	900	1.27	2.2
Lignite		2.0	
Limestone		0.54	
Line pipe		27	46.7
Mild Steel tubing		26	45
Mud	1500	0.75 - 1.5	1.3 - 2.6
Neoprene Rubber	-	0.17	0.3
Plastic coated pipe		20	34.6
Plastic coated tubing		20	34.6
Polyurathane Foam (dry)	30 - 100	0.011 - 0.023	0.02 - 0.04

Polyurthane Foam (wet)	-	0.023 - 0.034	0.4 - 0.6
PVC Foam (dry)	100 - 340	0.023 - 0.025	0.040 - 0.044
Sandstone		1.06	
Shale		0.7	
Stainless Steel	-	8.67	15
Stainless steel (13%)		18	31.14
Stainless steel (15%)		15	26
Syntactic Foam (dry)	500	0.052	0.09
Syntactic foam (wet)	-	0.17	0.3
Volcanics		1.6	
Wet Sand	1600	1.04 - 1.44	1.8 - 2.5

Related links:

[Flowline/riser catalog properties](#)

Thermal Conductivities in W/m/K (Liquids and Gases)

Fluid	Default	Temperature	Temperature	Temperature	Temperature
Air		5°C	20°C	100°C	200°C
Crude oil (30 API)	0.138	0.14	0.14	0.12	0.10
Glycol (DEG)		0.26	0.25	0.20	0.14
Natural gas (P=1 bara)	0.035	0.030	0.032	0.045	0.062
Natural Gas (P=100 bara)		0.045	0.045	0.052	0.070
Natural gas (P=200 bara)		0.071	0.067	0.064	0.074
Natural gas (P=300 bara)		0.090	0.085	0.076	0.083
Water	0.605	0.56	0.59	0.68	0.68

Default values can be changed - click the relevant link.

Related links:

[Flowline/riser catalog properties](#)

Permeability

For a gas well, this is gas permeability. For an oil well, this is total liquid permeability.

Typical values are:

- < 1 md : Very low
- 1 - 10 md: Low
- 10 - 50 md: Mediocre
- 50 - 200 md: Average
- 200 - 500 md: Good
- > 500 md: Excellent

Related links:

[Flowline/riser catalog properties](#)

Drainage radius

Common drainage radii are:

- 40 acres 745 ft (227 m)
- 80 acres 1053 ft (321 m)
- 160 acres 1490 ft (454 m)
- 640 acres 2980 ft (908 m)

Related links:

[Flowline/riser catalog properties](#)

Fittings

Related links:

[Flowline/riser catalog properties](#)**Model fittings**

Fittings (elbows, valves and tees) are modeled by the standard practice of utilizing equivalent length. From the fittings table determine the extra length of pipe that needs to be added to the model to exert the same pressure drop as the required fitting.

Related links:

[Flowline/riser catalog properties](#)**Valves - equivalent lengths of 100% open valves in feet**

Model as a pipe with the required ID and set the equivalent length as indicated in the table below. For example to model a 3/4 inch angle valve add a pipe section of ID 3/4 and a length of 12 feet.

Pipe Size	Gate Valve	Globe Valve	Angle Valve
(Inches)	(feet)	(feet)	(feet)
1/2	.35	17	8
3/4	.50	22	12
1	.6	27	14
1 1/4	.8	38	18
1 1/2	1.0	44	22
2	1.2	53	28
2 1/2	1.4	68	33
3	1.7	80	42
4	2.3	120	53
5	2.8	140	70
6	3.5	170	84
8	4.5	220	120
10	5.7	280	140
12	9	400	190
14	10	450	210
16	11	500	240
18	12	550	280
20	14	650	300
22	15	688	335
24	16	750	370

Related links:

[Flowline/riser catalog properties](#)**Elbows: Equivalent length of elbows in feet**

Model as a pipe with the required ID and set the equivalent length as indicated in the table below. For example to model a 3/4 standard elbow add a pipe section of ID 3/4 and a length of 2.2 feet.

Pipe Size:	St'd elbow	Med. sweep elbow	Long sweep elbow
Inches	feet	feet	feet
1/2	1.5	1.3	1
3/4	2.2	1.8	1.3
1	2.7	2.3	1.7
1 1/4	3.6	3	2.3
1 1/2	4.5	3.6	2.8
2	5.2	4.6	3.5
2 1/2	6.5	5.5	4.3
3	8	7	5.2
4	11	9	7
5	14	12	9
6	16	14	11
8	21	18	14

10	26	22	17
----	----	----	----

Related links:

[Flowline/riser catalog properties](#)

Tees: Equivalent length of Tees in feet

Model as a pipe with the required ID and set the equivalent length as indicated in the table below. For example to model a 3/4 inch Tee (straight through) add a pipe section of ID 3/4 and a length of 1.3 feet

Pipe Size:	Tee (straight through)	Tee (rt. angle flow)
Inches	feet	feet
1/2	1	3.2
3/4	1.3	4.5
1	1.7	5.7
1 1/4	2.3	7.5
1 1/2	2.8	9
2	3.5	12
2 1/2	4.3	14
3	5.2	16
4	7	22
5	9	27
6	11	33
8	14	43
10	17	53

Related links:

[Flowline/riser catalog properties](#)

Glossary

The PIPESIM help uses the following symbols:

Roman Letters

a	is the major axis of the drainage ellipse	ft	m
$A = \frac{\pi D^2}{4}$	is the pipe cross-sectional area	ft^2	m^2
$B = \frac{hR}{k}$	is the Biot number	dimensionless	dimensionless
B_o	is the oil formation volume factor	$bbl / STBO$	
c, C	is the specific heat capacity	$BTU / lb \cdot {}^\circ F$	$J / kg \cdot K$
d, D	is the pipe diameter	ft	m
E	is the specific total energy	BTU / lb	J / kg
f	is the friction factor	dimensionless	dimensionless
	is the frequency	Hz	Hz
F, R	is the gas/oil ratio	dimensionless	dimensionless
g	is the acceleration due to gravity	$= 32.17 \text{ ft} / s^2$	$= 9.81 m / s^2$
$Gr = \frac{L^3 \rho^2 \beta g \Delta T}{\mu^2}$	is the Grashof number	dimensionless	dimensionless
h	is the local heat transfer coefficient	$BTU / h \cdot \text{ft}^2 \cdot {}^\circ F$	$W / m^2 \cdot K$
$H = U + PV$	is the specific enthalpy	BTU / lb	J / kg
H_L	is the liquid holdup	dimensionless	dimensionless
$Head$	is the head	$\text{ft} \cdot lb_f / lb$	$N \cdot m / kg$
J	is the productivity index		

k	is the thermal conductivity is the absolute permeability	$BTU/h \cdot ft \cdot {}^{\circ}F$ ft^2	$W/m \cdot K$ m^2
L	is the pipe length is the horizontal well length	ft	m
m	is the mass	lb	kg
M	is the molecular weight is the number of magnetic poles in an ESP	lb/mol dimensionless	$kg/kmol$ dimensionless
n	is the polytropic coefficient is the number of moles	dimensionless mol	dimensionless mol
N	is the compressor speed		
$Nu = \frac{hL}{k}$	is the Nusselt number	dimensionless	dimensionless
p, P	is the pressure	psi or lbf/in^2	N/m^2
$Power$	is the power	hp	W
$Pr = \frac{\mu c_p}{k}$	is the Prandtl number	dimensionless	dimensionless
q	is the mass flow rate	lb/s	kg/s
Q	is the heat transfer rate is the average liquid rate	BTU/h	W
r	is the radial distance from the centre of well	ft	m
r_w	is the wellbore radius	ft	m
r_{ch}	is the drainage radius of a horizontal well	ft	m
R	is the pipe radius is the gas constant	ft $= 1545.35 lb_f \cdot ft/lb \cdot mol \cdot {}^{\circ}R$	m $= 8.314 J/K \cdot mol$
$Ra = Pr Gr$	is the Rayleigh number	dimensionless	dimensionless
Re	is the Reynolds number	dimensionless	dimensionless
S	is the specific entropy	$\frac{BTU}{lb \cdot {}^{\circ}F}$	$\frac{J}{kg \cdot K}$
$S = \frac{Q}{2\pi k \Delta T}$	is the pipe burial shape factor is the skin	dimensionless	dimensionless
t	is the well operating time	h	s
T	is the temperature	${}^{\circ}F, {}^{\circ}R$	K
U	is the specific internal energy is the overall heat transfer coefficient	BTU/lb $BTU/h \cdot ft^2 \cdot {}^{\circ}F$	J/kg $W/m^2 \cdot K$
v	is the fluid velocity is the ESP speed	ft/s rev/min	m/s rev/s
V	is the volume	ft^3	J/kg
wt	is the pipe wall thickness	ft	m
W_s	is the shaft work	BTU	J
z	is the vertical displacement above a gravitational datum level	ft	m
Z	is the compressibility is the pipe burial depth	ft	m

Greek Letters

θ	is the angle of the pipe to the horizontal		
$\theta_{bur} = \sin^{-1}\left(\frac{Z}{R}\right)$	is the angle of the buried arc of a partially buried pipe		
$\alpha = \frac{k}{\rho c_p}$	is the thermal diffusivity	ft^2/s	m^2/s
	is the volumetric thermal expansion coefficient	$1/{}^{\circ}F, 1/{}^{\circ}R$	$1/K$

$\beta = -\frac{1}{\rho} \left(\frac{\partial \rho}{\partial T} \right)_H$			
$\gamma = \frac{C_p}{C_v}$	is the ratio of specific heats is the specific gravity (relative density)	dimensionless dimensionless	dimensionless dimensionless
$\delta = \frac{d_{beam}}{d_{up}}$	is the choke diameter ratio	dimensionless	dimensionless
ϵ	is the pipe roughness	ft	m
η	is the efficiency, expressed as a fraction, $0 < \eta \leq 1$		
$\phi = \frac{Av_G}{Av_G + Av_L}$	is the void fraction	dimensionless	dimensionless
μ	is the fluid dynamic viscosity	$cp = 10^{-3} Pa \cdot s$	$Pa \cdot s = kg/m \cdot s$
ρ	is the density	lb/ft^3	kg/m^3
$\rho_{ns} = \lambda_L \rho_L + \lambda_G \rho_G$	is the no-slip density	lb/ft^3	kg/m^3
λ	is the flowing fraction	dimensionless	dimensionless
σ	is the interfacial (surface) tension	dynes/cm	N/m

Subscripts

<i>b</i>	bubble point
	bulk
<i>c</i>	critical
<i>G</i>	gas phase
<i>L</i>	liquid phase
<i>m</i>	mixture
<i>o</i>	oil
<i>r</i>	reduced
<i>R</i>	reservoir
<i>s</i>	gas/oil ratio, solution slip or slippage
<i>v</i>	vaporization or vapor phase volume or volumetric
<i>w</i>	water

Conversion factors

Common conversion factors used in PIPESIM are tabulated below.

Length

$$\begin{array}{|l|l|} \hline 1 \text{ ft} & 0.3048 \text{ m} \\ \hline 1 \text{ ft} & 12 \text{ in} \\ \hline \end{array} \quad \begin{array}{|l|l|} \hline 1 \text{ m} & 3.28084 \text{ ft} \\ \hline \end{array}$$

Volume

$$\begin{array}{|l|l|} \hline 1 \text{ ft}^3 & 0.02832 \text{ m}^3 \\ \hline 1 \text{ barrel} & 5.61458 \text{ ft}^3 \\ \hline 1 \text{ barrel} & 0.15899 \text{ m}^3 \\ \hline \end{array} \quad \begin{array}{|l|l|} \hline 1 \text{ m}^3 & 35.31467 \text{ ft}^3 \\ \hline 1 \text{ ft}^3 & 0.17811 \text{ barrel} \\ \hline 1 \text{ m}^3 & 6.28981 \text{ barrel} \\ \hline \end{array}$$

Mass

$$1 \text{ lb} = 0.4536 \text{ kg} \quad | \quad 1 \text{ kg} = 2.2046 \text{ kg}$$

Time

$$\begin{array}{c|c} 1 \text{ hour} = 3600 \text{ s} & \\ \hline 1 \text{ day} = 86400 \text{ s} & \end{array}$$

Gravity

$$\begin{array}{c|c} g = 32.18 \text{ ft} \cdot \text{s}^{-2} & g = 9.81 \text{ m} \cdot \text{s}^{-2} \\ \hline g = 1/144 \text{ psi} \cdot \text{ft}^2 \cdot \text{lb}^{-1} & \end{array}$$

Pressure

The engineering units of pressure psi, needs to be treated with care. One psi is one pound-force per square inch, or 144 pound force per square foot. A pound force is the force exerted by one pound weight, which is one pound times the acceleration due to gravity $g = 32.18 \text{ ft} \cdot \text{s}^{-2}$.

$$\begin{array}{c|c} 1 \text{ psi} = 144 \frac{\text{lbf}}{\text{ft}^2} = 144 \cdot g \text{ lb} \cdot \frac{\text{ft}}{\text{s}^2} \cdot \frac{1}{\text{ft}^2} & \\ \hline 1 \text{ bar} = 10^5 \text{ Pa} & 1 \text{ bar} = 14.504 \text{ psi} \\ 1 \text{ Atm} = 1.01325 \text{ bar} & 1 \text{ Atm} = 14.70 \text{ psi} \end{array}$$

Energy

$$\begin{array}{c|c} 1 \text{ BTU} = 1.055056 \text{ kJ} & 1 \text{ kJ} = 0.947817 \text{ BTU} \\ \hline & 1 \text{ kJ} = 10^{-3} \text{ Pa} \cdot \text{m}^3 \end{array}$$

Power

$$1 \text{ hp} = 550 \cdot g \text{ ft}^2 \cdot \text{lb} \cdot \text{s}^{-3} \quad | \quad 1 \text{ hp} = 0.7457 \text{ kW}$$

Dynamic viscosity

$$1 \text{ cP} = 10^{-3} \text{ Pa} \cdot \text{s}$$

Permeability

$$1 \text{ mD} = 10^{-10} \frac{\text{Pa}}{\text{Atm}} \cdot \text{m}^2$$

References

Adames, P.E.	"Analysis and comparison of three comprehensive mechanistic hydrodynamic models for vertical upward and deviated gas-liquid flow through pipes". MSc thesis, University of Calgary, 2009.
Aggour	"Hydrodynamics and Heat Transfer in Two-Phase Two-Component Flow", PhD thesis, University of Manitoba, Winnipeg, Canada (1978).
Al-Hussainy, R., Ramey Jr., H. J. and Crawford, P. B.	"The Flow of Real Gases Through Porous Media", JPT (1966) 624-636.
Alhanati, F. J. S., Schmidt, Z., Doty, D. R. and Lagerlef, D. D.	"Continuous Gas-Lift Instability: Diagnosis, Criteria, and Solutions", SPE 26554 (1993)
Alves,I.N., Alhanati, F. J. S. and Shoham,O.	"A Unified Model for Predicting Flowing Temperature Distribution in Wellbores and Pipelines", SPE 20632 (1992)
Ashford, F.E. and Pierce, P.E.	"Determining Multiphase Pressure Drops and Flow capacities in Down-Hole Safety Valves", Journal of Petroleum Technology, Paper No. SPE-5161, (September, 1975).
Aziz, K., Govier, G. W. and Forgasi, M.	"Pressure Drop in Wells Producing Oil and Gas," J. Cdn. Pet. Tech. (July-Sept. 1972) 38-48.
Babu, D. K. and Odeh, A. S.	"Productivity of a Horizontal Well", SPE Reservoir Engineering (November 1989) 417-421.
Baker, A., Nielsen, K., and Gabb, A.	"Pressure Loss, Liquid-Holdup Calculations Developed," Technology, Oil & Gas Journal (Mar. 14, 1988).
Baker, O. and Swerdloff, W.	"Calculation of Surface Tension - 3";, Oil & Gas Journal (Dec. 5, 1955) 141.
Beal, C.	"The Viscosity of Air, Water, Natural Gas, Crude Oil and its Associated Gases at Oil Field Temperatures and Pressures". SPE 946094, Trans AIME, December 1946.
Beggs, H. D.	"Gas Processing Operations", OCGI Publications, (1984), ISBN 0-930972-06-6
Beggs, H. D., and Brill, J. P.	"A Study of Two Phase Flow in Inclined Pipes", J. Pet. Tech. (May 1973) 607-617.
Beggs, H. D. and Robinson, J. R.	"Estimating the Viscosity of Crude Oil Systems", J. Pet. Tech. (Sept. 1975) 1140-1.
Behrmann, L., Grove, B., Walton, I., Zhan, L., Graham, C., Atwood, D., and Harvey, J.	"A Survey of Industry Models for Perforator Performance: Suggestions for Improvements", SPE 125020, Presented at the 2009 SPE ATCE, New Orleans, 4-7 October, 2009.

Behrmann, L.A., Hughes, K., Johnson, A.B. and Walton, I.C.	"New Underbalanced Perforating Technique Increases Completion Efficiency and Eliminates Costly Acid Stimulation," SPE 77364.
Bellarby, Jonathan	"Well Completion Design", Chapter 6, Elsevier, 2009.
Bendakhlia, H. and Aziz, K.	"Inflow Performance Relationships for Solution-Gas Drive Horizontal Wells", SPE paper 19823 presented at the Annual Technical Conference and Exhibition, San Antonio, (October 1989).
Bendiksen et al.	"The Dynamic Two-Fluid Model OLGA: Theory and Application," SPE Production Engineering, 171-180, May 1991.
Bergman, D. F. and Sutton, R. P.	"Undersaturated Oil Viscosity Correlation for Adverse Conditions", SPE 103144 (2006).
Bhatti and Shah	"Turbulent and Transition Flow Convective Heat Transfer in Ducts", Handbook of Single-Phase Convective Heat Transfer, ed. Kakac, Shah, Aung Wiley Interscience, NY (1987)
Brauner, N. and Ullmann, A.	"Modeling of Phase Inversion Phenomenon in Two-Phase Pipe Flows," Int. J. Multiphase Flow, 28, 1177, 2002.
Brill, J. P. et al.	"Analysis of Two-Phase Tests in Large Diameter Flow Lines in Prudhoe Bay Field", SPEJ (June 1981).
Brill, J. P. and Beggs, D. H.	"Two-Phase Flow in Pipes", 6th Edition, University of Tulsa, Tulsa, Oklahoma, (December 1988).
Brill, J.P. and Mukherjee, H.	"Multiphase Flow in Wells", SPE Monograph 17, (1999)
Brons, F. and Marting, V. E.	"The Effect of Restricted Fluid Entry on Well Productivity", Trans., AIME (1961) 222, 1972.
Brown, T.S., Niesen, V.G., And Erickson, D.P.	"Measurement and Predition of Kinetics of Paraffin Deposition", SPE 26548, 68th Annua Technical Conference and Exhibition of SPE Houston, TX, 3-6 October, 1993.
Brown, K.E.	"The Technology of Artificial Methods", Penwell Publishing Company, Tulsa, Oklahoma, 1984.
Butler, B.	"Success grows in pumping high-gas-fraction multiphase fluids", Petroleum Engineer International, July 1999.
Celier, G. C. M. R., Jouault, P. and de Montigny, O. A. M. C.	"Zuidwal: A Gas Field Development With Horizontal Wells", SPE paper 19826 presented at the Annual Technical Conference and Exhibition in San Antonio, October 1989.
Cheng, A.M.	"Inflow Performance Relationships for Solution-Gas-Drive Slanted/Horizontal Wells", SPE paper 20720 presented at the Annual Technical Conference and Exhibition, New Orleans, September 1990.
Chew, J. and Conally, C. A. Jr.	"A Viscosity Correlation for Gas Saturated Crude Oils", Trans., AIME (1974) 23.
Chu and Jones	"Convective Heat Transfer Coefficient Studies in Upward and Downward, Vertical, Two-Phase, Non-Boiling Flows", AIChE Symp. Ser., vol. 76, 79-90 (1980).
Cinco, H., Miller, F.G.,and Ramey H.J.	"Unsteady-State Pressure Distribution created By a Directionally Drilled Well," JPT 5131, (1975)
Cinco, H., Samaniego, V., and Dominguez A.	"Transient Pressure Behavior for a Well With a Finite-Conductivity Vertical Fracture", SPE 6014, August 1978.
Cinco-Ley, H., and Samaniego, F.	"Transient Pressure Analysis for Fractured Wells", JPT, 1749 - 1766, September 1981a.
Cinco-Ley, H., and Samaniego, F.	"Transient Pressure Analysis: Finite Conductivity Fracture Case versus Damage Fracture Case", SPE Paper 10179, 1981b.
Colburn	"A Method of Correlating Forced Convection Heat Transfer Data and a Comparison With Fluid Friction", Trans. AIChE, 19, 174 (1933) [reprinted in Int. J. Heat Mass Transfer, 7, 1359 (1964)..
Cooper, R.E., and Troncoso, J.C.	"An Overview of Horizontal Well Completion Technology", SPE paper 17582 presented at the International Meeting on Petroleum Engineering, Tianjin, China, (November 1988).
Crane Technical Paper 410	"Flow of fluids through valves, fittings and pipe", 1988, Crane Co.
Cunliffe, R.	"Prediction of Condensate Flow Rates in Large Diameter High Pressure Wet Gas Pipelines", APEA Journal (1978), 171-177
Dake, L.P.	"Fundamentals of Reservoir Engineering", Elsevier Scientific Publishing Co., New York, (1978).
De Ghetto, G. et al.	"Reliability Analysis on PVT Correlations", SPE 28904 (1994).
De Ghetto, G. et al.	"Pressure-Volume-Temperature Correlations for Heavy and Extra Heavy Oils", SPE 30316 (1995).
de Marolles, C. abd de Salis, J.	"Innovations in multiphase hydrocarbon operations", www.pump-zone.com, (1999).
C.de Waard, U. Lotz	"Influence of liquid flow velocity on CO2 corrosion: a semi-empirical model." CORROSION/95, Paper No. 128, NACE, 1995.
C.de Waard, U. Lotz, Milliams, D.E	"Predictive model for CO2 Corrosion Engineering in Natural Gas Pipelines", Corrosion, Vol. 47, No. 12, Dec. 1991 (976-985).
Dikken, B.J.	"Pressure Drop in Horizontal Wells and its Effect on Production Performance", JPT (November 1990) 1426-1433.
Dipprey and Sabersky	"Heat and Momentum Transfer in Smooth and Rough Tubes at Various Prandtl Numbers", Int. J. Heat Mass Transfer, 6, 329 (1963)
Dittus and Bolter	"Heat Transfer in Automobile Radiators of the Tubular Type", University of California Pub. Eng., 2, 443 (1930).
Dranchuk , P.M., Abou-Kassem, J.H.	"Calculation of Z Factors For Natural Gases Using Equations of State," J. Cdn. Pet. Tech. (July-Sept., 1975) 34-36
Drexel and McAdams	"Heat Transfer Coefficients for Air Flowing in Round Tubes and Around Finned Cylinders", NACA ARR No. 4F28, [also Wartime Report W-108 (1945)].
Dukler, E. A., et al.	"Gas-Liquid Flow in Pipelines, I. Research Results", AGA-API Project NX-28 (May 1969).

Duns, H., and Ros, N. C. J.	"Vertical Flow of Gas and Liquid Mixtures in Wells", 6th. World Pet. Congress (1963) 452.
Earlougher, R. C. Jr,	"Advances in Well Test Analysis", SPE Monograph 5, (1977)
Eaton, B. A.	"Prediction of Flow Patterns, Liquid Holdup and Pressure Losses Occurring During Continuous Two-Phase Flow in Horizontal Pipelines", Trans., AIME (1967) 815.
Economides, M.J., Hill, D.A., and Economides, C.E.	"Petroleum Production Systems", PTR Prentice Hall, 1994.
Economides, M.J., McLennan, J.D., Brown, E., and Roegiers, J.C.	"Performance and Stimulation of Horizontal Wells", World Oil, (July 1989) 69-76.
Eckert, E.R.G. and Jackson, T.W.	"Analysis of Turbulent Free Convection Boundary Layer on a Flat Plate", NACA Report 1015 (July 1950)
Elsharkawy, A.M. and Alikhan, A.A.	"Models for predicting the viscosity of Middle East crude oils", Fuel 78 (1999), 891-903.
Elamvaluthi and Srinivas	"Two-Phase Heat Transfer in Two Component Vertical Flows", Int. J. Multiphase Flow, vol. 10, no. 2, p. 237-242 (1984).
Fetkovich, M.J.	"The Isochronal Testing of Oil Wells", SPE 4259, (1973).
Fetkovich, M.J. and Vienot, M.E.	"Shape Factors, CA, Expressed as a Skin, sCA", JPT (February 1985) 321-322.
Flanigan, O.	"Effect of Uphill Flow on Pressure Drop in Design of Two-Phase Gathering Systems", Oil and Gas J. (March 10, 1958) 56, 132.
Folefac, A. N., Archer, J. S. and Issa, R. I.	"Effect of Pressure Drop Along Horizontal Wellbores on Well Performance", SPE paper 23094 presented at the Offshore Europe Conference held in Aberdeen (September 1991).
Forchheimer, Ph.	"Wasserbevegung durch Boden", Z. Ver. Deutch. Ing., Vol. 45 (1901) p. 1781 - 1788
Friend and Metzner	"Turbulent Heat Transfer inside Tubes and the Analogy among Heat, Mass, and Momentum Transfer", AIChE J., 4, 393 (1958).
Ghassan, H. A., and Maha, R. A.	"Correlations developed to predict two-phase flow through wellhead chokes", The Journal of Canadian Petroleum technology, Volume 30, No 6, 1991
Giger, F. M., Reiss, L. H., and Jourdan, A. P.	"The Reservoir Engineering Aspects of Horizontal Drilling", SPE paper 13024 presented at the Annual Technical Conference and Exhibition in Houston, September 1984.
Glasø, O.	"Generalized Pressure Volume Temperature Correlation", J. Pet. Tech. (May 1980) 785.
Golan, M. and Whitson, C.H.	"Well Performance", International Human Resources Corporation, Boston, MA (1986).
Gomez, L.E., Shoham, O., Schmidt, Z., Chokshi, R.N., and Northug, T.	"Unified mechanistic model for steady-state two-phase flow: Horizontal to vertical upward flow". SPE Journal, 5(3):339-350, 2000.
Goode, P. A. and Wilkinson, D. J.	"Inflow Performance of Partially Open Horizontal Wells", SPE paper 19341 presented at the SPE Eastern Regional Meeting, Morgantown, WV, October, (1989).
Gowen and Smith	"Turbulent Heat Transfer from Smooth and Rough Surfaces", Int. J. Heat Mass Transfer, 11, 1657 (1968)
Grolman, E.	"Gas-Liquid Flow with Low Liquid Loading in Slightly Inclined Pipes", Ph.D. Dissertation, U. of Amsterdam, Amsterdam, The Netherlands (1994).
Grolman, Commandeur, de Basst and Fortuin	"Wavy-to-Slug Flow Transition in Slightly Inclined Gas-Liquid Pipe Flow", AIChE Journal, vol 42. No. 4, p901 (1996)
Gurley, D. G., Copeland, C. T. and Hendrick, J. L.	"Design Plan and Execution of Gravel-Pack Completion," J. Pet. Tech. (Oct. 1977).
Hagedorn, A. R. and Brown, K. E.:	"Experimental Study of Pressure Gradients Occurring During Continuous Two-Phase Flow in Small-Diameter Vertical Conduits", J. Pet. Tech. (April 1965) 475-484.
Harvey, J., Grove, B., Zhan, L. and Behrman, L.	"New Predictive Model of Penetration for Oilwell-Perforating Shaped Charges", SPE 127920. Presented at the 2010 SPE International Symposium and Exhibition on Formation Damage Control, Lafayette, Louisiana, 10-12 February, 2010.
Hausen	"Neue Gleichungen fur die Wärmeübertragung bei freier oder erzwungener Stromung", Allg. Warmetchn., 9, 75 (1959).
Hawkins, M. F., Jr.	"A Note on the Skin Effect", Trans. AIME, 207: 356-357, (1956).
Hayduk, W. and Minhas, B.S.	"Correlations for Predictions of Molecular Diffusivities in Liquids", The Canadian Journal of Chemical Engineering, 60, 295 (1982).
Hernandez, O.C., Hensley, H., Sarica, C., Brill, J.P., Volk, M., Delle-Case, E.	"Improvements in Single-Phase Paraffin Deposition Modeling", SPE Production and Facilities, 237, (2004).
Hossain, M.S. et al.	"Assessment and development of Heavy-Oil Viscosity Correlations", SPE/PS-CIM/CHOA 97907, PS2005-407.
Hughmark, G. A.	"Holdup in Gas Liquid Flow", Chem. Eng. Prog., v.58, p.62.
Incropera, F. P. and DeWitt, D.P.	"Fundamentals of Heat and Mass Transfer", Fourth Edition, Wiley, New York. (1996).
ISO Standard 15136-1	"Petroleum and Natural Gas Industries – Progressing Cavity Pump Systems for Artificial Lift", Second Edition, 2009-11-15.
Jones, L.G., Blount, E.M. and Glaze, O.H.	"Use of Short Term Multiple Rate Flow Tests To Predict Performance of Wells Having Turbulence", SPE 6133 (1976).
Jones, L. G. and Slusser, M. L.	"The Estimation of Productivity Loss Caused by Perforation - Including Partial Completion and Formation Damage", SPE paper 4798 (1974).

Joshi, S. D.	"Horizontal Well Technology", Penwell Publishing Company, Tulsa, Oklahoma (1991).
Joshi, S. D.:	"A Review of Horizontal and Drainhole Technology", SPE paper 16868 presented at the Rocky Mountain Regional Meeting in Casper, WY (May 1988).
Kaminsky, R. D.	"Estimation of Two-Phase Flow Heat Transfer in Pipes", J Energy Res Tech, vol 121, p 75 (1999).
Karakas, M. and Tariq, S.M.	"Semianalytical Productivity Models for Perforated Completions", SPE 18247 (1991).
Karassik, I.J., Messina, J.P., Cooper, P., Heald, C. C.	"Pump Handbook," 3rd edition, McGraw-Hill Inc., 1991
Karassik, I. J.	"Pump Handbook," 3rd Edition. McGraw-Hill, New York, 2001.
Karassik, J. et al.	"Pump Handbook", 2nd edition, McGraw-Hill Inc., 1986
Kartoatmodjo, R.S.T. and Schmidt, Z.	"New Correlations For Crude Oil Physical Properties", SPE 23556 (1991).
Katz, D. L. et al.	"Handbook of Natural Gas Engineering", McGraw Hill Book Co., Inc., New York (1959).
Kawase and Ulbrecht	"Turbulent Heat and Mass Transfer in Dilute Polymer Solutions", Chem Eng Sci, 37, 1039 (1982)
Kawase and De	"Turbulent Heat and Mass Transfer in Dilute Polymer Solutions Flowing Through Rough Tubes", Int. J. Heat Mass Transfer, 27, 140 (1984)
Kern, D.Q. and Seaton, R.E.	"A Theoretical Analysis of Thermal Surface Fouling", British Chemical Engineering, Brit. Chem. Eng. 4, 258 (1959).
Khoze, Dunayev, Sparin	"Heat and Mass Transfer in Rising Two-Phase Flows in Rectangular Channels", Heat Transfer-Sov. Res., vol. 8, no. 3, p 87-90, (1976)
King	"Heat Transfer and Pressure Drop for an Air-Water Mixture Flowing in a 0.737 Inch I.D. Horizontal Tube", MS Thesis, University of California, Berkeley, CA, (1952).
Knott et al.	"An experimental Study of Heat Transfer to Nitrogen-Oil Mixtures", Ind. Eng. Chem., vol. 51, no. 11, p. 1369-1372 (1959).
Kreith, F. and Bohn, M.	"Principles of Heat Transfer", 5th Edition, PWS Publishing Company (1997).
Kudirka, Grosh, McFadden	"Heat Transfer in Two-Phase Flow of Gas-Liquid Mixtures", I&EC Fundamentals, vol 4, no 3, p 339-344 (1965)
Kunz, Klimeck	The GERG-2004 wide-range equation of state for natural gases and other mixtures. GERG TM15 2007. Fortschr.-Ber. VDI, Reihe 6, Nr. 557, VDI Verlag, Düsseldorf, 2007; also available as GERG Technical Monograph 15 (2007).
Kunz, Wagner	The GERG-2008 wide-range equation of state for natural gases and other mixtures: An expansion of GERG-2004. To be submitted to J. Chem. Eng. Data (2011).
Lasater, J. A.:	"Bubble Point Pressure Correlation", Trans., AIME (1958) 379.
Lee, A. L., Gonzales. M.H. and Eakin, B.E.	"The Viscosity of Natural Gases", Trans., AIME (1966), 237, 997-1000.
Lockhart, R. W. and Martinelli, R. C.	"Proposed Correlation of Data for Isothermal Two-phase, Two-Component Flow in Pipes", Chem. Eng. Prog. (January 1949) 45, 39.
Martin and Sims	"Forced Convection Heat Transfer to Water with Air Injection in a Rectangular Duct", Int. J. Heat Mass Transfer, vol 14, p 1115-1134, (1971).
Matzain, A.	"Multiphase Flow Paraffin Deposition Modeling", Ph.D. Dissertation, U. Tulsa, Tulsa, OK (2001).
Matzain, A., Apte, M.S., Zhang, H.-Q., Volk, M., Redus, C.L., Brill, J.P., Creek, J.L.	"Multiphase Flow Wax Deposition Modeling", Proceedings of ETCE 2001, ETCE2001-17114, 927 (2001).
Matzain, A., Apte, M.S., Zhang, H.-Q., Volk, M., Brill, J.P., Creek, J.L.	"Investigation of Paraffin Deposition During Multiphase Flow in Pipelines and Wellbores-Part 1: Experiments", Transactions of the ASME, 124, 180 (2002).
McAdams, W.H.	"Heat Transmission", McGraw Hill, New York (1954).
McCain, William D. Jr.	"Petroleum Fluids", edition 2.
McLeod, H. O.	"The Effect of Perforating Conditions on Well Performance", JPT (Jan. 1983).
Manabe, R.	"A comprehensive heat transfer model for two phase flow with high pressure flow pattern validation", University of Tulsa, (2001).
Manhane, J. M., Gregory, G. A. and Aziz, K.	"A Flow Pattern Map for Gas-Liquid Flow Pattern in Horizontal Pipes", Int. J. of Multiphase Flow.
Martinelli	"Heat Transfer to Molten Metals", Trans. ASME, 69, 947 (1947).
Minami, K. and Brill, J. P.	"Liquid Holdup in Wet Gas Pipelines", SPE J. Prod. Eng. (May 1987).
Mirza, K. Z.	"Progressing cavity multiphase pumping systems: expanding the possibilities", presented at BHR Conference Multiphase, 1999
Moody, L.	"An approximate Formula for Pipe Friction Factors", Transactions ASME, vol 69, pp. 1005 (1947)
Mukherjee, H. and Brill, J. P.	"Liquid Holdup Correlations for Inclined Two-Phase Flow", JPT (May 1983) 1003-1008.
Mukherjee, H. and Economides, M. J.	"A Parametric Comparison of Horizontal and Vertical Well Performance", SPE paper 18303 presented at the Annual Technical Conference and Exhibition in Houston, October 1988.
Muskat, M.	"The Flow of Homogeneous Fluids Through Porous Media", I.H.R.D.C., Boston (1937).
Mutalik, P. N., Godbole, S. P. and Joshi, S. D.	"Effect of Drainage Area Shapes on Horizontal Well Productivity", SPE paper 18301 presented at the Annual Technical Conference and Exhibition, Houston (October 1988).
Norris, L.	"Correlation of Prudhoe Bay Liquid Slug Lengths and Holdups Including 1981 Large Diameter Flowlines Tests", Internal Report Exxon (October 1982).

Nunner	"Wärmeübergang und Druckabfall in Rauhen Rohren", VDI-Forschungsheft 445, ser B, 22, 5 (1956) or 786-Atomic Energy Research Establishment, Harwell UK
Oliemans, R. V. A.	"Two-Phase Flow in Gas-Transmission Pipeline", ASME paper 76-Pet-25, presented at Pet. Div. ASME meeting Mexico City (Sept. 1976).
Oliver and Wright	"Pressure Drop and Heat Transfer in Gas-Liquid Slug Flow in Horizontal Tubes", Bri. Chem. Eng., vol. 9, no. 9, p 590-596 (1964)
Omana, R. et al.	"Multiphase Flow Through Chokes", SPE 2682, 1969
Orkiszewski, J.	"Predicting Two-Phase Pressure Drops in Vertical Pipes", J. Pet. Tech. (June 1967) 829-838.
Ouyang, L., Aziz, K	"Development of New Wall Friction Factor and Interfacial Friction Factor Correlations for Gas-Liquid Stratified Flow in Wells and Pipelines", SPE 35679, 1996.
Ovworrie, Chukwuemeka	"Steady-State Heat Transfer Models For Fully And Partially Buried Pipelines," SPE 131137, International Oil and Gas Conference and Exhibition in Beijing, China, 8-10 June 2010.
Oxley, K. C., Ward, J.M. and Derk, W.G.	"How multiphase pumping can make you money", presented at Facilities 2000 Conference, New Orleans 1999
Palmer, C. M.	"Evaluation of Inclined Pipe Two-Phase Liquid Holdup Correlations Using Experimental Data", M.S. Thesis, The University of Tulsa (1975).
Pan, S., Zhu, J., Zhang, D., Razouki, A., Talbot, M. and Wierczchowski, S.	"Case Studies on Simulation of Wax Deposition in Pipelines", IPTC-13420-PP, 7-9 December 2009
Park, H. Y., Falcone, G. and Teodoriu, C.	"Decision Matrix for Liquid Loading in Gas Wells for Cost/Benefit Analyses of Lifting Options," Journal of Natural Gas Science and Engineering 1 (2009) 72-83.
Payne, G. A.	"Experimental Evaluation of Two-Phase Pressure Loss Correlations for Inclined Pipe", M.S. Thesis, The University of Tulsa (1975).
Perry, R. H., Green, D. W.	"Perry's Chemical Engineering Handbook", 7th ed., McGraw-Hill, 1997.
Poettman, F. H. and Beck, R. L.	"New Charts Developed to Predict Gas-Liquid Flow Through Chokes", World Oil, March 1963, 95-101
Prandtl, L.	"Führer durch die Stromungslehre", Vieweg, Braunschweig, p 359 (1944)
Petrosky, G.E. Jr. and Farshad, F.F.	"Pressure-Volume-Temperature Correlations for Gulf of Mexico Crude Oils", SPE 51395 (1998)
Petukhov and Gnielinski	Int. Chem. Eng., 16-2, p 359, (1976)
Petukhov and Kirillov	"Heat Transfer and Friction in Turbulent Pipe Flow with Variable Physical Properties", Adv. Heat Tranfer, vol. 6, p 505-564 (1970)
Poling, B.E., Prausnitz, J.M. and O'Connell, J.P.	"The Properties of Gases and Liquids", Fifth Edition, McGraw-Hill
Pots, B. F. M., Bromilow, I. G. and Konijn, M. J. W.	"Severe Slug Flow on Offshore Flowline/Riser Systems", SPE paper 13723, (March 1985).
Prats, M.	"Effect of Vertical Fractures on Reservoir Behavior-Incompressible Fluid Case", SPEJ, pp. 105-118, June 1961.
Pucknell, J.K. and Mason J.N.E.	"Predicting the Pressure Drop in a Cased-Hole Gravel Pack Completion", SPE 24984, 1992.
Ramey, H.J.	"Wellbore Heat Transmission", JPT 435 Trans AIME, No. 225 (April 1962)
Ravipudi and Godbold	"The Effect of Mass Transfer on Heat Transfer Rates for Two-Phase Flow in a Vertical Pipe", Proc. 6th Int. Heat Transfer Conf.-Toronto, vol. 1, p 505-510, (1978)
Rawlins, E.L. and Schellhardt, M.A,	"Backpressure Data on Natural Gas Wells and Their Application to Production Practices", Monograph Series, USBM 7, (1935).
REFPROP: Lemmon, E.W., Huber, M.L., McLinden, M.O. NIST Standard Reference Database 23	Reference Fluid Thermodynamic and Transport Properties-REFPROP, Version 9.1, National Institute of Standards and Technology, Standard Reference Data Program, Gaithersburg, 2013
Renard, G. I. and Dupuy, J. M.	"Influence of Formation Damage on the Flow Efficiency of Horizontal Wells", SPE paper 19414 presented at the Formation Damage Control Symposium, Lafayette (February 1990).
Rezkallah and Sims	"An Examination of Correlations of Mean Heat Transfer Coefficients in Two-Phase and Two-Component Flow in Vertical Tubes", AIChE Symp. Ser., vol. 83, pp. 109-114, 1987.
Romero, D.J., Valko, P.P., and Economides, M.J.	"The Optimization Of The Productivity Index And The Fracture Geometry Of A Stimulated Well With Fracture Face And Choke Skins", SPE 73758, 2002.
Sandall et al.	"A New Theoretical Formula for Turbulent Heat and Mass Transfer with Gases or Liquids in Tube Flow", Can. J. Chem. Eng., 58, 443 (1980)
Scandpower PT Tech Note TN-11 (internal)	"TN-11: Heat Transfer Calculations", Scandpower PT, Oslo (February 2003).
Shell report SIEP 98-5463	"Satellite multiphase boosting - Multiphase boosting study", Siep-RTS, ABB Lummus Global
Scott, S. L., Shoham, O., and Brill, J. P.	"Prediction of Slug Length in Horizontal Large-Diameter Pipes", SPE paper 15103 (April 1986).
Schlunder, E.U. (ed)	VDI Wärmeatlas, VDI-Verlag, Düsseldorf (1984).
Schneider, G. E.	"An Investigation Into Heat Loss Characteristics of Buried Pipes", Journal of Heat Transfer Vol. 107 (pp696-699) (Aug 1985).
Shah	"Generalized Prediction of Heat Transfer during Two Component Gas-Liquid Flow in Tubes and Other Channels", AIChE Symp. Ser., vol. 77, no. 208, p. 140-151, (1981).
Sieder and Tate	"Heat Transfer and Pressure Drop of Liquids in Tubes", Ind. Eng. Chem., 28, 1429 - 1453 (April

	1936).
Singh, P.	"Gel Deposition on Cold Surfaces", U. of Michigan, Ann Arbor, Michigan (2000).
SPE Production Engineering Handbook	Volume IV, Chapter 15, Society of Petroleum Engineers, 2007.
Sonnad, J. and Goudar, C.	"Explicit Reformulation of the Colebrook-White Equation for turbulent Flow friction Factor calculation", Ind. Eng. Chem. Res, 46, pp. 2593-2600, (2007)
Span, R. and Wagner, W.	"A New Equation of State for Carbon Dioxide Covering the Fluid Region from the Triple-Point Temperature to 1100 K at Pressures up to 800 MPa," J. Phys. Chem. Ref. Data, 25(6):1509-1596, 1996.
Standing, M. B.	"Volumetric and Phase Behavior of Oil Field Hydrocarbon Systems", Society of Petroleum Engineers, (1977) 121.
Standing, M. B.	"A General Pressure Volume-Temperature Correlation for Mixtures Of California Oils and Greases," Drill. and Prod. Prac., API (1947) 275.
Standing, M. B. and Katz, D. L.	"Volumetric and Density of Natural Gases", Trans., AIME (1942) 140.
Taitel, Y. and Dukler, A. E.	"A Model for Predicting Flow Regime Transitions in Horizontal Gas-Liquid Flow", AIChE J. (vol. 22, no. 1) (Jan. 1976) 47-55.
Vasquez, M., and Beggs, H. D.	"Correlations for Fluid Physical Property Prediction", SPE paper 6719, presented at the 52nd Annual Technical Conference and Exhibition of the Society of Petroleum Engineers, Denver, Colorado (1977).
Venkatesan, R.	"The Deposition and Rheology of Organic Gels", U. of Michigan, Ann Arbor, Michigan (2004).
Vijay, Aggour, and Sims	"A Correlation of Mean Heat Transfer Coefficients for Two-Phase Two-Component Flow in a Vertical Tube", Proc. 7th Int. Heat Transfer Conf., vol. 5, p. 367-372 (1982).
von Karman,	"The Analogy Between Fluid Friction and Heat Transfer", Trans. ASME, 61, 705 (1939).
Vogel, J. V.	"Inflow performance relationships for solution gas drive wells", Journal Pet. Tech., SPE 1476, (1968)
Walton, Ian C., Johnson, Ashley B., Behrmann, Larry A. and Atwood, David C.	"Laboratory Experiments Provide New Insights into Underbalanced Perforating", SPE 71642.
Webb	"A Critical Evaluation of Analytical Solutions and Reynolds Analogy Equations for Turbulent Heat and Mass Transfer in Short Tubes", Warme-und Stoffübertrag, 4, 197 (1971).
Woelflin, W.	"The Viscosity of Crude-Oil Emulsions", Drill. and Prod. Prac., API (1942) 148.
Xiao, J.J., Shoham, O., and Brill J.P.	"A comprehensive mechanistic model for two-phase flow". In Proceedings of the 65th SPE Annual Technical Conference and Exhibition, pages 167-180, 1990.
Zhang, H.Q., Wang, Q., Sarica, C., Brill, J.P.	"Unified Model for Gas-Liquid Pipe Flow Via Slug Dynamics - Part 1: Model Development", ASME Journal of Energy Resources Technology, Vol.125 (December 2003) 274.
Zhang, H.-Q., Wang, Q., Sarica, C. and Brill, J.P.	"Unified Model for Gas-Liquid Pipe Flow Via Slug Dynamics - Part 2: Verification", ASME Journal of Energy Resources Technology, Vol.125 (December 2003) 266.
Zhang, H.-Q. and Sarica C.	"Unified Modeling of Gas/Oil/Water Pipe Flow – Basic Approaches and Preliminary Validation," SPE Project Facilities & Construction 1(2), pp. 1- 7, 2006.